

# **Microbiologically influenced corrosion in ship ballast tanks**

Anne Heyer



# **Microbiologically influenced corrosion in ship ballast tanks**

## **Proefschrift**

ter verkrijging van de graad van doctor aan de Technische Universiteit Delft,  
op gezag van de Rector Magnificus prof. ir. K.C.A.M. Luyben,  
voorzitter van het College voor Promoties,  
in het openbaar te verdedigen  
op maandag 15 april 2013 om 12.30 uur

door

**Anne HEYER**

Master of Science in Water Science, Universiteit Duisburg-Essen, Duitsland  
geboren te Duisburg, Duitsland

Dit proefschrift is goedgekeurd door de promotor:  
Prof. dr. J.H.W. de Wit

Samenstelling promotiecommissie:

Rector Magnificus	Voorzitter
Prof. dr. J.H.W. de Wit	Technische Universiteit Delft, promotor
Dr. ir. J.M.C. Mol	Technische Universiteit Delft, copromotor
Prof. dr. I. Richardson	Technische Universiteit Delft
Prof. dr. H. Terryn	Technische Universiteit Delft en Vrije Universiteit Brussel, België
Prof. dr. G. Muyzer	Universiteit van Amsterdam
Prof. dr. W. Sand	Universiteit Duisburg-Essen, Duitsland
MSc. G. Ferrari	TNO

The project was carried out under project number M32.6.08302 in the framework of the Research Program of the Materials innovation institute M2i ([www.m2i.nl](http://www.m2i.nl)). Additional support of TNO, Maritime Materials Performance Centre (MMPC) for lab facilities in Den Helder.

Title: Image of *Pseudomonas spp.* attached to stainless steel (atomic force microscope used for contact mode imaging in air of the metal substrate).

ISBN: 978-90-820590-0-7

Copyright © 2013 by A. Heyer

Printed by: Haveka drukkerij, Alblasserdam, The Netherlands

All rights reserved. No part of the material protected by this copyright notice may be reproduced or utilized in any form or by any means, electronic or mechanical, including photocopying, recording or by any information storage and retrieval system, without written permission from the author.

## Preface

Microbiologically influenced corrosion (MIC) has been in focus for some decades causing severe and rapid corrosion failure in industrial systems. Beside the damage to industrial applications as in power plants, oil and water industry failure due to MIC was also reported for materials exposed to freshwater, seawater and pure waters.

The microbiological processes are not causing corrosion damage directly, but these rather accelerate or initiate local electrochemical reactions. The type of corrosion damage is in itself not distinctive as the presence of organisms involved e.g. bacteria, fungi and algae make failure analysis quite difficult and imprecise.

The first report of MIC goes back to the 18<sup>th</sup> century and up to now MIC has been reported in various case studies including metallic and non-metallic materials. The central problem of MIC is the general underestimation in relation to costs. Until now only rough estimations of MIC related expenses are available but it is agreed that around 50% of the total corrosion costs are related to MIC worldwide (Fleming, 1996)\*.

This thesis will give an overview on the different approaches to determine MIC by interdisciplinary science including electrochemical, surface analytical and microbiological analysis. We will start our microbial corrosion journey by reviewing the structural properties of ship ballast tanks and the main environmental conditions in these enclosed marine structures in relation to various forms of corrosion.

The second chapter deals with a case study conducted in a real scale ballast tank and with the organisms associated with the corrosion sites.

The third chapter introduces several electrochemical detection techniques for lab scale experiments dealing with the impact of MIC.

The last chapter will give an outlook on more advanced local techniques to study MIC on the micron scale adding knowledge for future research.

The thesis is intended to give an overview on the topic of MIC in enclosed seawater environments, serving those interested in the impact of microorganisms in the deterioration of materials and helping them to prevent damage to vital structures in ships.

---

\* Fleming HC (1996) Economical and technical overview. In: Heitz E, Flemming HC, Sand W (eds) *Microbiologically Influenced Corrosion of Materials*. New York: Springer-Verlag, pp. 6-14.

## Research Aim and Outline

The overall scientific objective of the project is to conduct a detailed investigation into the chain of events leading to MIC at material/water interfaces in ship tank environments, aiming to fully understand the interactions between biological and electrochemical processes and to identify triggers that initiate crucial steps in the MIC pathway. The ultimate goal is to use this knowledge to better detect, prevent and manage MIC in ship ballast tanks (SBT).

MIC is known to be a dangerous process in ship tanks due to its rapid unpredictable occurrence, leading to extremely fast local corrosion, leading to perforation or severe reduction in strength in a short time. This project focuses on a fundamental understanding of MIC processes in ship tank environments where both aerobic and anaerobic biofilms develop resulting in aggressive corrosion.

Fundamental understanding of the dominant parameters considering Material, environment and bacteria will be addressed. The knowledge generated in this project will contribute the development of advanced MIC detection techniques. Major benefits from the project outcome include reduction of downtime, increased safety, reduced pollution risk and better MIC prevention technologies.

In this project the MIC process will be investigated in a multidisciplinary way, covering microbiology, biochemistry, surface chemistry and electrochemistry. The diagram below illustrates the general approach.

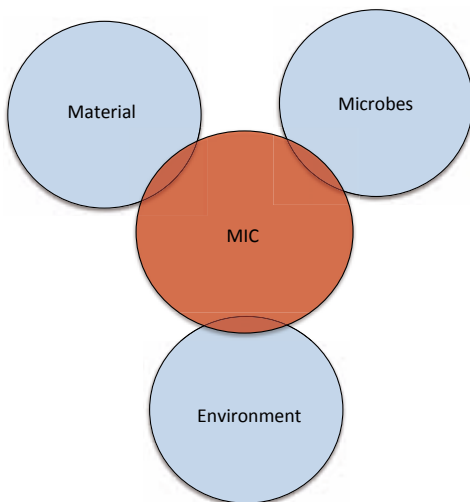


Fig. 1. Schematic structure of research approach

For this approach the research questions are treated in 4 different chapters (Figure 2).

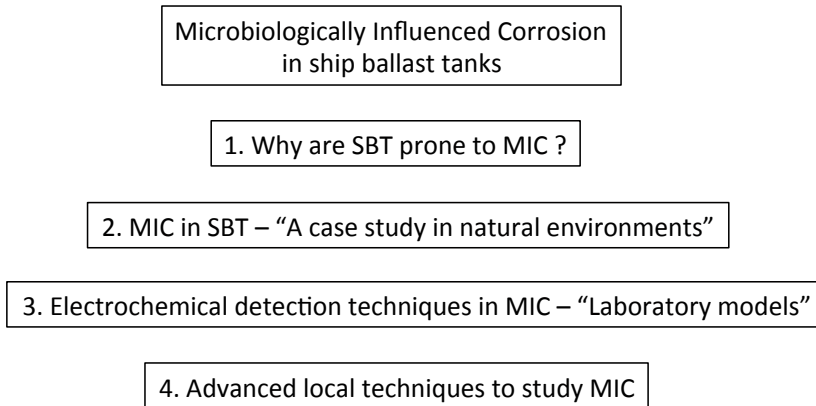


Fig. 2 Schematic structure of thesis chapters

- Chapter 1 reviews the problem of MIC in SBTs from environmental and electrochemical point of view.
- Chapter 2 comprises a field survey to study the microbial diversity shifts of attached biofilms within ship ballast tanks. Microbial community studies were combined with electrochemical corrosion rate measurements and revealed for the first time a correlation of microbial biofilms and corrosiveness in different height levels inside of a real ship ballast tanks.
- Chapter 3 covers a step-by-step investigation of the MIC chain of events. It covers a detailed investigation during built up of corrosive biofilms such as local corrosion phenomena. For this approach three different experimental routes were followed.
- Chapter 4 covers the study of localized corrosion reactions on metal surfaces caused or accelerated by microorganisms by local microscopic and electrochemical techniques.

## Abbreviations

Ag/AgCl	Silver/Silver Chloride electrode
AFM	Atomic force microscope
(m)-ASW	(modified) Artificial Seawater
APB	Acid-producing bacteria
BBS	Basal Salt Solution (minimal growth medium)
BBS+S°	Basal Salt Solution (minimal growth medium) + Sulfur
CPE	Constant phase element
DAPI	4.6-diamidin-2-phenylindole (nucleic acid dye)
EDX	Energy Dispersive X-ray spectroscopy
EFM	Epifluorescence microscope / microscopy
EIS	Electrochemical Impedance Spectroscopy
EPS	Extracellular polymeric substances
LPR	Linear Polarization Resistance
MIC	Microbiologically Influenced Corrosion
MICI	Microbiologically Influenced Corrosion Inhibition
OCP	Open Circuit Potential
OM	Optical microscope
SBT	Ship ballast tank
SECM	Scanning electrochemical microscope / microscopy
SEM	Scanning electron microscope / microscopy
SRB	Sulphate-reducing bacteria
SSTMS	Simulated ship tank model system
SVET	Scanning vibrating electrode technique
SW	Seawater



## Symbols and constants

C	Capacitance
D	Effective diffusion coefficient of the particle
$E_{\text{corr}}$	Corrosion potential
h	hours
$i$	Current density
I	Current
L	Effective diffusion thickness
n	CPE parameter
R	Electrical resistance
$R_s$	Solution resistance
$R_p$	Polarization resistance
t	time
Y	Admittance
$Y_o$	Admittance amplitude
$W_s$	Warburg diffusion element, semi-infinite diffusion
Z	Impedance
Z	Impedance magnitude

# Contents

Preface	I
Research aim and outline	II-III
Abbreviations and Symbols	IV-V
Table of contents	VI-VII
<b>1 Introduction</b>	
1.1 Ship ballast tanks a review from microbial and electrochemical point of view	1-29
<b>2 MIC in SBT- “A case study in natural environments”</b>	
2.1 Molecular Microbiology Methods applied on ship ballast tank samples Diagnosis of microbial corrosion in ship ballast tanks by combined molecular and electrochemical tools	31-50
2.2 A molecular and electrochemical approach to study corrosiveness and population dynamics of MIC biofilms inside of ship ballast tanks	51-72
<b>3 Electrochemical detection techniques in MIC – “Laboratory models”</b>	
3.1 Corrosion behaviour of ballast tank steel in the presence of sulphate reducing and acid producing bacteria	73-88
3.2 Corrosion of carbon steel in a simulated ship ballast tank in presence of a microbial community retrieved from an original site	89-108
3.3 Biodegradation of ballast tank coating investigated by microscopy and impedance spectroscopy	109-134
<b>4 Advanced local techniques to study MIC</b>	
4.1 A new approach to study local corrosion processes on steel surfaces by combining different microscopic techniques	135-150
4.2 Early-stages of Pseudomonas biofilm formation on stainless steel by means of local electrochemical techniques	151-169

<b>5</b>	<b>Conclusions</b>	171-176
	<b>Future Outlook</b>	177-179
	<b>Summary</b>	180-182
	<b>Samenvatting</b>	183-185
	<b>Zusammenfassung</b>	186-188
	<b>Publications</b>	189-192
	<b>Dankwoord</b>	193
	<b>Curriculum Vitae</b>	194

*Dedicated to my mother*

## Chapter 1

### **1.1**                                      *Ship ballast tanks a review from microbial and electrochemical point of view*

#### **Abstract**

Microbiologically Influenced Corrosion (MIC) is the term used for the phenomenon in which corrosion is initiated and/or accelerated by the activities of microorganisms. MIC is a very serious problem for the ship industry as it reduces structural lifetime and increases maintenance costs. This review aims to focus on the importance and mechanisms of MIC in ship ballast tanks (SBTs). Part one presents a literature review of general aspects of ballast tanks: structural properties including predominant environmental conditions. Part two summarizes the fundamental corrosion mechanisms within ballast tanks from an electrochemical point of view. Part three links microbial corrosion mechanism with electrochemical processes summarizing types of microorganisms, mechanisms of MIC and possible triggers for biofilm formation within this enclosed environment. Part four gives an outlook on surface treatment and coating application in SBT. The last paragraph considers the practical aspects of MIC detection, identification and possible counterstrategies for engineers and inspection personal. This paper gives a comprehensive overview of MIC processes in ship ballast tanks in particular addressing the practical relevance for engineers, equipment manufacturers and environmental scientists.

1. Ship ballast tanks

1.1 Historical aspects and application

A ballast tank is a compartment within a boat, ship or other floating structure that holds water. All vessels have ballast water tanks to adjust the ship’s draft, buoyancy and trim under different operating conditions. From the 1880s onwards, water was used for ship ballasting. This decreased time-consuming load of solid material e.g. stones used as ballast. Small vessels may have a single ballast tank in the middle or multiple ballast tanks typically on both sides. Large bulk carrier and oil tanker have several ballast tanks including double bottom tanks, wing tanks as well as forepeak and aft peak tanks. In ship construction, a ballast tank is usually centered at the lowest point of the hull (Figure 1). By positioning multiple ballast tanks around the ship, local weight reduction by fuel consumption and stormy weather conditions can be balanced increasing ship stability. Ballast tanks can be filled or emptied with water in order to adjust the amount of ballast force. Ballast tanks are usually filled when cargo is being offloaded, and discharged when cargo is being loaded. When ships take in water for ballast in port, they also take in organisms, which are present in the water. These organisms are then transported, and are potentially introduced into the waters of the harbors along the vessels' routes as ballast tanks are emptied each time cargo is loaded. It is well documented that ballast water is a major pathway for aquatic species introductions around the world (Haelegraeff and Bolch 1992; Hamer et al. 2000; Gollasch et al., 2002). Today 80% of the world's trade volume is transported by ships (Peters, 1993). In many cases half of a given voyage must be undertaken in ballast conditions to compensate the absence of cargo. This emphasizes the huge volume of ballast water, which is transferred all over the world and the importance of ship ballast tanks (SBT) on the lifetime and safety of a ship.

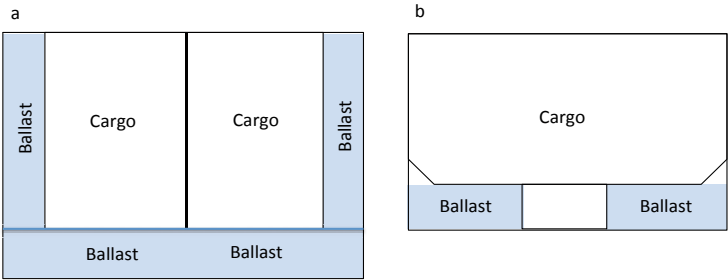


Fig. 1: Typical cross-sectional view of ballast tank positions within ships. (a) tanker; (b) bulk vessel

Typical vessel types and their ballast requirements can be broadly classified as provided in Table 1. The capacity, location and flexible use of ballast tanks are a crucial point in ship design. Rough operational conditions, such as wet/dry phases during load/unload conditions and structural aspects make SBTs difficult and expensive in maintenance and inspection.

The complex structure of a ballast tank results from stiffeners, edges and corners forming the basic skeleton of a ship. Inner surface areas of SBTs are enormous, classically in the range of 1.5 to 7 million m<sup>2</sup>. Ballast capacities depend on the ship size and therefore range from single cubic meters for sailing boats up to 200.000m<sup>3</sup> for large cargo carriers. Ballast water is taken on board using sea chests, pumps or by gravity feed. As a consequence of remaining water when off-loading (retarded by stiffeners) sediment accumulates within SBTs. Studies have shown that at least 65% of ships were carrying significant amounts of sediment on the bottom of their ballast tanks (Hallegraeff and Bolch, 1992; Hamer et al., 2000) which is a potential source for nonindigenous organisms (Gollasch et al., 1998).

Table 1

Ballast requirements and corresponding ship types.\*

Ballast requirement (Reason for ballast water uptake)	Ship types
<i>Cargo replacement</i>	Dry bulk carriers Ore carriers
<i>Return voyage</i>	Tankers Oil bulk ore carriers
<i>Control stability, trim</i>	Ferries General cargo vessels Passenger vessels Fishing vessels Fish factory vessels Military vessels
<i>Large volumes, discharged in same location</i>	Heavy lift vessels Military assault vessels Barge-carrying cargo vessels
<i>Vessel control</i>	Container ships

(\*Stemming the tide, Introduction of Nonindigenous Species by 'Ship Ballast Water by National Research Council (U.S.), 1996. Committee on ships' Ballast Operations)

### 1.2 MIC related costs for the ship industry

Ship ballast tanks are prone to MIC as they are continuously flushed and filled with seawater to trim the shipload with dry periods in between during which the humidity in the tanks may increase up to 95%. Corrosion rates ascribed to MIC in tanks of ships have been reported in literature. Huang et al. (1997) reported excessive pitting corrosion up to 2mm/yr on the uncoated carbon steel bottom plating. Cleland (1995) stated even 6mm/yr. for the bottom plating.

Water ballast tanks are an integral part of every ship and although these areas are not revenue earning, they can be a critical expense item particularly if steelwork replacement as a result of corrosion is required.

Due to the fact that large cargo vessels and oil tankers have hundreds of thousands square meter ballast tank surface, corrosion prevention and even more reconstruction if prevention fails is extremely costly.

Since 1990 water ballast tanks have become the subject of a number of regulations from institutions such as the International Association of Classification Societies (IACS) and the International Maritime Organization (IMO). One of the main reasons for increasing regulatory activity was the large number of ship losses that occurred in the 1980's where corrosion contributed to the failure of the construction. The break-up of the single hull tankers Exxon-Valdez (1989) and Erika (1999) should be mentioned here.

### 1.3 Material and environmental conditions

Nowadays mild and low carbon steels as listed in (Table 2) are typically used for ballast tank constructions due to their performance (ASTM A131) and cost efficiency.

Table 2  
Elemental composition of mild & low carbon steel

Elements	C	Si	Mn	P	S	Cu	Ni	Ti	V
Mild steel (higher strength steel)									
Composition in wt. %	0.17	0.25	0.70	0.018	0.007	0.04	0.01	0.002	0.001
Low carbon steel (ordinary strength steel)									
Composition in wt. %	0.15	0.40	1.45	0.015	0.015	0.035	0.025	-	-

The material is used in form of steel plates, shapes, bars, and rivets for ship construction. Beside choice and property of construction materials, important for SBT structural properties, environmental conditions as the water have to be taken into account. Depending on the uptake region of the ballast water, salinity, temperature and pH can vary considerably. Temperature of seawater shows a wide variety in the surface layers due to sun radiation, absorption, evaporation, rainfall and heat exchange with the atmosphere within a range from -2°C to 28°C (Pickard and Emery, 1982). Seawater salinity ranges between 3.3 and 3.8wt% (Yebra et al., 2004), containing a wide variety of ion species, but mainly NaCl, creating a “neutral” pH between 7.5 and 8.3. The following review part will give an outlook on corrosion processes in marine environments incorporating SBTs and microbial participation.

## 2. Corrosion and microbial interactions

### 2.1 Corrosion

The corrosion process in general can be defined as electrochemical interaction between a metallic material and its environment. A detailed discussion of corrosion processes is outside the scope of this review. For further information on this topic reviews (Jones, 1991; Groysman 2010) can be advised. However since microbiologically influenced corrosion is not a new type of corrosion, it is necessary to summarize briefly the electrochemical process of corrosion before the mechanisms of MIC are discussed.

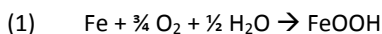


Corrosion occurs because of the natural tendency for most metals to return to oxidized species in nature originally in ores. This typical metal behavior will be illustrated by iron. The most common iron ore, hematite is an oxide of iron:  $\text{Fe}_2\text{O}_3$ .

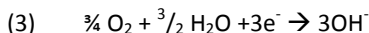
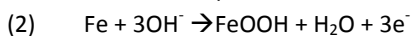
The most common product of the corrosion of iron is rust  $\text{FeOOH}$ , where iron has recovered its 3+ valency, due to interaction with the oxidizing environment.

A corrosion reaction involves the transfer of electrons through coupled oxidation and reduction processes. In electrochemical reactions, the electrons are produced at the anode (oxidation) and consumed at the cathode (reduction).

For iron the overall corrosion reaction in the presence of oxygen can be written as equation 1



The reaction is composed of the anodic reaction (2) and the cathodic reaction (3)



The character of the cathodic reaction depends on pH of the solution (electrolyte). In the pH range between 4 and 10 diffusion of dissolved oxygen to the metal surface controls the rate of corrosion. Low corrosion rates in this pH range will occur if oxygen is absent.

The corrosion rate is determined by the slowest partial reaction. All factors influencing either the anodic or the cathodic reaction may thus determine the overall rate. Consequently corrosion reactions can be faster or slower as a result of changes in pH, and temperature and due to the presence of microorganisms, if these influence the electron transfer process at the metal surface. Internal factors as type of metal, its properties (amorphous, heterogeneity), presence of surface films and mechanical properties (stresses) may also have a significant effect on the corrosion rate.

## 2.2 Microbial impact on corrosion

Microorganisms thus modify the corrosion process by changing the electrochemical conditions at the metal-solution interface. These modifications can have different effects ranging from microbiologically influenced corrosion inhibition (MICI) (Jayaraman et al. 1997; Ismail et al. 2002; Gunasekaran et al. 2004) to microbiologically enhanced corrosion (MIC) (Little et al. 1991; Beech 1999; Dinh et al. 2004) or localized corrosion. Actually it is the local change of environmental conditions (Ford and Mitchell, 1990; Walch, 1989; Breslin, 1997) that may cause a different route for the electron flow from anode to cathode. As mentioned for oxygen, corrosion rates can be influenced by diffusion processes. Biofilm accumulation on a metal surface may therefore influence the corrosion rate. The corrosion model is still valid under MIC but the process is unique due to the modification of the metal-solution interphase via biofilm formation. This exceptional feature is discussed in the following part summarizing microbial growth requirements for biofilms and emphasizing the diffusion processes through this biological layer. Microbial colonization commonly starts with single cell attachment to a surface covered with a so-called conditioning film.

Carbon steel is an easily corrodable surface in seawater, which is rapidly covered by deposits of corrosion products serving as a conditioning film. In marine environments layers of bacteria and microalgae embedded in adhesive exopolymeric substances (EPS) strengthen the corrosion product layers. Microorganisms are generally entrapped between corrosion product layers and EPS creating a sandwich structure. The existence of EPS formed by polysaccharides, proteins, lipids and nucleic acids and the roughness of irregular microbial colonies help to trap more particles and organisms. Additionally, this matrix allows sequestering nutrients from the water phase. The major component in the biofilm matrix is water, up to 97% (Geesey, 1982; Zhang et al., 1998), and the characteristics of the solvent are determined by the solutes dissolved in it, forming local pH gradients inside the biofilm. Wimpenny and Colasanti (1997) have also suggested that a biofilm structure is largely determined by metal substrate (composition and structural properties). Diffusion limitation arises readily in biofilm systems because fluid flow is reduced and the diffusion distance is increased in the biofilm. A dynamic biological system is formed at the interface and different transport processes e.g. diffusion will take place through the biofilm (Characklis, 1981). Within the biofilm local cell clusters with high cell densities and EPS compounds arrest the flow of water. Diffusion is therefore the predominant transport process within cell aggregates (de Beer et al. 1997; Stoodley et al. 1994). Diffusion times increase with increasing bacterial accumulation (biofilm thickness) e.g. 10 bacterial cells exhibit a diffusion time of 100 times longer than a single cell (Stewart 2003). For SBT biofilm formation was confirmed by community studies by PCR-DGGE (Heyer et al. 2011, personal communication). Diverse groups of organisms could be isolated and identified including  $\gamma$ -electroactive bacteria,  $\gamma$ -sulphur oxidizing (SOB),  $\gamma$ -iron oxidizing bacteria (IOB) and sulfate reducing bacteria (SRB). Based on these results it is obvious that diverse bacterial communities are present in ship ballast tanks and to some extent responsible for MIC. It is important to emphasize that MIC processes are rarely caused by only one distinct group of microorganisms. Many groups of microorganisms co-exist at the same time at the same place. Any microbial influenced corrosion occurring is probably the result of complex microbial interactions. This complexity has to be taken into account if risk evaluation of MIC within SBT is performed.

### *2.3 Biofilm formation within SBTs*

Microbial growth depends on many factors. A variation in pH, oxygen and temperature can be used to control bacterial growth. Fundamental growth requirements were correlated to environmental conditions found in SBT (Table 3). Care must be taken to ensure that no uncontrolled changes in these parameters do take place.

Table 3  
Requirements for microbial growth related to ballast tank conditions.

Requirements	Ballast tank
Water	Seawater (high salt content), brackish water, fresh water
pH	7.5 – 8
Temperature (°C)	-2-28 (depending on trading route)
Salinity (%)	0.3 - 3.5 %
Nutrients	(depending on trading route)

As can be derived from Table 3 all requirements for bacterial growth can be found in ballast tanks. All types of water (salty, fresh or brackish) are used for filling ballast tanks depending on the trading route of the vessel. The water temperature depends on the source water, within the ship temperature gradients are low and the water phase has a high load of nutrients. These points make a ship ballast tank an ideal environment for microbial growth and biofilms are an ideal form of life in these harsh environments. Biofilm formation and its structural properties are the outcome of microbial triggers in the system. A trigger can be seen as a stimulus for microorganisms to increase their growth rate or encouragement to produce more exopolymetric substances (EPS) for adhesion properties. Three different trigger mechanisms can be found which facilitate biofilm formation within ballast tanks (Table 4).

Table 4: Triggers for biofilm formation vs. the corresponding survival strategy of microorganisms.

Trigger for biofilm formation	Microbial survival strategy
Protection from harmful conditions (toxins)	Defense
Limitation in nutrients (Sequestration of nutrients out of the water phase)	Food supply (biofilm formation)
Energy loops (utilization of nutrients)	Independence (Metabolic interaction – cooperative benefit)

Biofilm formation is one of the most common microbial survival strategies: it allows bacterial species to form their own microenvironment for defense, food supply and metabolic interactions. The first trigger is presented in Table 4 by protection from harmful conditions. Bacteria form biofilms to protect themselves from toxic environmental substances. This preferred disposition provides the microorganisms with higher protection (10-1000 fold higher concentrations) from toxins (corrosion inhibitors, biocides). Low nutrient availability in the water phase can be seen as the second trigger in the system. Microbes growing in the biofilm can utilize more compounds from the water phase by exo-enzymes released and accumulated in the EPS matrix. The last trigger is cooperative benefit by re-using metabolic byproducts excreted by community members. This property makes the biofilm community independent from external impacts and is well known for acid producing bacteria (APB) and sulfate reducing bacteria (SRB) growing in close association. Overall it can be said that biofilm formation is favored by bacteria in SBTs, enhancing their chance of survival under severe environmental conditions (e.g. nutrient limitation and biocides).

## 2.4 MIC mechanisms

The classical mechanisms for microbial influenced corrosion can be reviewed as follows:

1. Metabolic production of aggressive compounds
  2. Oxygen concentration cell formation
  3. Acceleration of anodic or cathodic reactions by depolarization effect
  4. Hydrogen embrittlement (depolarization).
- 
- 1) Chemolithotrophic *Thiobacillus species* can be used to explain the first mechanism. *Thiobacilli* leach metal ores commonly found in natural environments. Part of their metabolism is the production of inorganic acid  $\text{H}_2\text{SO}_4$  (they can tolerate sulphuric acid up to 12%) through the oxidation of various, inorganic sulphur compounds as  $\text{S}_2\text{O}_3^{2-}$  (Cragolino and Tuovinen, 1984). These acids play an important role in MIC, first causing acid corrosion of iron and mild steel and in a second step, the acid can be metabolized by an oxidation reaction (Pope 1991) forming  $\text{SO}_4^{2-}$  and creating a nutrient source for sulphate reducing bacteria. Beside this inorganic acid-producing bacteria organic acids are produced by certain fungi, blamed for corrosion of steel and aluminium, (Hendey, 1964; McNamara et al., 2003; Rauch et al., 2005).
  - 2) The second mechanism, oxygen concentration cell formation, is relevant for corrosion resistant alloys (e.g., stainless steel) in the presence of biofilms. *Pseudomonas spp.* are slime forming and oxygen consuming organisms. Their growth forms oxygen concentration cells on the metal surface, resulting in a low oxygen concentration under the colony that acts as an anode. The surrounding area is indicated by a higher oxygen concentration forming the corresponding cathode. A corrosion cell is initiated, and the metal will dissolve faster leading to crevice corrosion or pitting (Walch et al., 1989; Videla, 1996; Wang, 1996). The same principle of surface separation can be found for iron-oxidizing bacteria. They isolate the metal surface into small anodic sites (beneath deposits of iron hydroxides and biomass in form of biofilms) and large surrounding cathodic areas (Tatnall, 1981; Borenstein, 1994).
  - 3) Sulphate reducing bacteria (SRB) are responsible for this type of mechanism. In particular the role of SRB has been documented in pitting corrosion of various metals and their alloys in both aquatic and terrestrial environments under anoxic as well as oxygenated conditions (Hamilton, 1985, 1998, 1999; Beech 2002). SRBs produce hydrogen sulphide during their metabolism; if SRBs are growing on metal surfaces, their biofilms are likely to promote the formation of pits beneath sulphide deposits (von Wolzogen, Kühr and van der Vlugt 1934; Jones et al. 2002). In the classical theory of SRB-influenced corrosion of metallic iron, electrons are transported from the metal surface to the bacterial sulphate reduction pathway through hydrogen intermediate.

This theory, suggests that only sulphate-reducing bacteria that are hydrogenase positive (hydrogenase is present) are responsible for the anaerobic corrosion of iron. Nowadays, it is widely accepted that this “depolarization mechanism” of the cathodic reaction by the enzyme hydrogenase plays no more than a secondary role in local corrosion of iron in the presence of SRB. More recent theories have been proposed in which the role of biogenic sulphide (King et al. 1973), the formation of a galvanic cell between the metal and the formed iron sulphide film (Costello, 1974), the role of elemental sulphur (Schaschl, 1980), the role of iron phosphates (Iverson, 1983) and the local acidification of anodes (Crolet et al. 1993) are discussed.

- 4) Hydrogen embrittlement refers to the depolarization mechanism that is influenced by microbial presence through the production of hydrogen sulphide as recognized for SRBs (King et al. 1973; Costello, 1974). The microbial influence on corrosion is indirect, causing cathodic depolarization with the consequent enhancement of iron dissolution. The term depolarization is used to indicate the change in the electrochemical behaviour of the system. Additionally, one important fact, generally not taken into account in the formulation of a mechanism for explaining the anaerobic corrosion of iron, is that in practical situations metal surfaces are generally covered with various deposits (oxides, sulphides and hydroxides). Thus, the mechanism proposed to explain the MIC process must include the breakdown of passivity by microbial activity as well.

In summary, all known cases of microbial corrosion can be attributed to known corrosion mechanisms. Several of these mechanisms can operate simultaneously or consecutively, but no single cause can account for all the corrosive effects of microorganisms. Microorganisms can influence corrosion by modifying the anodic or cathodic reaction with diverse effects. Anodic reactions can be accelerated by: Corrosive metabolites as sulphuric acid; metabolic substances that enhance corrosion such as biogenic sulphide in seawater. On the other hand, cathodic reactions can be altered by production of cathodic reactants (protons from acidic metabolic components), uptake or degradation of cathodic reactants (oxygen consumption) and cathodes can be indirectly accelerated by FeS participating in anaerobic corrosion (Costello 1974; Lee et al. 1995).

The following chapter focuses on the different zones of SBTs which depend on the load conditions of the vessel. In a second step a new approach is implemented which links the specific ballast tank zones with environmental conditions, microbial organisms and the resulting MIC corrosion mechanisms examined in the previous chapter.

3. Ballast tank zones

Based on engineering requirements, ballast tanks are commonly divided into two different zones: Fully submerged zone (*water phase*) and mid section (*air water phase*), see Figure 2a. This simple model is used for maintenance programs but does not reflect all relevant areas inside of SBTs considering MIC. Ballast tanks on board of vessels can be divided into four different zones (Heyer et al. 2009; Heyer et al. 2011) (Figure 2b). The presented “4 zone model” is based on a similar model which was developed for the waterfront of harbour pilings, namely, the Accelerated Low Water Corrosion (ALWC) (Little and Lee, 2007). From the author’s point of view, this model reflects the main cause why SBTs are prone to microbiologically influenced corrosion. Within these 4 different zones different environmental conditions (oxygen, nutrients, flow conditions) are established, these conditions will have a significant influence on bacterial communities and activities. These facts are addressed in the following section.

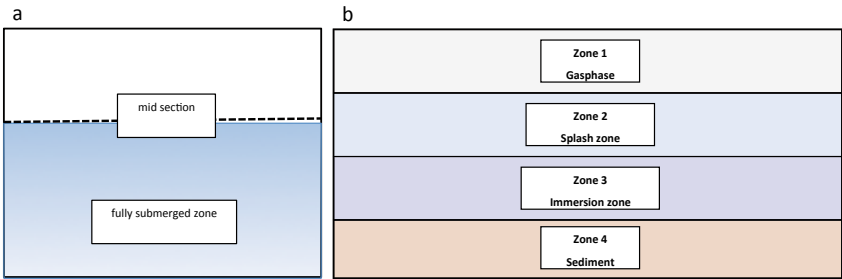


Fig. 2: Different zones in a ballast tank. (a) Common engineering model; (b) Model adapted to MIC requirements.

The proposed model in Figure 2b was supported by experimental work of the authors, who found increasing corrosion rates with decreasing oxygen concentrations from top to bottom in SBTs (Heyer et al. 2011). Interpretation and modelling of corrosion within SBTs is nowadays based on practical weight loss measurements gained in field studies (Tamburri et al. 2002, 2003, 2005; Suzuki et al. 2004), or corrosion depth measurements by ultrasonic instrumentation (Paik and Thayambali 2001; 2002; Paik et al. 2004). No model, however, has integrated bacterial species and MIC mechanisms so far. Based on this knowledge, a new model is proposed by the author, linking different SBT zones, corrosion rates, oxygen concentrations and microorganisms with their metabolic processes (Figure 3).

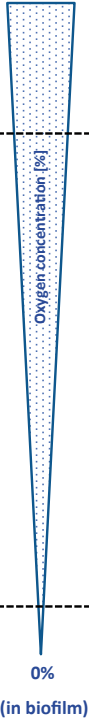

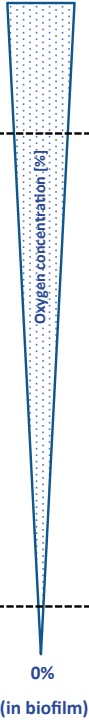

Zone	Oxygen concentration	Corrosion rate	Microorganisms	MIC processes
1 Gasphase	21% (in air) 	0,10mm/y 	Fungi  Slime forming bacteria ( <i>Pseudomonas</i> spp., <i>Clodstridium</i> spp., <i>Bacillus</i> spp., <i>Desulfovibrio</i> spp.)	organic acid production (Salvareza and Videla 1986) iron reducing mechanisms within tubercle (Emde et al. 1992)  biocatalyst of oxygen reduction (Pope et al. 1984; Scotto et al. 1993) acidic polysaccharide accumulation (Bremer and Geesey 1991) organic acid production (Little et al. 1988; Soracco et al. 1988.)
2 Splash Zone		>0,38mm/y 	Fungi	(see mechanism above)
3 Immersion Zone			Slime forming bacteria ( <i>Pseudomonas</i> spp., <i>Clodstridium</i> spp., <i>Bacillus</i> spp., <i>Desulfovibrio</i> spp.) <i>Thiobacillus</i> spp. ( <i>Thiomicrospira</i> )  IOB metal reducing bacteria ( <i>Pseudomonas</i> , <i>Shewanella</i> )  SRB ( <i>Desulfovibrio</i> spp.)	iron oxide reduction (Myers and Nealsom 1988)  cathodic depolarization (von Wolzogen Kühr and van der Vlugt 1934; Bryant et al. 1991) anodic depolarization (Dumas et al. 1988; Crolet 1992) sulfide production (Little et al. 1998) iron sulfide precipitation (King and Wakerley 1973) volatile high reactive phosphorous compounds (Iverson and Ohlson 1983) sulfide induced stress corrosion cracking (Edyvean et al. 1998) hydrogen induced cracking/ blistering (Edyvean et al. 1998)
4 Sediment	0% (in biofilm)	0,47mm/y	Electroactive bacteria  <i>Thiobacillus</i> spp. Slime forming bacteria SRB, IOB	electron shuttling shift of anodic cathodic processes (Dumas et al. 2005; Bergel et al. 2006)  (see mechanism above)

Fig. 3: Integral approach for a SBT linking zones of ballast tank with oxygen concentrations (assumptions), corrosion rates (Tamburri et al. 2002) and possible MIC mechanisms.

Figure 3 illustrates an integral approach for SBTs, linking environmental parameters such as oxygen concentration, corrosion rate, nutrient availability and the microbial species of this environment. The model specifies the SBT zones (column 1), oxygen concentration (column 2), corrosion rate (column 3), microbial species (column 4), and the metabolic process related to MIC (column 5). For each zone, oxygen concentration, corrosion rate, abundant microorganisms and the possible MIC process can be derived (from left to right). The gas phase and the sediment zone are separated, creating extreme zones within the ballast tank. The splash zone and the immersion zone in the middle of the tank are summarized as a result of similar environmental parameters and microorganisms therein. The scheme indicates that with decreasing oxygen concentrations increasing corrosion rates are determined in combination with bacterial activity in the system. This is an important observation because a decrease in oxygen concentration within ballast tanks is discussed as one of the future methods in preventing corrosion and invasive species.

It is well known that low oxygen concentrations slow down the general corrosion process of steel in seawater (Tamburri et al. 2002), and hypoxia is well known to have negative effects on many aquatic species (Grieshaber et al., 1994; Diaz and Rosenberg, 1995). However, it is not determined whether bacterial activity will be present in isolated areas of the tank. The presented data in columns 2 and 3 are based on experimental work of the author derived from a lab scale ship tank model system (Heyer et al. 2011), and on other researchers' findings (Tamburri et al. 2002). The results indicate that metabolic active bacteria increased local (pit shaped) corrosion effects in parallel with decreasing oxygen concentrations within zones 3 to 4. The blank set-up contained no bacteria and showed uniform corrosion rates in the range of 0.0466–0.0823 mm/y (Paik et al. 2004; Heyer et al., 2011). Microorganisms can actively influence their environment especially oxygen concentrations can be changed well known for biofilm communities (Kuenen 1986; Stewart and Franklin, 2008) this capability should not be underestimated for inaccessible areas as SBTs. Beside this active change of environmental parameters bacteria indicate a dynamic response on oxygen gradients this ability establish a diverse bacterial community inside the tank. This circumstance can be explained by different metabolic states of specific bacterial species that are unique for each zone. The presence of bacteria as well as their metabolic activity is significant. Uniform corrosion rates for ballast tanks can be accelerated into doubled or even higher rates; in the presence of SRB up to 8-13 mm/y (Cleland, 1994). This former observation can be explained with zone 4 in the figure above; it becomes apparent that mainly microorganisms responsible for aggressive local corrosion failure are predominant. It has to be highlighted that the rate of ballast water exchange determines the real impact of MIC in SBTs. Compared to closed seawater environments, in which electron acceptors are quickly exhausted, MIC might be irrelevant in some cases after some time. But SBTs are open systems, and ballast water exchange can be continued over the voyage time or locally in ports of arrival. A continuous input/output of nutrients ensures biofilm formation and growth of bacteria in inaccessible areas of SBTs because of their enclosed structure and their constant nutrient supply in form of water exchange. The presented microorganisms in column 4, and the corresponding MIC processes in column 5 will not be reviewed in detail; the mechanisms and corresponding organisms were discussed in detail in the previous section. For more details on the single mechanisms, the cited literature may be consulted. Finally, the following conclusions can be derived from the integral approach provided in Figure 3.

- The tank can be divided into three different risk regions for MIC; zone 1 low; zone 2 and 3 medium; zone 4 high;
- SBTs are prone to MIC because of their enclosed structure and their constant nutrient supply in form of water exchange. Within the four different zones, gradients in oxygen, nutrients and flow conditions are established these environmental conditions generate a diverse bacterial community;



- The corrosion process is characterized by rapid material loss forming deep pits at local sites. This condition is quite different from typical seawater corrosion, where low oxygen concentrations slow down the overall corrosion process, as explained in the former paragraph in respect to general corrosion reactions.

It can be recapitulated here that corrosion prediction models for SBTs are difficult to obtain because corrosion can be influenced by many factors, such as corrosion protection systems (coating and inhibitor) and various operational parameters. The operational parameters include maintenance, repair, percentage of time in ballast, frequency of tank cleaning, water quality, water temperature and sludge accumulation, as well as microbial contamination. In the case of ship structures, rigorous work aiming to understand the effect of many of these factors and their interactions is still lacking (Paik and Thayambali, 2002). Nevertheless, Paik and co-workers have proposed several models to predict general corrosion and its propagation within ship structures and ballast tanks for engineering purposes (Paik et al. 1998, Paik and Frieze 2001, Paik et al. 2004, Paik and Thayamballi, 2005). However, it becomes evident that incorporating MIC in corrosion estimations and reliability studies of SBTs is even more complex, and needs an interdisciplinary experts' approach (e.g., engineers, corrosion & coating experts and microbiologists).

## **4. Coatings and corrosion protection in ballast tanks**

### *4.1 SBT coatings*

Whilst the outer hull, external decks and superstructure may be in good condition, lifting the hatches of the water ballast tanks can reveal the real condition of the vessel and the true level of ship care and maintenance. If extensively corroded, the condition of the water ballast tanks can affect both the safety and the structural integrity of the vessel, and can also reduce its asset value. The International Maritime Organization (IMO) is the specialist United Nations agency which is tasked with improving maritime safety and with preventing pollution from ships. IMO adopted the new Performance Standard for Protective Coatings (PSPC) as resolution (MSC.215 (82) 2006). The PSPC is intended to improve the safety at sea by reducing the corrosion encountered in steel ships, and applies specifically to the protective coatings used for dedicated seawater ballast tanks in all types of ships, and also in the double-side skin spaces of bulk carriers. The aim of the new standard is to improve safety at sea by avoiding the effects of corrosion, thus enhancing the structural integrity of the vessels as a whole.

#### 4.2 Coating requirements and application

Coatings are applied for corrosion protection and act as a barrier layer between environment and metal surface. A coating is a semi-permeable membrane, and in the long term cannot permanently protect steel from corrosion. Coatings are mainly a dispersion of pigments and fillers, additives and solvents in a binder matrix (Munger, 1984; Geenen, 1991; Westing, 1992; Wicks et al. 1999; Forsgren and Schweitzer, 2006). They are generally applied to ship ballast tanks to protect the steel against corrosion. Prevention of corrosion is therefore one of the most important aspects of maintaining vessel safety plus preserving asset value.

The success of any program for protecting water ballast tank depends on:

1. The correct selection of the coating scheme during building
2. Correct surface preparation and application of the coating scheme at new building
3. Planned coating inspection in service
4. Planned and effective coating maintenance throughout the vessel's life

Neglect or poor practice at any of these four stages can lead to coatings defects and the rapid onset of de-adhesion and corrosion with possible, serious consequences. For ballast tanks, the metal surfaces are pre-treated by grid blasting to provide a clean rough surface for good interfacial bonding between metal and coating. Coatings are supposed to provide a physical barrier between the steel and the water.

However, imperfections and defects because of bad coating adhesion permit seawater to reach the steel and create anodic and cathodic sites. The result is accelerated coating wear and early de-adhesion. Furthermore, care must be taken during coating application to avoid cavities where microorganisms may grow with highly localized corrosion as a result. But in practice, a homogeneous surface structure that fulfils all these requirements is difficult to achieve due to:

- The presence of geometrically complex structural components and irregularities such as stiffeners;
- Uncontrolled environmental conditions during surface preparation;
- Moisture condensation and dust accumulation on the surface causing the coating to fail early.

### 4.3 Quality requirements for SBT coatings

Coal tar epoxies were used as ballast tanks coatings in former times. They were banned, however, due to their carcinogenic potential and will not be discussed in this review. Epoxy based coatings are mainly used for the protection of SBTs (IMO 1995; IACS 1998; DnV 1998; DnV 1999). Light coloured coatings are used nowadays to facilitate visual inspections of ballast tanks. The condition of coatings in water ballast tanks on existing ships became part of the classification scope of IACS (UR Z10.2 1993).

Based on this unified requirement, water ballast tank coating condition is to be evaluated by the ship's inspector and categorized as either: good, fair or poor. The coating conditions good, fair and poor are assigned on the basis of visual inspection and estimated percentages of areas with broken coating and rusty surfaces. The suggested integral approach for SBT can be linked to these coating categories as well.

In Figure 4, the coating category is linked to the possible risk of MIC.

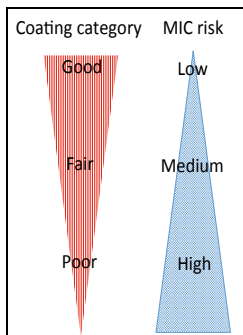


Fig. 4. Coating category estimated by visual inspection linked with possible MIC risk in the specific area.

Figure 4 indicates that with increasing coating loss (independent of SBT zone) the MIC risk increases. The danger of this fact is a reduced ship safety as a result of unpredictable structural fatigue. In short: visual coating inspection of SBTs should not only consider the quality of the applied coating by categorizing the system from good to poor. Rather, these inspections should be used to assess the MIC impact as well. A strategy of MIC assessment within the general SBT maintenance programs is provided in the last section of this review.

Epoxy solvent free coatings are new coatings to improve moisture resistance, flexibility and wetting properties of the coating. They were aimed to replace the coal tar epoxy coatings with all their positive characteristics without containing carcinogenic coal tar. Table 5 summarizes the advantages and drawbacks of a conventional epoxy ballast tank coating.

Table 5: Advantages and drawbacks of an epoxy coating for ballast water tanks.

Epoxy solvent free coating (Inorganic zinc ethyl silicate system)	
Advantages	Drawbacks
<ul style="list-style-type: none"> <li>• More tolerant to multilayer application</li> <li>• Reduced number of coating layers</li> <li>• Scratch resistance of surface</li> <li>• Better tolerant to water soluble salts (50 mg/m<sup>2</sup>), (decrease of water permeation of coating)</li> </ul>	<ul style="list-style-type: none"> <li>• Extensive pre-treatment (rust removal) before application</li> <li>• High costs due to preliminary surface preparation</li> </ul>

Nowadays, epoxy solvent free coatings are applicable in multi coating layers, thus simplifying coating repair and maintenance steps. This includes no additional surface treatment such as grid blasting; the coating can be applied on water jetted old coating surfaces, decreasing the dry dock time and repair costs. The number of preliminary coating layers can be reduced with decreasing costs for the ship owners. Modern coating systems for ballast tanks consist of at least two coating layers of a straight modified epoxy coating applied in a thickness of 250 micrometres, or solvent free epoxy coating with a thickness of 300 to 350 micrometres. The surface has a higher resistance to mechanical stresses, such as loading conditions, and can thus extend the lifetime of the coating. Beside these, one of the biggest benefits of epoxy coating systems is the high tolerance to salts (50 mg/m<sup>2</sup>), the net like chemical structure decrease water permeation/diffusion into the coating. This barrier property reduces blister formation, due to swelling of the coating. The only drawback for these coating systems is the extensive surface treatment (rust removal) by grid blasting (ISO Standard 8501-1, 2007) to optimize adhesion to the steel surface with a roughness profile between 50 and 100 microns.

#### 4.4 Coating breakdown and degradation

The breakdown of the coatings in ship ballast tanks is a well-known phenomenon, and has been addressed in several publications (IACS 1994; TSCF 1997; Paik et al. 1998; TSCF 1999; Paik and Frieze 2001). Several factors contribute to the short service life of the current coating systems: water compounds (mainly salt concentration), surface preparation of the steel surface, coating application and biodeterioration. Biodeterioration of SBT coatings by marine microorganisms should be considered, supported by experimental work of the authors showing that one SBT coating could be degraded by acid producing bacteria within 60 days (Ferrari et al. 2010). It is well recognized that polymeric coating materials can be affected by biodeterioration (Crabbe et al. 1994; Nakajima-Kambe et al. 1995; El-Sayed et al. 1996; Nakajima-Kambe et al. 1997; Little and Lee 2007; Gu 2003; Gu and Gu 2005).

The mechanisms of attack are as diverse as the material itself.

The type of attack can include:

- Acid attack by acids or enzymes excreted by microbes (bacteria or fungi);
- Utilization of organic additives as plasticizers, fillers and stabilizers as nutrients for microbial growth;

- Enhanced coating cracking due to calcareous deposits and gas evolution; biofilm formation can result in local chloride and sulphide concentration, which can destabilize coatings;
- Increase in ionic permeability resulting in moisture intrusion and osmotic blistering.

Consequently, SBT coatings are important to protect the ship structure from extensive corrosion maintenance, and visual inspections are important to increase the service lifetime and prolonged ship safety. Beside this inspection programmes, biodegradation of the coating should be taken into account, especially in areas where cavities accumulate MIC bacteria, allowing a close contact to the metal surface and leading to intensive localized corrosion. Beside coatings, corrosion protection systems are installed in ship ballast tanks to decrease the corrosion rate of unprotected tank areas. The next section gives a brief summary of the common protection system in SBTs.

#### *4.5 Alternative corrosion protection systems in ballast tanks*

The degree of corrosion impact depends on the type of corrosion protection system installed in a ballast tank. Some operators use only protective coatings, and some use protective coatings together with anodic protection (sacrificial anodes). Therefore, the corrosion attack is dependent on the type of corrosion protection system and the tank status (influenced by the loading condition). Zinc is commonly used as sacrificial anode because of its anodic behaviour against iron. However, if sacrificial anodes were installed, steel areas would be protected only when the tank is ballasted, but not when the tank is empty. Sacrificial anodes are only effective when the metallic surface is immersed in water (IACS, 2004), and it requires some time (a day or more) to become effective after the tank has been filled (Parente, 1996). When ballast tanks are full, the reported effectiveness of anodic protection is maximally 70 per cent (Weber, 1984).

#### *4.6 MIC assessment and maintenance strategies*

The most difficult issue is to face ship operators with respect to water ballast tank maintenance. MIC corrosion failure cannot be distinguished from 'normal' corrosion by one simple analysing method. It is rather the combination of local microbial techniques with electrochemical detection which makes it possible to evaluate the corrosion process in an appropriate way. This is intensively discussed by (Hamilton 1998, Beech 2004; Little et al. 2008) who summarized the combination of local detection techniques for MIC. Inspection and repair procedures of ship hulls and tanks are well defined by international rules by TSCF (1992, 1995, 1997, 1999, 2000). All these guidelines as discussed by (Paik et al. 2004; Paik and Thayamballi 2005), but they do not include the problem of MIC. As a future outlook for efficient MIC assessment in SBTs, Figure5 illustrates a scheme how MIC can be included in the international maintenance protocols of SBT inspection.

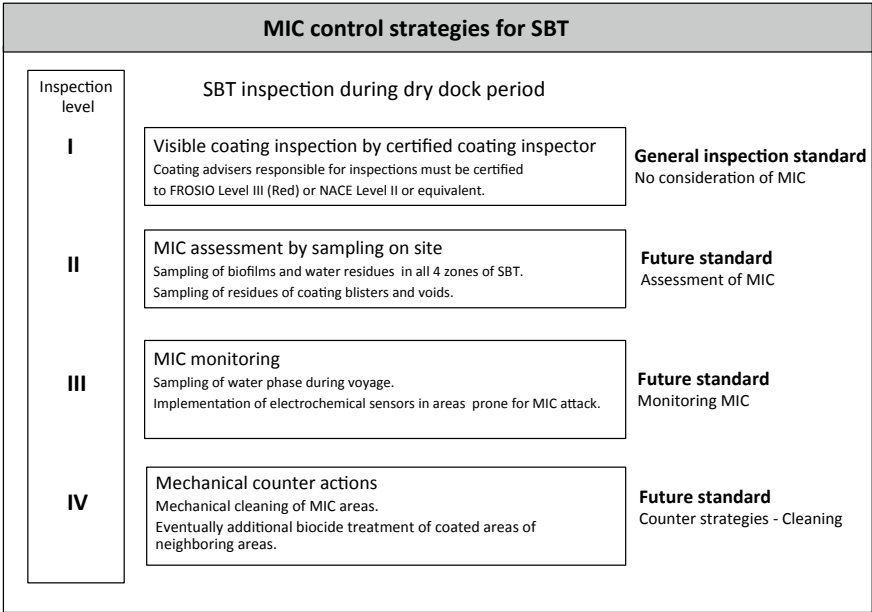


Figure 5: MIC assessment in SBT extended scheme for future inspection strategies.

An efficient MIC control strategy in ship ballast tanks should be based on four different levels which complement each other.

*Level I (International coating inspection standard)*

Maintenance programs for SBT, up to date, include only coating inspections performed inside the tanks; the inspections consider the coating quality and the amount of corrosion (TSCF 1992; TSCF 1995).

*Level II (Future standard – MIC assessment)*

Depending on the quality of the coating, sampling of bacterial communities at specific corrosion spots should be performed. Microbial rapid test kits can give first indications of bacterial activity, and additional analysis of scrapped biofilms by culture techniques in the lab will reveal the full extension of MIC in the specific tank area. The water phase should be controlled to observe changes of corrosive conditions that influence the electrochemical parameters (T, pH, oxygen); these may be used for the estimation of the occurrence of MIC.

*Level III (Future standard – Monitoring MIC)*

The third, most important step in MIC control for the future is monitoring the activity of sessile microorganisms (biofilms) on sidewalls of the tank under ballasted conditions (full tanks) to understand community structures and biocide efficiency over time. Chemical treatment of the water during voyage is one choice to lower bacterial activity inside the tank.

Another option might be ultraviolet (UV) radiation, which can be used for pre-treatment of the ballast water during intake instead of chlorination or biocide use. If biocides are used to lower bacterial activity, care has to be taken in the case of biofilms. Although all biocides are efficient in the water phase (planktonic bacteria), only a few are efficient against biofilms. This should be taken into account especially for older vessels where maintenance was poor (high amount of sediment), or less efficient pre-treatment systems for the water phase are installed. One MIC control strategy can be online monitoring by electrochemical sensors placed on high-risk spots (welding's, bottom) inside the tank. Up to now, the available ship hulls monitoring systems (Slaughter et al. 1997) do not consider ballast tanks. Currently it is difficult to differentiate between various forms of localized corrosion as many of them have a similar appearance. Therefore, electrochemical methods of MIC monitoring should be used with caution. Advanced detection methods, such as Open circuit potential (OCP) (Fonesca et al. 1996; Beech 2008), Linear Polarization Resistance (LPR) measurements (Little et al. 1988; Beech 2008), or Electrochemical noise measurements (ENM) (Iverson and Heverly 1986; Witham and Huizinga 1997; Padilla-Viveros et al. 2006) are able to give indications for biofilm formation or localized corrosion within ballast tanks, if limitations of the individual methods are anticipated.

#### *Level IV (Future strategy – Cleaning)*

If high amounts of corrosion failure can be related to bacterial activity, mechanical cleaning, e.g., with brushes of specific areas of the tank, should be performed. Additional cleaning/disinfection of surrounding areas with biocides can be one way to prevent further microbial activity. This MIC assessment and monitoring plan can be a useful approach to detect bacterial activity at local sites in a preliminary stage, leading to a decrease in maintenance costs and extensive repair programmes of local corrosion failures within SBTs.

## **5. Conclusions**

Rapid construction failure incidents of ship ballast tanks in practice have shown that fundamental understanding of the MIC processes involved becomes more and more important. Engineers do not realize the importance of the phenomenon because technical disciplines do not cover biological aspects. Another reason might be that only interdisciplinary approaches will supply enough information to understand the mechanisms for MIC. For engineers, the following points should be addressed:

- a. Structural changes which simplify cleaning strategies by reducing sediment accumulation – the source of MIC – should be considered.
- b. Perfect coating application should be aspired (no voids) to decrease the possible attachment sites of microorganisms. Biodegradation of ballast tanks coatings should be considered in the future in order to develop new strategies to overcome microbial

deterioration processes of the applied coatings. This will reduce the risk of MIC and will additionally fulfil the international coating guidelines provided by IMO.

c. Environmental parameters, such as water quality and surface structures of the SBT, have to be taken into account during dry dock inspections and during voyages to identify areas with a high MIC risk.

d. Nutrient availability, one of the growth requirements for microorganisms, has to be considered as well. Input and output of nutrients in SBTs will have a significant effect on bacterial activity, progression and, finally, MIC failures. Nutrient input/output in form of fresh ballast water in harbours or retention times of the ballast water can have a huge impact on the bacterial activity leading to changes in corrosion rates and corrosion initiation in local tank areas. Ballast water exchange should be performed outside the harbour to reduce the uptake of nutrient rich harbour water. For instance, exchange of ballast water on high sea is currently recommended to reduce introductions of invasive species (since coastal organisms are unlikely to invade open ocean areas, and vice versa), but the process is time-consuming and cannot be performed in rough sea conditions. A change of this recommendation into a standard operational method will decrease the nutrient load of the ballast water. Beside nutrient supply, sediment accumulation on the bottom of the tank, which is in general the hatchery for MIC bacteria and invasive species, will be reduced.

e. Deoxygenating the ballast water (by nitrogen stripping) is a technique that is effective in reducing invasive species and the general corrosion process on an environmentally friendly base; it is accepted by the shipping industry in terms of safety, time, and cost but it will not minimize the risk of MIC. In fact, it will enhance growth of sulphate reducing bacteria, commonly found in seawater, with the result of rapid localized corrosion attacks.

f. Ultimately, bacterial activity and diversity have a significant impact on the corrosion process. Biofilm formation and metabolic interactions are one of the key mechanisms of MIC in problematic accessible SBTs. Bacterial accumulation can be circumvented by pre-treatment of the ballast water, e.g., filtration and ozonation, to minimize the risk of MIC.

These considerations will help to design ships in more appropriate ways such that the corrosion effects enhanced by sediment residues and the bacteria therein can be decreased. There is no particular method which allows determining MIC occurrence. An evaluation of all conditions, such as abiotic and biotic conditions within ship ballast tanks, is necessary to understand the occurrence of MIC. Suitable and reliable methods for detection of MIC processes are available, but only the interdisciplinary diagnosis of all participating groups, such as engineers, ship owners, microbiologists and corrosion specialists, allows reducing life cycle costs and improving vessel safety.



More advanced maintenance programmes for all types of ships have to be developed, incorporating MIC as one of the major corrosion phenomena within these enclosed seawater environments.

## References

Aridgides, L.J., Doblin, M.A., Berke, T., Dobbs, F.C., Matson, D.O., Drake, L.A., 2004. Multiplex PCR allows simultaneous detection of pathogens in ships'ballast water. *Marine Pollution Bulletin* 48.

American Society for Testing and Materials (ASTM), A131, 2003. Standard specification for Structural Steel for Ships. ASTM International West Conshohocken.

Beech, I.B., Gaylarde, C.C., 1999. Recent advances in the study of biocorrosion – an overview *Revista de Microbiologis* 30, 177-190.

Beech, I.B., 2002. Biocorrosion: role of sulphate-reducing bacteria, in: Bitton G. (Ed.), John Wiley, New York.

Beech, I.B., Campbell, S.A., 2008. Accelerated low water corrosion of carbon steel in the presenc of a biofilm harbouring sulphate reducing and sulphur oxidizing bacteria recovered from a marine sediment. . *Electrochimica Acta* 14-21.

de Beer, D., Stoodly, P., Lewandowski, Z., 1997. Measurements of local diffusion coefficients in biofilms by microinjection and confocal microscopy. *Biotechnology Bioengineering* 53, 151-158.

Bergel, A., Feron, D., Mollica, A., 2005. Catalysis of oxygen reduction in PEM fuel cell by seawater biofilm. *Elctrochemistry Communications* 7.

Borenstein, S.W., 1994. *Microbiologically Influenced Corrosion Handbook*. Woodhead Publishing Ltd, Cambridge.

Bremer, P.J., Geesey, G.G., 1991. Laboratory-based model of microbially induced corrosion of copper. *Applied Environemntal Microbiology* 57, 1956-1962.

Bryant, R.D., Jansen, W., Bovin, J., Laishley, E.J., Costerton, J.W., 1991. Effect of hydrogenase and mixed sulfate reducing bacterial populations on the corrosion of steel. *Applied Environemntal Microbiology* 57, 2804-2809.

Cleland, J.H., 1995. Corrosion risks in ships'ballast tanks and the IMO pathogen guidlines. *Engineering Failure Analysis* 2, 79-84.

Costello, J.A., 1974. Cathodic depolarization by sulphate reducing bacteria. *South African Journal of Science* 70, 202-204.

Crabbe, J.R., Campbell, J.R., Thompson, L., Waltz, S.L., Schultz, W.W., 1994. Biodegradation of a colloidal ester-based polyurethane by soil fungi. *International Biodeterioration and Biodegradation* 33, 103-113.

Cragolino, G., Tuovinen, O.H., 1984. The role of sulphate reducing bacteria and sulphur oxidizing bacteria in the localized corrosion of iron-base alloys - a review. *International Biodeterioration and Biodegradation* 20, 9-26.

Crolet, J.L., Daumas, S., Magot, M., 1993. pH regulation by sulphate-reducing bacteria, NACE, New Orleans.

Daumas, S., Massiani, Y., Crousier, J., 1988. Microbiological battery induced by sulphate-reducing bacteria. *Corrosion Science* 28, 1042-1050.

Diaz, R.J., Rosenberg, R., 1995. Marine benthic hypoxia: a review of its ecological effects and the behavioral responses of benthic macrofauna. *Oceanography and Marine Biology Annual Review* 33.

Dinh, H.T., Kuever, J., Mußmann, M., Hassel, A.W., Stratmann, M., Widdel, F., 2004. Iron corrosion by novel anaerobic Microorganisms *Letters to Nature* 829-832.

Det Norske Veritas (DnV), 1998. Type approval programme for protective coating systems, Oslo.

Det Norske Veritas (DnV), 1999. Corrosion prevention of tanks and holds, Oslo.

Drake, L.A., Doblin, M.A., Dobbs, F.C., 2007. Potential microbial bioinvasions via ships' ballast water, sediment, and biofilm. *Marine Pollution Bulletin* 55, 333-341.

Drake, L.A., Meyer, A.E., Forsberg, R.L., Baier, R.E., Doblin, M.A., Heinemann, S., Johnson, W.P., Koch, M., Rublee, P.A., Dobbs, F.C., 2005. Potential invasion of microorganism and pathogens via "interior hull fouling": biofilms inside ballast water tanks. *Biological Invasions* 7, 969-982.

Dumas, C., Mollica, A., Basseguy, R., Etcheverry, L., Bergel, A., 2006. Marine microbial fuel cell: use of stainless steel electrodes as anode and cathode material. *Electrochimica Acta* 53. Edyvean, R.G.J., Benson, J., Thoas, C.J., Beech, I.B., Videla, H., 1998. Biological influences on hydrogen effects in steel in seawater. *Materials Performance* 37.

El-Sayed, A.H.M.M., Mohmoud, W.M., Davis, E.M., Coughlin, R.W., 1996. Biodegradation of polyurethane coatings by hydrocarbon-degrading bacteria. *International Biodeterioration and Biodegradation* 37, 69-79.

Emde, K.M.E., Smith, D.W., Facey, R., 1992. Initial investigation of microbially influenced corrosion (MIC) in a low temperature water distribution system. *Water Research* 26, 169-175.

Ferrari, G., Heyer, A., D'Souza F., Zhang, X., Bakuwel, H., Mol J.M.C., de Wit J.H.W., 2010. Susceptibility of epoxy coatings to microbial influenced degradation, Eurocorr, Moscow, Russia.

Fonesca, I.T.E., Feio, M.J., Lino, A.R., Reis, M.A., Reinha, V.L., 1998. The influence of the media on the corrosion of mild steel by *Desulfovibrio desulfuricans* bacteria: an electrochemical study. *Electrochimica Acta* 43.

Ford, T., Mitchell, R., 1990. Metal embrittlement by bacterial hydrogen—an overview. *Marine Technology Society Journal* 24, 29-35.

Fyske, E.M., Nilsen, T., Nielsen, A.D., Tryland, I., Delacroix, S., Blatny, J.M., 2012. Real time PCR and NASBA for rapid sensitive detection of *Vibrio cholera* in ballast tanks. *Marine Pollution Bulletin* 64, 200-206.

Geenen, F.M., 1991. Characterisation of Organic Coatings with Impedance Measurements. Technical University Delft.

Geesey, G.G., 1982. Microbial exopolymers: ecological and aconomic considerations. *ASM news* 48, 9-14.

Gollasch, S., Dammer, M., Lenz, J., Andres, H.G., 1998. Non-indeigenous organisms introduced via ships into German waters. ICES Cooperative Research Report, pp. 50-64.

Grieshaber, M.K., Hardewig, I., Kreutzer, U., Poertner, H.O., 1994. Physiological and metabolic responses to hypoxia in invertebrates, in: Blaustein, M.P. (Ed.), *Reviews of Physiology Biochemistry and Pharmacology* Springer, New York, pp. 43-147.

Groysmann A., 2010. Corrosion for everybody, Springer, Heidelberg.

Gu, J.D., 2003. Microbiological deterioration and degradation of synthetic polymeric materials: recent research advances. *International Biodeterioration and Biodegradation* 52, 69-91.

Gu, J.G., Gu, J.D., 2005. Methods currently used in testing microbial degradation and deterioration of a wide range of polymeric materials with various degree of degradability: a review. *Journal of Polymers and the Environment* 13, 37-42.

Gunasekaran, G., Chongdar, S., Gaonkar, S.N., Kumar, P., 2004. Influence of bacteria on film formation inhibiting corrosion. *Corrosion Science* 46, 1953-1967.

Hallegraeff, G.M., Bolch, C.J., 1992. Transport of diatom and dinoflagellate resting spores in ships' ballast water: Implications for plankton biogeography and aquaculture. *Journal of Plankton Research* 14, 1067-1084.

Hamer, J.P., Collin, T.A.M., Lucas, I.A.N., 2000. Dinoflagellate cysts in ballast tank sediments: between tank variability. *Marine Pollution Bulletin* 40, 731-733.

Hamilton, W.A., 1985. Sulphate reducing bacteria and anaerobic corrosion. *Annual Review Microbiology* 39, 195-217.

Hamilton, W.A., 1998. Sulfate reducing bacteria: Physiology determines their environmental impact. *Geomicrobiological Journal* 15, 19-28.

Hamilton, W.A., 1999. Metabolic interaction and environmental microniches: Implications for the modeling of biofilm process. *Review Microbiology* 30, 177-190.

Heyer, A., D'Souza, F., Ferrari G., Mol, J.M.C., de Wit, J.H.W., 2009. Microbiologically influenced corrosion (MIC) in a simulated ship tank model system, Eurocorr, Nice, France.

Heyer, A., D'Souza, F., Ferrari G., Mol, J.M.C., de Wit, J.H.W., 2011. EIS study of MIC in three different zones derived from ship ballast tank model system, NACE, Houston, USA.

Huang, R.T., McFarland, B.L., Hodgman, R.Z., 1997. Microbial influenced corrosion in cargo oil tanks of crude oil tankers, NACE, Houston, USA.

Ismail, K.M., Gehrig, T., Jayaraman A., Wood, T.K., Trandem, K., Arps, P.J., Earthman, J.C., 2002. Corrosion Control of Mild Steel by Aerobic Bacteria Under Continuous Flow Conditions. *Corrosion* 58, 417-423.

International Association of Classification Societies (IACS), 1993. Shipbuilding and repair quality standard. Recommendation No. 47.

International Association of Classification Societies (IACS), 1994. Bulk carriers: guidelines for surveys, assessment and repair of hull structure. Recommendation No. 76.

International Association of Classification Societies (IACS), 1998. Guidelines for acceptance, application and survey of semi-hard coatings on ballast tanks. Recommendation No. 54.

International Association of Classification Societies (IACS), 2004. "Guidelines for Coating Maintenance & Repairs for Ballast Tanks and Combined Cargo/Ballast Tanks on Oil Tankers". Recommendation 87.

International Maritime Organization (IMO), 1995. Guidelines for the selection, application and maintenance of corrosion prevention systems of dedicated seawater ballast tanks. Resolution A 798 (19).

International Maritime Organization (IMO), 1997. Guidelines for the control and management of ships' ballast water to minimize the transfer of harmful aquatic organisms and pathogens. Resolution A (868) 20.

International Maritime Organization (IMO), 2003. International convention for the Control and Management of Ships' Ballast Water and Sediment. International Conference on Ballast Water Management for Ships.

International Maritime Organization (IMO), 2006. Performance standard for Protective coatings (PSPC) London. Resolution MSC.215(82).

International Organization for Standardization (ISO) 8501-1, 2007. Preparation of steel substrates before application of paints and related products -- Visual assessment of surface cleanliness -- Part 1: Rust grades and preparation grades of uncoated steel substrates and of steel substrates after overall removal of previous coatings .

Iverson, I.P., Olson, G.J., 1983. Anaerobic corrosion by sulfate-reducing bacteria due to highly reactive volatile phosphorus compound, London.

Iverson, W.P., Heverly, L.F., 1986. Electrochemical Noise as an indicator of anaerobic corrosion, in: Moran, G.C., Labine, P. (Eds.), Corrosion Monitoring in Industrial plants using nondestructive testing and electrochemical methods ASTM STP 908. American society for Testing and Materials, pp. 459-471.

Jayaraman, A., Earthma, J.C., Wood, T.K., 1997. Corrosion inhibition by aerobic biofilms on SAE 1018 steel. Applied Environmental Microbiology 47, 62-68.

Jones, D.A., 1995. Principles and Prevention of Corrosion 2nd Edition, Prentice-Hall, New Jersey.

Jones, D.A., Amy, P.S., 2002. A thermodynamic interpretation of microbiologically influenced corrosion. Corrosion 58, 638-645.

King, R.A., Miller, J.D.A., Wakerley, D.S., 1973. Corrosion of mild steel in cultures of sulphate reducing bacteria: effect of changing the soluble iron concentration during growth. British Corrosion Journal, 89-93.

King, R.A., Wakerley, D.S., 1973. Corrosion of mild steel by ferrous sulphide. British Corrosion Journal 8, 41-45.

Kuenen, J.G., Jørgensen, B.B., Revsbech, N.P., 1986. Oxygen microprofiles of trickling filter biofilms. Water Research 20, 1589-1598.

Lee, W., Lewandowski, Z., Nielsen, P.H., Hamilton, W.A., 1995. Role of sulfate-reducing bacteria in corrosion of mild steel: A review. Biofouling 8, 165-194.

Little, B., Lee, J.S., 2007. Microbiologically Influenced Corrosion, in: Winston, R. (Ed.), Microbiologically Influenced Corrosion. Wiley-Interscience Wiley & Sons, Hoboken.

Little, B., Wagner, P., Duquette, D., 1988. Microbiologically-induced increase in corrosion current density of stainless steel under cathodic protection. Corrosion 44, 270-274.

Little, B., Wagner, P., Mansfeld, F., 1992. An overview of microbiologically influenced corrosion. Electrochimica Acta 37.

Matsuda, M., Kobayashi, S., Miyuki, H., Yoshida, S., 1999. An Anticorrosion Method for Ballast Tanks Using Nitrogen Gas (Ship and Ocean Foundation Technical Report).

McNamara, C., Perry, T.D., Leard, R., Bearce, K., Dante, J., Mitchell, R., 2005. Corrosion of Aluminum Alloy 2024 by microorganisms isolated from aircraft fuel tanks. *Biofouling* 21, 257-265.

Meyer, A.E., Baier, R., Hulsmann, N., Galil, B., Friedmann, D., Forsbergen, R., 2000. Risk assessment, prediction and limitation of transport invaders in biofilms, in: American society of Limnology and Oceanography, Aquatic Sciences Meeting, Copenhagen, Denmark.

Munger, C.G., 1984. *Corrosion Prevention by Protective Coatings*, 2nd Edition ed, Houston.

Myers, C., Nealson, K.H., 1988. Bacterial manganese reduction and growth with manganese oxide as the sole electron acceptor. *Science* 240, 1319-1321.

Nakajima-Kambe, T., Onuma, F., Akutsu, Y., Nakahara, T., 1995a. Determination of the polyester polyurethane breakdown products and distribution of the polyurethane degrading enzyme of *Comamonas acidovorans* Strain TB-35. *Journal of Fermentation and Bioengineering* 83, 456-460.

Nakajima-Kambe, T., Onuma, F., Kimpara, N., Nakahara, T., 1995b. Isolation and characterization of a bacterium which utilizes polyester polyurethane as a sole carbon and energy source. *FEMS Microbiology Letters* 129, 39-42.

Niimi, A.J., 2004. Role of container vessels in the introduction of exotic species. *Marine Pollution Bulletin* 49, 778-782.

Stemming the Tide: Introduction of Nonindigenous Species by Ship Ballast Water, 1996. National Academic Press, Washington D.C.

Padilla-Viveros, A., Garcia-Ochoa, E., Alazard, D., 2006. Comparative electrochemical noise study of the corrosion process of carbon steel by sulfate-reducing bacterium *Desulfovibrio alaskensis* under nutritionally rich and oligotrophic culture conditions. *Electrochimica Acta* 51, 3841-3847.

Paik, J.K., 2004. Corrosion Analysis of Seawater Ballast Tank Structures. *International Journal of Maritime Engineering* 146, 1-12.

Paik, J.K., Frieze, P.A., 2001. Ship structural safety and reliability. *Progress in Structural Engineering and Materials* 3, 198-210.

Paik, J.K., Thayamballi, A.K., 2002. Ultimate Strength of Ageing Ships. *Journal Engineering for the Maritime Environment* 216, 57-77.

Paik, J.K., Thayamballi, A.K., 2004. A Time-dependent Corrosion Wastage Model for Seawater Ballast Tank Structures of Ships. *Corrosion Science* 46, 471-486.

Paik, J.K., Thayamballi, A.K., 2005. Reliability assessment of ships, in: Nikolaidis, E., Ghiocel, D.M., Singhal, S. (Eds.), *Engineering Design Reliability Handbook*. CRC Press, New York.

Paik, K.P., Kim, S.K., Lee, S.K., 1998. Probabilistic corrosion rate estimation model for longitudinal strength members of bulk carriers. *Ocean Engineer* 25, 837-860.

Parente, J., 1996. Commercial Ship Design and Fabrication for Corrosion Control SR-1377, MR&S Report No. 5087.10N-1.

Peters, J.H., 1993. The Maritime Transport Crisis Discussion Paper 220, Development, The international Bank for Reconstruction and Development, World Bank Discussion Washington D.C.

Pickard, G.L., Emery, W.J., 1982. Descriptive Physical Oceanography: An Introduction, Pergamon Press, Oxford (fourth enlarged edition.), Wiley, New York.

Pope, D.H., Duquette, D.J., Johannes, A.H., Wayner, P.C., 1984. Microbially influenced corrosion of industrial alloys. *Materials Performance* 23, 14-18.

Rauch, M.E., Graef, H.W., Rozenzhak, S.M., Jones, S.E., Bleckmann, C.A., Kruger, R.L., Naik, R.R., 2006. Characterization of microbial contamination in United States Air Force aviation fuel tanks. *Journal of Industrial Microbiology and Biotechnology* 33, 29-36.

Salvarezza, R.C., Videla, H.A., 1986. Electrochemical behaviour of aluminium in *Cladosporium resinae* cultures, in: Barry, S. (Ed.), *Biodeterioration*. Elsevier, London, pp. 212-217.

Schaschl, E., 1980. Elemental sulphur as a corrodent in deaerated, neutral aqueous solutions. *Materials Performance* 7, 9-12.

Slaughter, S.B., Cheung, M.C., Sucharski, D., Cowper, B., 1997. State of the art in hull monitoring systems. Ship Structure Committee, Washington D.C.

Soracco, R.J., Pope, D.H., Eggers, J.M., Effinger, T.N., 1988. Microbiologically influenced corrosion investigations in electric power generating stations, NACE, Houston.

Stewart, P.S., 1998. A review of experimental measurements of effective diffusive permeabilities and effective diffusion coefficients in biofilms. *Biotechnology Bioengineering* 59, 261-272.

Stewart, P.S., 2003. Diffusion in biofilms. *Journal of Bacteriology* 185, 1485-1491.

Stoodly, P., de Beer, D., Lewandowski, Z., 1997. Liquid flow in biofilm systems. *Applied Environmental Microbiology* 60, 2711-2716.

Suzuki, S., Muraoka, R., Obinata, T., Endo, E., Horita, T., Omata, K., 2004. Steel products for shipbuilding, JFE Technical Report

Tamburri, M.N., Little, B.J., Ruiz, G.M., Lee, J.S., McNulty, P.D., 2003. Evaluations of Venturi Oxygen Stripping TM as a ballast water treatment to prevent aquatic invasions and ship corrosion, in: Organization, I.M. (Ed.), *International Ballast Water Treatment R&D Symposium*, London.

Tamburri, M.N., Ruiz, G.M., 2005. Evaluation of a ballast water treatment to stop invasive species and tank corrosion, SNAME Annual Meeting. The Society of Naval Architects and Marine Engineers, Houston.

Tamburri, M.N., Wasson, K., Matsuda, M., 2002. Ballast water deoxygenation can prevent aquatic introductions while reducing ship corrosion. *Biological Conversation* 103.

Tatnall, R.E., 1981. Fundamentals of bacteria induced corrosion. *Materials Performance* 20, 32-38.

Tanker Structure Cooperative Forum (TSCF), 1992. Condition evaluation and maintenance of tanker structure, TSCF work group report, London.

Tanker Structure Cooperative Forum (TSCF), 1995. Guidance manual for the inspection and maintenance of double hull tanker structure, London.

Tanker Structure Cooperative Forum (TSCF), 1997. Guidance manual for tanker structures. TSCF, London.

Tanker Structure Cooperative Forum (TSCF), 1999. Condition evaluation and maintenance of tanker structures.

Tanker Structure Cooperative Forum (TSCF), 2000. Guidelines for ballast tank coating system and edge preparation. TSCF, London.

von Wolzogen Kühr, C.A.H., van der Vlugt, L.S., 1934. De grafiteering van Gietijzer als electrobiochemisch Proces in anaerobe Gronden. *Water (den Haag)* 18, 147-151.

Videla, H.A., 1996. Corrosion inhibition by bacteria, *Manual of Biocorrosion*. CRC Press, Boca Raton, pp. 121-136.

Walch, M., Ford, T.E., Mitchell, R., 1989. Influence of hydrogen-producing bacteria on hydrogen uptake by steel. *Corrosion* 45, 705-709.

Wang, J.S., 1996. Hydrogen induced embrittlement and the effect of the mobility of hydrogen atoms, in: Thompson, A.W., Moody, N.R. (Eds.), *Hydrogen Effects in Materials*. The Minerals, Metals and Materials Society, Warrendale, pp. 61-75.

Weber, P.F. 1984. "Structural Surveys of Oil Tankers". *Transactions IME*

Westing van, E.P.M., 1992. Determination of coating performance with impedance measurements. Technical University Delft.

Whitham, T., Huizinga, S., 1997. Aspects of Microbiolocilly Induced Corrosion, in: *Shell research and Technology Thormton*, pp. 89-102.



Wicks, Z.W., Jones, F.N., Pappas, S.P., 1999. *Organic Coatings: Science and Technology* 2nd ed. Wiley Interscience, New York.

Wimpenny, J.W.T., Colasanti, R., 1997. A more unifying hypothesis for biofilm structures – a reply. *FEMS Microbiology Ecology* 24, 185-186.

Yeber, D.M., Kill, S., Dam-Johanson, K., 2004. Review Antifouling technology – past, present and future steps towards efficient and environmentally friendly antifouling coatings. *Progress in Organic Coatings* 50, 75-104.

Zhang, X.Q., Bishop, P.L., Kupferle, M.J., 1998. Measurement of polysaccharides and proteins in biofilm extracellular polymers. *Water Science Technology* 37, 345-348.



## Chapter 2

### ***2.1 Molecular Microbiology Methods applied on ship ballast tank samples***

#### **Abstract**

Microbiologically influenced corrosion (MIC) of steel is a serious problem in the marine environment including offshore and shipping industries. The uses of molecular techniques and electrochemical techniques for evaluating microbial corrosion effects have continued to gain importance. This chapter summarizes a large-scale approach of a simultaneous direct investigation of corrosion and microbial community within a practical ship ballast tank (SBT) environment. The corrosion behaviour of ASTM A131 steel, grade EH36 exposed to natural seawater was investigated at two different height levels of the SBT - sediment and immersion zone. Biofilm samples were scraped from exposed corrosion coupons and subjected to DGGE of PCR-amplified 16S rRNA genes and sequence analysis to characterize the microbial community on the sidewall of ship ballast tanks as well as the water phase. In parallel, corrosion was monitored by open circuit potential (OCP) and linear polarization resistance (LPR) measurements, indicating a difference in corrosion behaviour for sediment and immersion zone related to the variation in bacterial community changes. Detailed information was gained on microbial community composition and the corresponding corrosiveness within ship ballast tanks. This chapter demonstrates the problem of attached biofilms in the corrosion of ship ballast tanks, which is characterized by a combination of electrochemical and molecular tools.

## 1. Introduction

### *MIC in the Ship industry*

Ship Ballast Tanks (SBTs) are essential parts of the structure of vessels. The large and complex structure of a ballast tank combined with rough operational conditions, such as wet/dry phases during loading/unloading of the ballast tanks and also extreme corrosive environment makes them one of the highest maintenance prone areas for ship owners. Corroded steel structures on a vessel decrease seaworthiness, therefore extensive measures are taken to prevent corrosion and repair. The cost to prevent, maintain, and repair corrosion on individual vessels can run into the millions of dollars (e.g., \$5.5 million to replace 1400 tons of ballast tank steel (Marine Engineering Review, 1991). The cost to paint ballast tanks is typically at least \$5 to \$10 per square meter with the cost to repair corroded areas at approximately \$500 per square meter (Fairply, 1993). With large cargo vessels and oil tankers having hundreds of thousands of square feet of ballast tank surface area, preventing and treating corrosion is extremely costly. Moreover, measures that are engaged to control invasive species through ship ballast water are known to indirectly impact the corrosion protection. For example, both chlorination (McCracken, 2001) and ozonation (Andersen, 2001) of seawater sterilization methods are believed to intensify corrosion of steel. The most corrosive operating condition is one in which carbon steel is exposed to alternating aerobic/anaerobic conditions (Hardy and Bown, 1984; Lee et al., 1993). This condition prevails in the ship ballast tanks where the aerobic and anaerobic microorganism results in unpredictable pitting type of corrosion. The uptake of organisms in association with wet or dry ballast is well known and controlled for human health requirements (Carlton, 1985, 1996; Ruiz et al., 2000). Almost all tanks used for holding ballast water accumulate sediments at the bottom of the tanks and the amount of sediment varies according to the ports vessels visit. Accumulations of sediments can become sufficient to support a bacterial community (Gollasch, 2002). To minimize the risk of spreading aquatic nuisance species at the coast, the International Maritime Organization (IMO) developed a convention on ballast water management (BWM, 2005). Existing methods beside chemical treatment include the exchange of coastal ballast water for open oceanic water while in transit or chemical and physical treatment by biocides and ozone. This ballast water exchange (BWE) may act to reduce the likelihood of species transport in some instances, but these activities may not dislodge any sediment that has accumulated at the bottom of the ballast tank along with bacterial community in attached biofilms. Corrosion resulting from the activities of naturally occurring microaerophilic, facultative or obligate anaerobic bacteria, acid-producing bacteria (APB) and sulphate reducing bacteria (SRB) growing under oxic/anoxic conditions and produce corrosive metabolic by-products are defined as biocorrosion or microbiologically influenced corrosion (MIC) (Borenstein, 1994; Flemming and Schaule, 1996).

A thorough understanding of the microbial ecology and electrochemical environments where microbial corrosion occurs is necessary to implement preventive measures or appropriate controls to improve structural integrity. The use of traditional culture methods (involving liquid culturing) is inadequate to comprehensively assess the composition of microbial communities and their interactions, since the great majority of microorganisms in nature occur as biofilms and are yet uncultivated (Amann et al., 1995). In the last decades, molecular tools have been developed to overcome the limitations imposed by traditional cultivation techniques to study bacterial diversity in corrosive biofilms that form in diverse environments (Stahl et al., 1988; Amann et al., 1995; Schäfer and Muyzer et al. 2001; Marty et al. 2012). The technique involves amplification of 16S rRNA gene sequences by polymerase chain reaction (PCR) amplification of the extracted and purified nucleic acids. The PCR products can be evaluated using community-fingerprinting techniques such as denaturing gradient gel electrophoresis (DGGE). Each DGGE band is representative of a specific bacterial population and the number of distinctive bands is indicative of microbial diversity. For example, the diversity of the microbial populations of biofilms and water phase in an enclosed marine environments was examined by DGGE analysis of PCR-amplified 16S rRNA gene fragments in order to gain data on corrosiveness and biodiversity in this specific environment (Schäfer and Muyzer, 2001).

However, detailed information regarding the microbial corrosion of SBTs exposed to seawater is practically non-existent. The current work is a large-scale approach of a direct investigation of microbial community in the ship ballast tank and also their corrosiveness simultaneously. The approach to determine the corrosiveness in the ship ballast tanks includes monitoring the electrochemical activity of carbon steel exposed to seawater by measuring the corrosion potential by OCP (Fonesca, 1998; Beech and Campbell, 2008) and the corrosion rate by LPR (Little et al., 2007; Beech and Campbell, 2008).

## **2. Case**

### ***2.1 Electrochemistry and MIC***

MIC monitoring techniques based on electrochemistry have been introduced over the years in the laboratory (Scott et al., 1988; Dexter et al., 1991; Videla, 1996; Schmitt, 1997) and also in technical applications such as cooling water, heat exchangers, storage tanks and piping systems (ASTM G96-90, 2008; Groysman, 2008). The monitoring technique that has to be chosen for each case depends on technical considerations and requirements such as control of biofilm formation, hygienic standards or corrosion control in a system exposed to bacteria e.g. cooling water systems. Broad ranges of online monitoring devices are available for corrosion such as, LPR, zero resistance ammetry, potentiodynamic polarization, electrochemical impedance spectroscopy, electrochemical noise analysis and deposition accumulation monitoring.

Under perfect conditions an online monitoring tool should detect biofilm formation under real time conditions and measure the actual corrosion rate with simple data analysis without any disturbance to biofilm and steel structure.

## 2.2 Electrochemical techniques

Two electrochemical techniques that are applied in this study, namely OCP and LPR, are discussed briefly based on their positive aspects and drawbacks in relation to MIC monitoring.

*Open circuit potential (OCP)* is used as a qualitative characteristic of the corrosion process on the metal surface. The corrosion potential is the electric potential of a metal established in an electrolyte, when no net electric current flows through the material. This means that the current due to the anodic (oxidation, e.g. dissolution of metal) reactions are balanced with the cathodic (reduction, e.g. of oxygen) reactions. The corrosion potential of a corroding metal is the difference between the metal immersed in the environment and a reference electrode (e.g. calomel electrode, silver/silver chloride or copper/copper sulphate electrodes). Normally, during this measurement no external potential is applied. This method has the lowest impact on microbial activity and settling properties (Hilbert, 2000; Javaherdashti, 2008). The general trend among electrochemical techniques in the field of MIC seems to be that OCP measurements are considered to be one of the safest methods in recognizing and monitoring MIC because it does not impose voltages upon microbes (Dexter, 1995; Olesen et al., 2000). Moreover, OCP changes provide important qualitative information about the on-going corrosion process and also environmental conditions.

*Linear polarization resistance (LPR)* is the most common technique for monitoring corrosion in corrosion science (ASTM, G96-90) and MIC (Beech and Campbell, 2005). LPR is considered a non-destructive method and can be conducted on probes (carbon steel coupons) in a conductive media such as seawater. Probes designed for LPR consists of 2 or 3 electrodes: a working electrode, an auxiliary electrode and optionally a reference electrode. The working electrode is polarized by imposing a potential difference between the working electrode and the reference electrode, causing a current to flow between the auxiliary electrode and the working electrode in fundamental terms, a small voltage (or polarization potential) is applied to an electrode in solution. The corrosion reactions developing on the working electrode, which occur independently from polarization, can be determined by measuring the current, gaining the corrosion rate.

The method is best suited for use whenever there are substantial corrosion rate changes may occur (ASTM G96-90, 2008). Table 1 gives an overview on the positive and negative aspects of the discussed electrochemical techniques and their relation to MIC.

Table 1 Pros and cons of electrochemical methods applied to MIC

	Pros	Cons	MIC
OCP	Simple Fast	No corrosion rate, only qualitative  No anodic/cathodic process detection No type of corrosion (pitting, crevice)	Study film formation (Tuovinen, 1986)  Study SRB activity (Fonseca; Keresztes, 1998)
LPR	On-line Real time	No localized corrosion Scaling increase resistance (Biofilm & corrosion products)  Deposits on the probe  Redox reactions contribution (caused by microorganisms)	Bridging and fouling effects (ASTM G96-90)  Adsorptive processes (sulphide films) (Dexter, 1995) Masking steel by ferrous sulphide film (wrong data interpretation, leading to high corrosion rates (Thompson, 1994)

To study the microbial corrosion processes the ballast tank is divided into different zones with respect to specific corrosion processes. These zones were related to the waterfront of well-known Accelerated Low Water Corrosion (ALWC) process on harbour pilings, as discussed by (Beech and Campbell, 2008). The experimental ballast tank set-up was compared with the immersion zone and sediment zone of the ALWC. The following paragraph summarize the experimental set-up conducted in a test ballast tank originally designed for evaluation and certification of ballast water treatment systems (such as ozonation or chlorination) on the north coast of the Netherlands.

### 3. Experimental set-up

#### 3.1 Test facility (operational conditions)

An international test facility for the certification of and research on ballast water treatment systems at the Royal Netherlands Institute for Sea Research (Royal NIOZ) was used in this study to assess the bacterial dynamics and corrosion in the ballast tank environment. A coated concrete tank (epoxy ballast tank coating) with the capacity of 100 m<sup>3</sup> volume was used to simulate the ballast water tank of a ship. The test facility at the dockside with a typical ballast water pump (capacity of ca. 250 m<sup>3</sup>) provided the North Sea water directly from the harbour. The tank was filled in the beginning of the experiment and remained undisturbed over the experimental time period of 14 weeks.

From the microbial corrosion point of view and the different processes and mechanisms that are involved in MIC, ballast tanks can be divided into four different zones (Heyer et al., 2009).

The proposed model in Figure 1a was supported by experimental work of the authors, who found increasing corrosion rates with decreasing oxygen concentrations from top to bottom in SBTs (Heyer et al. 2011). Interpretation and modelling of corrosion within SBTs is nowadays based on practical weight loss measurements gained in field studies (Tamburri et al. 2002, 2003, 2005; Suzuki et al. 2004), or corrosion depth measurements by ultrasonic instrumentation (Paik and Thayambali 2001; 2002; Paik et al. 2004). No model, however, has integrated zones and oxygen concentrations so far. Based on this knowledge, a new model is proposed by the author, linking different SBT zones, corrosion rates and oxygen concentrations. (Figure 1a illustrates the combination of the four zones with the corresponding corrosion rates (filled triangle), which have been measured during weight loss experiments of field studies within ship tanks (Tamburri et al., 2002; 2003, 2005; Suzuki et al., 2004). Figure 1b represents the experimental set-up where corrosion coupons and electrochemical OCP and LPR sensors were placed at two different height levels of the tank corresponding to sediment and immersion zone.

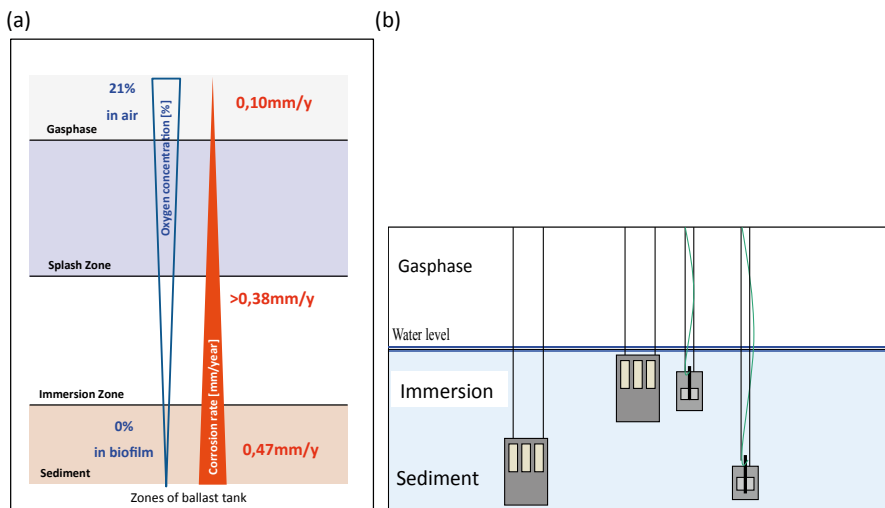


Fig. 1 Schematic figures: (a) corresponding environmental conditions e.g. (corrosion rate/ oxygen concentration); (b) ballast tank

### 3.2 Test coupon preparation

Carbon steel coupons of ASTM A131 Steel, grade EH36 were used to monitor bacterial attachment. This particular low carbon steel was chosen as it is used in ship construction, typically in ship ballast tanks. The rectangular coupons with a dimension of (30 x 20 x 1) mm were fixed on epoxy plates and immersed in the ballast tank at two different height levels, with a total exposed area of 6 cm<sup>2</sup>. The steel surface was uncoated to simulate uncoated bare ship steel.



### 3.3 Biofilm sampling

The biofilms were collected from immersion zone and sediment zone of the ballast tank. Sample coupons were immersed and taken out at fixed sampling periods of 4 and 14 weeks. In parallel, 1 liter sea water was sampled and immediately filtered through a sterile 0.2  $\mu\text{m}$  filter to concentrate the planktonic biomass. Sediment water was taken by bypass on the bottom of the tank immersion zone water could be taken by sampling bottle. The corroded coupons and filters were transferred into a sterile 50ml falcon tubes in an icebox and transferred to the laboratory. The coupons and filters were stored at - 80°C until DNA analysis.

### 3.4 DNA extraction, PCR amplification and DGGE

The frozen biofilms including corrosion products were scraped off from the coupons. The material was grinded with a pestle in a mortar filled with liquid nitrogen to prevent sample thawing. 0.1mg of sample was transferred to a cryo tube and kept frozen until DNA extraction. For seawater biomass filters, the filter fibers were cut with a sterile blade and scissors before being introduced in a PowerSoil™ DNA isolation Kit (without beads) preliminary transferred in a sterile 50 ml reaction tube. The solution with the cut fibers was subsequently vortexed for 1 minute and centrifuged at 10.000 g for 10 minutes. The liquid fraction obtained was transferred back to the PowerSoil Tube with beads. Genomic DNA from both grinded corrosion deposits and seawater was extracted using the PowerSoil™ DNA isolation Kit as described by Marty et al. (2012). 16S rRNA genes were amplified and DGGE analysis was performed as described by Schäfer and Muyzer (2001). Bands were excised from the denaturing gel and stored for 2 days at 4 °C in 40  $\mu\text{l}$  TRIS-HCl buffer. An aliquot of 0.5  $\mu\text{l}$  was used for re-amplification. A commercial company sequenced purified products.

### 3.5 Phylogenetic analysis (16SrDNA sequence)

The rDNA sequences were checked manually using the software program CodoncodeAligner (CodonCode Corporation, LI-COR Inc). The corrected sequences were compared to sequences stored in GenBank database using the MegaBLAST algorithm and the highest score sequence affiliated to a known bacterial relative was selected. Subsequently, the sequences were aligned to sequences in the SILVA SSU database Ref NR 108 and a phylogenetic tree was constructed using the software program ARB (Ludwig et al., 2004). The DGGE profiles and band intensities were normalized using the GelComparII v5.0 software. The percentages of band intensities per profile were determined by the relative surface value, correcting manually the densitograms whenever necessary. The similarities between the DGGE profiles were determined using the Pearson correlation index.

### 3.6 Electrochemical corrosion measurements

All electrochemical measurements were performed using a portable potentiostat with an USB powered device to avoid any external noise disturbance and controlled by IVIUM software version 1.705. Linear Polarization Resistance (LPR) data was modelled with Z<sub>view</sub> software version 3.0. ASTM A131 working electrodes were used in combination with water immiscible silver/silver chloride electrode. A platinum mesh electrode was implemented as a counter electrode. The electrode configuration was custom made and was equipped with duplicate working electrodes of 1 cm<sup>2</sup> to ensure reliable data acquisition.

### 3.7 Pit characterization using Microscopy

Initially working electrodes were stripped of corrosion products by adding Clarke acid cleaning solution (1L 36% (v/v) HCl, 20 g Sb<sub>2</sub>O<sub>3</sub> and 50 g SnCl<sub>2</sub>) for 10-15 sec. The cleaned exposed sample surface was finally rinsed with distilled water, cleaned in absolute ethanol, and dried under a flow of nitrogen gas. The surfaces were later examined under an optical microscope (Olympus X51) with 20x magnification. Pit depth was measured by adjusting the focus point to the bottom of the pit and the surface layer, 10 individual pits were measured averaged from 3 coupons. Pitting factor was determined at the deepest metal penetration divided by average metal penetration according to G46-94 (ASTM, 1994). A pitting factor close to 1 represents uniform corrosion and increasing numbers represents higher degree of pitting.

## 4. Results

### 4.1 PCR-DGGE analysis

The experimental set-up had good replicates giving 80% minimum similar community structures proven by Pearsons correlation index (data not shown). The bacterial diversity of the samples was evaluated by DGGE analysis of 16S rRNA gene amplicons (Figure 2). Each band represents a specific bacterial population and the number of distinctive bands in each lane indicates the microbial diversity in the sample. Dominant bands were excised from the gel by visual determination under UV light and sequenced. Only those bands that gave the clean sequences (these are numbered bands) were used for phylogenetic analysis.

Several bands shared similarity between the samples i.e. the biofilms from different zones and also to that of the water phase. For example, similarities were found between band 1 & 9 (i.e. biofilm from immersion zone) and band 23 & 20 (biofilm from sediment zone). Additionally, bands 34, 36, 37, 45, 46, 47, 53, and 54 were unique for the planktonic community and also Band 2, 4–24 that were associated to the biofilm community showing a high diversity in the mid molecular weight sector of the gel.

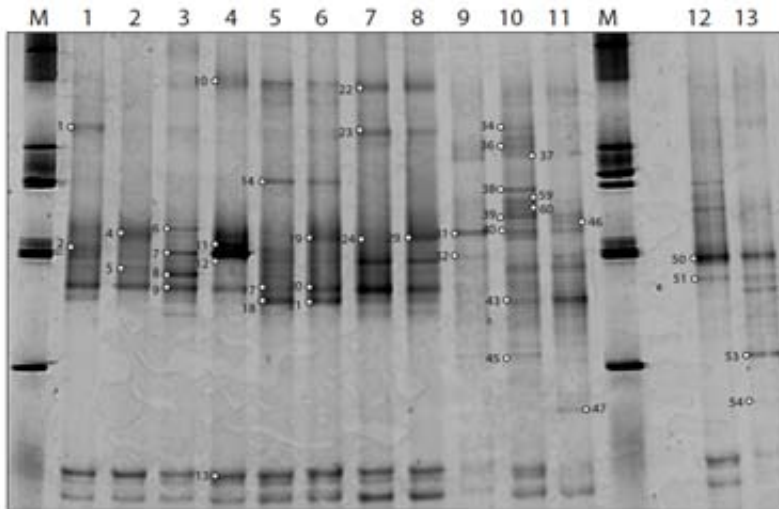


Figure 2. DGGE gel pattern used for verification of species from the ballast tank samples. Biofilm immersion zone (1,2 → 4 weeks; 3,4 → 14 weeks), Biofilm sediment zone (5,6 → 4 weeks; 7,8 → 14 weeks) Water phase (9 → start), water phase bottom (10 → 4 weeks; 11 → 14 weeks; water phase immersion (12 → 4 weeks; 13 → 14 weeks). \*M representing marker bands. Marked bands were excised and sequenced. Replicate samples show no significant variation supporting the reproducibility of the data.

#### 4.2 Phylogenetic analysis

The sequences retrieved from the denaturing gradient gel were affiliated to five major subclasses of the *Proteobacteria* i.e.  $\alpha$ ,  $\beta$ ,  $\gamma$ ,  $\delta$  and  $\zeta$ . The other class of bacteria that were abundant includes the *Bacteroidetes*, the *Gemmatimonadetes* and the *Actinobacteria* (data not shown). The bacteria analysis were carried out for the biofilm samples from the immersion zone and sediment zone and also to that of the water phase in the ballast tank. The relative abundance is given in percentage and is based on the intensity measurements. Figure 3 and 4 are the relative abundance of bacteria in the biofilm and water phase samples collected from the immersion and sediment zone, respectively. The summarized community data indicate clear differences between water phase and biofilms as well as immersion and sediment samples.

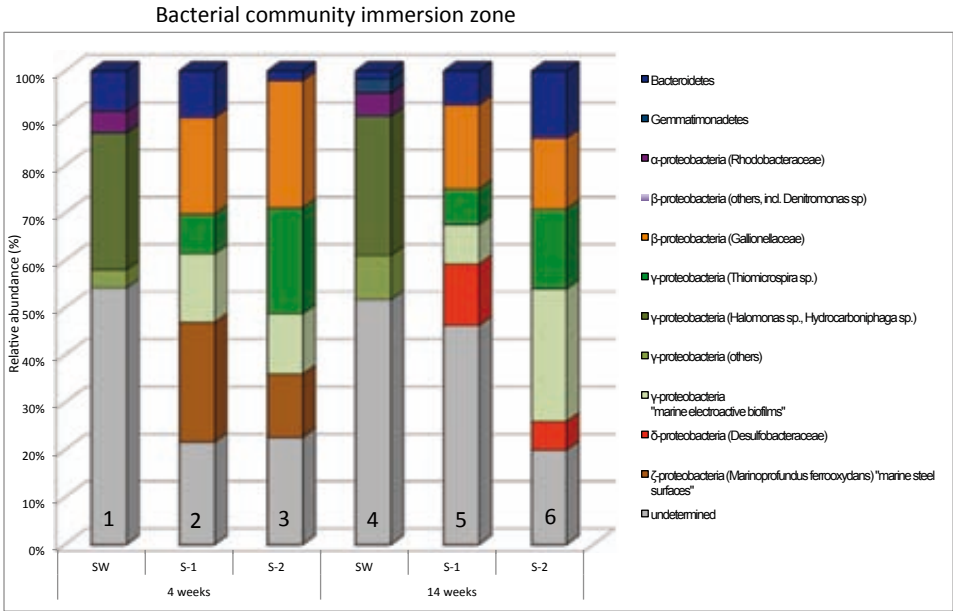


Figure 3. Relative bacterial abundance in percent over experimental time in weeks. Water phase (1 → 4 weeks; 4 → 14 weeks); Biofilm immersion zone (2,3 → 4 weeks; 5,6 → 14 weeks).

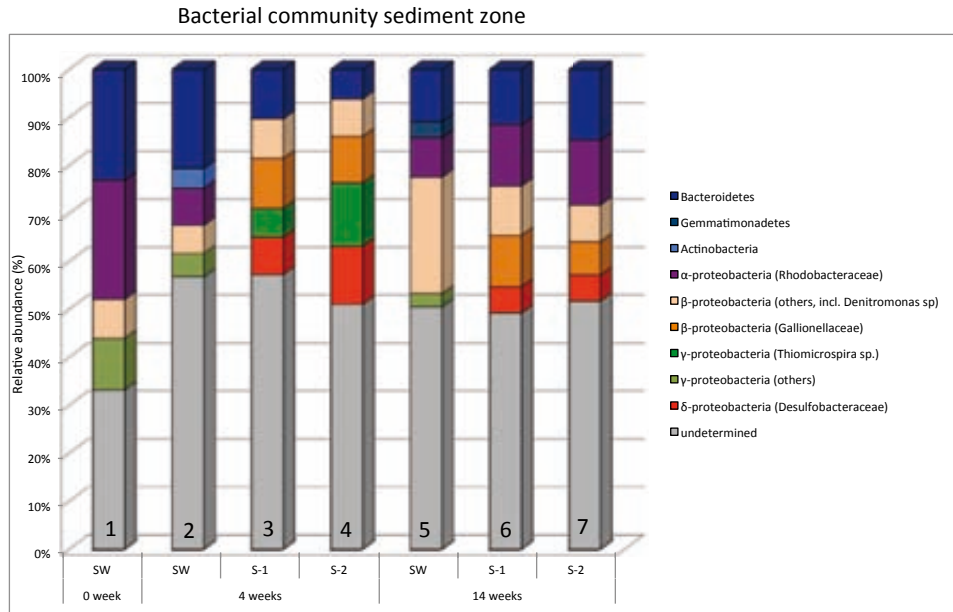


Figure 4. Relative bacterial abundance in percent over experimental time in weeks. Water phase (1 → start; 2 → 4 weeks; 5 → 14 weeks); Biofilm sediment zone (3,4 → 4 weeks; 6,7 → 14 weeks).

*(i) Biofilm communities in the immersion zone*

Within the first four weeks Bacteroidetes,  $\beta$ -Proteobacteria (*Denitromonas* and *Gallionella* sp.),  $\gamma$ -Proteobacteria (*Thiomicrospira* sp.), were abundant in the biofilm community. During the first four weeks of the experiment no SRBs  $\delta$ -Proteobacteria (*Desulfobacteraceae*) were found within the biofilm of the immersion zone, whereas  $\zeta$ -Proteobacteria such as *Mariprofundus ferrooxydans*, and  $\beta$ -Proteobacteria such as *Gallionella* sp. are abundant in the biofilm community. Bacteroidetes and Proteobacteria form electroactive biofilms.

*Mariprofundus* is a neutrophilic Fe-oxidizing bacterium (IOB), which plays an important role in Fe deposit formation (Juniper et al. 1988; Kato et al. 2009) and *Gallionella* sp. deposit ferric oxide on the cell surface under microaerophilic conditions. It can be deduced for the immersion zone that the oxygen concentration was still high enough to avoid SRB growth within the biofilm community up to four weeks. After 14 weeks SRB were developed in the anaerobic niche of the biofilm (underneath of oxygen consuming bacteria) and these mixed community of SRB and IOB increased the electroactive activity community i.e.  $\gamma$ -Proteobacteria as supported by DGGE analysis.

*(ii) Biofilm communities sediment zone*

The only difference towards the immersion zone is the abundance of *Denitromonas* species as a result of the presence of SRB from the beginning of the experiment within the sediment zone. *Denitromonas* utilize the metabolic compounds of the SRBs (sulfide or thiosulfate) as an electron acceptor. *Gallionella*, *Thiomicrospira* and *Desulfobacteriaceae* form a closed metabolic loop (as discussed before) for the immersion zone. This community diversity illustrates that microbial activity is a closed loop of metabolic reactions in a specific microenvironment driven by oxygen concentration and nutrient availability in the environment.

4.3 Electrochemical data

Open circuit potential measurements - Fig. 5 details the OCP value changes for the carbon steel exposed to seawater in practical ballast tanks at different heights i.e., at sediment and immersion zone over the period of 14 weeks. Each data point is an average of three replicate measurements.

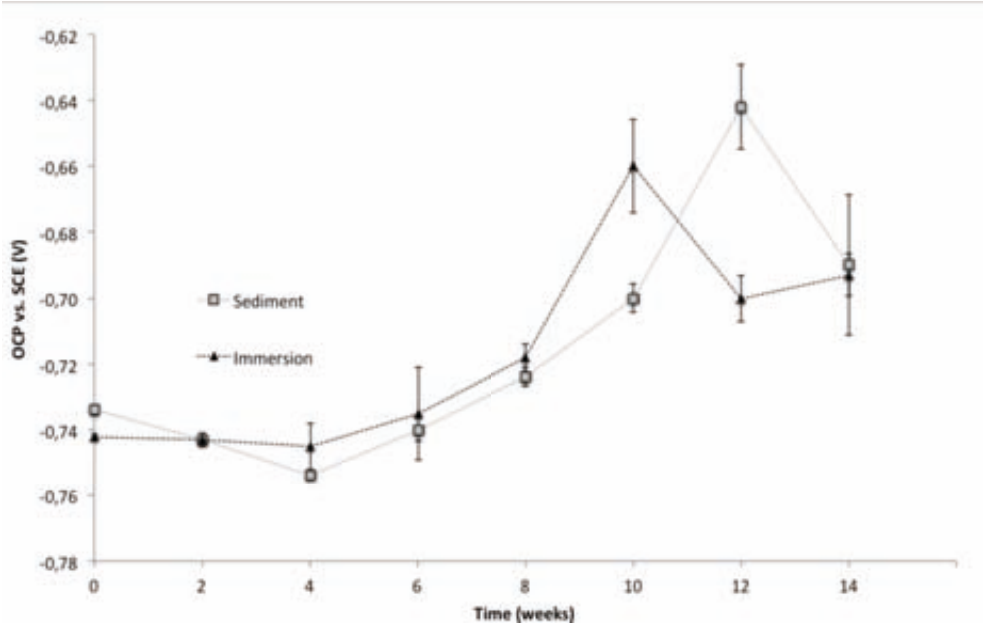


Figure 5. OCP values vs. SCE electrode (triangle: immersion zone 2; square (dashed line) sediment zone).

At the start of the experiment until the first three weeks, the OCP values remained constant for both the zones. Subsequently, the OCP showed a gradual increase and reached maximum value in 10 weeks in the case of immersion zone and 12 weeks for the sediment zone. After these maximum peaks the OCP values decreased slightly down to ~ -0.70 for both zones until the end of the experiment but not as low as in the beginning. These potential data are in line with findings by Beech and Campbell (2008) who reported potential values between -0.71V and -0.68V for steel electrodes covered with a biofilm after 8 weeks.

4.4 LPR measurements

Table 2 summarize corrosion rates of the carbon steel immersed in the ballast tank near the surface and at the sediment zone over period of 14 weeks. Corrosion rates were monitored by LPR measurements and are given in mm/y for three experimental times (0 weeks, 8 weeks, 14 weeks).

Table 2. General corrosion rates of carbon steel coupons exposed to different levels in ballast tank over the experimental time of weeks.

General corrosion rate (mm/y)			
Zone	0 weeks	8 weeks	14 weeks
Immersion	0.75±1.5	0.46±0.9	0.49±0.9
Sediment	0.38±0.3	0.49±0.2	0.59±0.3

The corrosion rates of carbon steel showed a gradual decreased over the period of time in the immersion zone (i.e. near to surface water). On the contrary, for sediment zone a constant increase in corrosion rate was observed (14 weeks Table 2). The average corrosion rates for the immersion zone was 0.5 mm/y and for the sediment zone it was 0.6 mm/y.

4.5 Pitting corrosion

Pitting factor was determined based on the pit depth for the carbon steel exposed to different levels in ballast tank. Table 3 are the data of the 10 different measured pits for both immersion and sediment zone.

Table 3. Pit depth and pitting factor (PF) of carbon steel coupons exposed to different levels in ballast tank.

Zone	Pit depth (micron), 10 individual pits										Average depth	PF
Immersion	10	12	16	6	9	34	11	13	24	27	17	2
Sediment	31	23	19	24	37	31	15	27	24	33	26	1.4

Pitting factor close to 1 represents uniform corrosion and increasing numbers represents higher degree of pitting.

The values indicate that the average pit depth is higher for the sediment zone than the immersion zone. In contrast, the PF values are low for the sediment.

## 5. Discussion

This chapter highlighted the problem of attached biofilms in the field of corrosion in ship ballast tanks and will open new ways in practical applications to combat this serious corrosion problem. The genetic variability between the water phase and MIC biofilm was significant. Overall it can be said that the bottom zone was more dominated by MIC bacteria such as (*Gallionella*, *Thiomicrospira* and *Desulfobacteraceae*) than the immersion zone (irrespective planktonic or sessile).

Higher pitting rates could be due to synergetic effects of various bacterial groups such as acid producing bacteria, slime producing bacteria, sulphur-oxidizing, sulphate reducing and metal oxidizing bacteria enabling the proliferation of local corrosion damage. All these results highlight the strong genetic variability among these bacterial populations and their fast adaptability to different conditions, underlining once more the difficulty in finding a correlation between electrochemical activity and composition of microbial populations. Such type of consortium is unlikely to be fully unveiled by only cultivation techniques. The combination of OCP and the use of DGGE as a screening tool can be one way in the future to monitor corrosion behaviour in enclosed seawater environments. The results in this study clearly point out how important PCR-DGGE work is to determine the type of bacterial species in such a specific enclosed environment.

The combination of molecular tools and electrochemistry can be one of the future aims to combat microbial corrosion in marine environments for the ship industry. A more effective monitoring and treatment system in form of effective preventing and treating biofilms on sidewalls of ship ballast tanks will help to reduce costly material replacements. Therefore, any measure for controlling aquatic invasive species in ballast tanks should consider the impact on corrosion in form of sessile communities in the future, which has been an underestimated problem so far. The summarized work in this chapter can be one-way for the future to build up a database of bacterial species, which are involved in corrosion or coating degradation on-board of ships. This will help on the one hand to fulfil international coating guidelines provided by IMO for ballast water treatment and coatings to secure our environment and human health on a very high level. Another important step in MIC control for the future is monitoring the activity of sessile microorganisms (biofilms) on sidewalls of the tank under ballasted conditions (full tanks) to understand community structures and biocide efficiency over time. Chemical treatment of the water during voyage is one choice to lower bacterial activity inside the tank. Another option might be ultraviolet (UV) radiation, which can be used for pre-treatment of the ballast water during intake instead of chlorination or biocide use. If biocides are used to lower bacterial activity, care has to be taken in the case of biofilms. Although all biocides are efficient in the water phase (planktonic bacteria), only a few are efficient against biofilms.



This should be taken into account especially for older vessels where maintenance was poor (high amount of sediment), or less efficient pre-treatment systems for the water phase are installed. One MIC control strategy can be online monitoring by electrochemical sensors placed on high-risk spots (welding's, bottom) inside the tank. Up to now, the available ship hulls monitoring systems (Slaughter et al. 1997) do not consider ballast tanks. Currently it is difficult to differentiate between various forms of localized corrosion as many of them have a similar appearance. Therefore, electrochemical methods of MIC monitoring should be used with caution.

Suitable and reliable methods for detection of MIC processes are available, but only the interdisciplinary diagnosis of all participating groups, such as engineers, ship owners, microbiologists and corrosion specialists, allows reducing life cycle costs and improving vessel safety. More advanced maintenance programmes for all types of ships have to be developed, incorporating MIC as one of the major corrosion phenomena within these enclosed seawater environments.

## References

- Al-Hashem A., Carew J. and Al-Borno A. (2004). Screening test for six dual biocide regimes against planktonic and sessile populations of bacteria. Proceedings of NACE Paper no. 04748.
- Amann R.I., Ludwig W., Schleifer K. (1995). Phylogenetic identification and in situ detection of individual microbial cells without cultivation. *Microbiol Rev* 59, 143-169.
- Andersen, A.B. (2001). Ballast Water Treatment by Ozonation. International Ballast Water Treatment R&D Symposium IMO, London.
- ASTM. (1994). Standard guide for examination and evaluation of pitting corrosion. p. G46-94.
- ASTM (1996). Standard Guide for On-line Monitoring of corrosion in plant Equipment. p. G96-90.
- BWM (2005). International Convention on the Control and Management of Ship's Ballast Water and Sediments. International Maritime Organization, London, United Kingdom; [www.imo.org](http://www.imo.org).
- Borenstein, S.W. (1994). Microbiologically Influenced Corrosion Handbook. Woodhead. London, Cambridge, p. 12.
- Beech I.B. and Sunner J. (2004). Biocorrosion: towards understanding interactions between biofilms and metals. *Curr. Opin. Biotechnol.* 15, 181-186.

Beech I.B and Campbell S.A. (2008). Accelerated low water corrosion of carbon steel in the presence of a biofilm harbouring sulphate-reducing and sulphur-oxidising bacteria recovered from a marine sediment. *Electrochimica Acta* 54, 14-21.

Carlton J.T. (1985). Transoceanic and interoceanic dispersal of coastal marine organisms: the biology of ballast water. *Ocean Mar Biol Ann Rev* 23, 313-371.

Carlton J.T. (1996). Pattern, process, and prediction in marine invasion ecology. *Biol Cons* 78, 97–106.

Cleland, J. H. (1995). Corrosion risks in ships’ ballast tanks and the IMO pathogen guidelines. *Engineering Failure Analysis* 2, 79-84.

Cullimor D.R. (2000). *Microbiology of well biofouling* (CRC Press Chapman and Hall, Boca Raton).

Dexter S.C. and Gao G.Y. (1988). Effect of seawater biofilms on corrosion potential and oxygen reduction of stainless steel. *Corrosion* 44, 717-723.

Dexter S.C. (1995). Microbiological effects. In: *Corrosion Tests and Standards, Application and Interpretation*, Robert Baboian, eds. ASTM Manual Serie, MNL 20.

Eashwar M.S., Maruthamuthu S., Sathiyarayanan S., Blakrishnan K. (1996). The ennoblement of stainless alloys by marine biofilms: the neutral pH and passivity enhancement model. *Corrosion Science* 38, 1407-1422.

Fairply (1993). Special report: Paints and Coatings Covering the Costs.

Farmali M., Chelossi E., Pavanello G., Benedetti A., Vandecandelaere I., de Vos P., van Damme P. and Mollica A. (2010). Electrochemical activity and bacterial diversity of a natural marine biofilm in laboratory closed-systems. *Bioelectrochemistry* 78, 30-38.

Flemming H.C., Schaule. G. (1996). Measures against biofouling. In *Microbially influenced corrosion of materials – scientific and technological aspects*. Sand W., Heitz E. and Flemming H.C. eds. (Heidelberg, Germany: Springer), pp. 121-139.

Fonesca I.T.E., Feio M.J., Lino A.R., Reis M.A., V.L. Rainha (1998). The influence of the media on the corrosion of mild steel by *Desulfovibrio desulfuricans* bacteria: an electrochemical study. *Electrochimica Acta* 43, 213-222.

Ford, T., Black J.P., and Mitchell R. (1990). Relationship between bacterial exopolymers and corroding metal surfaces. National Association of Corrosion Engineers. Houston, TX. Corrosion paper no. 110

Geenen, F.M. (1991). Characterization of Organic Coatings with Impedance Measurements, Pasmans Offsetdrukkerij B.V., 's-Gravenhage, p. 30.

Geesey G.G. and L.W. Costerton (1986) The microphysiology of consortia with adherent bacterial populations, pp. 238-242. In Proceedings of the 4<sup>th</sup> International Symposium on Microbial Ecology. Ljubljana, Yugoslavia.

Geesey G.G., Mittelman M.W., Iwaoka T. and Griffiths P.R. (1986). Role of exopolymers in the deterioration of metallic copper surfaces. *Mater. Perform.* 25, 37-40.

Gollasch S. (2002). The importance of ship hull fouling as a vector of species introductions into the North Sea . *Biofouling* 18, 105-121.

Groysman A. (2008). Corrosion monitoring in Industry. In: *Corrosion Science and Technology*, U. Kamachi Mudali and B. Raj eds., (Narosa Publishing House, New Dehli, India), pp. 500-550.

Heyer A., D’Souza F., Ferrari G., Mol J.M.C. and de Wit J.H.W. (2009). Microbiologically influenced corrosion (MIC) in a simulated ship tank model system. *Proceedings of Eurocorr* paper no. 7852.

Heyer A. D’Souza F., Ferrari G., Mol J.M.C. and de Wit J.H.W. (2011). EIS study of MIC in three different zones derived from ship ballast tank model system. *Proceedings of NACE* paper no. 19148.

Hilbert L.R. (2000) Monitoring Microbially Influenced Corrosion. PhD thesis Technical University of Denmark. IPT 0125-00.

Huang, R.T., McFarland, B.L. and Hodgman, R.Z. (1997). Microbial influenced corrosion in in cargo oil tanks of crude oil tankers. *Proceedings of NACE* paper no. 535.

Iyer P., Bruns M.A., Zhang H., Van Ginkel S. and Logan B.E. (2004). H<sub>2</sub> producing bacterial communities from a heat-treated soil inoculum. *Appl Microbiol Biotechnol* 66, 166–173.

Javaherdashti R. (2008). Microbiologically influenced corrosion an engineering insight. Derby B. eds. (London, England: Springer), pp. 101-104.

Jeffrey R. and Melchers R.E. (2009). Corrosion of vertical strips in seawater. *Corrosion Science* 51, 2291-2297.

Juniper S.K. and Fouquet Y. (1988). Filamentous iron silica deposits from modern and ancient hydrothermal sites. *Can. Mineral.* 26, pp. 859-869.

Kajiyama F. (1994) Bacterial-Environmental Interactions in Corrosion on buried Pipes In: *Environmental Oriented Electrochemistry* eds. C.A.C. Sequeira *Studies in Environmental Science* 59, Elsevier.

Kato S., Kobayashi C., Kakegawa T. and Yamagishi A. (2009). Microbial communities in iron silica rich microbial mats at deep-sea hydrothermal fields of the Southern Mariana Trough. *Env. Microbiol.* 11, 2094-2111.

Keresztes Z. Telegi J., Beczner J. and Kalamán E. (1998) The influence of biocides on the microbiologically influenced corrosion of mild steel and brass, *Electrochimica Acta* 43, 77-85.

Landoulsi, J., El Kirat K., Richard C., Feron D., and Pulvin S. (2008). Enzymatic approach in microbial-influenced corrosion: a review based on stainless steels in natural waters. *Environ. Sci. Technol.* 42:2233–2242.

LaQue F.L. (1951) Corrosion testing (Edgar Marburg Lecture) *Proc. ASTM*, 51, pp. 495–582.

Lee, W.C., Lewandowski, Z. Okabe, S., Characklis, W.G. and Avci R. (1993). Corrosion of mild steel underneath aerobic biofilms containing sulfate-reducing bacteria part I: At high dissolved oxygen concentration. *Biofouling* 7, 197-216.

Little, B.J., and J. R. Depalma. (1988). Marine biofouling. *Treatise on Material Science and Technology* 28:89–119.

Little, B.J. and Lee J.S., (2007). Microbiologically influenced Corrosion, Chapter 2. In: Winston R. eds. (Wiley-Interscience, Inc., Hoboken, New Jersey).

Little B.J., Lee J.S. and Ray R., (2007). A review of green strategies to prevent or mitigate microbiologically influenced corrosion. *Biofouling* 23, 87-97.

Little B.J., Lee J.S., Ray R., (2007). A review of green strategies to prevent or mitigate microbiologically influenced corrosion. *Biofouling* 23: 87-97.

Melchers R.E. (2003). Mathematical modeling of the diffusion controlled phase in marine immersion corrosion of mild steel. *Corrosion Science* 45, 923-940.

Melchers R.E. (2005). The effect of corrosion on the structural reliability of steel offshore structures. *Corrosion Science* 47, 2391-2410.

Melchers R.E. and Jeffrey R. (2005). Early corrosion of mild steel in seawater. *Corrosion Science* 47, 1678-1693.

Melchers R.E. and Wells T. (2006). Models for the anaerobic phases in marine immersion corrosion. *Corrosion Science* 48, 1791-1811.

Naderi, R., Attar, M.M. and Moayed, M.H. (2004). EIS examination of mill scale on mild steel with polysterepoxy powder coating. *Progress in Organic Coatings*, 50, 162.

Olesen B.H., Nielsen P.H. and Lewandowski Z. (2000). Effect of biomineralized manganese on the corrosion behavior of C1008 mild steel. *Corrosion* 56: 80-89.

Paradies H.H., Haenßel I., Fisher W. and Wagner D. (1990). Microbial Induced Corrosion of Copper Pipes. New York, INCRA Report No. 444:16.

Roe, F.L., Lewandowski Z., and Funk T. (1996). Simulation microbiologically influenced corrosion by depositing extracellular biopolymers on mild steel surfaces. *Corrosion* 52, 744–752.

Ruiz G.M., Fofonoff P.W., Carlton J.T., Wonham M.J. and Hines A.H. (2000). Invasion of coastal marine communities in North America: apparent patterns, processes, and biases. *Ann Rev Ecol Syst* 31, 481-531.

Schäfer H. and Muyzer G. (2001). Denaturing gradient gel electrophoresis in marine microbial ecology. *Methods Microbiol* 30, 425-468.

Schmitt G. *Sophisticated Electrochemical Methods for MIC Investigation and Monitoring, Materials and Corrosion*, Vol. 48, pp. 586-601, 1997.

Stahl S., Hultman T., Olsson A, Moks T. and Uhlén M. (1988). Solid phase DNA sequencing using the biotin-avidin system. *Nucl. Acids Res.* 16, 3025-3038.

Scott J.F.D., Skerry B.S. and King R.A. (1988). Laboratory evaluation of materials for resistance to anaerobic corrosion caused by sulphate reducing bacteria: Philosophy and practical design. The use of synthetic environments for corrosion testing. ASTM STP 970 Franci P.E. and Lee T.S. eds. 98-111 ASTM.

Starosvetsky J.O., Armon R., Yahalom J. and Starosvetsky D. (2001). Pitting corrosion of carbon steel caused by iron bacteria. *Inter. Biodeter. & Biodegrad.* 47, 79.

Suzuki, S., Muraoka, R., Obinata, T., Endo, S., Horita, T. and Omata, K. (2004). Steel products for shipbuilding, JFE Technical Report No. 2.

Tamburri, M.N., Wasson, K. Matsuda, M. (2002). Ballast water deoxygenation can prevent aquatic introductions while reducing ship corrosion. *Biological Conversation* 103, 331-341.

Tamburri, M.N., Little, B.J., Ruiz, G.M., Lee, J.S. and McNulty, P.D. (2003). Evaluations of Venturi Oxygen Stripping TM as a ballast water treatment to prevent aquatic invasions and ship corrosion. *Proceedings of the 2nd International Ballast Water Treatment R&D Symposium*, International Maritime Organization, London.

Tamburri, M.N. and Ruiz, G.M. (2005). Evaluation of a ballast water treatment to stop invasive species and tank corrosion. Presented at the SNAME Annual Meeting, The Society of Naval Architects and Marine Engineers, Houston

Tatnall, R.E. (1981). Fundamentals of bacteria induced corrosion. *Mater. Perform* 20, 32–38.

Thompson N.G., Oldfield J.W. and Scholified M.J. (1994). Corrosion Monitoring of Process control *Proceedings from the sixth middle east NACE-BSE Conference 1994, Bahrain*, Vol. 2, pp. 679-695.

Torsvik V. and Øvreås I. (2002). Microbial diversity and function in soil: from genes to ecosystems. *Current Opinion in Biotechnology* 5, 240-245.

Tuovinen O.H. Cragolino G. (1986) A review of microbiological and electrochemical techniques in the study of corrosion induced by sulphate reducing bacteria, *Corrosion Monitoring in Industrial Plants using nondestructive testing and electrochemical methods*, ASTM STP 908, Moran G.C. and Labine P., eds. (American Society for Testing and Materials, Philadelphia), pp. 413-432.

Videla H.A. (1996). *Manual of Biocorrosion*. (CRC Press Chapman and Hall, Boca Raton).

Xu K., Dexter S.C. and Luther G.W. (1998). Voltametric microelectrodes for biocorrosion studies. *Corrosion* 54, 814-823.

Yaseen, M. (1981). Permeation properties of organic coatings in the control of metallic corrosion. In: *Corrosion Control by Organic Coatings*, Leidheiser H., eds. (NACE), pp. 24-27.

## ***2.2 A molecular and electrochemical approach to study corrosiveness and population dynamics of MIC biofilms inside ship ballast tanks***

### **Abstract**

Microbiologically influenced corrosion of steel is a serious problem in the marine environment and many industries, such as offshore and shipping industry. Under natural conditions biofilms form heterogeneous patchy surfaces, which eventually result in pitting corrosion. While electrochemical measurements, such as Open Circuit Potential (OCP) and linear polarization resistance (LPR), have been used in corrosion monitoring for several years the combination with microbiological techniques were always underestimated in sense of studying microbial communities in combination with corrosion rates. A new experimental approach was established by operating a full-size ship ballast tank to assess the impact of microbes on ship corrosion. A full-scale set-up was chosen to simulate the impact of bacterial growth on the corrosion of ship steel as realistic as possible. This cannot be performed under lab conditions of a smaller volume where nutrient limitation and environmental conditions such as flow or stagnation will influence the natural growth conditions. This new approach covered realistic pumping rates of the used seawater and a representative volume of ballast water under dark stagnant conditions as commonly found within ballast tanks in ships over long trans oceanic travel routes. Working electrodes were immersed at two different height levels of the ship ballast tank, sediment and immersion zone to compare the corrosion behavior of ASTM A131 Steel grade EH36 exposed to natural seawater. These specific zones Based on engineering requirements, ballast tanks are commonly divided into two different zones: Fully submerged zone (*water phase*) and mid section (*air water phase*). This simple model is used for maintenance programs but does not reflect all relevant areas inside of SBTs considering MIC. Ballast tanks on board of vessels can be divided into four different zones (Heyer et al. 2009; Heyer et al. 2011). This model reflects the main cause why SBTs are prone to microbiologically influenced corrosion. Within these 4 different zones different environmental conditions (oxygen, nutrients, flow conditions) are established, these conditions will have a significant influence on bacterial communities and activities. It has to be highlighted that the rate of ballast water exchange determines the real impact of MIC in SBTs. Compared to closed seawater environments, in which electron acceptors are quickly exhausted, MIC might be irrelevant in some cases after some time. But SBTs are open systems, and ballast water exchange can be continued over the voyage time or locally in ports of arrival. A continuous input/output of nutrients ensures biofilm formation and growth of bacteria in inaccessible areas of SBTs because of their enclosed structure and their constant nutrient supply in form of water exchange.

Interpretation and modelling of corrosion within SBTs is nowadays based on practical weight loss measurements gained in field studies (Tamburri et al. 2002, 2003, 2005; Suzuki et al. 2004), or corrosion depth measurements by ultrasonic instrumentation (Paik and Thayambali 2001; 2002; Paik et al. 2004). Corrosion rates ascribed to MIC in tanks of ships have been reported in literature. Huang et al. (1997) reported excessive pitting corrosion up to 2mm/yr on the uncoated carbon steel bottom plating. Cleland (1995) stated even 6mm/yr for the bottom plating. No model, however, has integrated bacterial species and MIC mechanisms so far. Until now little information is available on microbial community composition and the corresponding corrosiveness within ship ballast tanks. This lack of knowledge was investigated by combining electrochemical detection techniques and molecular screening tools to gain new data of corrosive biofilms in enclosed seawater environments. The experimental procedure included sampling of biofilms from exposed corrosion coupons were subjected to denaturing gradient gel electrophoresis (DGGE) of PCR-amplified 16S rRNA genes. The microbial community on the corrosion coupons (representing the sidewall of the tank) and in the water phase was investigated by DGGE. The genetic variability The water phase and the formed biofilms indicated a significant difference in species grown demonstrating that the bottom zone was more dominated by MIC bacteria than the immersion zone. The information on the bacterial community was combined with conventional electrochemical on-site measurements, such as OCP and LPR, to evaluate the corrosion processes with regards to the bacterial communities. A substantial difference in corrosion rates for bottom and immersion zone was detected and could be linked to the bacterial populations in these zones. This research paper summarizes for the first time the problem of attached biofilms in the field of corrosion in ship ballast tanks combining electrochemical and molecular tools.



## 1. Introduction

Ship ballast tanks are designed to hold enormous quantities of water; each has a capacity of hundreds, even thousands of metric tonnes. The ballast tanks are crucial to the ship's cargo operations and safety at sea as it's maximizing the ship's stability in rough waves and increases propulsion efficiency. Ballast capacities depend on the ship size and therefore range from single cubic meters for sailing boats up to 200.000m<sup>3</sup> for large cargo carriers. Ballast water is taken on board using sea chests, pumps or by gravity feed. As a consequence of remaining water when off-loading (retarded by stiffeners) sediment accumulates within SBTs. Studies have shown that at least 65% of ships were carrying significant amounts of sediment on the bottom of their ballast tanks (Hallegraeff and Bolch, 1992; Hamer et al., 2000) which is a potential source for nonindigenous organisms (Gollasch et al., 1998) and MIC bacteria. The International Maritime Organization (IMO) developed a convention on ballast water management for the control of marine flora and fauna (IMO 2005; Hewitt et al. 1999). Existing methods include the exchange of coastal ballast water for open oceanic water while in transit. The ballast water exchange may act to reduce the likelihood of species transport to some extent, but these activities will not dislodge any sediment that has accumulated at the bottom of the tank (Hallegraeff and Bolch, 1992; Hamer et al., 2000) and bacterial biofilm developed on the tank surface. Blistering type of corrosion is mostly prevalent in most cases at the bottom horizontal position of the tanks, where sediment is normally accumulated. Extensive corrosion failures have been recognized in the form of local corrosion in the ballast tanks (Tamburri et al. 2002; Suzuki et al. 2004). Further, not much information is available on the role of microbes in corrosion process in the ship ballast tanks. This study aims to characterize the microbial biodiversity in the ship ballast tank environment and also their role in corrosion processes. The microbial population is examined using DGGE analysis of PCR-amplified 16S rRNA gene fragments revealing qualitative data on the bacterial community. The methodology has been adapted in many laboratories as a convenient tool for the assessment of microbial diversity in natural samples (Muyzer 2000; Schäfer and Muyzer 2001) and was used to follow up trends in community shifts over time. The microbial diversity in the water and biofilm sample in the ship ballast tank environment were inspected and the shift in the population over the period of time is determined. Different sampling periods were considered based on preliminary experiments performed by the authors prior to the long term experiment (data not shown) indicating that shifts in the biofilm community are occurring after exposure of 4 weeks. Furthermore, corrosion processes in the ballast tank are monitored using electrochemical techniques such as open circuit potential measurements (OCP) and linear polarization resistance (LPR). Both these techniques have been widely used for monitoring of corrosion processes of steel in different environment (Fonesca et al. 1996; Little et al. 2007; Beech and Sunner 2004; Beech and Campbell 2008).

The main questions that are investigated in this study include (i) what is the microbial community differences and shift, at different water height levels within a ship ballast tank with time? (ii) What is community difference between the water phase and the biofilm developed at the bottom of the ship ballast tank (near sediment zone) (iii) Does the microbial community have a significant impact on the corrosion mechanism or/and rate in the ship ballast tank closed environment? In order to address these queries the experiments were performed in a large practical test ballast tank designed for evaluation and certification of ballast water treatment systems at the north coast of the Netherlands

## 2. Materials and methods

### 2.1 Practical ballast tank facility (operational conditions)

An international test facility for the certification of ballast water treatment systems at the Royal Netherlands Institute for Sea Research (Royal NIOZ) was used to study microbial dynamics and corrosion rates in a closed ballast tank environment. For the study a coated (epoxy ballast tank coating) tank (dimensions 31.05 x 3.10 x 3.55 meters) was used to simulate the ballast tank of a ship ballast tank conditions (Figure 1). At the dockside a ballast water pump (working speed 300m<sup>3</sup>/h) was used to pump fresh North Sea water (end volume 140 m<sup>3</sup>) directly from the harbour of Den Helder at a water temperature of 9.1 °C. The tank was filled at the beginning of the experiment and was not replaced or disturbed over the experimental time of 14 weeks. A control experiment without bacteria cannot be performed for this kind of set-up and is not necessary due to the fact that the community shifts and corrosion rates within 2 different height levels in the tank were compared.

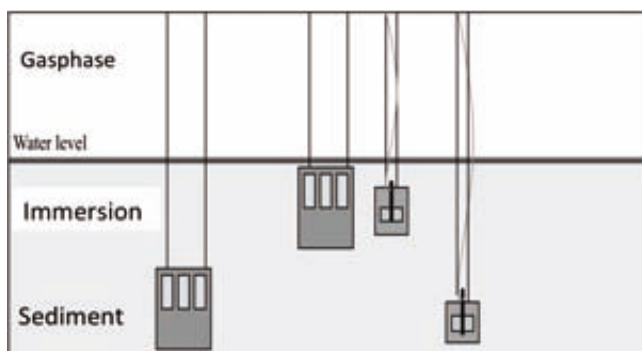


Figure 1. Experimental set-up of ballast tank including sampling coupons and electrochemical corrosion sensors in different height levels of the tank.

## 2.2 Test coupon preparation

Carbon steel coupons of ASTM A131 Steel, grade EH36 elemental composition (C 0.15; Si 0.40; Mn 1.45; P 0.05; S 0.015; Cu 0.035; Mn 0.025 wt %) was chosen as it is used in ship construction, typically in ship ballast tanks. The rectangular coupons with a dimension of 30 x 20 x 1mm were fixed on epoxy plates and immersed in the ballast tank at two different height levels (sediment zone & immersion zone). An epoxy plate with mounted coupons was fixed near bottom of the tank (~ 2m), which is considered as near sediment zone and the other plate is fixed in the immersion zone (near to surface water i.e. ~ 15 cm from the surface water) (Figure 1). The coupons remained immersed for the period of 14 weeks for the development of a biofilm and for estimation of the corrosion rate using electrochemical techniques as detailed later. The steel surface was uncoated to simulate pure carbon ship steel, this is a realistic approach due to the fact that coating failure in ship ballast tanks is well known and considered in ballast tank inspections. The normal classification society method of quantifying ballast tanks gives three categories: “good”, “fair” and “poor” (IACS 1993). The coating conditions are assigned based on visual inspection and estimated percentages of areas with broken down coating and rusty surfaces. Therefore the use of uncoated steel coupons will cover a broad range of ballast tanks considering practical and realistic conditions onboard of ships worldwide. The seawater pumped in the ballast tank remained stagnant throughout the experimental period of time.

## 2.3 Biofilm sampling

The biofilm developed on the steel coupons over the period of 14 weeks were collected from both the sediment and immersion zones of the practical ballast tank. Duplicate steel coupons were retrieved at fixed sampling periods of 4 and 14 weeks based on data of preliminary experiments (data not shown). Water from the sediment zone was taken through a valve on the bottom of the tank accessible from a cellar underneath the tank. Immersion zone water could be collected by a sterile bottle drawn to the water level with a rope. The sampled water was immediately filtered through a sterile 0.2 µm Sterivex filter to concentrate the planktonic biomass. The corroded coupons with biofilm and seawater biomass filters were transferred immediately into sterile 50ml falcon tubes in an icebox and transported to the laboratory. The coupons and filters were stored at -80°C until DNA analysis.

## 2.4 DNA extraction, PCR amplification and DGGE

The biofilm was frozen in liquid nitrogen by introducing the coupon with a tweezer inside a thermal isolated nitrogen jar, corrosion/biofilm products were scraped off the coupons. The material was ground with a pestle in a mortar filled with liquid nitrogen to prevent sample thawing. Around 0.1 mg of sample was transferred to an Eppendorf tube and kept frozen until DNA extraction.

For seawater filters, the housing was aseptically cut and removed with a hot blade and filter fibers were cut with a sterile blade and scissors before being introduced in the PowerSoil Tube solution (without beads) preliminary transferred in a sterile 50 ml Falcon tubes. The solution with the cut fibers was subsequently vortex with short interruptions of 1 min and fibers were pressed along the tube wall with sterile forceps to drain the fibers and centrifuged at 10,000 g for 10 min. The liquid fraction obtained was transferred back to the PowerSoil Tube with beads. Genomic DNA from both grinded corrosion deposits and sea water extract was extracted using the PowerSoil DNA isolation Kit (Mo Bio Laboratories, USA). The protocol for isolation is described by Marty et al. (2012). 16S rRNA genes were amplified and DGGE analysis was performed as described by Schäfer and Muyzer (2001). Several separated bands were excised from the denaturing gel and stored during 2 days at 4 °C in 40 µl TRIS-HCl buffer. An aliquot of 0.5 µl was used for re-amplification. Purified products were sent for sequencing at a commercial company (Macrogen Inc., South, Korea).

### *2.5 Phylogenetic analysis (16SrDNA sequence)*

The rDNA sequences were checked manually using the software program CodonCodeAligner (CodonCode corporation, LI-COR Inc). The corrected sequences were compared to sequences stored in GenBank database using the MegaBLAST algorithm and the highest score sequence affiliated to a known bacterial relative was selected. Subsequently, the sequences were aligned to sequences in the SILVA SSU database Ref NR 108 and a phylogenetic tree was constructed using the software program ARB (Ludwig et al. 2004). The DGGE profiles and band intensities were normalized using the GelComparII v5.0 software. The percentages of band intensities per profile were determined by the relative 1D surface value correcting manually the densitograms whenever necessary. The similarities between DGGE profiles were determined using the Pearson correlation index (Boon et al. 2002; Smalla et al. 2007).

### *2.6 Electrochemical corrosion measurements*

Along with the biofilm steel coupons, two working electrodes (area 1 cm<sup>2</sup>) of the same steel grade (ASTM A131) were also mounted on the epoxy plates. The electrode configuration for electrochemical measurements consisted of working electrode, water immiscible silver/silver chloride electrode as reference electrode and a platinum mesh as a counter electrode. All electrochemical measurements were performed using a portable potentiostat (IVIUM Technologies, The Netherlands) an USB powered device to avoid any external noise disturbance controlled by IVIUM software version 1.705. LPR and OCP measurement were carried out for the electrodes placed in both zones i.e., sediment and immersion zone. For LPR measurements, a  $\pm 10$  mV potentiodynamic potential versus open circuit potential (OCP) was applied.

LPR data were modelled with  $Z_{view}$  software version 3.0. OCP was monitored vs. SCE reference electrode for five minutes in the beginning to enable the system to stabilize. Measurements were performed in triplicate.

### 2.7 Surface characterization of working electrodes

The corrosion products and biofilm were stripped from the working electrodes by adding Clarke acid cleaning solution (ASTM G 1-90, 1999) (1L 36% (v/v) HCl, 20 g  $Sb_2O_3$  and 50g  $SnCl_2$ ) for 10-15sec. The exposed sample surface was finally rinsed with distilled water, cleaned in absolute ethanol and dried under a flow of nitrogen gas. The electrode surface was examined using an optical microscope (Olympus X51) at 20X magnification. Microscope images of the surface were made and the pit depth at different spots was characterized gaining qualitative data on the corrosiveness of the attached biofilm. Pit depth was measured by adjusting first the microscope focus point at the bottom of the pit and later at the electrode surface. The height difference is defined in this paper as the depth of the pit. A total of ten individual pits were measured on each electrode surface i.e. at two different zones (immersion and sediment) in the practical ballast tank.

## 3. Results and Discussion

### 3.1 Environmental parameters

Temperature, pH and suspended particulate matter (SPM) were measured during the experimental study as shown in Table 1 below.

Table 1. Environmental parameter (pH, T, SPM) for immersion & sediment zone over time.

	pH	Temperature	SPM
Immersion Zone			
0	8.5	5.3	195.2
4 weeks	7.9	5.3	-
14 weeks	7.8	7.3	42.3
Sediment Zone			
0	8.5	5.3	195.2
4 weeks	7.6	7.0	-
14 weeks	6.5	7.5	45.5

\*Suspended particulate matter

The water temperature was relatively low over the experiment study period as a result of winter conditions. This fact will have a strong impact on the bacterial activity leading to the conclusion that all measured values must be seen as minimum values due to less metabolic activity and harvested cells due to low temperature. The pH in the sediment zone showed a large drop was lower as compared to the immersion zone. The difference in the pH will enable growth of diverse bacterial communities in these zones. Suspended particulate matter load of the ballast tank water decreased from ~ 195 mg/ to ~ 42 mg/L over the experimental period of time due to sedimentation as indicated in Table 1. Accumulation of sediment rich in organic component at the bottom of ship ballast tanks can result in development of anaerobic environments that will later facilitate the growth of anaerobic sulphate reducing bacteria (SRB). The establishment anaerobic conditions in these environments are discussed in two research papers of the authors that are under review. Aerobic biofilms can enhance corrosion as well due to colonization of anaerobic pockets by SRB, which cause an increase in corrosion by the removal of hydrogen and also by the production of hydrogen sulfide and Fe sulfide. The decrease of SPM in water is also an indication of nutrient limitation in the water phase over the period of time in such enclosed stagnant environments.

### 3.2 DGGE Analysis

The bacterial communities structure in the seawater that was pumped into the ship ballast tank and the biofilms that were developed in the tank over a period of time were examined by DGGE analysis of 16S rRNA gene fragments. DGGE results of bacterial fragments are shown in Figure 2. The structures of bacterial communities established on replicate steel coupons were highly similar (80% similarity minimum) (data not shown). The experimental set-up had good replicates giving 80% minimum similar community structures proven by Pearsons correlation index (data not shown). Dominant bands were excised from the gel by visual determination under UV light and sequenced. Only those bands that gave the clean sequences (these are numbered bands) were used for phylogenetic analysis.

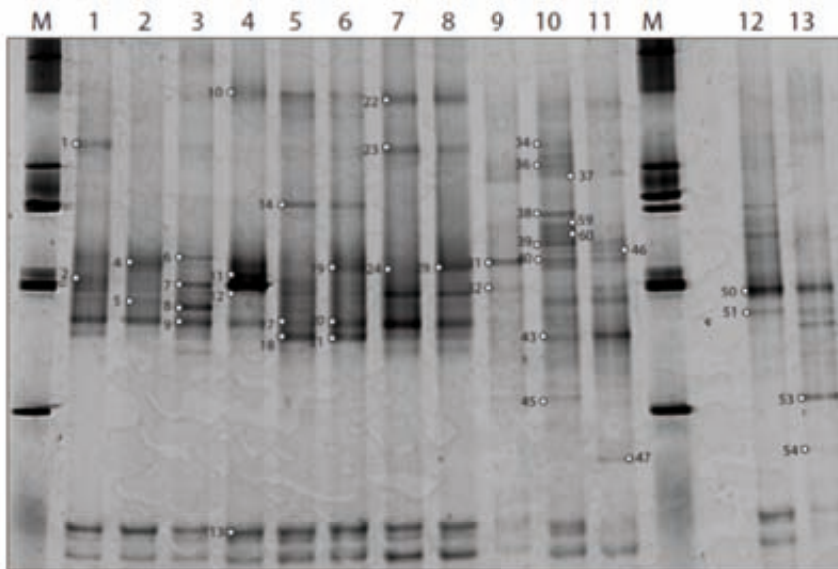


Figure 2. DGGE gel pattern used for verification of species in the biofilm and water samples from practical ship ballast tank during different experimental time period.

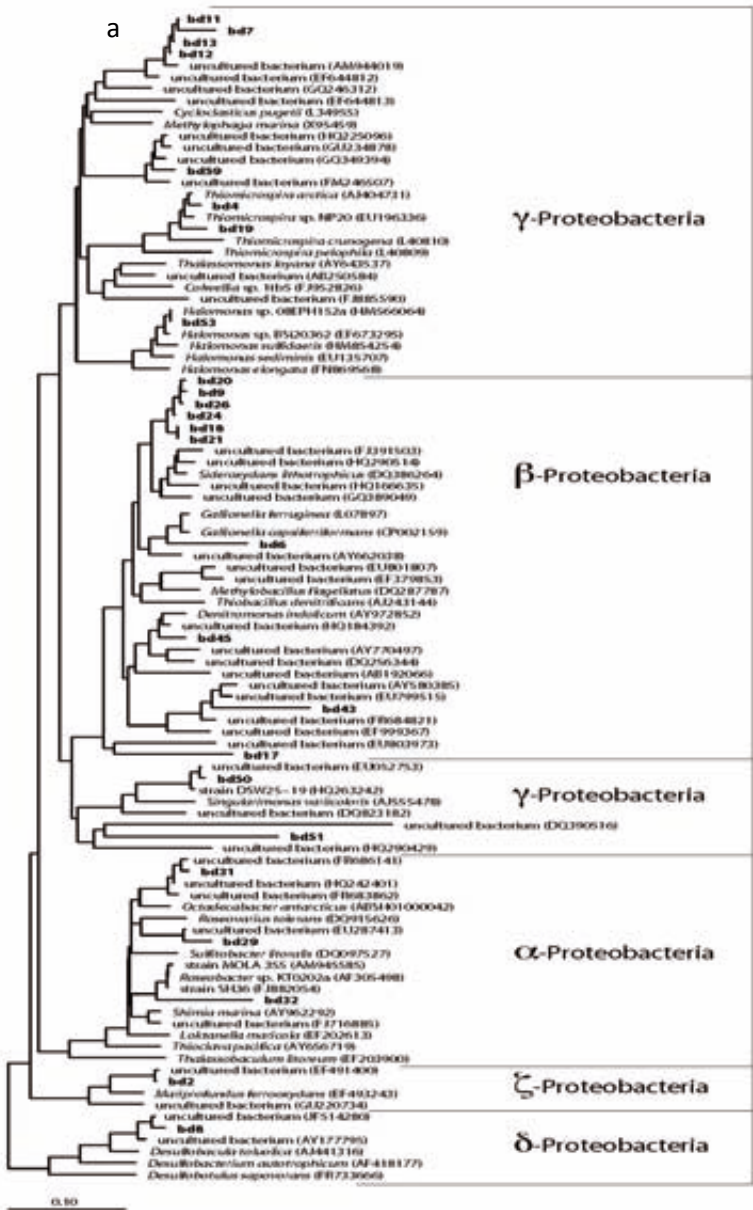
*Biofilm samples* in duplicate - Immersion zone 4 weeks (lane 1, 2) & 14 weeks (lane 3,4); sediment zone lane 4 weeks (lane 5,6) & 14 weeks (lane 7,8);

*Water phase samples* - Day 0 (lane 9); sediment zone 4 weeks (lane 10) & 14 weeks (lane 11); immersion zone 4 weeks (lane 12) & 14 weeks (lane 13). M representing marker bands

The numbered bands of the DGGE gel were used for phylogenetic analysis in the next section. In general, the communities in the water phase contained higher numbers of visible bands (lane 9-12) than the biofilm samples (lane 1-8). It was observed that the bacterial communities in the water phase collected from the immersion zone (12, 13) showed less diversity (indicated by the number of bands), whereas, the water collected from the bottom of the tank (lane 10, 11) was highly diverse leading to more identified bands per lane. Several bands were shared between the biofilms that were developed at immersion and sediment zones, e.g., band 1 (immersion zone) & band 23 (sediment zone), band 9 (immersion zone) & band 20 (sediment zone), and also between different zones and the water phase, such as bands 50 & 51 from the water phase. Besides, bands 34, 36, 37, 45, 46, 47, 53, and 54 were unique to the planktonic community. Band 2 and 4–24 associated to the biofilm community showed a high diversity of organisms.

3.3 Phylogenetic analysis

The sequences retrieved from the denaturing gradient gel were affiliated to five major sub-classes of the Proteobacteria,  $\alpha$ ,  $\beta$ ,  $\gamma$ ,  $\delta$  and  $\zeta$  (Figure 3a) as well as Bacterioidetes, Gemmatimonadetes and Actinobacteria (Figure 3b)





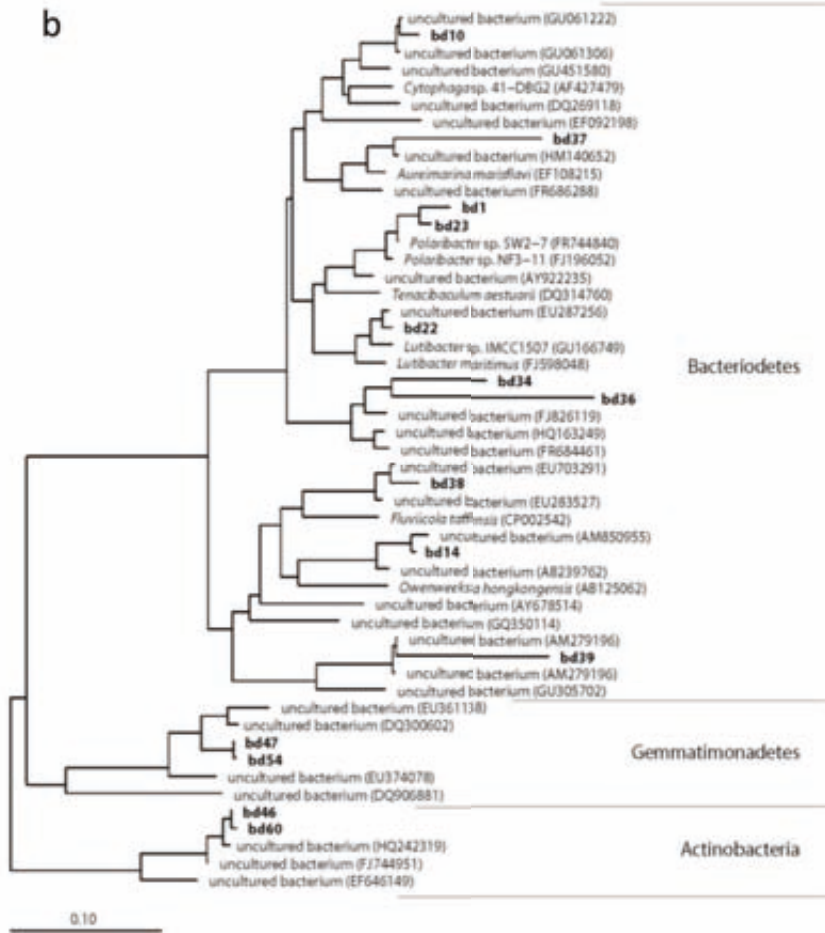


Figure 3. Neighbour joining trees showing the phylogenetic affiliation of the sequences retrieved from water phase and biofilms of immersion (Figure 3a) and bottom zone (Figure 3b). The sequences determined in this study are printed in bold. The accession numbers of the sequences are between brackets. The bars represent 10% estimated sequence divergence.

(i) *Planktonic community in immersion zone and sediment zone*

At the beginning of the experiment, the water phase indicated  $\alpha$ -Proteobacteria represented by bd31 as *Octadecabacter antarcticus* and *Roseovarius tolerans*. Additional species of *Shimia marina* (AY962292), *Loktanella marivola* (EF202613) and *Thalassobaculum litoreum* (EF203900) were identified as subgroups of (bd32). In later stages the bacterial species changed to  $\gamma$ -Proteobacteria as *Singularimonas variicoloris* (AJ555478) (bd50) and *Halomonas spp.* (bd53) within the immersion zone (Figure 2, lane 13). A different pattern could be found for the bottom level of the ballast tank water containing additional *Gemmatimonadetes* (bd 46, 47) (Figure 2, lane 11) after 14 weeks.

(ii) *Sessile community of the immersion zone*

For the biofilms in the immersion zone (Figure 2, lane 1-2) a higher diversity was found after 4 weeks in form of  $\zeta$ -Proteobacteria *Mariprofundus ferrooxydans* (EF493243) (bd2) and *Thiomicrospira sp.* NP20(EU196336) (Figure 2, bd4). Figure 2 (lane 1-2) represents the biofilm of the immersion zone after 14 weeks. Species of  $\beta$ -Proteobacteria become predominant as *Thiobacillus denitrificans* (AJ243144) (bd6). Sulphate reducing bacteria could be found likewise in form of *Desulfobacterium autotrophicum* (AF418177) and *Desulfobacula toluolica* (AJ441316).

(iii) *Sessile community at the bottom zone*

$\beta$ -Proteobacteria are forming the main community within the bottom zone (Figure 2, lane 5-6) after 4 weeks such as *Gallionella ferruginea* (L07897) (bd6) and many uncultured  $\beta$ -Proteobacteria (Figure 3a bd21 and 24). Bacterioidetes appeared as *Owenweeksia hongkongensis* (AB125062) within the bottom biofilm (Figure 3b, bd14). End of the experiment, different bacterioidetes could be found in the biofilm formed at the sediment zone (Figure 2, lane 7-8) such as *Fluviicola taffensis* (CP002542) (bd38), *Lutibacter sp.* IMCC1507 (GU166749) (bd22), *Polaribacter sp.* SW2-7 (FR744840) and NF3-11 (FJ196052) (bd23). These bacteria were originally isolated from sea ice and water from the Arctic and the Antarctic. The occurrence of these microorganisms in the present study might be explained by the low water temperatures observed over the course of the experiment. Unique for the planktonic biofilm community were  $\alpha$ -Proteobacteria and  $\gamma$ -Proteobacteria which are dominating the biofilm including highly specialized species such as *Acidithiobacillus spp.* and *Polaribacter spp.*  $\gamma$ -  $\zeta$ - and  $\delta$ -Proteobacteria could be found in the sessile community, giving a clear indication that the sessile community contains a more complex species community.

### 3.4 Quantitative analysis of the different community members

The bacterial community structure of the water phase and the attached biofilms were analyzed by PCR-DGGE. Figure 3 and 4 in chapter 2.1 illustrate the bacterial community structure in the near surface immersion zone and sediment zone i.e. bottom of the ship ballast tank. Pearson similarity index (intensities) measurements indicated that the experimental set up was reproducible giving replicates with at least 80% similar community structure. In Figure 3 and Figure 4 a shift in the bacterial community from planktonic cells to sessile biofilms can be identified underlying the overall estimation that biofilm communities are more diverse and able to adapt to more harsh conditions than the surrounding planktonic cells. Biofilm formation and its structural properties are the outcome of microbial triggers in the system. A trigger can be seen as a stimulus for microorganisms to increase their growth rate or encouragement to produce more exopolymetric substances (EPS) for adhesion properties. Biofilm formation is one of the most common microbial survival strategies: it allows bacterial species to form their own microenvironment for defense, food supply and metabolic interactions. Low nutrient availability in the water phase can be seen as a trigger in the system. Microbes growing in the biofilm can utilize more compounds from the water phase by exo-enzymes released and accumulated in the EPS matrix. Another trigger is cooperative benefit by re-using metabolic byproducts excreted by community members. This property makes the biofilm community independent from external impacts and is well known for acid producing bacteria (APB) and sulfate reducing bacteria (SRB) growing in close association.

Figure 3 in chapter 2.1 illustrates the bacterial community profile of the planktonic and sessile bacteria at the near surface immersion zone. The water phase i.e., column 1 is characteristically represented by  $\gamma$ -Halomonas,  $\alpha$ -Rhodobacteriaceae and  $\beta$ -Proteobacteria in the first 4 weeks stagnant conditions in the practical ship ballast tank. Subsequently, after 14 weeks the bacteria community in the stagnant water phase shifted slightly i.e., column 4  $\gamma$ -Halomonas (25%) which are typical seawater organisms and tolerant to a wide range of NaCl concentrations coexists with  $\alpha$ -Rhodobacteriaceae (5%), which are chemoorganotrophic organisms that remained in the water throughout. A characteristic change that was observed after 14 weeks is the decrease of  $\beta$ -Proteobacteria groups of bacteria which can fixate nitrogen were almost replaced by Gemmatimonadales gram-negative, aerobic, polyphosphate-accumulating micro-organisms. This shift in the community of the water phase gives an indication of nutrients shortage within the tank where organic compounds containing nitrogen and carbon are utilized first and more specialist organisms such as the Gemmatimonadales are rising for utilization of specific compounds in the later stages. It can be summarized here that the microbial community shift in the water phase that occurred near the surface of the ballast tank over the period of 14 weeks is driven by nutrient availability. The biofilm community showed a complete different bacterial diversity than the planktonic community in the immersion zone.

Within first 4 weeks (i.e., column 2&3) Zeta-proteobacterium (as early colonizers),  $\gamma$ -electroactive bacteria,  $\gamma$ -Thiomicrospira (*Thiomicrospira artica*) and  $\gamma$ -iron oxidizing bacteria (IOB) were the main colonizers, next to the non-sequenced groups of 18%. Later by 14 weeks (i.e., column 5&6) a shift in the biofilm community can be found where Zeta-proteobacteria are replaced by sulphate reducing (SRB), which make up 10% of the whole community. The main changes that were observed after 14 weeks is enrichment of gamma-electroactive bacteria and SRB in the biofilm developed in the immersion zone (near surface) on carbon steel (column 5&6 of figure 3 in chapter 2.1). It can be deduced for the immersion zone that the oxygen concentration was still high enough to avoid SRB growth within the biofilm community up to four weeks. After 14 weeks SRB were developed in the anaerobic niche of the biofilm (underneath of oxygen consuming bacteria) and these mixed community of SRB and IOB increased the electroactive activity community i.e.  $\gamma$ -Proteobacteria as supported by DGGE analysis.

Figure 4 in chapter 2.1 indicates the planktonic and sessile community changes over the period of 14 weeks in the sediment zone (near sediment) of the ship ballast tank. At the beginning of the experimental (day 0 i.e., column 1), the bacterial community in the water phase contains  $\beta$ -Proteobacteria (8%),  $\alpha$ -Rhodobacteraceae (25%) followed by some uncultured Bacteroidetes (17%) and uncultured Chroococcidiopsis (5%). After 4 weeks (i.e., column 2), the overall percentage composition in the community was slightly shifted and Actinobacteria (4%) were found. A major change in the community was observed after 14 weeks in the dark bottom water of the ballast tank were  $\beta$ -Proteobacteria (25%) and  $\alpha$ -Rhodobacteraceae (8%) reversed their abundances and also Gemmatimonadales (4%) were found. The community in the water at the bottom of the tank is characterized by  $\beta$ -Proteobacteria nitrogen fixing organisms and  $\alpha$ -Rhodobacteraceae chemoorganotrophic organisms. Interestingly, Gemmatimonadales were found in both the bottom water phase as well as at the surface water layer, indicating limitation of nutrients in the water phase. At the sediment zone, it can be highlighted that chemoorganotrophic organisms and nitrogen fixing organisms are predominant in water. In the biofilm a different community pattern could be found in 4 weeks this includes  $\gamma$ -IOB (5%),  $\gamma$ -electroactive bacteria (30%),  $\gamma$ -Thiomicrospira (12%), SRB (10%) and uncultured Bacteroidetes (10%) (Fig. 4. column 3&4 of chapter 2.1). After 14 weeks a community shift was identified towards SRB (5%),  $\gamma$ -IOB (4%) and  $\gamma$ -electroactive bacteria (31%). *Thiomicrospira* species were replaced by  $\alpha$ -Rhodobacteraceae (13%) and uncultured Bacteroidetes of (8%) (Fig. 4. column 6&7 of chapter 2.1). Electroactive bacteria, SRB, IOB and Rhodobacteraceae that play a crucial role in MIC, dominate the biofilm community at the bottom of the ballast tank. The overall PCR-DGGE results highlight the strong genetic variability between water phase and biofilm community and their fast adaption to different conditions such as darkness, low temperature and low nutrient availability. It is well known from literature that environmental changes influence biofilm formation and growth conditions.

The exact structure of any biofilm is probably a unique feature of the environment, in which it develops. Under natural conditions, monospecies biofilms are rare; as a result most biofilms are composed of mixtures of microorganisms. This adds to the interspecies and intraspecies interactions and to the general complexity of the macromolecular mixture present. Differences in bacterial species composition of biofilm consortia and resulting differences in metabolic activities within such biofilms could explain why, in two identical systems under the same environmental conditions, corrosion rates can vary significantly. For example, carbon steel corrosion can vary from a rate of 0.05 mm/year in one system to 3 mm/year in another. This phenomenon has been reported for steel piling structures in several European harbors and has also been observed in certain secondary oil recovery systems (Beech, in review). Consortia of metal depositing bacteria (MDB) and SRB often exist as biofilms on corroding metal surfaces.–Until now these kind of research was limited by possible identification techniques. Such type of consortium is unlikely to be fully revealed by only cultivation techniques. Molecular tools developed in the last decades overcome this limitations imposed by traditional cultivation techniques and have been used to study bacterial diversity in corrosive biofilms that form in diverse environments. Several studies revealed synergism between SRB, Clostridia and Enterbacteriaceae in accelerating metal corrosion (Bermont-Bouis et al. 2007, Duan et al. 2008; Jan-Roblero et al. 2008). The results indicate that after 14 weeks, Bacteroidetes and Proteobacteria forming electroactive biofilms dominated the biofilms in both investigated zones of the ballast tank. Immersion zone and sediment were chosen as representative areas typically influenced by pitting corrosion as explained before. These bacteria can influence the corrosion process on the steel surface due to kinetic mechanisms in form of electron shuttling by exopolymeric compounds and conductivity of the biofilm itself (Beech and Campbell 2004; Heyer et al. 2009).

### 3.5 Corrosion processes in the ship ballast tank

#### Open circuit potential

It is well known that active passive alloys in natural seawater undergo a shift of open circuit potential (OCP) towards more noble potential values. This behaviour in marine environments was experimentally correlated to the presence of a biofilm (Mollica 1976). Fig. 4 showed the measured OCP of carbon steel at near surface immersion zone and sediment zone in the ballast tank, over the experiment period of 14 weeks. Each data point is an average of three replicate measurements.

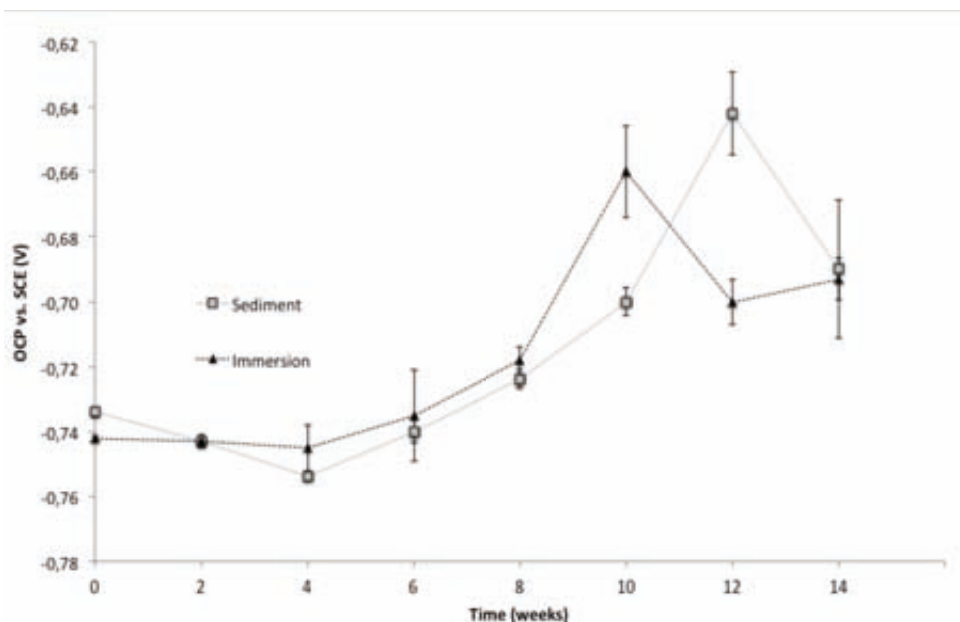


Figure 4. OCP values against SCE electrode - triangle: immersion zone; square: sediment zone. Bar indicates standard deviation of duplicate measurements.

The OCP measurements of the carbon steel exposed to both the zones in the ballast tank showed a gradual shift towards noble potential. The measured value were  $\sim -0.73$  V at the start of the experiment and reached a maximum value of  $\sim -0.64$  V for both immersion and sediment zone. The data are in agreement with potential data monitored by (Beech and Campbell 2008) reporting OCP values between  $-0.71$  V to  $-0.68$  V for electrodes covered with a biofilm after 55 days. The measured data give an indication that a biofilm was formed on the electrode surface confirmed by PCR-DGGE analysis.

*Corrosion rate*

LPR measured corrosion rate in Fig. 6 showed a sharp increase during the initial four weeks in both immersion and sediment zone of the ballast tank. Thereafter, corrosion rate gradually decreased over the experimental period of 14 weeks. The decrease could be due to formation of a thicker corrosion layer on the surface that will lower the overall corrosion rate or oxygen diminishing effects in the stagnant environment. The average corrosion rate was ~ 0.6 mm/y for both zones. Immersion zone showed a slightly higher corrosion rate than the sediment zone, this could be due the difference in dissolve oxygen concentrate near the surface layer. Our findings are in agreement with the literature (Beech 2008) reported corrosion rates of 0.518 mm/y.

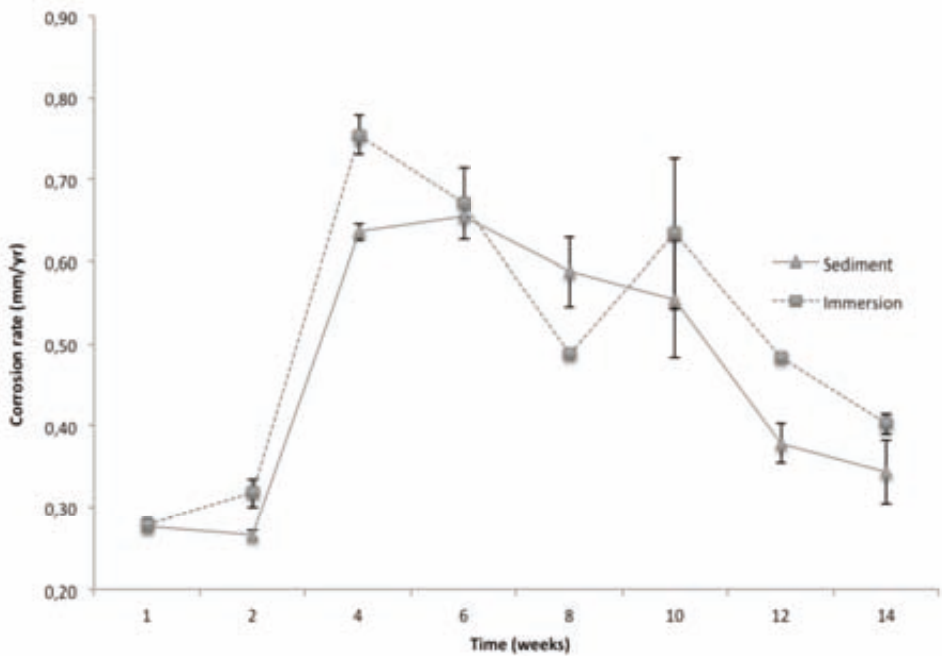


Figure 5. Corrosion rate gained from LPR measurements of carbon steel in immersion and sediment zone of the ship ballast tank over the period of 14 weeks. Bar indicates standard deviation of duplicate measurements.

*Pitting index*

Table 2 represent the pitting indexes which were determined using stereomicroscope after cleaning the surface of the carbon steel working electrodes. The pitting that was observed on the electrode surface support findings reported by (Starrovetsky et al. 2001, Beech and Campbell 2008, Faimali et al. 2010) who described that ennoblement is coupled to pitting corrosion in the presence of bacteria.

Table 2. Pit depth of carbon steel coupons exposed to different levels in ballast tank.

Zone	Pit depth (micron), 10 individual pits										Average depth
Immersion	10	12	16	6	9	34	19	12	24	27	17
Sediment	31	23	19	24	37	31	15	22	24	33	26

The averaged pit depth values measured from the 10 different pits showed higher pitting in the sediment zone than the immersion zone. Sediment zone (average pit depth 26  $\mu\text{m}$ ) is strongly influenced by pitting than immersion zone (average pit depth 17  $\mu\text{m}$ ). The values are relatively low as compared to the previous studies and reports of ballast tank corrosion who claim an average corrosion rate within ship ballast tanks of 0.2 mm/y (Suzuki et al. 2004; Tamburri et al. 2002). Huang et al. (1997) has documented excessive pitting corrosion up to 2 mm/yr in the uncoated carbon steel bottom plating and other authors even 6 mm/yr for the bottom plating (Cleland, 1995). The reduced pit depths in this study are a result of the relatively low water temperature.

*3.6 DGGE results v/s pitting corrosion*

The DGGE analysis revealed that the genetic variability between the water phase and biofilm were significant. Overall, the bottom zone was more dominated by MIC bacteria such as (*Gallionella*, *Thiomicrospira* and *Desulfobacteraceae*) than the immersion zone (irrespective planktonic or sessile). Higher pitting rates at the bottom zone could be due to synergetic effects of various bacterial groups such as acid producing bacteria, slime producing bacteria, sulphur-oxidizing, sulphate reducing and metal oxidizing bacteria enabling the proliferation of local corrosion damage. For example, corrosive SRB bacteria were active in the biofilm developed in the sediment zone within the first four weeks, which were not found in the immersion zone biofilm. SRB produce hydrogen sulfide that can react with steel in sulfate-containing environments. Sulfide produced by the SRB then migrates to edges of the deposits where it can be oxidized to thiosulphate or reduce to elemental sulfur which are well-known activator of pitting corrosion (Felder and Stein 1994; Jones and Amy 2002). This initial activity of SRB in the sediment zone probably contributed to more pitting.



In contrast, the pitting depths that were measured were not as comparable to that reported for the ship ballast tank. Environmental conditions have to be taken into account such as bacterial growth and activity. Bacterial metabolic activity strongly depends on temperature (10°C rule, increase of 10°C will double metabolic reaction kinetic) and due to the fact that the overall temperature was relative low during the experimental period, we can assume the lowest possible indication of bacterial metabolic activity and therefore the gained corrosion rates will indicate the lowest possible rate. If a higher temperature is to be considered, the corrosion will increase, due to kinetic reactions rates enhancing the process of corrosion and on the other hand due to a higher growth rates. The results highlight the strong genetic variability among these bacterial populations and their fast adaptability to different conditions, underlining a correlation between electrochemical activity and composition of microbial populations. It was possible to show that the sediment zone is strongly influenced by pitting than the immersion zone supported by the presence of *Denitromonas* and SRB forming a closed loop of metabolic interactions by utilizing the metabolic compounds of the SRBs (sulfide or thiosulfate) as an electron acceptor. Such type of consortium is unrevealed by only cultivation techniques. But it has to be mentioned here that if the right media are used cultivation techniques may be as good as molecular ones. Nevertheless the combination of OCP and the use of DGGE as a screening tool can be one way in the future to monitor corrosion behaviour in enclosed seawater environments.

#### 4. Conclusions

A marine electrochemical active biofilms was developed in a closed seawater system under mature conditions (stagnant for 14 weeks). The genetic variability between water phase and biofilm could be identified by PCR method. Higher pitting rates could be found at bottom of the tank due to synergetic effects of various bacterial groups and especially due to the presence of SRB at the early stages of biofilm formation. The results in this study clearly point out how important that PCR-DGGE work can be one way in the future to determine the type of bacterial species in such a specific enclosed environment. The combination of molecular tools and electrochemistry can be one of the future aims to combat microbial corrosion in marine environments for the ship industry. A more effective monitoring and treatment system in form of effective preventing and treating biofilms on sidewalls of ship ballast tanks will help to reduce costly material replacements. Therefore, any measure for controlling aquatic invasive species in ballast tanks should also consider the impact on corrosion from the sessile communities, which has been an underestimated problem so far. The results presented here provide useful information for further studies of corrosion in ship ballast tanks and up scaled MIC laboratory studies.

The work also summarizes for the first time the problem of attached biofilms in the field of corrosion in ship ballast tanks and will open new ways in practical applications to combat this serious corrosion problem.

## References

ASTM G1-90 1999, Standard Practice for Preparing, Cleaning, and Evaluating Corrosion Test Specimens. NACE, Houston TX.

Beech IB, Sunner J. 2004. Biocorrosion: towards understanding interactions between biofilms and metals, *Curr. Opin. Biotechnol.* 15:181-186.

Beech IB, Campbell SA. 2008. Accelerated low water corrosion of carbon steel in the presence of a biofilm harbouring sulphate-reducing and sulphur-oxidising bacteria recovered from a marine sediment. *Electrochimica Acta* 54: 14-21.

Bermont-Bouis D, Janvier M, Grimont PAD, Dupont I, Vallaey, T. 2007, Both sulfate-reducing bacteria and Enterobacteriaceae take part in marine biocorrosion of carbon steel. *Journal of Applied Microbiology*, 102:161–168.

Boon N, de Windt W, Verstraete W, Top EM. 2002. Evaluation of nested PCR–DGGE (denaturing gradient gel electrophoresis) with group-specific 16S rRNA primers for the analysis of bacterial communities from different wastewater treatment plants. *FEMS Microbiol. Ecol.* 39:101-112.

Cleland JH. 1995. Corrosion risks in ships'ballast tanks and the IMO pathogen guidelines. *Engineering Failure Analysis*, Vol. 2, p. 79-84.

Duan J, Wu S, X. Zhang, Huang G, Du M., Hou B 2008. Corrosion of carbon steel influenced by anaerobic biofilm in natural seawater, *Electrochimica Acta* 54:22-28.

Farmali M, Chelossi E, Pavanello G, Benedetti A, Vandecandelaere I, de Vos P, van Damme P, Mollica A. 2010. Electrochemical activity and bacterial diversity of a natural marine biofilm in laboratory closed-systems. *Bioelectrochemistry* 78:30-38.

Felder CM, Stein AA. 1994. Microbiologically influenced corrosion of stainless steel weld and base metal-four-year field test results. *Corrosion* 50:275.

Fonesca ITE, FMJ, Lino AR, Reis MA, Rainha VL. 1998. The influence of the media on the corrosion of mild steel by *Desulfovibrio desulfuricans* bacteria: an electrochemical study. *Electrochimica Acta* 43:213-222.

Gollasch S, 2002a. The importance of ship hull fouling as a vector of species introductions into the North Sea. *Biofouling* 18:105-121.

Gollasch S, 2002b. Ballast water management in the north-east Atlantic, in: F., T. (Ed.), Report to aid decision making on ballast water in the Oslo-Paris Commission (OSPAR). Biological Diversity Committee. North Sea Directorate, the Netherlands, p. 48.

Heyer A, D'Souza F, Ferrari G, Mol JMC and de Wit JHW. 2009. Microbiologically influenced corrosion (MIC) in a simulated ship tank model system. Proceedings of Eurocorr paper no. 7852.

Hewitt CL, Campbell ML, 1999. The introduced species of Port Phillip Bay, Victoria. Thresher RE, Martin RB. Eds. Centre for Research on Introduced Marine Pests Technical Report No. 20. CSIRO Marine Research, Hobart.

Huang RT, McFarland BL, Hodgman RZ. 1997. Microbial influenced corrosion in in cargo oil tanks of crude oil tankers, NACE, Houston, USA.

Hülsmann N, Galil BS. 2002. Protists – a dominant component of the ballast – transported biota., in: Leppäkoski E., G.S., Olenin S. (Ed.), *Invasive aquatic species of Europe: distribution, impact and management*. Kluwer, Dordrecht, pp. 20-26.

International Maritime Organization (IMO). 2005. International Convention on the Control and Management of Ship's Ballast Water and Sediments. International Maritime Organization, London, United Kingdom; [www.imo.org](http://www.imo.org).

Jan-Roblero J, Posadas A, Zavala Díaz de la Serna J, García R, C.Hernández-Rodríguez C. 2008. Phylogenetic characterization of bacterial consortia obtained of corroding gas pipelines in Mexico, *world Journal of Microbiology and Biotechnology* 24:1775-1784.

Jones DA, Amy PS. 2002. A thermodynamic interpretation of microbiologically influenced corrosion, *Corrosion* 58:638-645.

Little BJ, Lee JS, 2007. *Microbiologically Influenced Corrosion*, . Wily Interscience Wiley & Sons, Inc., Hoboken New Jersey.

Ludwig W, Strunk O, Westram R, Richter L, Meier H, Yadhukumar, Buchner A, Lai T, Steppi S, Jobb G, et al. 2004. ARB a software environment for sequence data *Nucl. Acids Res.* 32:1363-1371.

Marty F, Ghiglione JF, Païssé S, Gueuné H, Quillet L, van Loosdrecht MCM and Muyzer G. 2012. Evaluation and optimization of nucleic acid extraction methods for the molecular analysis of bacterial communities associated with corroded carbon steel *Biofouling* 28:363-380.

Mollica A, Trevis A. 1976. Correlation entre la formation de la pellicule primaire et de la modification de la cathodique sur des aciers inoxydables expérimentés en eau de mer aux vitesses 0.3 à 5.2m/s, Proc. Fourth Congress on Marine Corrosion and Fouling, Antibes, France. p. 351–365.

Muyzer G. 2000. Genetic fingerprinting of microbial communities - present status and future perspectives. Atlantic Canada Society for Microbial Ecology, Halifax.

Schäfer H, Muyzer G. 2001. Denaturing gradient gel electrophoresis in marine microbial ecology. *Methods Microbiol* 30:425-468.

Smalla K, Oros-Sichler M, Milling A., Heuer H., Baumgarte S, Becker R, Neuber G, Kropf S, Ulrich A, Tebbe CC. 2007. Bacterial diversity of soils assessed by DGGE, T-RFLP and SSCP fingerprints of PCR-amplified 16S rRNA gene fragments: Do the different methods provide similar results? *Journal of Microbial Methods* 69:470-479.

Starosvetsky JO, Armon R, Yahalom Y, Starosvetsky D. 2001. Pitting corrosion of carbon steel caused by iron bacteria. *Inter.Biodeter. & Biodegrad.* 47:79.

Suzuki S, Muraoka R, Obinata T, Endo S, Horita T, Omata K. 2004. Steel products for shipbuilding. JFE Technical Report No. 2.

Tamburri MN, Wasson K, Matsuda M. 2002. Ballast water deoxygenation can prevent aquatic introductions while reducing ship corrosion. *Biological Conservation* 103: 331-341.

## Chapter 3

### 3.1 *Corrosion behavior of ballast tank steel in the presence of sulphate-reducing and acid-producing bacteria*

#### **Abstract**

Microbiologically influenced corrosion (MIC) is a serious problem in the marine environment for industries such as the shipping industry. Generally, MIC is a localized, pitting-type corrosion, so a relatively fast rate of failure has been reported as compared to abiotic, anaerobic corrosion. The influence on localized corrosion on carbon steel by two anaerobic bacterial strains isolated from a ship ballast tank was investigated by using linear polarization resistance (LPR), electrochemical impedance spectroscopy (EIS), scanning electron microscopy (SEM) and energy-dispersive analysis (EDX). The results show that the corrosion rate increased in the presence of bacteria, in comparison with the rate observed in the sterile medium for the same exposure time. Localized corrosion attack in the form of pitting was observed on the steel surface in the presence of bacteria. The synergy of sulfate-reducing bacteria (SRB) and acid-producing bacteria (APB) yielded the highest general corrosion rate. The interactions between the metal surface, abiotic corrosion products, chloride anions, bacterial cells and their metabolic products in the presence of both SRB and APB increased the general corrosion rate but lowered the accelerated local corrosion attack relative to SRB and APB alone.

## 1. Introduction

Ballast water tanks, with their complex structural architecture, have a high surface-area-to-volume ratio, and large areas of biofilms can accumulate in them to form “interior hull fouling.” Most abundant aquatic organisms, including species provoking MIC, are transported in ballast water [1, 2] all over the world. Field experiments have demonstrated that biofilm communities are formed on multiple types of artificial surfaces deployed in a ballast tank during a transoceanic voyage [3]. These communities contain SRB as well as APB, which grow synergistically [4]. On the one hand, the biofilm forms a barrier layer, reducing the exposure of the solid surface to the external environment. However, on the other hand, it can also result in localized corrosion of the metal and deterioration of polymers [5, 6]. The presence of microorganisms on a metal surface often leads to highly localized changes in the concentration of electrolytes, pH and oxygen concentration [7, 8]. These microorganisms and their metabolic activity severely influence the corrosion process, i.e., they often stimulate localized corrosion. Nevertheless, the importance of microbial synergy on carbon steel in the presence of anaerobic SRB and APB is still unknown. The purpose of this study is to investigate the influence of microbial synergy in the presence of SRB and APB, isolated from a ship ballast tank, on carbon steel ASTM A131 grade EH36 by interdisciplinary electrochemical and microbiological techniques. Electrochemical impedance measurements are suitable for biofilm monitoring since small potential perturbations have only a minor effect on bacteria [9]. The drawback of this method is that changes in culture media and bacterial metabolism during growth may significantly influence the measurements [10-12]. Therefore, a correlation of electrochemical analysis with the extent of bacterial adhesion is necessary. For this, we combined SEM-EDX microscopy and fluorescent imaging techniques together with EIS to study bacterial attachment, corrosion attack morphology and corrosion product formation.

## 2. Experimental

### 2.1 Metal sample preparation

For electrochemical measurements, electrodes from carbon steel grade EH36 were mounted in epoxy resin and the surface ground up to 2400 SiC-paper (Struers) to obtain a smooth surface. The ground probes with an exposed surface area of 1 cm<sup>2</sup> were used as working electrodes in duplicate.

### 2.2 Microbial techniques

#### 2.2.1 Biofilm sampling

For biofilm sampling, a real ship ballast tank was investigated in the dry dock period of the ship. Inside the ballast tank, the sidewall was scraped using a sterile cotton swab. An area of 20 cm<sup>2</sup> was scraped, and both the swab and attached material was placed in a sterile 50 ml centrifuge tube.

The end of the swab was broken off, leaving the cotton sample end in the tube filled with sterile ASW for transportation. Duplicate samples were taken of the biofilm; the tubes were capped, transported in a dark, insulated cooler to the laboratory and processed immediately.

### 2.2.2 Medium

*Sulphate-reducing bacteria* and *acid-producing bacteria* were isolated from the ship ballast tank. The cultures were enriched and purified from the natural rust layer biofilm by sub-culturing in the lab (data not shown). Cultures were maintained continuously in a recommended liquid medium for SRB (DSM15121) and APB (DSM142) from the Deutsche Sammlung von Mikroorganismen und Zellkulturen (DSMZ, Germany). APB growth was revealed by a change in color from red to yellow of the fermentative anaerobic culture medium. Electrochemical measurements were performed using low-nutrient loaded artificial seawater (ASW) to simulate natural seawater conditions. The modified medium consisted of two parts. Part A consisted of NaCl 23.93 g; Na<sub>2</sub>SO<sub>4</sub> 4.01 g, KCl 0.68 g, NaHCO<sub>3</sub> 0.197 g, KBr 0.099 g, H<sub>3</sub>BO<sub>3</sub> 0.03 g and NaF 0.01 g dissolved in 750 mL deionized water. Part B consisted of 1.0M MgCl<sub>2</sub>·6H<sub>2</sub>O 53.27 ml, 1.0M CaCl<sub>2</sub>·2H<sub>2</sub>O 10.33 ml and 1.0M SrCl<sub>2</sub>·6H<sub>2</sub>O 0.90 ml. Parts A and B were combined into 1 liter. Modification was made by an additional nutrient supply of 4.2 ml lactate and 0.01 g yeast extract. The medium was sterilized by autoclaving for 20 min at 121°C at 1.5bar. The pH of the medium was 7.5±0.3 for in the experimental setup. For both enrichment strains, a supplementary solution containing FeSO<sub>4</sub>·H<sub>2</sub>O 0.004 g, Na<sub>3</sub>C<sub>6</sub>H<sub>5</sub>O<sub>7</sub>·2H<sub>2</sub>O 0.30 g and C<sub>6</sub>H<sub>8</sub>O<sub>6</sub> 0.10 g dissolved in 10 ml distilled water was added to support growth.

### 2.2.3 Bacterial cultivation and inoculation

Experiments were performed in acrylic tubes with a total volume of 120 ml (10.5 cm diameter and 8 cm height, Fig. 1a). The electrochemical tubes were filled with 80 ml sterile ASW medium and inoculated with 20 ml bacterial culture from the exponential phase (10<sup>7</sup> cells/ml). SRB growth was supported by gently flushing with N<sub>2</sub> for 5 min. Bacterial cultures were run in semi-continuous mode: 50% medium was removed under sterile conditions and replaced with an equal amount of fresh medium stripped with N<sub>2</sub> to supply enough nutrients once a week. For the dual culture experiment, 10 ml of each culture was used as inoculum. The blank control contained sodiumazide to avoid bacterial growth over the course of the experiment.

## 2.3 Electrochemical measurements

### 2.3.1 Electrochemical cell setup

All measurements were performed in a custom-made setup to simulate the corrosion processes on uncoated steel type ASTM A131 grade EH36 typically used for ballast tank structures (Fig. 1b). The tubes were sealed on both edges; the working electrodes were fixed in a vertical position to avoid accumulation of corrosion products over the course of the experiment. A standard Ag/AgCl electrode (Ref 201 Red rod, Radiometer Analytical, France) was used as a reference electrode in combination with a platinum mesh counter electrode. All potential values presented in this paper are relative to the Ag/AgCl reference electrode.

The counter and the reference electrode were sealed in the cell; a detailed schematic overview can be seen in Fig. 1a. The cells and all components were sterilized with 70% EtOH for 1h prior to assembly and mounted under sterile clean bench conditions. As a reference, blank measurements were performed containing no bacteria.

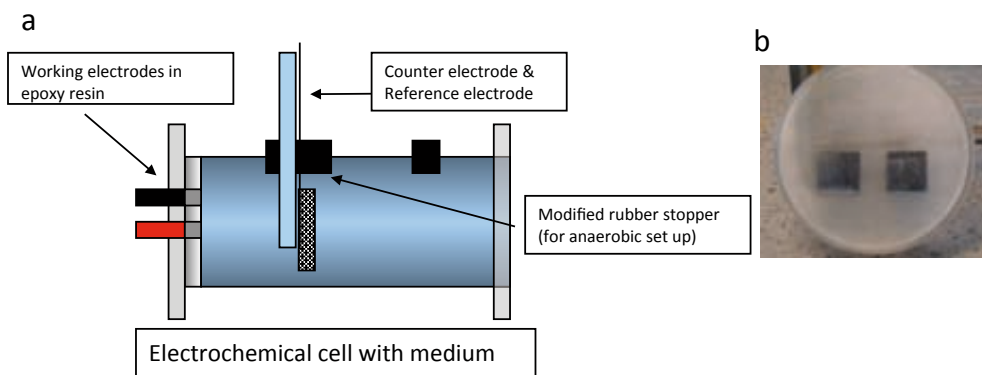


Fig. 1. Experimental setup of the electrochemical cell. a. Electrochemical cell and vertically arranged working electrodes; b. Optical micrograph of the duplicate working electrodes embedded in epoxy resin.

### 2.3.2 Open circuit potential (OCP), linear polarization resistance (LPR) and electrochemical impedance spectroscopy (EIS) measurements

All electrochemical measurements were performed using a potentiostat (IVIUM Technologies, Netherlands) controlled by IVIUM software version 1.901. The OCP of the carbon steel was monitored by determining the potential difference between the metal immersed (the carbon steel) and a reference electrode of Ag/AgCl; during the measurement, no external potential was applied. Linear polarization resistance (LPR) was measured using a potentiodynamic method to obtain the potential current (E-I) ratio, applying  $\pm 10$  mV overpotential, with respect to the OCP. EIS measurements were performed at the OCP using a 10 mV amplitude sinusoidal signal over frequencies ranging from 10.000 to 0.01 Hz at 21°C over an exposure time of 21 days in total. The impedance data was analyzed acquiring equivalent circuits by using software Z<sub>view</sub> 3.0 (Scribner Associates Inc., USA). The goodness of the fit was evaluated by using error plots, and the data was validated by Kramer-Kronig transform analysis [13-15].

## 2.4 Surface analysis

### 2.4.1 Epifluorescent microscope (EFM)

Bacterial colonization of the working electrode surface for the biotic and abiotic setups was studied after the total exposure time of 21 days. Electrode surfaces were gently rinsed twice with sterile oxygen-free deionized water. The nucleic acid dye 4,6-diamidin-2-phenylindole DAPI (25μM) was used for staining. Bacterial biofilms were imaged at 20x magnification using an Olympus BX51 fluorescent microscope (Olympus America Inc., USA).



The data obtained from the electrodes was used to calculate the surface coverage with AnalySIS 5.0 imaging software (Olympus America Inc., USA).

2.4.2 Scanning electron microscope (SEM) and energy-dispersive X-ray (EDX) analysis

The electrode surfaces were examined for their surface biofilm and corrosion features using SEM and EDX. The samples were dried in a nitrogen atmosphere to determine the corrosion layers and stored in a glove box (Interflow) in a nitrogen atmosphere until imaging. The SEM JSM-5800LV (Joel, Japan) was operated at an accelerating voltage of 10kV with a working distance of 12 mm at 100x magnification. For energy-dispersive X-ray (EDX) spectroscopic analysis, the system was equipped with a Noran 5 elemental analyzer (Thermo Scientific, Germany). NSS 2.2 x-ray microanalysis (Thermo Scientific, Germany) analysis software was used for elemental analysis. Subsequently, the steel surface was stripped of corrosion products by adding Clarke acid cleaning solution (1l 36% HCl, 20g Sb<sub>2</sub>O<sub>3</sub> and 50g SnCl<sub>2</sub>) for 10-15 sec. The exposed sample surface was finally rinsed with distilled water, cleaned in absolute ethanol and dried under nitrogen flow before the final analysis of the corrosion attack morphology.

3. Results and Discussion

3.1.OCP vs. time

The bacteria isolated from a ship ballast tank were identified as an anaerobic acid-producing species and sulfate-reducing bacteria. Figure 2 shows the variations of the OCP of steel with immersion time in a sterile medium, APB, SRB and SRB+APB solutions vs. Ag/AgCl. The error bars given justify the significance of differences found for the different bacterial setups.

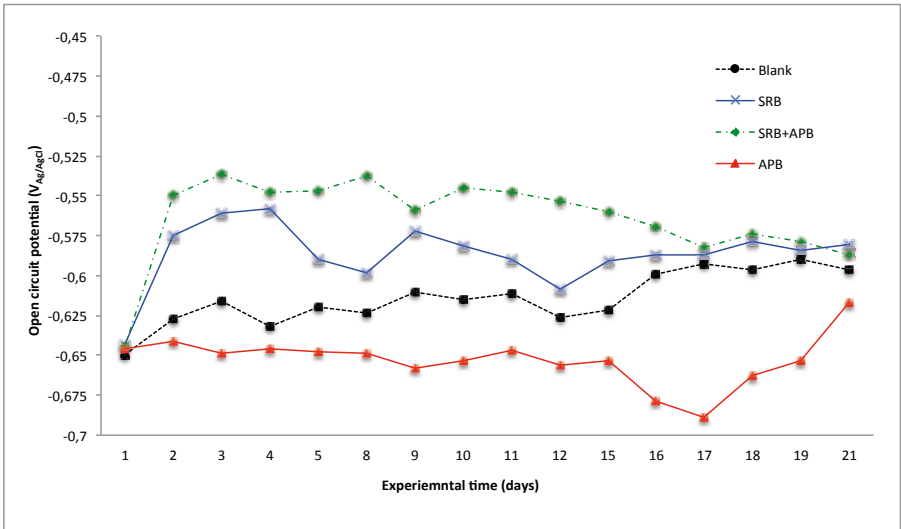


Fig. 2. Variation of the OCP with time for carbon steel. Blank (dot), SRB (cross), SRB+APB (rhomb) and APB (triangle) represent shifts in the OCP over time in different bacterial solutions.

This method has the lowest impact on microbial activity and settling properties. The general trend among electrochemical techniques in the field of MIC seems to be that OCP measurements are considered to be one of the safest methods in recognizing and monitoring MIC because they do not impose voltages upon microbes [16, 17]. Moreover, OCP changes provide important qualitative information about both the ongoing corrosion process and environmental conditions. In the blank test cell, the OCP was found to remain relatively constant, staying in the range of -712mV to -661mV during the 21-day exposure. The SRB culture showed a clear increase to -597mV after establishing bacterial growth in the cell; this shift is coupled to sulphide production by bacterial activity. This ennoblement shift of 100 mV is typical for carbon steel immersed in pure cultures of SRB [18-20]. The OCP shifts for the SRB culture are consistent with the sequential medium refreshment after seven and 14 days. After each refreshment, a significant increase in OCP can be found due to bacterial activity reaching OCP values of -605mV and -607mV. For the mixed species, a similar behavior of the OCP was found with two maximum peaks after the medium exchange. Values of -621mV were measured, indicating a shift to more positive values in the range of 100 mV. The lowest impact on the OCP were found for the APB alone. The value increases slightly from -708mV to -643mV over the experimental time of 21 days. This is a slight increase in the noble direction of around 50 mV but not as significant as for the combination with SRB or SRB alone.

3.2 EIS measurements

Electrochemical impedance measurements were conducted with all electrochemical cells inoculated with diverse bacterial cultures. Impedance spectra obtained experimentally were analyzed using Z plot equivalent circuit software; two time-constant equivalent circuits in Fig. 3 are proposed as the base for the models for the carbon steel/solution systems.

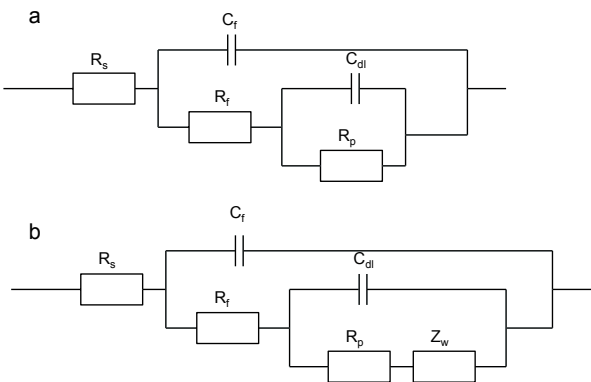


Fig. 3 Two equivalent circuits used in the fitting impedance data of carbon steel at different conditions. a. Circuit used for blank b. Circuit used for bacterial presence.

Data for carbon steel in sterile medium was first analyzed using the equivalent circuit illustrated in Fig. 3a; the impedance expression is written as formula (1). It was necessary to use the circuit in Fig. 3b for a better fit of the data in the presence of bacteria, where a Warburg impedance ( $Z_w$ ) was introduced to account for a diffusion process within a heterogeneous surface layer over the metal using formula (2). The two time-constant equivalent circuits fitted the impedance at all frequencies.

$$Z = R_s + \frac{1}{j\omega C_f + \frac{1}{R_f} + \frac{1}{j\omega C_{dl} + \frac{1}{R_p}}}$$

(1)

$$Z = R_s + \frac{1}{j\omega C_f + \frac{1}{R_f} + \frac{1}{j\omega C_{dl} + \frac{1}{R_p + Z_w}}}$$

(2)

$R_s$  represent the electrolyte resistance,  $R_f$  and  $C_f$  represent the resistance and capacitance of a heterogeneous surface layer and  $R_p$  and  $C_{dl}$  represent the polarization resistance and double layer capacitance, respectively.  $Z_w$  represents the diffusion impedance through the porous film layer. In addition, both  $C_f$  and  $C_{dl}$  were replaced with a constant phase element (CPE) in the fitting procedure due to the non-ideal capacitive response of the interface carbon steel/solution. The impedance of CPE is written as  $Z_{CPE}=Y_o^{-1}(j\omega)^{-n}$ , where  $w$  is the angular frequency in rad/s,  $Y_o$  is the admittance magnitude of CPE that can be approximately converted into a capacitance and  $n$  is the exponential term that can vary between 1 for pure capacitance and 0 for pure resistor [21]. In this context,  $n$  can be used as the measure of surface inhomogeneity, its decrease being correlated to an increase in surface metal roughening [22]. The fitted results of EIS spectra for carbon steel in sterile medium and for 3 different bacterial solutions are given in Table. 1. The goodness of the fit is presented by Chi squared in Table 1. Data validation was performed by a Kramers-Kronig transform analysis, indicating a good fitting procedure because the data shows a non-steady state or non-linear behavior.

**Table 1** Fitted results for EIS spectra after 21 days of exposure.

	R1 [Ω*cm <sup>2</sup> ]	Y <sub>o-f</sub> [Ω <sup>-1</sup> *cm <sup>-2</sup> ]	n <sub>f</sub>	R <sub>f</sub> [Ω*cm <sup>2</sup> ]	Y <sub>o-dl</sub> [Ω <sup>-1</sup> *cm <sup>-2</sup> ]	n <sub>dl</sub>	R <sub>p</sub> [Ω*cm <sup>2</sup> ]	Z <sub>w</sub> [Ω <sup>-1</sup> ]	Chi-squared
Blank	10,4	5,3*10 <sup>-5</sup>	0,97	5460	2,87*10 <sup>-5</sup>	0,67	2,50*10 <sup>5</sup>	-	5,2*10 <sup>-4</sup>
APB	11,0	4,7*10 <sup>-4</sup>	0,90	369	2,21*10 <sup>-5</sup>	0,70	5,53*10 <sup>4</sup>	7,78*10 <sup>-5</sup>	6,6*10 <sup>-4</sup>
SRB	11,4	3,8*10 <sup>-4</sup>	0,86	158	2,32*10 <sup>-5</sup>	0,71	4,48*10 <sup>4</sup>	8,41*10 <sup>-5</sup>	5,8*10 <sup>-4</sup>
SRB+APB	10,7	8,2*10 <sup>-4</sup>	0,93	117	2,35*10 <sup>-5</sup>	0,73	3,89*10 <sup>4</sup>	5,32*10 <sup>-5</sup>	3,5*10 <sup>-4</sup>

The value of  $n_f$  for carbon steel in the sterile medium was found to be close to one, which reflects some degree of film heterogeneity. A lower value of  $n$  was observed in the presence of APB, SRB+APB and SRB. The lowest value was found in the presence of SRB. The decrease of  $n_f$  values indicates the increment of the surface inhomogeneity due to corrosion. The surface roughness is influenced by patchy biofilms leading to localized corrosion that increases the surface heterogeneity. The values of  $R_f$  and  $R_p$  at the same exposure time of carbon steel and three bacterial solutions can be ranked by size: R (sterile medium) followed by APB, SRB and SRB+APB. This decrease in  $R_f$  and  $R_p$  values indicates an increment in the corrosion rate, which could be due to the metabolic synergies between the metal surface, abiotic corrosion products, and bacterial cells and their metabolic products, which are produced and remain in the biofilm at the metal surface.

3.3 LPR measurements correlated to bacterial surface coverage

LPR is the electrochemical technique probably most used for monitoring purposes [23] for corrosion rate measurements. To avoid interference from fouling on top of the electrode [23], very slow scan rates were applied to maintain steady state conditions, avoiding an overestimation of the corrosion rate [24]. In a second step, this corrosion rate data was linked to the bacterial surface coverage by epifluorescence microscopy after terminating the experiment. Both sets of data were combined in Fig. 4, illustrating the surface coverage in percentages combined with the corrosion rate after 21 days.

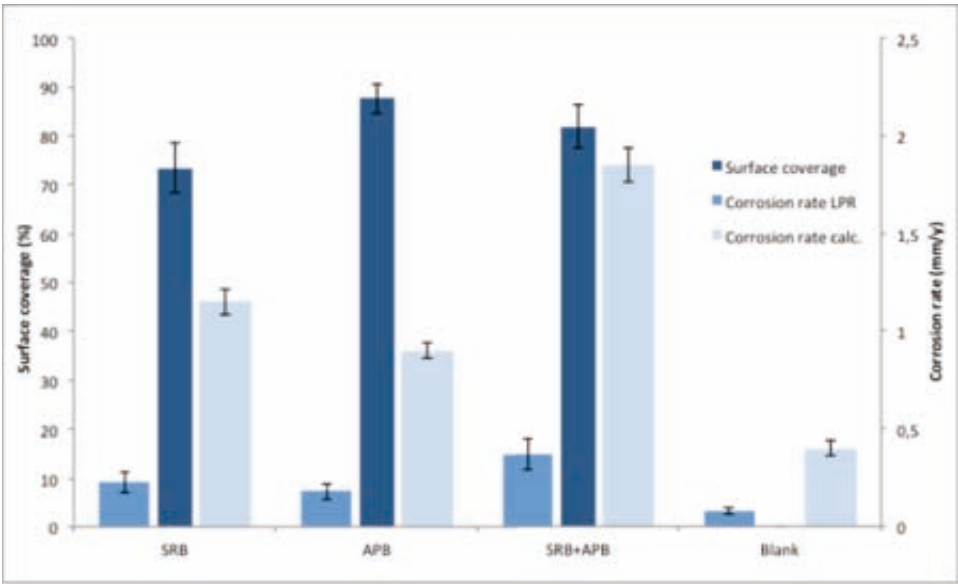


Fig. 4. Comparison between bacterial surface coverage (%) (first axis) and corrosion rate (mm/y) (second axis) of carbon steel exposed to different bacterial solutions. The first column corrosion rate is determined by LPR (mm/y), the second column surface coverage by bacteria (%) and the third column corrosion rate is calculated in (mm/y).

As shown in Fig. 4, surface coverage and corrosion rate are not related. All biological test solutions indicate a surface coverage of 73% for SRB, 87% for APB and 82% for SRB+APB. That demonstrates that for all test setups, a significant change in bacterial growth could be found, and biofilm formation was present as indicated in the SEM images in section 3.3. A clear difference could be found for the corrosion rates in the different bacterial solutions. This was observed before by [25] showing that a high concentration of bacteria does not necessarily imply that the corrosion rates increase. The blank set indicated a very low corrosion rate of 0.10 mm/y after 21 days for the carbon steel. A clear sign for an anaerobic test setup where corrosion is prevented on the metal surface. APB bacteria indicated the lowest corrosion rate with a value of 0.18 mm/y compared to SRB and the mixed species. For the SRB, a rate of 0.23 mm/y could be found. The highest rate was discovered for the mixed species of SRB+APB with 0.37 mm/y. This increment in the corrosion rate can be explained by the combination of both species: a hydrogen sulphide-producing bacteria and an organic acid-producing bacterium on the other side will create an aggressive local environment enhancing the general corrosion process [8] even under anaerobic conditions. If a realistic corrosion rate is considered based on the surface defects, the corrosion rate is in general five times higher than the measured rates by LPR [4]. The third column for each setup highlights the calculated corrosion rates in diagram 4. The columns indicate that the corrosion rate determined by LPR alone underestimates the real corrosion impact. The values calculated reach maximum values of 1.15 mm/y for SRB, 0.9 mm/y for APB alone and 1.85 mm/y for the mixed species. These results clearly underline how important it is to distinguish between measured corrosion rates and the surface covered by bacteria, which will not necessarily give a clear indication for the severity of corrosion attack and the existent corrosion rate.

### 3.3. SEM-EDX analysis

Supplementary SEM was carried out to verify the corrosion product film on carbon steel in the presence of diverse bacteria. Figure 5 provides the corrosion products developed on the carbon steel surface exposed to: (a) blank, (b) SRB, (c) APB and (d) SRB+APB after 21 days, respectively.

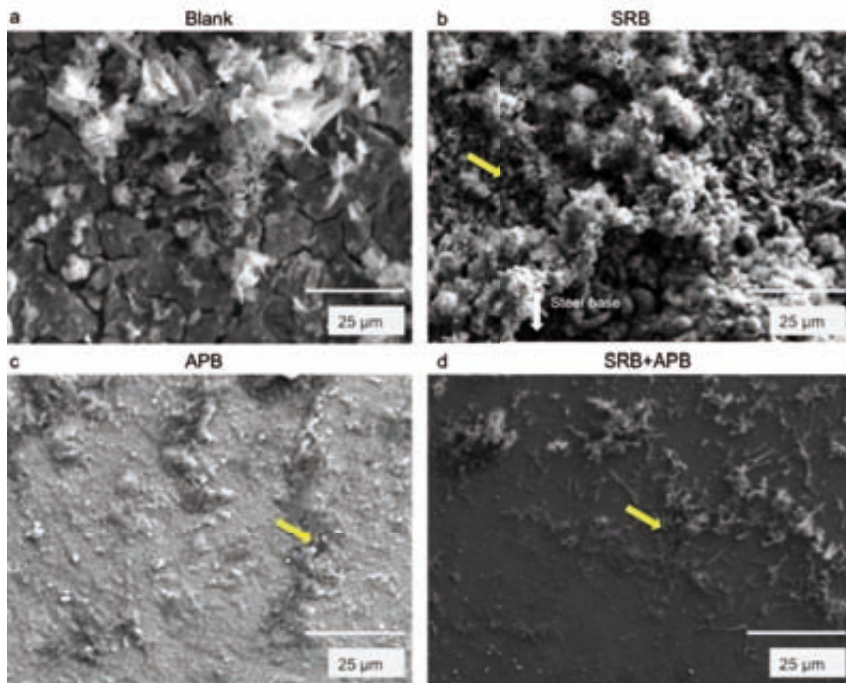


Fig. 5 SEM images providing corrosion products and biofilms formed on carbon steel after 21 days' exposure to bacteria; scale bar 25 µm. (a) Blank, (b) SRB, (c) APB and (d) SRB+APB. Arrows indicate bacterial attachment (biofilm).

For the blank, the corrosion products formed are of a crystalline structure imaged in white (Fig. 5a) whereas the surrounding surface indicated a surface containing various cracks. The surface was still visually smooth and turned gray under anaerobic conditions. Figure 5b illustrates the SRB cells attached to the surface. Bacterial cells can be made out in a net-like structure close to the metal surface (arrow), typically rod-shaped, 2 microns in size and embedded in corrosion products. Corrosion products are brittle and loosely attached to the carbon steel, forming a porous layer of biofilm, iron oxides, iron chlorides and iron sulfides (Table 2). This is demonstrated by the presence of tiny cracks in the sulphide film. As a result, these cracks may lead to active corrosion cells between the sulphide (cathode) and the exposed steel base (anode), inducing local pits (Fig. 5b). In Fig. 5c, the biofilm of APB is presented as filamentous cells, which are embedded in a layer of exopolymeric substances (EPS) (arrow), where the cells adhere to the carbon steel surface. The metal surface itself is smooth and no corrosion products can be observed next to the EPS films, which are heterogeneously distributed over the metal surface. This observation is supported by EDX results in Table 2, indicating no iron oxides on the surface.

Nevertheless, a high sulphur peak was found based on the bacterial metabolism-producing elemental sulfur and thiosulfate, suggesting that bacterial growth was well developed inside the test cell, which was confirmed before by biofilm staining. For the combination of SRB+APB, the carbon steel surface was covered with a filamentous, heterogeneous biofilm (arrow, Fig. 5d).

The metal surface itself is smooth and no clusters of corrosion products were found next to the biofilm. EDX analysis showed mainly iron sulphides on the surface as a clear indication for the presence of SRB+APB on the surface. It can be summarized for the described corrosion product layers that the blank interface exhibits a thin, flat distribution of hard corrosion products at the interface. The biotic interfaces show a high degree of porosity in all cases, and for all bacterial setups a high sulphur content was observed in the individual EDX spectra (Table 2).

**Table 2** EDX results of the corrosion products of the carbon steel after 21 days.

Wt %	Blank	SRB	APB	SRB+APB
C	9.99	-	20.45	40.87
O	8.98	8.48	10.15	-
Si	1.58	-	4.29	-
S	5.85	20.40	21.35	14.37
Fe	65.36	67.16	43.75	24.22

The results of the chemical analysis of biofilms show that iron sulphides are the main metabolites of SRB and APB microorganisms. The element O should be ascribed to the iron oxides produced by the oxidation of sulphide when small quantities of oxygen enter the electrochemical cell. The same can be seen for the blank where iron oxides were found on the steel surface. In a second step, the carbon steel electrodes were cleaned for further SEM investigation. The corresponding images are presented in Fig. 5, and show the pitted appearance on the surface of the carbon steel.

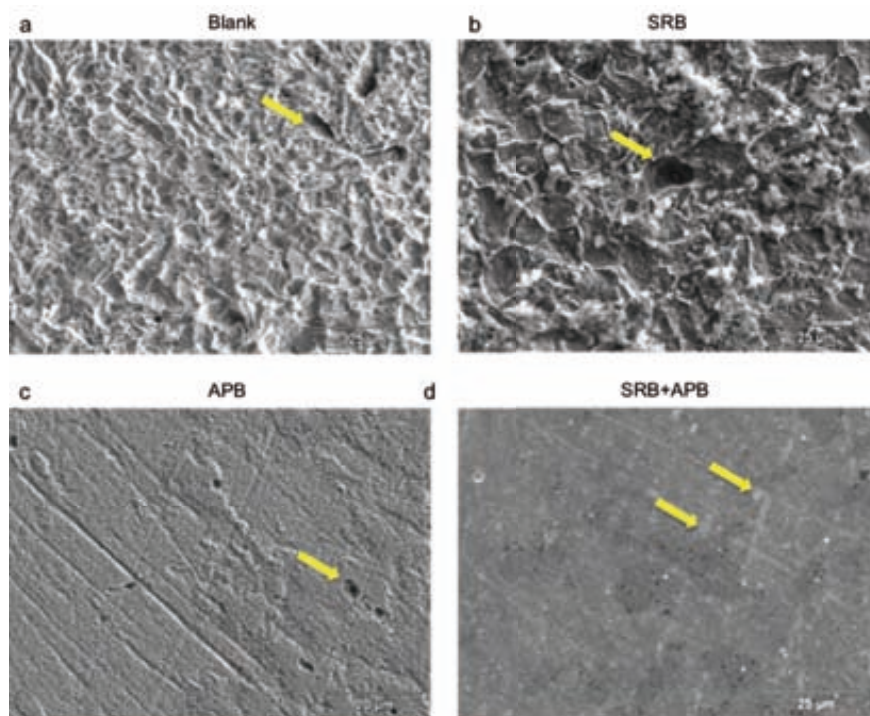


Fig. 6. SEM images showing corrosion pits on carbon steel after 21 days exposure. (a) Blank, (b) SRB, (c) APB and (d) SRB+APB corrosion pits are indicated by arrows.

The corresponding SEM images in Fig. 6 support these findings. In Fig. 6a, the working electrode of the blank setup is shown, indicating a rough, homogeneously corroded surface with a regular corrosion pattern. Small pits with regular edges can be observed for the blank with no significant seize (arrow, Fig. 6a and table 3). Once the corrosion product film was removed from the carbon steel, localized corrosion processes become visible for the bacterial setups as shown in Fig. 6(b)-(d). The carbon steel exposed to SRBs indicates a rough surface; the most predominant feature is one deep pit on the electrode surface (arrow, Fig. 6b). The SRBs indicated a mean hemispherical pit of 11-14  $\mu\text{m}$ . This clearly validates the significance of severe local attack by SRB (Table 3). Other pits were hemispherical in shape and were clustered in groups. Clustered hemispherical pits are known as one of the characteristics of SRB-related MIC [26-28]. Microbiologically produced hydrogen sulfide is very corrosive to ferrous metals and further reacts with dissolved iron to form an iron sulfide ( $\text{FeS}$ ) film on the metal substrate. Therefore, galvanic coupling between an iron sulfide film and the nearby metal substrate is established and corrosion is accelerated [29, 30]. In Fig. 6(c) the carbon steel surface exposed to APB is shown; the depth of attack was not as deep as that of the pit-like attack (arrow), and small round holes could be identified with a diameter of 3,4  $\mu\text{m}$  (Table 3). The corroded areas were broad, irregular and highly striated. These striations are usually associated with rapid corrosion and caused by preferential attack along longitudinally oriented microstructural inclusions of the material.



Striations are known to occur when the pH is acidic and can be clearly seen after cleaning. In this case, it is reported that this striation is the fingerprint of APB activities [26, 31]. In Fig. 6(d) the surface for the mixed species of SRB+APB is given, showing a similar striated surface as indicated for the APB alone. The amount of local pitting attack was significantly reduced (arrow). For the combination of both cultures, flat defects could be made out on the surface of only a few microns in diameter and with no penetration (Table 3). Nevertheless, in the combination of SRB+APB, the localized corrosion damage by pits was less than that for APB or SRB alone. The above results indicate that the degree of pitting corrosion for carbon steel in combination with just SRB is the most severe and is less in the APB and mixed cultures, respectively. Based on these observations, it can be concluded that there is a clear difference in the type of local pit formation varying on the bacterial culture. The similarity between the dimensions of bacterial cells attached to the surface and the structural appearance and the dimensions of corrosion pits indicates a possibility that the pits are initiated at the sites where the microbes were attached [32, 33].

**Table 3** Pit shape and size gained for carbon steel exposed to diverse bacterial solutions for a period of 21 days.

	Pit shape	Length (μm)	Width (μm)
Blank	Elongated pits	-	-
SRB	Hemispherical pits	11±3.45	8±5.31
APB	Hemispherical pits	3.4±2.03	1±0.82
APB+SRB	flat bean shaped defects (no pits)	1.5±0.89	0.5±0.74

4. Conclusions

The impact of enriched pure acid-producing bacteria and sulfate-reducing bacteria on the corrosion of carbon steel was investigated. The results demonstrated well that bacteria have the ability to increase corrosion rates as compared to when they are exposed to abiotic, sterile media. A correlation between an increase in sulphide production and the OCP of steel could be found as a result of biofilm formation and ferrous sulphide production analyzed by SEM-EDX. Electrochemical impedance measurements showed the influence of a biofilm on the corrosion; diffusion through the biological layer will be rate limiting, based on our EIS evaluation. SEM imaging indicated different surface morphologies for the diverse setups. The blank electrode was characterized by a rough surface as expected for general corrosion; SRBs lead to very local corrosion defects in the form of pits, implementing a large cathode surface with a smooth surface. APB bacteria, however, resulted in a more uniform attack on the surface as expected from acidic environments. The combination of both species influenced the local corrosion process of carbon steel, decreasing the pit size and local defects. SRB and APB together demonstrated higher corrosion rates than those observed in the presence of SRB and APB alone. These indications are noteworthy for further studies on natural systems, revealing that the combination of species or beneficial biofilm can be one way in the future to lower the local corrosion.

## References

- [1] G. Ruiz, T. Rawlings, F. Dobbs, L. Drake, T. Mullady, A. Hug, R. Colwell, Global spread of microorganisms by ships, *Nature* 408 (2000) 49-50.
- [2] L. Drake, C. KH, G. Ruiz, F. Dobbs, Global redistribution of bacterioplankton and virioplankton communities, *Biological Invasions* 3(2001) 193-199.
- [3] A. Meyer, R. Baier, N. Hülsmann, B. Galil, D. Friedmann, R. Forsberg, Risk assessment, prediction, and limitation of transport of bioinvaders in biofilms, in: A.S.o.L.a. Oceanography (Ed.) Aquatic Sciences Meeting, 2000, Copenhagen, 2000, pp. 22.
- [4] A. Heyer, F. D'Souza, G. Ferrari, J. Mol, J.d. Wit, EIS study of MIC in three different zones derived from ship ballast tank model system, in: N. International (Ed.) NACE, Houston, 2011.
- [5] J. Gu, Microbiological deterioration and degradation of synthetic polymeric materials: recent research advances. , *International Biodeterioration and Biodegradation*, 52 (2003) 69-91.
- [6] J. Paik, Corrosion Analysis of Seawater Ballast Tank Structures, *International Journal of Maritime Engineering*, 146 (2004) 1-12.
- [7] J. Costerton, Z. Lewandowski, D. Caldwell, D. Korber, H. Lappin-Scott, Microbial biofilms, *Annual Review Microbiology*, 49 (1995) 711.
- [8] S. Gerakov, B. Little, P. Wagner, Probing microbiologically induced corrosion, *Corrosion*, 42 (1986) 689-692.
- [9] M. Franklin, D. Nivens, J. Guckert, D. White, Effect of electrochemical impedance spectroscopy on microbial biofilm cell numbers, viability, and activity, *Corrosion*, 47 (1991) 37-42.
- [10] L. Yang, C. Ruan, Y. Li, Detection of viable *Salmonella typhimurium* by impedance measurements of electrode capacitance and medium resistance, *Biosensors and Bioelectronics*, 19 (2003) 495-502.
- [11] A. Dheilly, I. Linossier, A. Darchen, D. Hadjiev, C. Corbel, V. Alonso, Monitoring of microbial adhesion and biofilm growth using electrochemical impedance spectroscopy, *Applied Microbiology and Biotechnology*, 79 (2008) 157-164.
- [12] X. Munoz-Berbel, C. Garcia-Aljaro, F. Munoz, Impedimetric approach for monitoring the formation of biofilms on metallic surfaces and the subsequent application to the detection of bacteriophages, *Electrochem. Acta*, 53 (2008) 5739-5744.

- 
- [13] B. Boukamp, A nonlinear least square fit procedure for analysis of immittance data of electrochemical systems, *Solid State Ionics*, 20 (1986) 31-44.
- [14] B. Boukamp, Electrochemical impedance spectroscopy in solid state ionics recent advances, *Solid State Ionics*, 169 (2004a) 65-73.
- [15] B. Boukamp, Impedance Spectroscopy Strength and Limitations, *Technisches Messen*, 71 (2004b) 454-459.
- [16] E. Valencia-Cantero, J. Pena-Cabriales, E. Martinez-Romero, The corrosion effects of sulfate- and ferric-reducing bacterial consortia on steel, *Geomicrobiology Journal*, 20 (2003) 157-169.
- [17] E.v. Westing, Determination of coating performance with impedance measurements, Delft University of Technology, Delft, 1992.
- [18] S. Chongdar, G. Gunasekaran, P. Kumar, Corrosion inhibition of mild steel by aerobic biofilm, *Electrochimica Acta*, 50 (2005) 4655-4665.
- [19] B. Little, P. Wagner, D. Duquette, Microbiologically-induced increase in corrosion current density of stainless steel under cathodic protection, *corrosion*, 44 (1988) 270-274.
- [20] F.v.d. Ende, H. Gemerden, Sulfide oxidation under oxygen limitation by *Thiobacillus thioparus*, *FEMS Microbiology Ecology*, 13 (1993) 69-78.
- [21] G. Stefess, Oxidation of sulfide to elemental sulfur by aerobic thiobacilli *Biotechnology*, Technical University Delft, Delft, 1993.
- [22] D. Pope, T. Zintel, Methods for the investigation of under-deposit microbiologically influenced corrosion, *NACE Corrosion*, NACE International, Houston, 1988.
- [23] J. Slatter, M. Davidson, J. Grapiglia, W. Wong, DC voltage gradient technique to assess coating defects on buried pipelines, *Materials Performance*, 32 (1993) 35-38.
- [24] S. Li, Y. Kim, K. Jeon, Y. Kho, Microbiologically Influenced Corrosion of Underground Pipelines under the Disbonded Coatings *Metals and Materials*, 6 (2000) 281-286.
- [25] H. Videla, Microbially induced corrosion: an updated overview, in: H. Roossmore (Ed.) *Biodeterioration and biodegradation* elsevier Applied Science, London, 1991, pp. 63-88.
- [26] W. Lee, W. Characklis, Corrosion of mild steel under anaerobic biofilm, *Corrosion*, 49 (1993) 186.

[27] H. Herro, MIC Myth – does pitting cause MIC, in: N. International (Ed.) NACE, San Diego, CA, 1998.

[28] R. Eckert, H. Aldrich, C. Edwards, B. Cookingham, Microscopic differentiation of internal corrosion initiation mechanisms in natural gas pipeline systems. , Corrosion, NACE International, Houston, TX, 2003.

[29] J. Telegdi, Z. Keresztes, G. Paalinkas, E. Kalaman, W. Sand, Microbiologically influenced corrosion visualized by atomic force microscopy, Applied Physics A, 66 (1998) 639.

### **3.2      *Corrosion of carbon steel in a simulated ship ballast tank in the presence of a natural microbial community***

#### **Abstract**

Investigations were undertaken to elucidate causes of severe localized corrosion within ship ballast tanks (SBTs). Visual inspection revealed features characteristic of localized corrosion such as blister formation located on the sidewall and on the tank bottom. Representative samples of blisters were retrieved from selected areas for microbiological and microscopy analyses. A mixed microbial community was enriched from an internal SBT sidewall. A simulated ship ballast tank model (SSBTM) was implemented to reproduce the environmental conditions i.e. sediment and construction material to determine corrosion rates. It was possible to distinguish different corrosion zones in the SSBTM due to bacterial interaction and sediment accumulation. For the first time a natural bacterial community was used to investigate corrosion rates of carbon steel in the presence of sediment accumulation and ship rolling. Linear polarization resistance (LPR) measurements revealed that the corrosion rate of the carbon steel exposed to the enrichment culture ( $0.48 \text{ mm y}^{-1}$ ) was higher than the recorded in artificial seawater alone ( $0.02 \text{ mm y}^{-1}$ ). The LPR measurements gave a good indication for material loss in form of general corrosion but the local corrosion loss was underestimated by this technique. To confirm these findings weight loss measurements were used to confirm the gained electrochemical data. Additional surface analysis by scanning electron microscopy (SEM) imaging demonstrated enhanced local corrosion on the carbon steel in presence of the bacterial community as compared to abiotic controls.

## 1. Introduction

As intensively discussed in literature, corrosion in ship tank environments is shown to be a serious problem for decades (Cleland 1995, Huang et al. 1997). Since 1990 water ballast tanks have become the subject of a number of regulations from institutions such as the International Association of Classification Societies (IACS) and the International Maritime Organization (IMO) (IMO 1997; 2003). One of the main reasons for increasing regulatory activity was the large number of ship losses that occurred in the 1980's where corrosion contributed to the failure of the construction. Ship ballast tanks (SBTs) are prone to MIC as they are continuously flushed and filled with seawater to trim the shipload with dry periods in-between. General corrosion within ballast tanks is intensively described by (Tamburri et al. 2002; Suzuki et al. 2004). The main problem is residual sediment on the bottom of SBTs accumulating bacteria known as invasive species (Hallegraeff and Bolch 1992; Gollasch et al. 1998; Hamer et al. 2000). Sulfate reducing bacteria (SRB) are one of the mayor classes of organisms detected in the sediment zone inducing microbiologically influenced corrosion (MIC) (Magot et al. 1997; Crolet and Magot 1993; Santana Rodriguez et al. 2006; Abedi et al. 2007). Previous studies showed that living SRB accelerate corrosion of metals (Magot et al. 1997; Santana Rodriguez et al. 2006; Abedi et al. 2007; Javaherdashti et al. 2006) and influence environmental parameters by metabolic products (Garcia et al. 2001; Benedetto et al. 2005). Ballast tanks on board of vessels can be divided into four different zones (Heyer et al., 2009) detailed in Fig. 1(a). The "4 zone approach" is based on a model which was developed for the waterfront of harbour pilings, namely, the Accelerated Low Water Corrosion (ALWC) (Little and Lee, 2007). From the author's point of view, this model reflects the main cause why SBTs are prone to MIC. Within these 4 different zones diverse environmental conditions (oxygen, nutrients, flow conditions) are established. These circumstances will have a significant influence on bacterial communities and activities. In closed seawater environments, in which nutrients are quickly exhausted, MIC might be irrelevant in some cases after some time. SBTs are open systems, and ballast water exchange can be continued over the voyage time or locally in ports of arrival. Ballast water exchange, ensures a continuous input of nutrients and output of waste products which is crucial for biofilm formation and growth of bacteria in inaccessible areas of SBTs. Interpretation and modelling of corrosion within SBTs is at present based on practical weight loss measurements gained in field studies (Tamburri et al. 2002, 2003, 2005; Suzuki et al. 2004), or corrosion depth measurements by ultrasonic instrumentation (Paik, 2004; Paik and Thayambali 2002, 2004, 2005). Using natural biofilm communities recovered from a SBT sidewall and carrying out electrochemical evaluation of corrosion using conditions as close to the field environment as possible is needed to identify and evaluate MIC as a potential corrosion source in SBTs. However to the authors' knowledge, there are no reports focusing on the role of different risk levels within ship ballast tanks and accumulated sediment therein.

The here reported laboratory investigations were undertaken (i) to determine if distinctive corrosion rates can be monitored in different height levels of an SBT and (ii) to investigate if sediment accumulation will have an effect on the corrosion behaviour in the presence of bacteria. Based on this information, a new model was implemented in the lab to study the corrosion rates of carbon steel in different levels in a simulated ship ballast tank (SSBT) considering sediment accumulation and low oxygen concentrations in the water phase. Electrochemical experiments using linear polarization resistance measurements (LPR) were implemented to determine whether corrosion rates similar to the rates reported for SBTs in the field could be studied under laboratory conditions.

## **2. Experimental**

### *2.1 Sample collection*

A ship ballast tank was examined in dry dock for indications of blister and pit formation. Selected blisters were taken with a sterile scalpel. Sediment samples were retrieved from the bottom of the tank. Corrosion products and sediment residues were placed in sterile Schott flasks 100 ml and transported to the laboratory in a cooler.

### *2.2 Enrichment*

Biofilms formed on the sidewall of a ballast tank (not visible by naked eye) were swabbed repeatedly at random places with sterile cotton swabs and transferred immediately into a flask containing 100 ml of sterile artificial seawater (ASW). Collection was continued until the clear ASW appeared slightly turbid.

The basic ASW medium contained the following compounds, Part A: NaCl 23.93 g; Na<sub>2</sub>SO<sub>4</sub> 4.01 g, KCl 0.68 g, NaHCO<sub>3</sub> 0.197 g, KBr 0.099 g, H<sub>3</sub>BO<sub>3</sub> 0.03 g, NaF 0.01 g dissolved in 750 ml deionized water. Part B: 1.0M MgCl<sub>2</sub>·6H<sub>2</sub>O 53.27 ml, 1.0M CaCl<sub>2</sub>·2H<sub>2</sub>O 10.33 ml, 1.0M SrCl<sub>2</sub>·6H<sub>2</sub>O 0.90 ml. Part A and B are combined to 1 liter. The isolated culture was maintained prior to experiment for 1 weeks in ASW supplemented with 0.02% yeast as nutrient source at 28°C. The community composition was tested with a commercial available MIC rapid test (BTI products) confirming the presence of SRB, APB, IRB and LNB bacteria commonly associated with MIC.

### 2.3 Material preparation

All measurements were performed in a costume made set-up to simulate the corrosion processes on uncoated steel type ASTM A131 grade EH36 typically used for ballast tank construction. Working electrodes were mounted in epoxy resin and the surface was ground using a series up to 2400 SiC-paper. The total exposed surface area was 1 cm<sup>2</sup> and were fixed in epoxy resin and afterwards fixed in vertical position to avoid precipitation of corrosion products directly on the electrode surface. A detailed schematic overview can be derived from Fig. 1(a). The polished electrodes with a surface area of 1 cm<sup>2</sup> were fixed in three different height levels inside the cell Fig. 1(b).

### 2.4 Linear polarization resistance (LPR)

LPR measurements were carried out using an IVIUM potentiostat (IVIUM technologies, Netherlands) controlled by IVIUM software version 1.901. LPR measurements were conducted in sealed measurement cells at ambient temperature (25°C) over a period of 3 weeks. The experimental period was chosen based on literature data where researchers commonly used the time period of 3-4 weeks for bacterial communities containing SRBs (Castaneda and Benetton 2008; Beech and Campbell 2007). ASW served as electrolyte as either control solution or solution supporting growth of the natural community. Electrochemical measurements were carried out using in-house designed electrochemical cells to simulate the corrosion processes on uncoated low carbon steel type ASTM A131 (grade EH36) used for ballast tank construction. The material was exposed to artificial seawater (ASW) and sediment to perform the experiments under realistic environmental conditions. For this purpose acryl-measuring cells had a size of 10.5 cm diameter and 8 cm height with a total volume of 500 ml. The top cover was configured with openings for three Ag/AgCl reference electrodes (Radiometer Analytical) in combination with platinum mesh counter electrodes. Counter and reference electrode were sealed using rubber stopper and silicone rubber. Prior to immersion electrodes were rinsed with distilled water, degreased with acetone, sterilized in 70 % ethanol for 30 min and maintained under sterile conditions before mounting inside the cell under sterile conditions. The cells and all compounds were sterilized with 70% EtOH, prior to assembly. In a final step the electrochemical cells were placed on a three dimensional shaker (15 rpm) to imitate the rolling of a ship Fig. 1(c). The movement of the shaker allowed simulating the splash zone of a ballast tank with continuous wet/dry conditions.



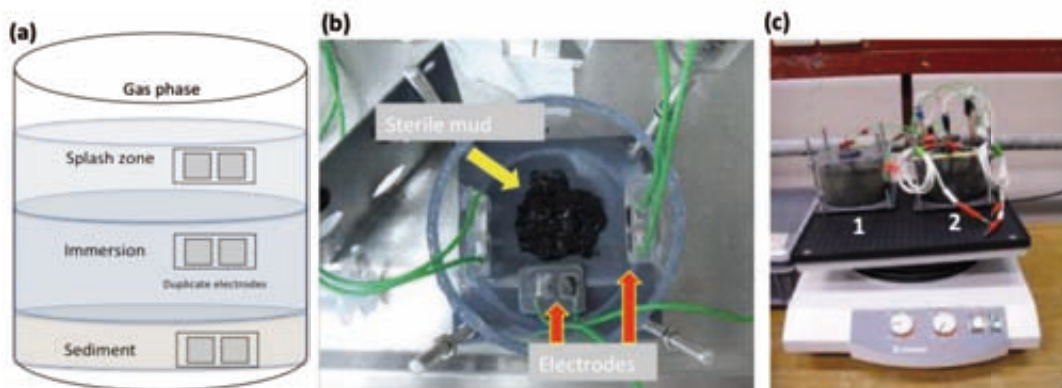


Fig. 1. Electrochemical cells designed to measure corrosion rates of carbon steel in different height levels in the SSBT: (a) Schematic overview of cell incl. the 4 different zones and fixed working electrodes; (b) top view photograph of cell with implemented electrodes and sediment and (c) assembled cells on 3 dimensional shaker (1 cell for weight loss measurements without electrodes, 2 electrochemical set-up + bacteria).

### 2.5 Electrochemical control cell

The electrochemical control cell was filled as for bacterial community containing 400ml of ASW+0.02% yeast and was kept sterile throughout the experiment by addition of 0.02% sodium azide.

### 2.6 Electrochemical cell with isolated community

The electrochemical cell was filled with 380ml of ASW+0.02% yeast and 20ml of the enrichment culture (taken from exponential growth phase  $10^7$  cells/ml). The cell was supplemented with 15.0g (wet weight), heat sterilized (1.5 bar, 121°C, 30 min) sediment sample, recovered from a ship ballast tank. The electrolyte was flushed afterwards with nitrogen for 10 min with gently flow to gain a semi anaerobic environment. Each week 100ml ASW was removed from each cell (control and bacteria) to maintain a steady supply of nutrients. All procedures were carried out aseptically.

### 2.7 Weight loss measurements

Steel coupons were prepared as described above and weighed on a 0.1mg readability balance (Mettler Toledo, Germany) triplicate measurements. The coupons were placed aseptically in the same test cells without electrodes. The cells contained ASW supplemented with sediment, for control and bacteria placed on a 3 dimensional shaker. After 3 weeks of exposure at 25°C, samples were removed and degreased in Clarke acid cleaning solution (1L 36% (v/v) HCl, 20 g  $\text{Sb}_2\text{O}_3$  and 50 g  $\text{SnCl}_2$ ), after which they were rinsed with 70% ethanol and dried under a stream of nitrogen.

Weights were recorded in triplicate and weight loss of each sample was obtained from mean values. Corrosion rates were calculated from weight loss measurements according to the ASTM standard (ASTM D2688-05).

## 2.9 Microscopy

### 2.9.1 Epifluorescent microscope (EFM)

Bacterial growth over the period of time was monitored by periodically removal of test coupons from stainless steel 316. Stainless steel was the first choice of material avoiding background fluorescence of the material in the staining procedure. For biofilm imaging, the coupons were taken out of the cell and transferred into QuadriPerm plates with deionized water. Bacterial biofilms were imaged in water by an immersible objective in liquid to avoid structural disturbance of the 3 dimensional biofilm with 40x magnification using an Olympus BX51 fluorescent microscope (Olympus America Inc., NY). The nucleic acid dye 4,6-diamidin-2-phenylindole DAPI (25µM, 15 min in the dark) was used for staining. Surface coverage was analysed by analySIS auto 5.1 Software (Olympus America Inc., NY).

### 2.9.2 Scanning electron microscope (SEM) and EDX analysis

Biofilms, generated on electrode surfaces, were fixed in 2.5% (v/v) glutaraldehyde in cacodylate buffer (0.01M) for 24 h and dehydrated in a 30, 50, 70, 90 and 100% isopropanol/water series (15 minutes in each solution). The samples were sputter-coated with gold in order increase the contrast of the images. The coupons were stored prior to SEM observation in a desiccator with silica gel to maintain a dry atmosphere. SEM analysis was performed with a JSM-5800LV (Joel, Japan) scanning electron microscope. Images were taken with a working distance of 7-12 mm and 800x magnification. Elemental analysis was performed using an Energy Dispersive X-Ray (EDX) spectroscopic analysis the system equipped with a Noran 5 elemental analyser (Thermo Scientific, Germany). An accelerated voltage of 12 kV was used for both secondary electron imaging and EDX. The analysis software NSS 2.2 x-ray microanalysis (Thermo Scientific, Germany) was used for elemental analysis.

## 3. Results and Discussion

The susceptibility of uncoated carbon steel to MIC was evaluated in a series of microscopic, electrochemical and analytical investigations.

### 3.1 Morphology of samples and microbial growth

Blisters that were observed on the sidewall of the SBT were removed for SEM investigations Fig. 2(a). The corresponding SEM image revealed the presence of filamentous fungi (yellow arrow) Fig. 2(b).

The presence of fungi was proven by selective growth medium on petri dishes revealing diverse fungi in the tested area Fig. 2(c). Accumulated bacteria inside the blister indicated by (dotted white arrow) in Fig. 2(b), corresponds mainly to spiral rod shaped SRB cells of 2  $\mu\text{m}$  in length. All collected field samples (biofilm and sediment residues) confirmed the presence of SRB, APB, IRB and LNB as bacterial growth was detected in their respective enrichment medium determined by liquid rapid tests\* Fig. 2(d).

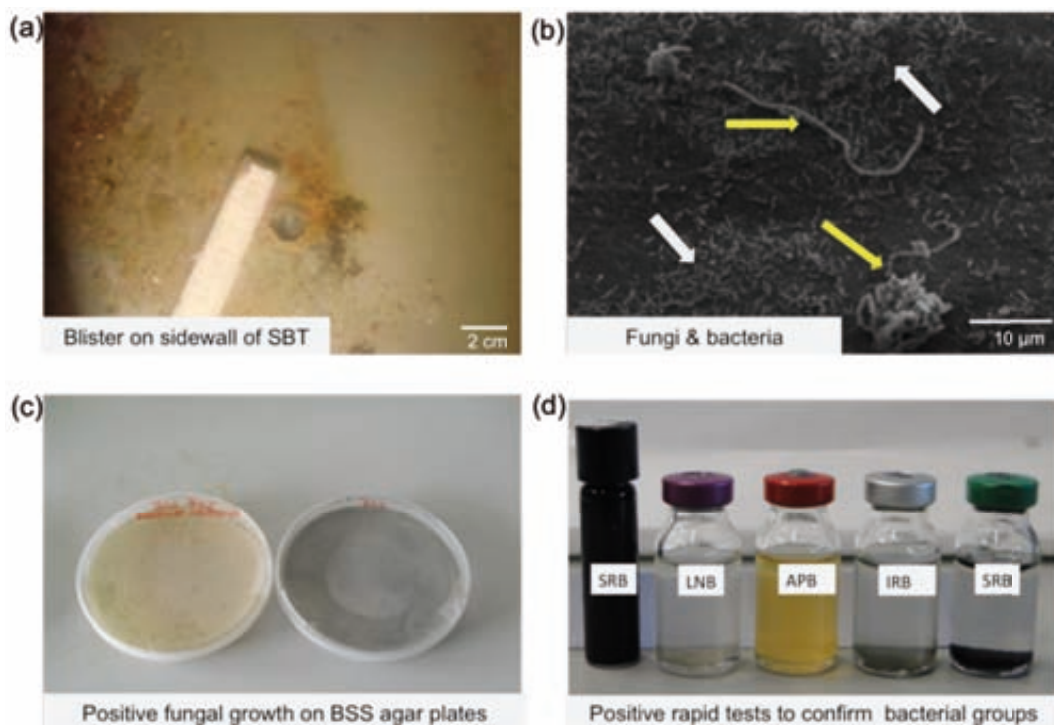


Fig. 2. Photographs of sampling site and obtained laboratory results: (a) blister on a sidewall of a ship ballast tank; (b) SEM image of fungi (yellow arrow) and bacteria (dotted arrow) accumulated inside the removed blister, (c) positive fungal growth on BSS agar plates and (d) MIC test kit to enumerate viable bacteria of different groups (indicated in image).

These preliminary tests validated that under natural conditions mixed bacterial communities are involved in blister and pit formation in SBTs.

\*Rapid check tests can be used on site and requires no background information. The tests normally rely on visual effects caused by presence of bacteria (Javaherdashti, 2008).

### 3.2 Microscopy observation

Fluorescent staining over the course of the experiment monitored the bacterial growth and biofilm formation. Representative material coupons were periodically removed from the test cells to study bacterial colonization. Fig. 3 (a) illustrates and verifies the bacterial growth in the test cells. It can be observed that a significant bacterial growth was developed in three weeks period. The total bacterial surface coverage of the coupons was calculated (in percentage) and the corresponding data are given in Fig. 3 (b). The diagram indicates a clear proliferation in surface coverage by bacterial cells over time where the initial coverage was 54%, which gradually increased to 88% after 21 days.

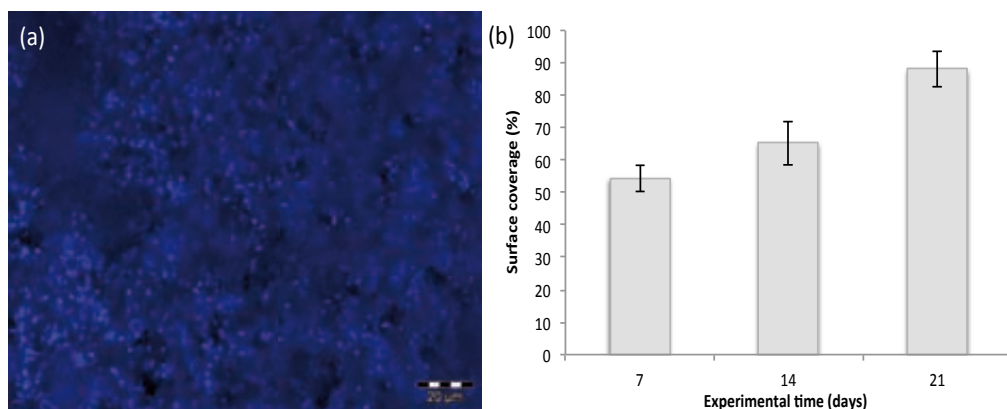
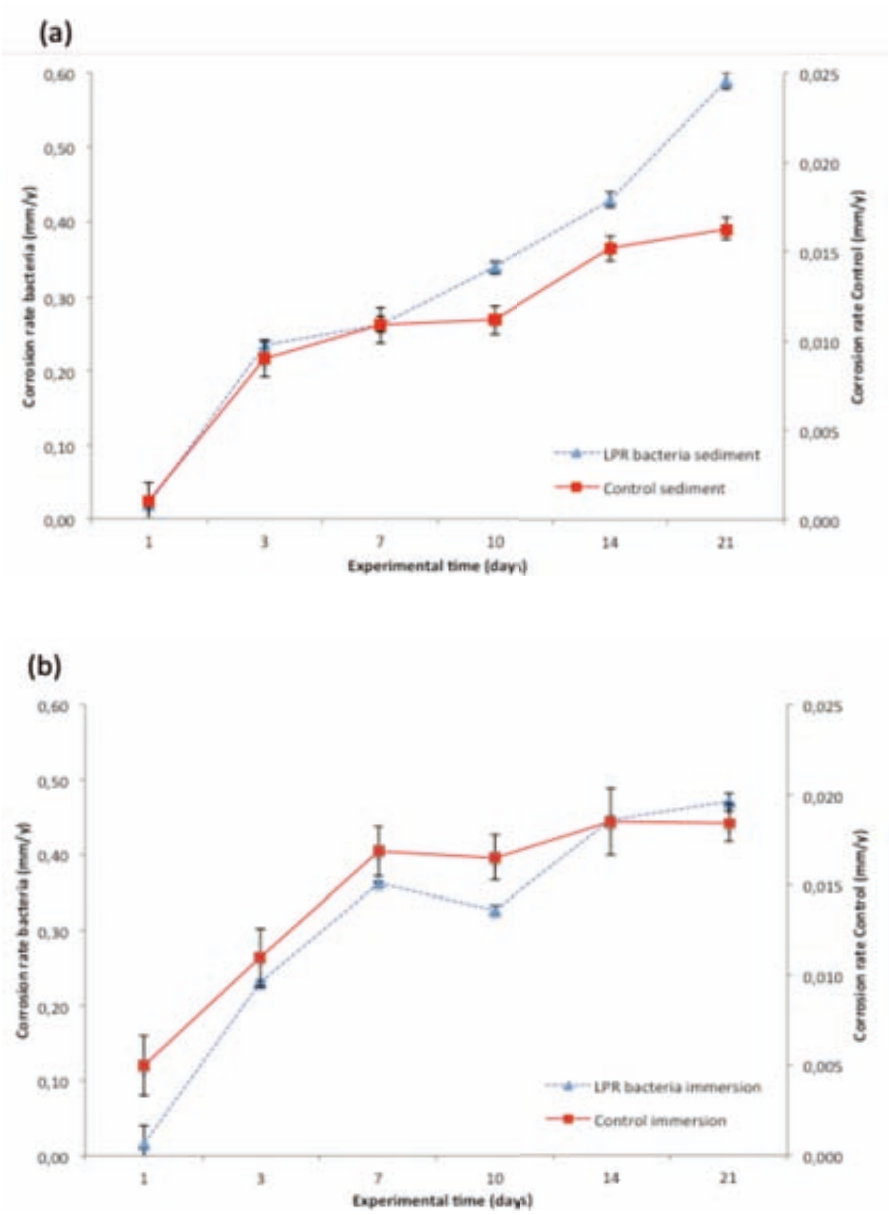


Fig. 3. DAPI stained biofilms on test coupons: (a) 21d old biofilm; scale bar 20 μm, (b) diagram indicating bacterial surface coverage in % on top of test coupons over the period of time.

### 3.3 Corrosion studies

Linear polarization resistance (LPR) is the electrochemical technique probably most applied for monitoring purpose (11ASTM G96-90). LPR is a simple on-line technique that can be run with fairly cheap equipment. Figure 4 (a)-(c) display the corrosion rates monitored in the three zones for the control experiment i.e., without bacteria (square, line) and in combination with the bacterial community (triangle, dashed line). The primary x-axis indicates the corrosion rate monitored for the bacterial community whereas the secondary x-axis represents in all figures the control experiment (without bacteria).



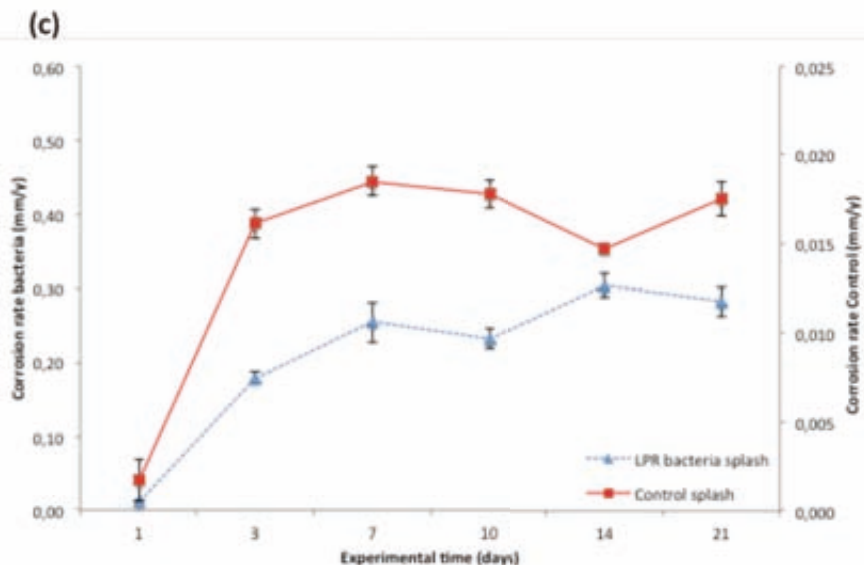
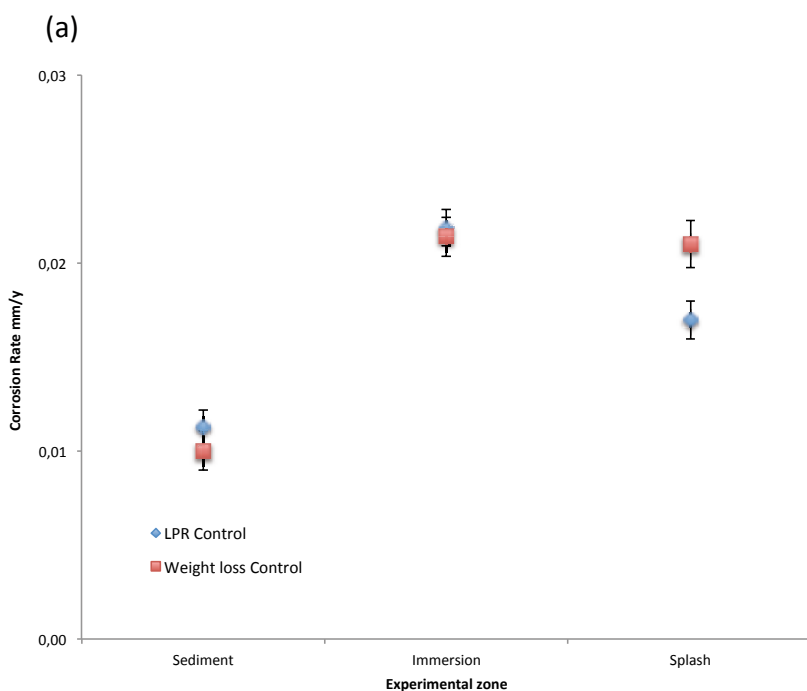


Fig. 4. LPR data for control corrosion rates (square, line) of carbon steel exposed to different levels in simulated SBT in combination with bacterial community (triangle, dashed line), (a) splash zone; (b) immersion zone and (c) sediment zone. Corrosion rates are expressed in mm/y.

For the control experiment the corrosion rate reached a value of 0.02 mm/y in the splash zone shown in Fig. 4(a). However the measured corrosion rate for the bacterial community in the splash zone, reached a value of 0.28 mm/y after the 3 weeks test period. These data is in accordance with literature values (Little et al. 2007). Fig. 4(b) shows the immersion zone of control and corresponding bacterial cell the corrosion rate increased slightly to 0.018 mm/y in the sediment for the control, while in the immersion zone of the bacterial cell the final corrosion rate increased to 0.48 mm/y. Fig. 4(c) indicates the sediment zone the corrosion rate for the bacterial set-up increased to 0.59 mm/y whereas the control experiment indicated a corrosion rate of 0.016 mm/y in the sediment zone. The corrosion rates for the control experiment have not changed much and stayed rather low over the course of the experiment. These values correspond to literature values of carbon steel in seawater (Cheung et al., 1994; Little et al. 2007) with the predicted rates of 0.025-0.060 mm/y depending on aeration and seawater pH. The control was continuously showed low corrosion rate with a maximum value of 0.018 mm/y. Due to the fact that the test cell was stripped with nitrogen the corrosion rate indicates marginally lower values. Additional a small amount of yeast as nutrient supply was added which can lead passivation of the electrode surface resulting in corrosion inhibition (Little et al. 2007). The use of such media can sometimes lead to misleading conclusions while performing LPR measurements. This is one reason why the amount of yeast extract was kept as low as possible 0.01% in our experiment.

In contrast, the bacterial community set-up indicated strong shifts in the corrosion rates for all the three zones as triggered due to bacterial activity. In summary, averaged LPR data demonstrated an increased corrosion rate for the immersion zone (0.47 mm/y) and sediment zone (0.59 mm/y) in the presence of bacteria. The bacterial set-up represents an increase in corrosion rate to a value typically for piling affected to ALWC (Little et al. 2007) and ballast tanks (Tamburri et al. 2002; Paik et al. 2004). Additionally, the corrosion data gained from weight loss measurements for control and bacterial community are summarized in Fig. 5(a) and (b). To verify the reliability of the LPR data in MIC monitoring, weight loss measurements were performed. The use of coupons makes it possible to study the corrosion attack with a metallographic examination and analysis of the corrosion products. This also gives the opportunity to determine pit depths and pit density in the case of localized corrosion that is underestimated by LPR alone. In general the overall corrosion trend is the same in both set-ups indicating different corrosion rates for all the three zones. The sterile control containing no bacteria indicates a corrosion trend as expected for the different zones in a SBT, the highest corrosion rates were detected in the splash zone due to constant wet and dry conditions followed by sediment and immersion zone Fig. 5(a).



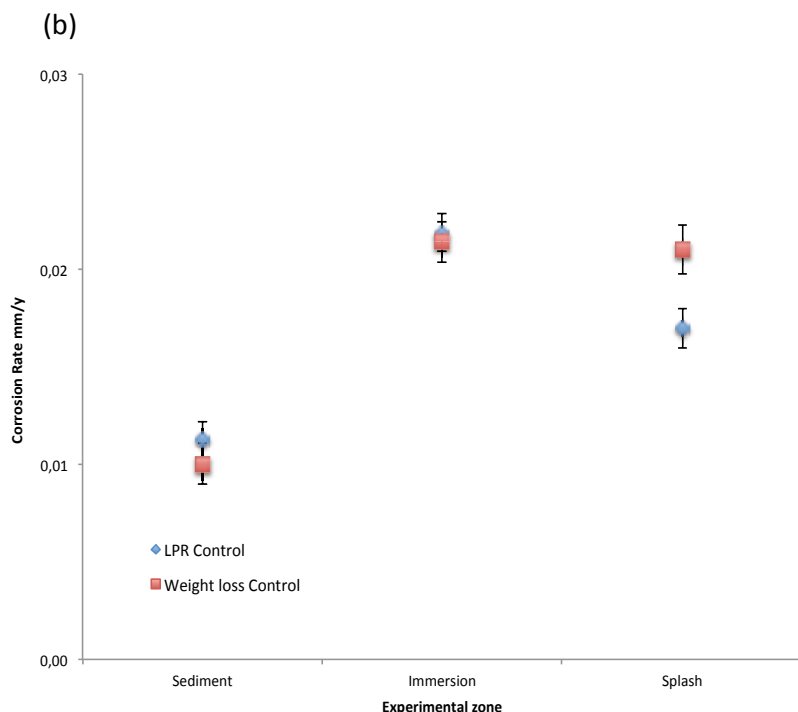


Fig. 5. Corrosion rates of carbon steel exposed to different levels in simulated SBT determined by weight loss measurements: (a) bacterial community (b) control (rhomb LPR; square weight loss). Corrosion rates are expressed in mm/y.

The contrary effect for the corrosion rate could be observed for the natural bacterial community, the highest corrosion rates could be determined for the sediment zone followed by the immersion zone and the splash zone Fig. 5(b). This decreasing trend in corrosion behaviour was expected and is typical for steel exposed to MIC bacteria in a system with low oxygen concentrations (Cheung et al. 1994; Little et al. 2007; Hilbert 2000). The sediment and immersion zones showed the highest corrosion rates due to bacterial activity. The lowest corrosion rate was identified for the splash zone that is explainable by the fact that continuous shaking conditions will disturb bacterial accumulation and is therefore lower than in areas where biofilm growth is promoted such as in the immersion zone. It has to be mentioned here that there are a number of problems related to the use of LPR technique for MIC monitoring. Material precipitation in form of fouling has a significant impact on the technique used. The biofilm formed can introduce a capacitance and a resistance and additional electrochemical reactions and adsorptive processes which can affect the results and interpretation of the technique (Dexter 1995). These effects could be observed for our experimental set-up indicating higher corrosion rates measured by LPR than weight loss measurements, similar findings are reported by Tuovinen et al. (1986). There are indications that this might be related to the formation of ferrous sulphide films.



The presence of species that can be oxidized like ferrous sulphides limit the use of LPR as the reaction in the ferrous sulphide film masks the response from the steel coupon (Thompson 1994). This idea was followed up in the next section where SEM-EDX was used to determine the corrosion products on the electrode surface. It can be summarized that the corrosion rates of the steel in the control and bacterial samples Fig. 4as determined by weight loss measurements Fig. 5, confirmed the trend observed with the LPR data with significantly higher corrosion rates observed for the steel samples exposed to microbial community.

To avoid the underestimation of the localized corrosion the corrosion rate for each zone was calculated. Based on SEM microscopy images the local corrosion surface coverage was expected to be 20% of the total surface area. The bacterial community gives a clear trend in the corrosion rate showing the highest values for the sediment followed by immersion and sediment zone. If the LPR data is now considered as an average value of the corrosion rate underestimating the local corrosion impact the following Eq. (1) can be used to estimate the local impact of pits on an average surface coverage of 20%.

$$\text{Corrosion rate LPR} * 5 \text{ (20\% local defect)} = \text{total loss (mm/y)} \quad (1)$$

The gained and calculated corrosion rates are presented in Fig. 6. The diagram clearly indicates that there is a significant shift in the corrosion rate if the local corrosion effect is considered. The corrosion rates range from 2.95 mm/y for the sediment layer followed by 2.35 mm/y for the immersion and 1.4 mm/y for the splash zone. This effect is attributed to the sediment in the cell creating a niche for anaerobic bacteria as established and reported for SBTs (Hallegraeff and Bolch 1992; Gollasch et al. 1998; Hamer et al. 2000). Low oxygen concentration values were supported by visual observations of the test cells indicating SRB growth by blackening of the water phase near the bottom and the characteristic smell of H<sub>2</sub>S while sampling the water phase (Hilbert, 2000). The gained data correspond to literature data and weight loss measurements obtained by (Paik and Thamballi 2004, 2005; Cleland, 1996). The calculated corrosion rates highlight visually the made observations in the test cell showing the highest corrosion rate in the sediment zone, followed by immersion zone and splash zone. This effect was not observed and described for an experimental ship ballast tank before. An indication that the chosen experimental approach incorporating sediment and wave movement provided a realistic copy of the natural conditions. The determined corrosion rates by LPR are lower if the localized corrosion effects are not considered. Showing how important it is to consider effects on the electrode surface in form of rapid localized corrosion phenomena. It can be summarized here that it was possible to identify different corrosion rates within different height levels of the electrochemical cell. The determined rates correspond to previous observations made for real ballast tanks.

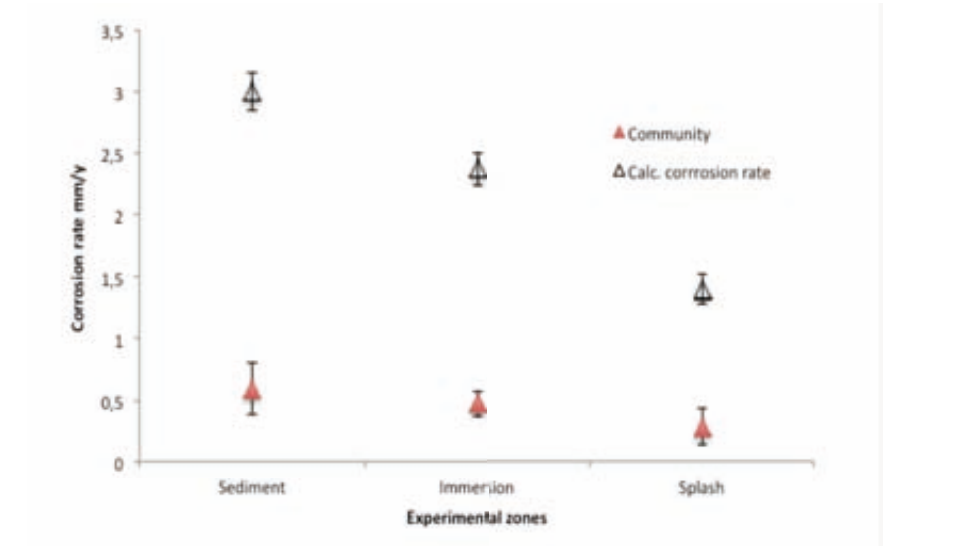


Fig. 6. Calculated corrosion rates for the experimental cell considering the localized corrosion phenomena observed on the working electrode surfaces. Calculated realistic corrosion rate derived from LPR measurements (empty triangle) considering that 20% of surface are indicating defects by Eq. 1, data gained from experimental approach (filled triangle).

3.4 SEM imaging and EDX analysis

SEM imaging of the working electrodes after immersion was performed providing the microscopic image series of Figure 7. The images highlight the structural surface properties and equivalent EDX spectra gave the elemental composition of the corrosion layers as presented in Table 1 and 2. Table 1 summarizes the elemental composition in weight % of the control. The EDX analysis of the corroded steel surface confirms no carbon and low amounts of sulphur indicating that SRB growth could be suppressed during the experimental time of 3 weeks by sodium azide. The bacterial set-up (Table 2) indicates carbon and sulphur accumulation on top of the surface revealing the presence of biological residues.

**Table 1**  
EDX analysis of corrosion products on control electrodes exposed to ASW for 3 weeks.

EDX analysis (w/w%)								
Control	Electrode	O	Na	Mg	Si	S	Cl	Fe
	Immersion	30.3	2.5	12.7	4.7	0.6	3.3	46.1
	Sediment	23.1	4.9	7.8	1.5	0.7	4.5	57.5

**Table 2**

EDX analysis elemental composition of corrosion products on electrodes exposed to natural community after exposure to ASW for 3 weeks.

EDX analysis (w/w%)								
Bacteria	Electrode	C	O	Na	Mg	S	Cl	Fe
	Immersion	17.5	16.3	14.7	4.9	10.7	15.5	16.2
	Sediment	29.2	16.6	11.5	3.0	11.6	8.7	16.7

In summary, control and biotic system showed differences in distribution and composition of the corrosion products formed. In the presence of the natural community comprising SRB, APB, IRB and LNB accumulation of sulphur-based compounds were found underlying the hypothesis that the bacterial accumulation and metabolic activity is supported by decreasing oxygen concentrations throughout the test cell where anaerobic conditions are established. This supports the previous findings as presented in Fig. 4 that bacterial attachment and biofilm formation change the corrosion product morphology forming ferrous sulphide on top of the electrode which limits the use of LPR for localized corrosion.

Representative SEM images of the working electrodes were obtained in order to compare the pitting type for bacteria and control as shown in Fig. 7.

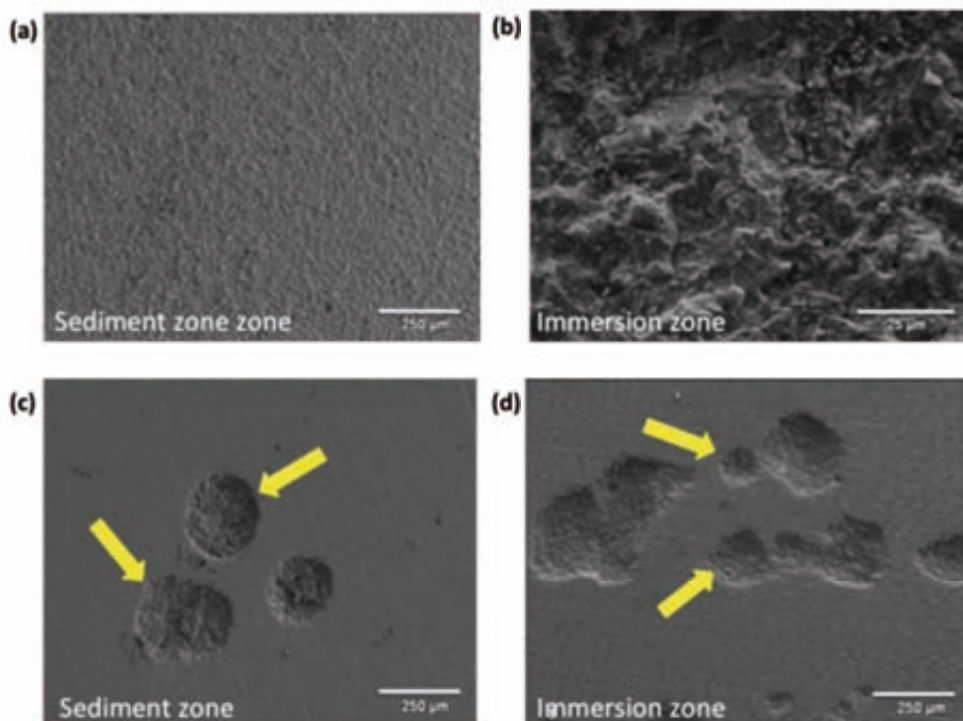


Fig. 7. SEM images of working electrodes after 3 weeks immersed to ASW+bacteria. (a) sediment zone control; (b) immersion zone control (c) sediment zone natural community; (d) immersion zone natural community. Scale bar 250  $\mu\text{m}$ .

The cleaned electrodes of all zones are presented in Fig. 7 (a)-(d) summarizing control and bacterial set-up. Fig. 7(a) shows the sediment zone of the control after 3 weeks of exposure to ASW. No pitting can be found and uniform corrosion is indicated by a homogeneous surface. The immersion zone of the control reveals a similar smooth surface without pits as shown in 7(b) scale bar 25  $\mu\text{m}$ . The previous findings are supported by a close up image of the surface indicating no localized corrosion attack. A contrary effect could be observed for the bacterial set-up, localized corrosion was evident for the sediment as well as the immersion zone of the bacterial community in Fig. 7(c) and (d), specified on the SEM micrographs by yellow arrows. Spherical pits of up to 250  $\mu\text{m}$  in diameter coalescing with those of smaller diameter are evident in Fig. 7(c). The data is supported by findings of (Yuan et al. 2007) reporting that SRB can induce pitting attack by large hemispherical pits of 2 mm diameter and many micropits. The immersion zone is characterized by less profound rounded holes in chains and groups as also reported by (Xu et al. 2007) shown in Fig. 7(d).

#### 4. Conclusions

For the first time a model system was used to study the impact of sediment and wave movement in different zones of a simulated SBT. The study confirmed that the metabolic activity of bacterial species as well as environmental conditions have a strong influence on local corrosion attack. Visual inspection of SBT revealed the presence of blister and poorly adherent, corrosion products of varying morphology on sidewalls of the tanks. These macroscopic observations are indicative for MIC attack within these enclosed environments. Removal of such blister revealed the presence of fungi and various level of bacteria associated with MIC such as SRB, APB and IRB. These findings together with literature data confirmed that MIC attack of these structures should be of concern. A contrary effect for the corrosion rates could be found in the sediment zone for the abiotic and biotic experiments. The presence of sediment in the test cell supported anaerobic conditions favourable for the growth of anaerobic and acid producing bacteria increasing the potential risk of pitting corrosion. Electrochemical LPR measurements performed in the presence of the natural community, comprising SRB, SOB, IRB and APB isolated from a SBT biofilm and grown under semi anaerobic shaking conditions, confirmed higher corrosion rates of steel samples exposed to ASW containing these microorganisms. LPR measurements revealed corrosion rate values of 0.59 and 0.47 mm/y in the presence of the isolated community. These values indicate a 20-fold increase in corrosion, compared to the control where a corrosion rate of 0.02 mm/y was monitored. The data was gained under semi-anaerobic conditions in the test cell indicating once more that the performance of the electrochemical technique determines the result supported by or findings. While LPR measurements provide relatively straightforward information in the case of general corrosion, the technique can also be used to estimate localized corrosion phenomena with the assumption of local corrosion surface coverage and attack morphology. SEM imaging demonstrated enhanced pitting for the mixed community for the sediment and immersion zone. Our study was the first one to reveal the contribution of sediment and a mixed species community to MIC attack in a simulated SBT.

#### References

- American society for Testing Materials (ASTM) ASTM (2005) Standard Test Methods for Corrosivity of Water in the Absence of Heat Transfer (Weight Loss Methods). ASTM D2688-05
- Abedi SS, Abdolmaleki A, Adibi N (2007) Failure analysis of SCC and SRB induced cracking of a transmission oil products pipeline. *Failure Analysis* 14:250-261
- Beech IB and Campbell SA (2007) Accelerated low water corrosion of carbon steel in the presence of a biofilm harbouring sulphate-reducing and sulphur-oxidising bacteria recovered from marine sediment. *Electrochimica Acta* 54:14-21

Benedetto JS, Almeida SKd, Gomes HA, Vazoller RF, Ladeira ACQ (2005) Monitoring of sulfate-reducing bacteria in acid water from uranium mines *Minerals Engineering* 18 (13-14):1341-1343

Castaneda H, Xochitl D., Benetton D (2008) SRB-biofilm influence in active corrosion sites formed at the steel-electrolyte interface when exposed to artificial seawater conditions. *Corrosion Science* 50:1169–1183

Cheung CWS, Walsh FC, Campbell SA, Chao WT, Beech IB (1994) Microbial contributions to the marine corrosion of steel piling. *Inter. Biodeter. Biodegr.* 34: 259-274

Cleland JH (1995) Corrosion risks in ships ballast tanks and the IMO pathogen guidelines. *Engineering Failure Analysis* 2:79-84

Crolet JL, Daumas S, Magot M (1993) pH regulation by sulphate-reducing bacteria. Paper presented at the NACE, New Orleans.

Garcia C, Moreno DA, Ballester A, Blasquez ML, Gonzalez F (2001) Bioremediation of an industrial acid mine water by metal-tolerant sulphate-reducing bacteria *Minerals Engineering* 14 (9):997-1008

Gollasch S, Dammer M, Lenz J, Andres HG (1998) Non-indigenous organisms introduced via ships into German waters. vol 224. ICES Cooperative Research Report.

Hallegraeff GM, Bolch CJ (1992) Transport of diatom and dinoflagellate resting spores in ships' ballast water: Implications for plankton biogeography and aquaculture. *Journal of Plankton Research* 14:1067-1084

Hamer JP, Collin TAM, Lucas IAN (2000) Dinoflagellate cysts in ballast tank sediments: between tank variability. *Marine Pollution Bulletin* 40:731-733

Heyer A, D'Souza F, Mol JMC, deWit JHW (2009) Microbiologically influenced corrosion (MIC) in a simulated ship tank model system. Paper presented at the Eurocorr, Nice, France

Hilbert L (2000) Monitoring Microbially Influenced Corrosion. Technical University of Denmark, Copenhagen

Huang RT, McFarland BL, Hodgman RZ (1997) Microbial influenced corrosion in in cargo oil tanks of crude oil tankers. Paper presented at the NACE, Houston, USA

International Maritime Organization (IMO), (1997) Guidelines for the control and management of ships' ballast water to minimize the transfer of harmful organisms and pathogens.

International Maritime Organization (IMO), (2003) International convention for the Control and Mangement of Ship's ballast water and Sediment. Conference on Ballast Water Management for Ships.

Javaherdashti R, Raman RKS, Panter C, Pereloma EV (2006) Microbiologically assisted stress corrosion cracking of carbon steel in mixed and pure cultures of sulfate reducing bacteria. *International Biodeterioration and Biodegradation* 58:27-35

Little B, Lee JS (2007) Microbiologically Influenced Corrosion. In: Winston R (ed) *Microbiologically Influenced Corrosion*. Wiley-Interscience Wiley & Sons, Hoboken

Magot M, Ravot G, Campaignolle X, Ollivier B, Patel BKC, Fardeau ML, Thomas P, Crolet JL, Garcia JL (1997) *Dethiosulfovibrio peptidovorans* gen. nov., sp. nov., a New Anaerobic, Slightly Halophilic, Thiosulfate-Reducing Bacterium from Corroding Offshore Oil Wells. *Int J Syst Bacteriol* 47:818-824

Paik JK (2004) Corrosion Analysis of Seawater Ballast Tank Structures. *International Journal of Maritime Engineering* 146:1-12

Paik JK, Thayamballi AK (2002) Ultimate Strength of Ageing Ships. *Journal Engineering for the Maritime Environment* 216:57-77

Paik JK, Thayamballi AK (2004) A time-dependent corrosion wastage model for seawater ballast tank structures of ships. *Corrosion Science* 46:471-486

Paik JK, Thayamballi AK (2005) Reliability assessment of ships. In: Nikolaidis E, Ghiocel DM, Snghal S (eds) *Engineering Design Reliability Handbook*. CRC Press, New York.

Rodriguez IJS, Hernandez FJS, Gonzalez JE (2006) Comparative study of the behaviour of AISI 304 SS in a natural seawater hopper, in sterile media and with SRB using electrochemical techniques and SEM. *Corrosion Science* 48:1265-1278

Suzuki S, Muraoka R, Obinata T, Endo ES, Horita T, Omata K (2004) Steel products for shipbuilding. JFE Technical Report Vol No. 2.

Tamburri MN, Little BJ, Ruiz GM, Lee JS, McNulty PD Evaluations of Venturi Oxygen Stripping TM as a ballast water treatment to prevent aquatic invasions and ship corrosion. In: Organization IM (ed) International Ballast Water Treatment R&D Symposium, London, 2003

Tamburri MN, Ruiz GM Evaluation of a ballast water treatment to stopinvasive species and tank corrosion. In: SNAME Annual Meeting, Houston, 2005. The Society of Naval Architects and Marine Engineers.

Tamburri MN, Wasson K, Matsuda M (2002) Ballast water deoxygenation can prevent aquatic introductions while reducing ship corrosion. *Biological Conversation* 103:331-341



### **3.3** ***Biodegradation of ballast tank coating investigated by impedance spectroscopy and microscopy***

#### **Abstract**

This research paper addresses the biodegradation process for ballast tank coatings in marine environments. As part of this new approach, a commercial available ballast tank coating was exposed to bacteria obtained from a culture collection and to a natural bacterial community isolated from a real ballast tank. The natural community was chosen to explore progression and interaction of natural biofilms on the coating, an aspect, factors which are not covered in standard procedures. The behaviour of a ballast tank coating against microbial degradation was studied, showing that biological activity significantly affects the coating properties. As a result of such a phenomenon, micro-cracks and holes have been identified by AFM. The overall effect of this degradation was examined using the EIS technique. The non-bacterial exposed samples (blank) exhibited a reasonably proper corrosion resistance. However, the bacterial affected coatings (exposed to acid producing bacteria and a natural ballast tank community) showed a decrease in corrosion resistance. It is therefore necessary to include natural communities in coating degradation studies to identify possible degradation mechanisms and the severity of the attack over time.

## 1. Introduction

As ballast tank conditions can affect the structural integrity and security of the vessel, coatings are applied for safety reasons. Epoxy coatings are commonly used in ship ballast tanks for corrosion protection, in accordance to several legislation requirements (IMO 1995; IACS 1998; DnV 1998; DnV 1999). In 2006, the International Maritime Organization (IMO) adopted a new resolution (MSC.215 (82)) aiming to improve safety at sea by avoiding the effects of corrosion, thus enhancing the structural integrity of the vessels as a whole. This performance standard includes a correct selection of coating, surface preparation, inspection and extensive maintenance programs. Coating inspections are certified for maintenance efficiency, and greater attention is paid to coating failures within ship ballast tanks. On the one hand, the breakdown of the coatings in ship tanks is a well-known phenomenon, yet relatively difficult to predict (IACS 1994; TSCF 1997; Paik 1998; TSCF 1999). On the other hand, the biodegradation/biodeterioration of ballast tank coatings is underestimated within these specific coating guidelines. According to ASTM D 6400-99 (1976), a biodegradable polymer is defined as a degradable plastic in which the degradation results from the actions of naturally occurring microorganisms such as bacteria, fungi and algae. Several test methods assessing the potential biodegradability of polymers have been developed by the International Standard Organization (ISO) and American Society for Testing and Materials (ASTM). The methods used can be divided into quantitative methods as gravimetry, respirometry and characterising weight loss, carbon dioxide production, bacterial activity and changes in chemical and physical properties (Gu et al. 1992; Kemnitzer et al. 1992; ASTM D5271-92 1993; Gu et al., 1994; Gu et al. 1997). The evaluation of visible changes in polymers can be taken as a first indication of any microbial attack (e.g. roughening of the surface, formation of holes or cracks, biofilm formation). Either scanning electron microscopy (SEM) or atomic force microscopy (AFM) (Ikada, 1999, Kikkawa et al., 2002) can then be used to obtain more detailed information about the initial degradation of the surface. Supplementary sensitive electrochemical impedance spectroscopy (EIS) can be useful to quantitatively evaluate the integrity of polymeric composites (Gu et al. 1996; Gu et al. 1997a; Gu et al. 1997b) or polymeric coatings (Gilmore et al. 1992; van Westing et al. 1993; van Westing et al. 1994a, van Westing et al. 1994b; Geenen and de Wit 1990; Mitchell et al. 1996). Further test methods are based on ASTM standards, incorporating microorganisms for testing the biodegradation of polymers under simulated environmental conditions (e.g. D5209-92; D5210-92; G21-90; G22-76). These methods offer advantages including the reproducibility of the test conditions and pre-selection of known microorganisms (Gilmore et al., 1992; Kemnitzer et al. 1992; Imam et al., 1999). Although these standard procedures are generally accepted and used in coating tests worldwide, the broad variety of natural environments are not considered. This represents a major drawback, since the chosen microorganisms might not be relevant to local environmental conditions.

For example, bacterial communities in a ship ballast tank will be very different from microbial life in municipal sewage sludge or wastewater, which is commonly, used in ASTM test methods (D5209-92; D5210-92; D5271-92). In response to this lack in environmental significance, new evaluation methods for soils, marine, freshwater and strictly anaerobic conditions should be included in ASTM standards in the future. This adaption would reduce the risk of misleading results for new polymeric compounds tested with bacteria that are not relevant for the proved material. This research paper addresses the biodegradation process for ballast tank coatings in marine environments. For this new approach, a commercial available ballast tank coating was exposed to bacteria obtained from a culture collection and to a natural bacterial community isolated from a real ballast tank. The natural community was chosen to explore the progression and interaction of natural biofilms on the coating, an aspect not covered in standard procedures. The study combined three well-known techniques for coating degradation analyses (EIS, coating thickness measurements and AFM) to gain fresh insight into the sensitivity of ballast tank coatings to biodegradation. EIS measurements were implemented to examine the coating performance exposed to diverse bacteria in salty water over time. Fluorescent microscopy was used to determine the bacterial coverage and resulting defects, as traditional paint thickness instruments do not detect pinholes. Consequently, Atomic Force Microscopy (AFM) was used to investigate pinhole formation on a local scale. The outcomes of the three techniques were finally linked, to acquire a biodegradation model for ballast tank coatings exposed to marine bacteria.

## 2. Experimental

### 2.1 Materials

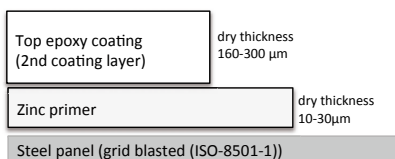
#### 2.1.1. *Paint and metal substrate*

The experiments used a commercial epoxy based coating intended for ballast tanks (secrecy agreement with the coating company). No primer was used, as the primary objective of the research was to investigate the degradation of the top coating by microorganisms. Relatively corrosion resistant stainless steel (AISI 316, size 150 x 70 mm) was chosen as substrate to minimize EIS signal interference. The steel surface was degreased by acetone followed by ethanol, rinsed with deionized water and dried before the coating application. The coating application was performed in accordance with the producer's guidelines (surface preparation, curing time, thickness). The coating was applied in one layer by airless spray, with a dry thickness of approximately 230  $\mu\text{m}$ . The surface was grinded ( $\pm 5 \mu\text{m}$ ) to increase the points of mechanical adhesion of the coating by surface pits, anchoring the coating to the substrate. Proper adhesion of anticorrosive coatings to the substrate is essential for the anticorrosive properties of the coating system.

## 2.2 Sample preparation

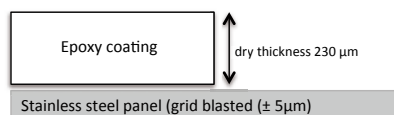
As shown in Fig. 1a, the normal ballast tank coating systems are multi-layered and contain a zinc primer with a topcoat of epoxy. No primer was used in the experiments, to increase the sensitivity for the electrochemical measurements in order to achieve a direct response on the working electrode by coating degradation. The thickness of the coating and main function of the layers are presented in Fig. 1b.

**a Conventional ballast tank coating application**



Zinc rich primer :  
good adhesion  
corrosion inhibition

**b Experimental coating application**



Top epoxy coating:  
build the total film thickness enhance overall protection  
decrease permeability of oxygen and water

Fig. 1. Schematic representation of (a) general multilayer ballast coating application and (b) experimental application without primer.

The schematic chemical structure of an amine cured epoxy coating is provided in Fig. 2, consisting of an epoxy resin (part A) and an epoxy curing agent (part B). In most cases, Bisphenol A is used as an epoxy resin due to its low cost and excellent alkali resistance. Cycloaliphatic amines are used as curing agents to improve coating resistance to water uptake by crosslinking reactions and better chemical resistance (Iijima et al., 1992).

The presence of stable carbon-carbon and ether bonds in the backbone of the epoxy molecule has been ascribed as the reasons for the high chemical stability of cured epoxy (Rouw, 1998). The coating system used in this experiment is a typical commercial grade ballast tank coating.

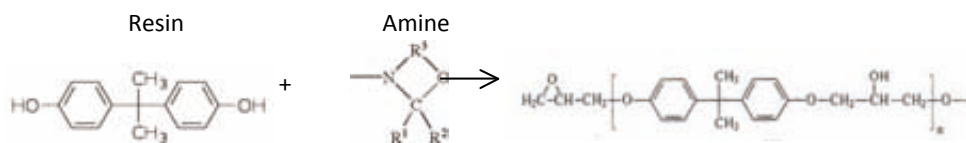


Fig. 2 Bisphenol A + cycloaliphatic amine forming epoxy coating structure.

## 2.3 Cultures and Medium

### 2.3.1 Lab cultures

This study used one pure bacterial culture, *Acidithiobacillus thiooxidans* (DSM 504), obtained from the German culture collection (DSMZ). The culture was maintained continuously in the recommended liquid medium (*Acidithiobacillus* DSM 35) of DSMZ. The culture was selected as representative organisms acid-producing bacteria. The medium was sterilised via autoclave for 20 min at 121 °C with overpressure. *Acidithiobacillus thiooxidans* was grown under shaking conditions for efficient oxygen supply. All cultures were grown at ~ 28 °C. For the coating experiments, all cultures were adapted to BSS+S° in several transfer steps to acquire cultures growing in seawater environments.

### 2.3.2 Natural bacterial consortium (isolated from practical ballast tank)

Biofilms formed on a coated ballast tank were swabbed repeatedly at random places using sterile cotton swabs, and immediately transferred into a flask containing 100 ml of sterile artificial seawater (ASW). The basic ASW medium contained the following compounds, Part A: NaCl 23.93 g; Na<sub>2</sub>SO<sub>4</sub> 4.01 g, KCl 0.68 g, NaHCO<sub>3</sub> 0.197 g, KBr 0.099 g, H<sub>3</sub>BO<sub>3</sub> 0.03 g, NaF 0.01 g dissolved in 750 ml deionized water. Part B: 1.0M MgCl<sub>2</sub>·6H<sub>2</sub>O 53.27 ml, 1.0M CaCl<sub>2</sub>·2H<sub>2</sub>O 10.33 ml, 1.0M SrCl<sub>2</sub>·6H<sub>2</sub>O 0.90 ml. Part A and B combined to 1 litre. Biofilms were collected until the clear ASW appeared slightly turbid. The stock culture (gained from sampling) was later transferred into an appropriate enrichment medium. Basal salt solution (BSS) (Majumdar et al. 1999) was used to isolate epoxy degrading bacteria from a biofilm sample collected from a ship ballast tank during dry dock service time.

The composition of the BSS medium (w/v) was as follows: NaCl, 30.00 g; KCl, 0.75 g; MgSO<sub>4</sub>, 7.00 g; NH<sub>4</sub>Cl, 1.00 g; K<sub>2</sub>HPO<sub>4</sub> (10%) 7.00 ml; KH<sub>2</sub>PO<sub>4</sub>(10%) 3.00 ml; Trace metal solution ,1.00ml; Distilled water 1000 ml; Trace metal solution had the following composition H<sub>3</sub>BO<sub>3</sub> , 2.85 g; MnCl<sub>2</sub>·7 H<sub>2</sub>O, 1.80 g; FeSO<sub>4</sub>·7H<sub>2</sub>O, 2.49 g; Na-Tartarate, 1.77 g; CuCl<sub>2</sub>, 0.03 g; ZnCl<sub>2</sub> , 0.02 g; CoCl<sub>2</sub>, 0.04 g; Na<sub>2</sub>MoO<sub>4</sub>·2 H<sub>2</sub>O, 0.02g; Distilled water , 1000 ml. The pH of the medium was adjusted to 7.5 using 1N NaOH.

Enrichment of a natural bacterial community, able to utilize the coating, was achieved by selectively choosing the coating as a sole carbon source in the growth medium. A film of epoxy coating was prepared by drying the coating on flexible plastic foil. The cured coating layer was then removed and crushed into small flakes, and added to the medium as a carbon source (Fig. 3a). This enriched bacterial consortium was used for the experiment. The presence of acid producing bacteria in this consortium could be confirmed by lowering the medium pH from 7.5 to 4 to 5.

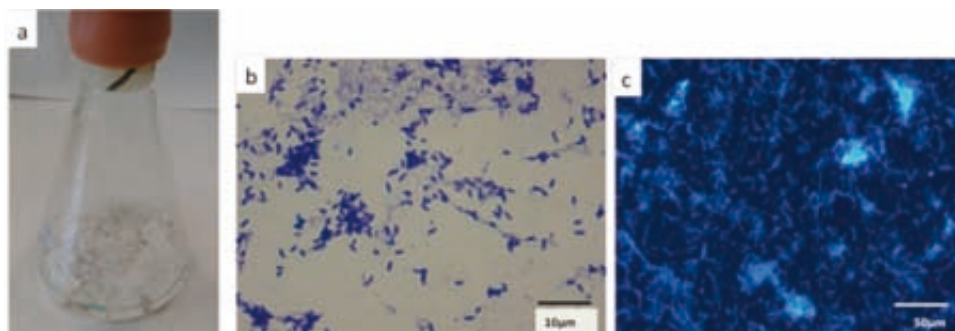


Fig. 3. (a) Enrichment culture with isolated bacteria + coating flaks (b) Isolated natural community crystal violet stained culture stained (c) pure culture of *A.thiooxidans* DAPI stained.

By fluorescent staining of the cultures, growth and attachment at the coating surface was followed. Examples of the natural community stained with crystal violet and of acid producing bacteria with DAPI are illustrated in Figs. 3b and c.

## 2.4 Experimental techniques

### 2.4.1. Electrochemical cell set-up

For the electrochemical measurements, a typical flat plate set up for coating tests was used. Measurements were performed in duplicate using two identical cells (Fig. 4a). The coated test plate acting as the working electrode was horizontally placed. Acrylic tubes (88 mm long; internal diameter 40 mm) were permanently glued to the coated-stainless steel surface as an electrolyte reservoir. Measurements were conducted using an Ag/AgCl saturated reference electrode, in combination with a parallel positioned platinum mesh counter electrode to guarantee efficient current distribution (Fig. 4b). The cells were sterilized with 70 % ethanol prior to bacterial inoculation and left to dry in a sterile flow chamber.

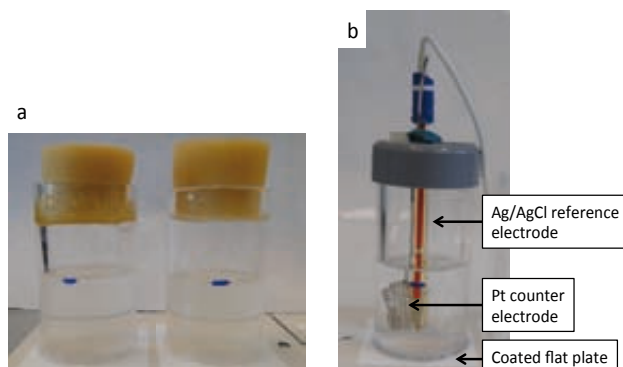


Fig. 4. Experimental set-up for degradation study (a) Duplicate test cells with bacteria + BSS medium (b) Electrochemical test cell for biodegradation - flat plate test cell composed of: working electrode (coated panel) sealed acrylic tube and electrodes therein.

#### 2.4.2 Bacterial inoculation

ASW was the first choice of a growth medium to reproduce marine conditions, due to its conductive characteristics and well-known elemental composition. Bacterial inoculation ( $10^{-6}$  cells/mL) was completed under sterile conditions, and 10% inoculum was transferred to 60 mL ASW. All cells were closed with a sterile sponge for oxygen supply and to prevent contamination (Fig. 2a). For EIS measurements, the cells were transferred to the flow chamber, and sterilised electrodes were added for the measurements before being directly removed afterwards, as illustrated in Fig. 2b. Blanks were kept sterile with the addition of 0.02% sodiumazide to avoid bacterial contamination throughout the experiment (e.g. from air).

#### 2.4.3 Electrochemical impedance measurements

All electrochemical measurements were performed using a potentiostat (IVIUM technologies, Netherlands) controlled by IVIUM software version 1.901. The impedance response was measured over a range of frequencies from 10 KHz to 0.01 Hz. All experimental set ups were analyzed for impedance responses over the period of 1, 7, 14, 21, 29, 40 and 60 days. EIS data was modelled with  $Z_{view}$  software version 3.0.

#### 2.4.4. Fluorescent staining and quantitative bacterial coverage

An upright optical/epifluorescence microscope (Olympus BX 51, Japan) with a 10x and 20x objective was used. The nucleic acid dye 4,6-diamidin-2-phenylindole DAPI ( $25\mu\text{M}$ ) and crystal violet ( $25\mu\text{M}$ ) were used for staining. The percentage surface cover was determined by imaging software (Adobe Photoshop CS3). 9 individual images were taken and analysed and the surface coverage and structural pattern of the biofilms were determined and graphically correlated with blister and hole formation of the coating analysed by AFM.

#### 2.4.5. AFM surface scans

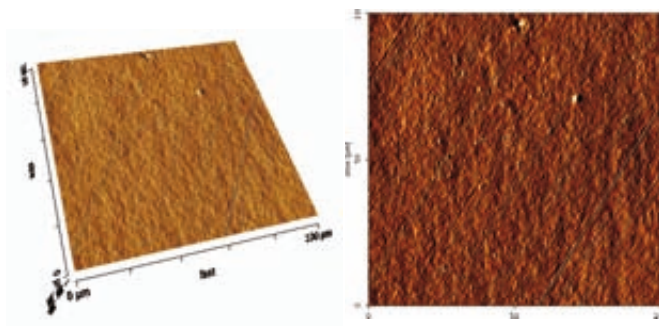
The coating morphology and roughness measurements were performed with an atomic force microscope (NanoWizard II, JPK Instruments, Germany), in air by intermittent contact mode to lower tip surface interactions. The commercially available silicon cantilever CSC37 A (Mikromasch, Estonia) was used, with the following features: length 250  $\mu\text{m}$ ; width 35  $\mu\text{m}$ ; thickness 2  $\mu\text{m}$ ; resonance frequency 41 kHz and a nominal force/spring constant of 0.65 N/m. Each AFM image consists of 512 by 512 pixels. The AFM image acquisition details are specified in the legend of the figure.

### 3. Results and discussion

#### 3.1. Surface analysis by AFM

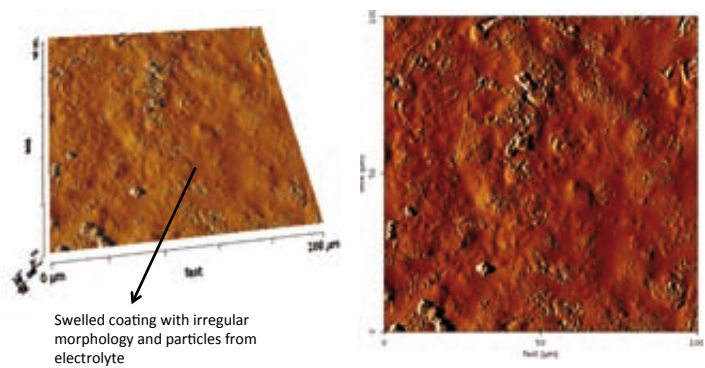
Previous AFM studies on solvent cast PVC have revealed that contact mode AFM induces surface erosion (Vancsco and Liu 1996; Vancsco et al. 1996). The noncontact mode, here termed as the intermittent contact mode, was therefore chosen for our study. The image series of Fig. 5 represents a topographic overview of the coating surfaces before and after exposure to bacterial species.

a Blank coating surface before exposure

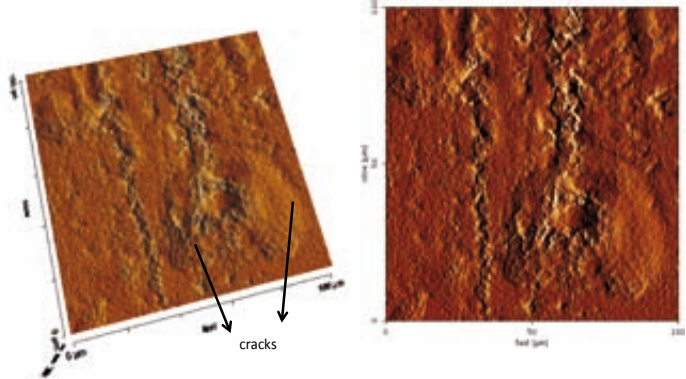




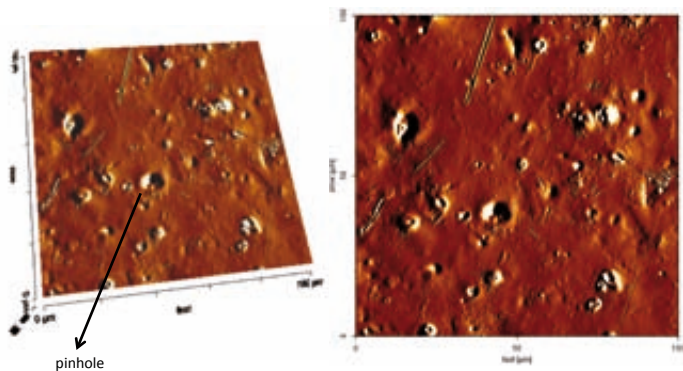
b Coating exposed to BSS pH 7 after 60 days



c Coating exposed BSS pH 2 after 60 days



d Coating exposed to acid producing bacteria after 60 days



## e Coating exposed natural community after 60 days

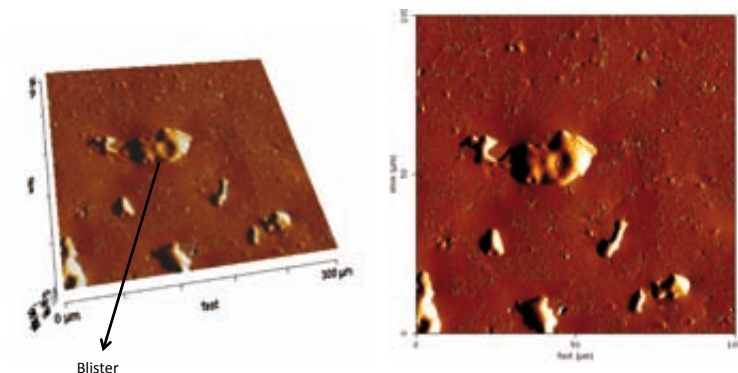


Fig. 5. AFM scans of epoxy ballast tank coating, before and after exposure to bacteria. Intermittent contact scans in air, line rate 0.2 Hz, scan area 100x100  $\mu\text{m}$ . (a) Blank control (no exposure). Effect of exposure time (60 days) on coating morphology: (b) Blank pH 7; (c) Blank pH 2; (d) *A. thiooxidans*; (e) natural community (isolated from ballast tank). Arrows indicate cracks/pinholes/blister on the surface.

No noticeable surface defects can be observed for the coating before exposure to BSS. The blank coating suggests a smooth surface; small irregularities in the form of parallel lines result from the application procedure (spray coating) (Fig. 5a). The second AFM image provides the coating after exposure to BSS (pH 7) for 60 days. One can identify swelling of the surface and precipitates from the medium on top of the coating in Fig. 5b. A different coating behaviour can be derived from Fig. 5c, which illustrates the coating immersed to BSS (pH 2) for 60 days. The outer coating layer has become brittle, indicated by leached areas and micro cracks on the surface. Fig. 5d represents the coating exposed to acid producing bacterial strain *A. thiooxidans*. A clear difference between the two coating surfaces can be identified. Holes in form of small round dots become visible for the acidic bacteria. The final image represents the coating exposed to the natural ballast tank community Fig. 5e. This coating surface is characterised by micro blisters all over the surface. However, the biological influenced coatings show a clear indication of hole and blister formation by AFM analysis on micron level. To prove the existence of holes, Fig. 6 provides a close up image of the coating surface without preliminary surface cleaning.

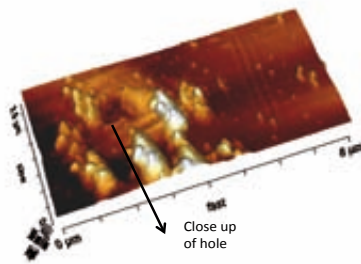


Fig. 6. Close up 3D AFM image of coating exposed to acidic bacteria after 60 days, contact scan in air, line rate 0.2 Hz, scan area  $3.5 \times 8 \mu\text{m}$ . Scan represents a circular pinhole (indicated by frame), surrounded by bacterial cells attached to the coating.

A circular hole can be noticed, surrounded by bacterial residues and dried out cells. The bacteria appear in the form of white clusters on the surface (a result of drying the sample before imaging), and the attached bacteria lose their original cell shape under the “shrinking effect” (Mangold et al., 2008). The coating surface is recognisably still smooth and homogeneous, and the bacterial effect is very local and aggressive, leading to hole formation in an apparently intact coating. Ageing of polymeric materials subjected to aggressive media consist first of all, in oxidation resulting in the formation of carbonyl groups  $\text{C}=\text{O}$  (Decker and Balandier, 1982; Katnarowska, 1999; Narrisawa, 1987). Oxidised surface layers of polymeric coatings show increased brittleness, resulting in cohesion loss in the pigment /binder resin system. In the next stage of coating ageing, pigment and filler particles are released from surface layers leading to increased surface roughness (Katnarowska, 1999). In turn, higher surface roughness results in lower protective efficiency, due to the resultant micro cavities gathering contaminants. This triggers the development of biological degradation, generating etching pits in the coating structure (Zyska, 1994). Another conclusion derived from the observed coating imperfections is that hydrolysis reaction and etching by acids occur favourably where cross-linking density is low (Osterhold and Patrick, 2001). Therefore, the lower cross-linking areas are removed during the course of degradation, while the higher crosslinking areas remain intact (hole formation with conductive path to the metal surface). To highlight and compare the effects of acidic bacteria and the natural community on the epoxy coating degradation, the mean hole and crack sizes were measured by AFM (Table 1).

**Table 1**

Mean hole and crack size of the coating samples exposed to BSS and BSS+bacteria.

Sample	Hole/Blister size (µm)		Crack size (µm)		
	Depth	Width	Depth	Length	Width
Blank pH 7 (before)	No hole	-	No crack	-	-
Blank pH 2 (before)	No hole	-	No crack	-	-
Blank pH 7 (after)	No hole	-	No crack	-	-
Blank pH 2 (after)	No hole	-	<i>Big cracks</i>		
			0.94±0.70	66.24±1.42	4.06±0.12
			<i>Small cracks</i>		
			0.61±0.91	35.79±1.01	7.53±0.58
Acidic bacteria	0.25- 0.99±0.26	4.8-9.1±1.59	No crack	-	-
Natural community	0.23- 0.57±0.16	4.4-10.2±2.33	No crack	-	-
			Particle/Precipitates	2.88-8±1.83	1.01-1.24±0.6

The mean whole widths and depths for the acidic bacteria are 4.8 to 9.1 µm and 0.25 to 0.99 µm, respectively. This clearly demonstrates the consequence of severe etching mechanism by biological metabolism. For the natural community, blister formation could be observed with 0.23 to 0.57 µm in height and an average width of 4.4 to 10.2 µm. For the pure culture of acid producing bacteria, hole formation can be observed on the surface, whereas the natural community containing diverse bacterial species is characterised by blister formation. Based on the aforementioned explanations, biological produced inorganic acids causes hole formation during the course of degradation. On the nano-scale, these effects change the behaviour of water uptake. This mainly arises from the changes in hydrophobicity of degraded parts, resulting in a more facilitated diffusion of electrolytes into the coating/metal interface. It is commonly acknowledged that coating porosity can play a key role in the film absorbing more water. This will negatively affect the epoxy coating, decreasing the anti-corrosive properties.

The following mechanism of microbial attack can be summarised after AFM imaging:

- Microbial attack is initiated from the surface, taking place through penetration of the coating, and forming channels throughout the coating.
- Excreted metabolites on the surface are responsible for the breakdown. The properties of the coating may thus be changed; first, the coating becomes hard and brittle, showing that the bacteria have altered the chemical composition of the film, and consequently it becomes prone to the physical causes of blistering.

In the first step, the surface coverage by bacteria was examined by fluorescent microscopy. The corresponding data from 9 individual images are presented in Fig. 5. The surface coverage of the bacterial set ups were initially compared with each other, resulting in an average bacterial surface coverage of 21% for the acid producing organisms and 14% for the natural community. The second approach included a more detailed investigation of the coating imperfections by fluorescent microscopy, involving the selection of 9 individual surface spots exhibiting characteristic surface defects, i.e. holes and blister.

These specific areas were determined and the bacterial attachment was related to the defects. For blister formation, a slight increase in coverage of 3% (from 14 to 17%) was observed for the natural community. A significant expansion from 21 to 33% (an increase of 12%) in surface coverage was found for the acid-producing bacteria next to the coating holes. Such shifts in surface attachment can be linked to the natural growth pattern of the biofilms. A schematic model correlating surface imperfection and biofilm structure is provided in Fig. 7.

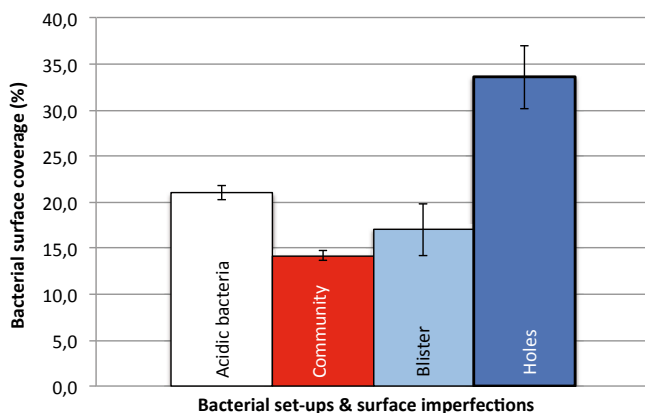


Fig. 7. Bacterial surface coverage in % depending on bacterial culture (average of whole surface) and type of coating defect.

Fig. 8a illustrates a perfect barrier coating with local cell cluster formation. The general surface coverage was 14-21% for both bacterial set-ups. The biofilm model indicates a patchy model of heterogeneous distributed cells on the surface, with no significant influence on fluid flow.

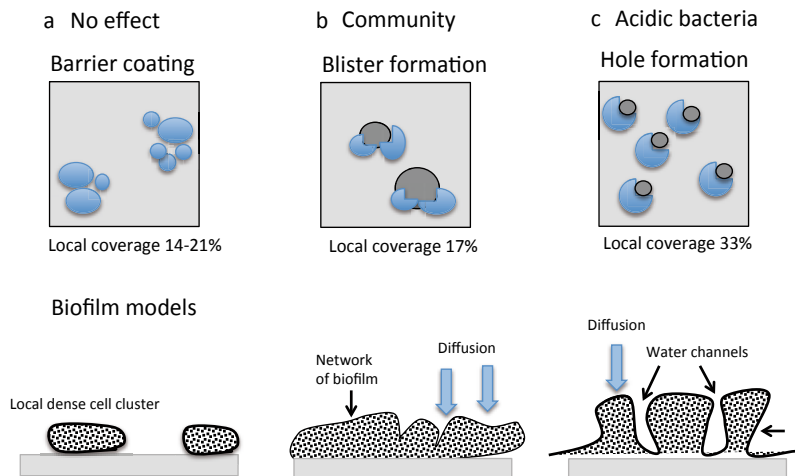


Fig. 8. Schematic model of coating defects correlating biofilm structure and mechanism of coating attack.

A different observation can be derived for the blister formation model presented in Fig. 8b, occurring as a consequence of bacterial attack in the form of a thick 3D biofilm. Diffusion reactions became the rate limiting reaction for water and oxygen down to the coating surface. The dense biological matrix acts as a diffusion barrier between coating and electrolyte, where acidic metabolic by-products accumulate in the interface of coating and biofilm matrix initiating blister formation of the polymer coating. The third form of attack was identified as hole formation, displayed in Fig. 8c in the presence of acidic bacteria. This was the most severe form of attack during the experiment, with the local attack caused by biofilms as discussed with the previous case. Nevertheless, the difference of attack can be explained by the circumstance whereby the biofilm structure not only acts as a diffusion barrier, rather it is the formation of water channels throughout the biofilm network that makes this type of attack so aggressive. One explanation is that the biofilm acts as a diffusion barrier for water and oxygen as mentioned above. However, the overall coverage of 33% and exposure time prompts the assumption that an altered biofilm is formed beside and on top of the holes. A mature biofilm is characterised by fluid channels creating a highly viscous structure. These channels will quantitatively increase the fluid flow towards the coating surface. The initially attacked coating, etched by acidic metabolic compounds of the bacteria, will easily take up water which leads to hole formation due to loss of the binder matrix system on local spots.

### 3.2 Electrochemical studies

The Nyquist plots of the blank samples and the bacterial set-ups at different immersion times are shown in Fig. 9.

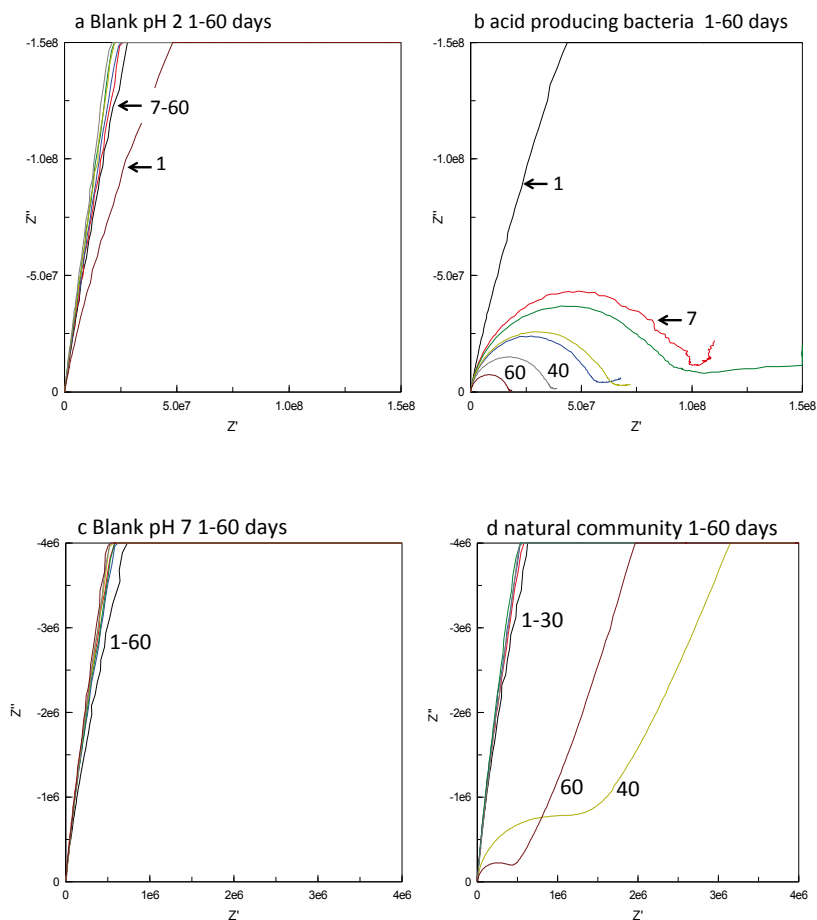


Fig. 9. Nyquist plot representation of the impedance results measured on ballast tank coating exposed to BSS and BSS+bacteria at different immersion times (1-60 days) (a) Blank (pH 2), (b) acidic bacteria, (c) Blank (pH 7), (d) natural community.

Coating resistance and phase angle parameters of the blank samples (coating without bacteria) were studied, based on the fitted values of Nyquist plots as shown in Fig. 9. Results indicated a two-time constant semi-circle for the immersion time (1-60 days) of the blank set-ups (Figs. 9a and 9c).

No significant changes were observed in coating resistance for pH 2 and pH 7 during these times. The coating prepared is usually partially heterogeneous and contains micropores. A slight shift can be recognised for both blanks after day 1, where the impedance shifts closer to an ideal capacitor (parallel to  $Z''$ ). These phase shifts are the result of interactions of water molecules and micropores. Water molecules have good isolating properties and can block the coating pores due to their dimension. From day 7 to 60 the blank coating exhibits an excellent barrier performance against electrolyte diffusion. The appropriate equivalent circuit used to fit the measured EIS data is shown in Fig. 10.

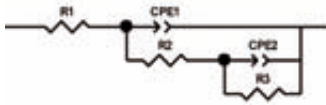


Fig. 10. Two-time constant electrical circuit model used for EIS results fitting of the ballast tank coating exposed to BSS (pH 2 and 7) blank samples.

The different electrical elements shown in this model, i.e.  $R_1$ , CPE1,  $R_2$ , CPE2 and  $R_3$ , represent the electrolyte resistance, coating capacitance, coating pore resistance, double layer capacitance and charge transfer resistance, respectively. It should be noted that the coating capacitance measured by EIS is non-ideal capacitance. Therefore, a constant phase element has to be used to replace the capacitance to gain a better fit. The relation between constant phase element and capacitance is the ideal coating capacitances measured using Eq. (1) (Mahdavian and Attar, 2006):

$$C = \frac{(Y_o \cdot R_p)^{\frac{1}{n}}}{R_p} \quad (1)$$

Where  $R_p$  represents the total resistance, and  $Y_o$  and  $n$  represent CPE (constant phase element) parameters. The data obtained from fitting EIS information ( $R_p$  and CPE) and from Nyquist and Bode plots (phase angle and  $Z'$ ) gained for the blank samples are shown in Table 2. Measured low frequency data (0.01 Hz) by EIS shows considerable sensitivity and variation to changes in the impedance, due to the uptake of water. The higher the impedance at low frequency, the more effective the coating is. The variation of phase angles  $\Phi$  at 10 Hz over time is very close to the variation of coating resistance, and hence can qualitatively reflect the coating performance (Zuo et al., 2008).



**Table 2**

Different electrochemical parameters obtained from Bode plots and EIS fitting results of the coating exposed to blank electrolyte (BSS, pH 2 and pH 7) at different immersion times; 1 to 60 days.

<b>Blank pH 2</b>					
	R <sub>p</sub> (M·Ω·cm <sup>2</sup> )	CPE1 (μF cm <sup>-2</sup> )	-Φ (°) at 10 Hz	Z  at 0.01 Hz	Chi-Squared of fitting
Time in days		Mean	Mean	(G·Ω)	
1	6030	0.000418	78.21	4.47	0.00014
7	12888	0.000426	78.45	8.78	0.00027
15	8806	0.000425	80.37	4.85	0.00053
21	6822	0.000436	77.89	4.69	0.00028
30	2210	0.000445	76.15	2.56	0.00088
40	8340	0.000490	77.06	6.68	0.00021
60	797	0.000528	76.13	8.25	0.00028

<b>Blank pH 7</b>					
	R <sub>p</sub> (M·Ω·cm <sup>2</sup> )	CPE1 (μF cm <sup>-2</sup> )	-Φ (°) at 10 Hz	Z  at 0.01 Hz	Chi-Squared of fitting
Time in days		Mean	Mean	(G·Ω)	
1	23480	0.000439	78.27	5.08	0.00021
7	31340	0.000547	80.61	9.76	0.00013
15	41108	0.000530	80.37	10.02	0.00011
21	47017	0.000523	80.89	5.35	0.00011
30	96508	0.000573	81.15	9.47	0.00026
40	188200	0.000531	82.06	9.02	0.00028
60	478480	0.000491	82.31	13.35	0.00053

Based on the coating resistance and impedance magnitude at 0.01 Hz and the blank sample during the immersion to BSS pH 7, a slow decrease in resistance and increase in phase angle can be attributed to the swelling of the coating during its interaction with the electrolyte (salt solution 3.5%). The increase in phase angle magnitude of the blank sample over the course of the experiment arises from its excellent barrier effect. This can be explained by the observations made by AFM images of the blank sample in Fig. 3. According to this figure, no defect, hole or pore can be found after 60 days. For the blank set-up with a pH 2, a different effect can be observed. Directly after exposure the coating indicated a continuous decrease in coating resistance and an increase in impedance magnitude. These phenomena can be attributed to crack formation and coating deterioration during exposure to a low pH electrolyte (pH 2). Soon after immersion, the coating loses the barrier effect, as supported by AFM data in Fig. 3b, and a crack formation becomes visible. The hypothesis, based on which the coating impedance magnitude (at 0.01 Hz) is believed to decrease, relates to degradation and can be explained by the information obtained from the phase angle. Phase angle is a suitable parameter of EIS method for describing coating degradation during its interaction with a corrosive electrolyte (Mahdavian and Attar, 2006; Mahdavian and Attar, 2009). Phase angle (-Φ) magnitude varies from 0° to 90°. This parameter is close to 90° for an intact coating on a metal substrate. However, when coating is exposed to a corrosive electrolyte, the deterioration causes the phase angle to decrease.

Therefore, the closer the phase angles ( $-\Phi$ ) of a coating to  $90^\circ$ , the lower the deterioration during the immersion. As can be seen from Table 2, an increase in phase angle can be observed for the blank with pH 7 ( $78.27^\circ$  to  $82.31^\circ$ ), a slight decrease in phase angle ( $-\Phi$ ) could be found for the blank with a pH 2 ( $77.82^\circ$  to  $76.13^\circ$ ). This observation clearly demonstrates lower coating resistance at higher exposure times. The size of cracks created by hydrolysis produced some conductive paths in the coating at pH 2.

**Table 3**

Different electrochemical parameters obtained from Bode plots and EIS fitting results of the coating exposed to acid producing bacteria (*A. thiooxidans*) and natural community (isolate from ballast tank) at different immersion times; 1 to 60 days.

<b>A. thiooxidans</b>	Rp ( $M\cdot\Omega\cdot cm^2$ )	CPE1 ( $\mu F\ cm^{-2}$ ) Mean	$-\Phi$ ( $^\circ$ ) at 10 Hz Mean	IZI at 0.01 Hz ( $G\cdot\Omega$ )	Chi-Squared of fitting
Time in days					
1	9641	0.000513	77.73	2.80	0.00020
7	95	0.000496	66.82	0.11	0.00026
15	52	0.000517	59.26	0.06	0.00039
21	82	0.000518	64.49	0.24	0.00095
30	56	0.000549	60.15	0.07	0.00034
40	31	0.000583	48.62	0.04	0.00016
60	12	0.000669	33.79	0.02	0.00012

<b>Natural Community</b>	Rp ( $M\cdot\Omega\cdot cm^2$ )	CPE1 ( $\mu F\ cm^{-2}$ ) Mean	$-\Phi$ ( $^\circ$ ) at 10 Hz Mean	IZI at 0.01 Hz ( $G\cdot\Omega$ )	Chi-Squared of fitting
Time in days					
1	5770	0.000495	76.58	2.81	0.00018
7	12273	0.000427	79.27	6.08	0.00011
15	14554	0.000463	80.04	4.41	0.00009
21	14659	0.000463	80.37	4.48	0.00010
30	87	0.000429	51.75	0.45	0.00180
40	5	0.000417	41.91	0.27	0.00014
60	2	0.000363	46.88	0.21	0.00014

Unlike the behaviour of the blank samples, those exposed to bacterial species show significant changes in electrochemical parameters. One further equivalent electrical circuit was used to fit EIS data, for the purpose of comparison.

The two time constant model could be used for all immersion times. At higher immersion times for 40 to 60 days, the model was extended with the Warburg diffusion element for the acidic bacteria. The semi-circle observed for the ballast tank coating in contact with acidic bacteria in Fig. 7b indicates higher diffusion behaviour. For the second bacterial set-up with a natural bacterial community isolated from a ship ballast tank, a more pronounced diffusion behaviour can be observed for 40 to 60 days. The two time constant model remained valid, and could be used to fit the corresponding data.

The equivalent circuits applicable to fit the EIS data for the bacterial set-ups are shown in Fig. 11. Fig. 11a represents the two-time constant model as described in Fig. 10, and Fig. 11b shows the circuit with added Warburg diffusion element.

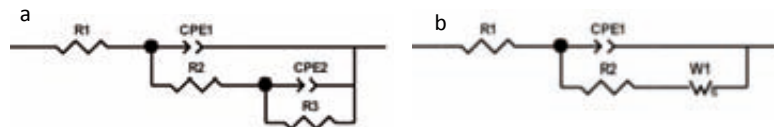


Fig. 11. Two-time constant electrical circuit models used for EIS results fitting of the ballast tank coating exposed to bacteria (a) circuit used for natural community (1-60 days) and acidic bacteria (1-30 days); (b) circuit used for acidic bacteria (40-60 days).

The Warburg diffusion element is well known and described for several bacterial experiments (Lee et al. 2006; Castaneda et al. 2008). The different electrical elements shown in this model for Fig. 9b, i.e.  $R_1$ ,  $CPE_1$ ,  $R_2$  and  $W_s$ , represent the electrolyte resistance, coating capacitance, pore resistance, and Warburg diffusion respectively. By comparing the results of Table 3 with the findings in Table 2, there are noticeable differences between blank and bacterial set-ups. For the bacterial set-up with acidic bacteria low phase angles ( $-\Phi$ ) at very short immersion times correspond to biologically metabolism and therefore biodegradation of the coating. The two time constant Nyquist plot appearing at low immersion times suggests that the corrosion resistance of the coating is poor. The corresponding coating resistance and impedance at 0.01 Hz are much lower for the biological sample with a pH of 2. This clearly illustrates the effect of biological degradation on coating performance. This lower coating resistance and smaller phase angle can be explained by the previously discussed AFM data. The impedance magnitude (at 0.01 Hz) after 60 days was  $0.019 \text{ G}\cdot\Omega$  for acidic bacteria, whereas those of the natural community showed a value of  $0.21 \text{ G}\cdot\Omega$ . These results indicate that the anti-corrosive performance of biologically degraded coatings decreases significantly after 60 days of immersion. Another parameter showing the low anticorrosive properties of these coatings is phase angle, measuring at 10 Hz from Bode plots. As indicated in Table 3, phase angles ( $-\Phi$ ) of ballast tank coating degraded by acidic bacteria and natural community changed for the acidic bacteria from  $77.73^\circ$  to  $33.79^\circ$  and  $78.27^\circ$  to  $66.88^\circ$ , respectively. This can be attributed to a severe degradation is taking place through biological activity and metabolic by-products. Furthermore, strong conformity between the results of Tables 2 and 3 can be seen. The phase angle changes of each sample immersed at different times in electrolyte are compared and provided in Fig. 12.

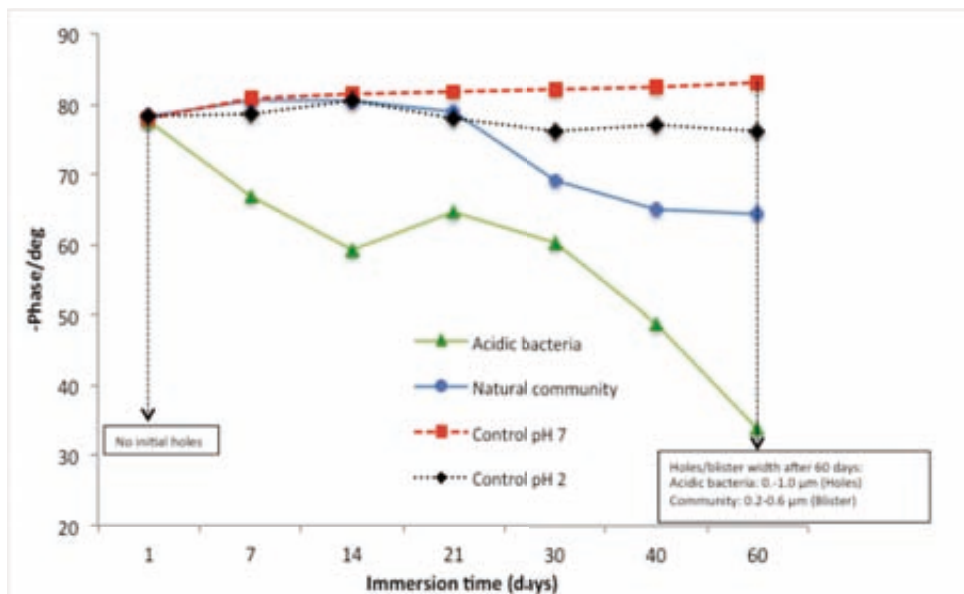


Fig. 12. Comparing the phase angle (at 10 Hz) changes of different samples and their relation to the size and type of defect at the surface.

According to Fig. 12, the greater decrease in phase angle of the sample degraded by acidic bacteria (triangle) could be related to the existence of holes, resulting in a higher diffusion of electrolyte into the coating. This in turn leads to reduction in phase angle and subsequently to a higher degradation. The fact that the phase angle of the blank (pH 2, rhomb) has decreased in parallel is a result of the indicated cracks in the coating surface leading to diffusion of electrolyte. Nevertheless, a clear difference can be noticed between blank and acidic bacteria for low pH ranges, however both coating surfaces indicate a decrease in phase angle and therefore a loss of the barrier property of the coating. On the other hand, the blank (pH 7, cross) has not changed significantly, due to the lack of surface holes. The corresponding natural community (dot) shows a lower decrease in phase angle with a clear signal for coating biodeterioration in relation to the blank (dot). The Warburg diffusion element was added in the circuit for the ongoing experiment, to fit the related EIS data, with the diffusion resistance decreasing after 40 to 60 days. This indicates that the biofilm layer has conductive pathways or water channels for transport properties. If the diffusion process increases due to a thick biofilm, a longer conductive pathway will result. The Warburg resistance is lowered by a factor of 1.5 at the end of the experiment for acidic bacteria. This decrease in diffusion could have two possible explanations:

1. Decrease in biofilm thickness over time due to less metabolic active bacteria, 2. Change in biofilm architecture, establishing water filled channels rather than diffusion-limited pores throughout the biological layer. To make a clear statement on these assumptions, the relative thickness of the acidic biofilm was calculated using Eq. (2).

$$W_s T = \frac{L^2}{D} \Rightarrow L_{days} = \sqrt{W_s T * D_{(oxygen)}} \quad (2)$$

The Warburg diffusion element  $W_s$  is the solution of the one-dimensional diffusion equation of a particle interpreted as  $W_{sT} = L^2/D$ . Where  $L$  is the effective diffusion thickness and  $D$  is the effective diffusion coefficient of the particle. To calculate the thickness of the biofilm, the diffusion coefficient of oxygen ( $20.0 \times 10^{-6} \text{ cm}^2/\text{s}$ ) at  $25^\circ\text{C}$  was used as a representative parameter influencing biofilm built up. The equation was solved according to  $L$  for specific days to interpret the gained data.

**Table 4**

Calculated oxygen diffusion derived from Warburg diffusion element for acidic bacteria after 40 and 60 days.

Acidic bacteria	$L_{max}$ = biofilm thickness ( $\mu\text{m}$ , $25^\circ\text{C}$ )
$L_{40}$	17.5
$L_{60}$	14.3

A thinner biofilm results in a decrease in the  $L$  value, with increased transport probabilities in form of pores with water channels therein. This allows the transport of salts and oxygen (penetration of electrolyte) towards the coating layer in a rapid manner. The data in table 4 supports previous observations that the diffusion effect of the biofilm decreases over time due to bacterial activity and changes in biofilm architecture (discussed in Fig. 6 of this paper). The biofilm consists of tightly packed mushroom-shaped clusters that are between  $17.5$  and  $14.3 \mu\text{m}$  in height. The time required for a solute from the liquid phase (medium) to reach the base of a uniformly thick biofilm (assumed for calculation) is simply provided by Eq. 3 (Stewart, 2003):

$$t = 1.03 \frac{L^2}{D_e} \quad (3)$$

Here,  $L$  is the biofilm thickness, and  $D_e$  the effective diffusion coefficient in the biofilm. The value of the effective diffusion coefficient in the biofilm will be reduced compared to the diffusion coefficient in water, due to the presence of microbial cells, extracellular polymers, and abiotic particles or gas bubbles trapped in the biofilm. This reduction is denoted by the ratio  $D_e/D_{aq}$ . Experimental measurements of this ratio, termed the relative diffusivity, have been reviewed elsewhere (Stewart, 1998).

The calculated diffusion times of  $\text{Cl}^-$ ,  $\text{SO}_4^{2-}$ , acetic acid and oxygen are listed in Table 5.

**Table 5**

Calculated diffusion times for oxygen, acetic acid, chloride, sulphate through acidic biofilm after 40 and 60 days.

Solute	Diffusion coefficient $D_{\text{aq}}10^{-6} (\text{cm}^2/\text{s})$	$D_e(\text{factor})$	$L_{40} (\mu\text{m})$	Diffusion time (min)	$L_{60} (\mu\text{m})$	Diffusion time (min)
Oxygen	20.0	0.7	175	3.63	143	2.43
Acetic acid	12.1	0.7	175	6.02	143	4.02
$\text{Cl}^-$	20.3	0.7	175	3.60	143	2.38
$\text{SO}_4^{2-}$	10.6	0.7	175	6.86	143	4.58

It is evident from the table that the diffusion times obtained decreased over time depending on the biofilm architecture. The diffusion times are within the range of several minutes are typical for diffusion processes through biofilms as reported by (Stewart, 2003). It is valuable to mention that for the experimental set-up discussed here aggressive compounds such as acids and chloride are rapidly transported and concentrated close to the coating surface, causing serious damage in the presence of bacteria.

#### 4. Conclusions & Recommendations

It can be concluded that the bacterial deterioration effect is as severe as other types of degradation, leaving the coating system highly vulnerable to deterioration in real environmental conditions. It is therefore necessary to include natural communities in coating degradation studies to identify possible degradation mechanisms and the severity of attack over time. The behaviour of a ballast tank coating against microbial degradation was studied, indicating that biological activity significantly affect the coating properties. As a result of such a phenomenon, micro-cracks and holes were identified by AFM. The overall effect of such degradation was studied using the EIS technique, with the non-bacterial exposed samples (blank) exhibiting a reasonably proper corrosion resistance.

However, the bacterial affected coatings (exposed to acid producing bacteria and natural ballast tank community) show a decrease in corrosion resistance. For the acidic environment with a low pH, EIS measurements indicate a decline in corrosion resistance over the course of the experimental time regardless of whether there was a bacteria presence. This demonstrates that low pH solution has a significant impact on the coating barrier property, resulting in crack and hole formation. This effect was attributed to electrolyte diffusion through the biofilm. It is also revealed that the coating corrosion resistance declines after 40 days of exposure for the natural community, leading to the formation of blisters. Bacterial settling could be linked to some specific biofilm patterns affecting different types of coating attack. It is possible to model and explain the impact of the biofilm on the ballast tank coating responsible for serious coating deterioration. Overall, the natural bacterial community shows a less aggressive type of deterioration than the pure culture alone.

---

## References

American Society for Testing and Materials ASTM (1976). vol D 6400-99. Philadelphia, Pennsylvania

American Society for Testing and Materials ASTM (1993a). Annual Book of ASTM Standards, Volume 08.03, 5209-92. Philadelphia, Pennsylvania

American Society for Testing and Materials ASTM (1993b). Annual Book of ASTM Standards, Volume 08.03, 5210-92. Philadelphia, Pennsylvania

American Society for Testing and Materials ASTM (1993c). Volume 08.03, D5271-92. Philadelphia, Pennsylvania

American Society for Testing and Materials ASTM (1993d). Volume 08.03, G22-76. Philadelphia, Pennsylvania

American Society for Testing and Materials ASTM (1993e). Annual Book of ASTM Standards, vol Volume 08.03, G21-90. Philadelphia, Pennsylvania

Castaneda H, Benetton XD (2008) SRB-biofilm influence in active corrosion site formed at the steel-electrolyte interface when exposed to artificial seawater conditions. *Corrosion Science* 50:1169-1183

Decker C, Balandier M (1982) Degradation of poly (vinyl chloride) by UV radiation – I Kinetics and quantum yields. *European Polymer Journal* 18:1085-1091

Det Norske Veritas (DnV) (1998) Type approval programme for protective coating systems. vol No. 1-602.1. DnV, Oslo

Det Norske Veritas (DnV) (1999) Corrosion prevention of tanks and holds. vol No. 33.1. DnV, Oslo

Geenen FM, de Wit JHW (1990) An impedance spectroscopy study of the degradation mechanism for a model epoxy coating on mild steel *Prog Org Coat* 18 (3):299-312

Gilmore DF, Antoun S, Lenz RW, Goodwin S, Austin R, Fuller RC (1992) The fate of biodegradable plastics in municipal leaf compost. *Journal of Industrial Microbiology and Biotechnology* 10:199-206

Gu JD, Ford TE, Mitchell R (1996) Susceptibility of electronic insulating polyimides to microbial degradation. *J Appl Polm Sci* 62:1029-1034

Gu JD, Gada M, Kharas G, Eberiel D, McCarthy SP, Gross RA (1992) Degradability of cellulose acetate (1.7 and 2.5, d.s.) and poly(lactide) in simulated composting bioreactors. *Polymer Materials Science and Engineering* 67:351–352

Gu JD, Lu C, Thorp K, Crasto A, Mitchell R (1997a) Fiber-reinforced polymeric composite materials are susceptible to microbial degradation. *Journal of Industrial Microbiology & Biotechnology* 18:364-369

Gu JD, Lu C, Thorp K, Crasto A, Mitchell R (1997b) Fungal degradation of fiber-reinforced composite materials. *Materials Performance* 36:37-42

Gu JD, Mitton DB, Ford TE, Mitchell R (1998) Microbial degradation of polymeric coatings measured by electrochemical impedance spectroscopy. *Biodegradation* 9 (1):39-45

Iijima T, Arai N, Takematsu K, Fukuda W, Tomoi M (1992) Toughening of epoxy resins by N-phenylmaleimide-styrene copolymers. *European Polymer Journal* 28 (12):1539-1545

Imam SH, Gould JM, Gordon SH, Kimney MP, Ramsey AM, Tosteson TR (1992) Fate of starch-containing plastic films exposed in aquatic habitats. *Current Microbiology* 25:1-8

International Association of Classification Societies (IACS) (1998) Guidelines for acceptance, application and survey of semi-hard coatings on ballast tanks. Recommendation, vol No. 5.

International Maritime Organization (IMO) (1995) Guidelines for the selection, application and maintenance of corrosion prevention systems of dedicated seawater ballast tanks. vol Resolution A 798 (19) London

Katnarowska D (1999) Influence of ultraviolet radiation and aggressive media on epoxy coating degradation. *Progress in Organic coatings* 37:149-159

Kemnitzer JE, McCarthy SP, Gross RA (1992) Poly( $\beta$ -hydroxy-butyrate) stereoisomers: a model study of the effects of stereochemical and morphological variables on polymer biological degradability. *Macromolecules* 22:6143-6150

Kikkawa Y, Yamashita K, Hiraishi T, Kanesato M, Doi Y (2006) Dynamic Adsorption Behavior of Poly(3-hydroxybutyrate) Depolymerase onto Polyester Surface Investigated by QCM and AFM *Biomacromolecules* 6:2084-2090

Kotnarowska D (1999) Influence of ageing on mechanical properties of epoxy coatings. In: *Advances in corrosion protection by organic coatings*. Cambridge, pp 1-10

Lee AK, Buehler MG, Newman DK (2006) Influence of a dual-species biofilm on the corrosion of mild steel. *Corrosio Science* 48:165-178

Mahdavian M, Attar MM (2006) Another approach in analysis of paint coatings with EIS measurement: phase angle at high frequencies. *Corros Sci* 48:4152-4157

Mahdavian M, Attar MM (2009) Electrochemical behaviour of some transition metal acetylacetonate complexes as corrosion inhibitors for mild steel. *Corros Sci* 51:409-414



Majumdar I, D'Souza F, Bhosle NB (1999) Microbial exopolysaccharides: Effect on corrosion and partial chemical characterization. *J Indian Inst Sci* 79:539-550

Mangold S, Harneit K, Rohwerder T, Claus G, Sand W (2008) Novel Combination of Atomic Force Microscopy and Epifluorescence Microscopy for Visualization of Leaching Bacteria on Pyrite. *Appl. Env. Microbiol.* 74: 410-415

Osterhold M, Patrick G (2001) Influence of weathering on physical properties of clearcoats. *Prog Org Coat* 41:177-182

Ramezanzadeh B, Mohseni M, Yari H (2010) On the electrochemical and structural behavior of biologically degraded automotive coatings; Part 1: Effect of natural and simulated bird droppings *Prog Org Coat* 71:19-31

Rouw AC (1997) Model epoxy powder coatings and their adhesion to steel. *Prog Org Coat* 34 (1-4):181–192

Stewart PS (1998) A review of experimental measurements of effective diffusive permeabilities and effective diffusion coefficients in biofilms. *Biotechnol Bioeng* 59:261–272

Stewart PS (2003) Diffusion in biofilms. *J Bacteriol* 185 (5):1485

Tanker Structure Cooperative Forum (TSCF) (1997) Guidance manual for tanker structures. Witherby & Co. Ltd., London

Tanker Structure Cooperative Forum (TSCF) (1999) Condition evaluation and maintenance of tanker structures. Witherby & Co. Ltd., London

Uchida E, Ikada Y (1997) Topography of Polymer Chains Grafted on a Polymer Surface Underwater. *Macromolecules* 30:5464–5469

Vancsco GJ, Allston TD, Chun I (1996) Surface Morphology of Polymer Films Imaged by Atomic Force Microscopy. *Int J Polym Anal Charact* 3:89

Vancsco GJ, Liu G Surface morphology of polymer films by scanning probe technique In: ANTEC'96, 1996.

van Westing EPM, Ferrari GM, de Wit JHW (1994a) The determination of coating performance using electrochemical impedance spectroscopy *Electrochem Acta* 39 (7):899-910

van Westing EPM, Ferrari GM, de Wit JHW (1994b) The determination of coating performance with impedance measurements—II. Water uptake of coatings. *Corrosion Science* 36:957-977

Zuo Y, Pang R, Li W, Xiong JP, Tang YM (2008) The evaluation of coating performance by variations of phase angles in middle and high frequency domains by EIS. *Cor Sci* 50 (12):3322–3328

## Chapter 4

### **4.1    *A new approach to study local corrosion processes on steel surfaces by combining different microscopic techniques***

#### **Abstract**

Corrosion studies of materials on the micro or even nano-scale level are cumbersome due to instrumental limitations and handling procedures. If biological processes are involved the spatial resolution is even more important and sample preparation is usually the limitation. Attachment of bacteria on stainless steel surface is a complex interfacial process including interactions of bacterial cells and bacterial extracellular polymeric substances with the surface. To overcome the limitations in sample preparations and resolution we present a new stainless steel sample holder to switch among Epifluorescent Microscope (EFM), AFM and SEM at exactly the same position. Exemplary bacterial accumulation was studied by staining the bacterial DNA with a fluorescent dye over time. It was possible to distinguish among bacteria and other surface characteristic such as deformations or grain structures. Also surface topographic features such as roughness at the grain boundaries and deposits were quantified. All three techniques complement one another in the way that AFM is a high-resolution technique that does not allow to distinguish directly bacterial cell structures, whereas EFM offers excellent bacterial identification based on staining at a low resolution that can complement AFM images. Application of SEM in the last step will reveal inclusions and grain structure and combined with EDX gives the composition of the substrate, inclusions and corrosion deposit. The combination of the three high-resolution techniques enables a more detailed understanding of surface phenomena. The method itself is quite elegant and easy to handle which is an important item in materials research, especially when a high sample throughput is needed.

## 1. Introduction

Attachment and growth of bacteria on metal surfaces can lead to the formation of a biofilm and the importance of biofilm in corrosion of metals and alloys has recently gained considerable interest [1-2]. Corrosion due to presence of bacteria and their activity is termed bio-corrosion or microbiologically influenced corrosion (MIC). MIC mostly manifests itself as localized corrosion, since microscopic organisms tend to settle on metal surfaces as discrete colonies rather than continuous films. Due to the strong impact of bacterial presence on localized corrosion of steel it is important to characterize how bacteria initiate and influence corrosion. While propagation steps of MIC are well modelled and documented [3-5], the initial steps of MIC are not well understood until now and one of the ways to study such phenomena is using surface characterization techniques such as microscopy.

Conventional optical microscopic techniques such as light microscopy (LM) are intensively used for surface analysis to investigate the occurrence and characteristic features of MIC [6-8]. Epifluorescence microscopy (EFM) has proven to be a powerful tool for selective and specific visualization of labelled bacteria and molecules, which makes it possible to follow cellular processes and to monitor the distribution of living cells [9]. Besides this some researchers started to combine fluorescent microscopy and SEM imaging to understand structural properties of natural biofilms [10,11]. EFM and SEM coupling is also used for corrosion studies under protective coatings by using fluorescent probes [12]. The use of the fluorescent dye for the investigation of the localized corrosion behaviour of aluminium alloys allows the identification of the anodic dissolution site within a few minutes after exposure to the test solution. It is therefore a powerful tool for investigation of the corrosion processes and the characterization of inhibitor efficiency [13].

Atomic force microscopy (AFM) is receiving considerable attention in the field of surface science and engineering because of its ability to image surfaces, either conducting or non-conducting, in situ and with up to atomic scale resolution. Most of the previous studies are, however, related to the atomic imaging of well-defined surfaces [14], AFM has not yet been used widely in corrosion studies [15] despite its enormous potential in revealing shape evolution at the nanoscale level during corrosion or surface treatment, at/or near fine surface inhomogeneity's associated with cellular boundaries, grain boundaries, or precipitates or inclusions of exceedingly fine sizes. On the other hand AFM is widely used for biological samples because of its high in-situ resolution, while it requires minimum sample preparation and can be operated under wet and dry conditions [16]. The technique was used to study MIC intensively and is well discussed in literature in recent years [17-23]. Further, several local microscopic techniques have been combined for bacterial applications such as the combination of optical and atomic force microscopy (AFM) [20] or the combination of AFM and confocal microscopy [21]. Combination of optical and atomic force microscopy (AFM) is a powerful tool to obtain comprehensive information on a variety of samples. The advantage of combining fluorescence microscopy and the AFM technique is that they are complementary and provide detailed characterization of living component and processes:

the fluorescence provides information about the location of labelled cells and the AFM scanning gives a more comprehensive topology picture of the cells. The scanning electron microscope (SEM) generally has the high lateral resolution and a relatively large field-of-view making it an excellent tool for surface analysis [24]. It has been used to detect the degradation of or damage to coatings in polymer blends [25], relaxation and physical aging effects [26], water sorption, diffusion in films [27-29] and reaction kinetics [29,30]. The energy dispersive X-ray spectroscopy (EDX) is a comfortable technique that has the ability to perform a timely, non-destructive, semi-quantitative chemical analysis of environmental particles [31], corrosion effects [32] or coatings [33]. The combination of EFM, AFM and SEM in general seems to be a powerful tool for investigations of biological processes on surfaces and corrosion. In this paper, we demonstrate for the first time the feasibility of combining the three microscopic techniques operated subsequently in time at exactly the same area spot at the surface, by using a custom-made sample stage and an additional shuttle stage, thus pioneering the way for a powerful tool for the investigation of surface processes, coatings or even interfacial reactions.

## 2. Experimental

### 2.1 Metal coupons and bacterial attachment

Stainless steel 316L coupons (30 mm x 15mm x 1mm) were used in the experiment. The coupons were sequentially ground with a series of grit SiC papers (220, 500, 1200, 2400 and 4000) to a smooth surface, and were finally polished to a mirror-finish surface using 0.3 to 0.1 micron diamond paste. The polished coupons were first degreased with acetone, followed by rinsing with ethanol and dried immediately. Finally, the sample was treated with V2A acid solution ( $\text{HNO}_3/\text{H}_2\text{O}/\text{HCl}$ ) commonly used for macroetching of iron and steel surfaces to visualise the grain boundary structure. To identify the same sample spot precisely an indent was made on the surface of the coupon. The indent is mounted on the surface of the metal coupon in such a way that it corresponds to the centre of the SEM stage (point 0 of the SEM axis) when the metal coupon is placed in the SEM sample holder. Further, the indent will enable to reach any spot on the surface by using fixed x and y-axis coordinates in the SEM vacuum chamber. After indentation the prepared coupon was sterilized by immersion in 70% ethanol for 4 h, and dried aseptically in air.

The stainless steel coupon was exposed for 48h to natural seawater, which is pumped continuously through a basin containing 1 m<sup>3</sup> of water to obtain initial bacterial accommodation on the surface from a natural source. To investigate the changes on the steel surface after bacteria attachment, coupons were investigated before and after exposure with a combination of different microscopes i.e. EFM, AFM and SEM providing more accurately visualization of the same spot of the surface at a micron level before and after immersion.

## *2.2 Sample stages for microscopy*

To characterise exactly the same sample spot of the surface before and after immersion at the micron level, it was necessary to design an in-house sample holder and stages for the microscopes. Figure 1a is a custom-made sample holder that can hold a coupon in the groove with minimum movement. The sample holder has the same size as a normal glass slide in order to be used on stages of different microscopes. Figure 1b displays the AFM shuttle stage (which is commercial available by JPK Instruments) in combination with the house made sample holder to combine LM, EFM and AFM. Figure 1c shows the homemade SEM shuttle stage with the new sample holder that was used to further combine AFM and SEM. The combination steps are further detailed below in the methodology part. By combining the sample holders, transfer stages and additional surface indentation of the sample, it was possible to combine and locate the same sample spot with different microscopes before and after the experiment on micron scale. In the following paragraph the shuttling procedures are described to help visualizing the new methodology and the combined results of the three techniques.

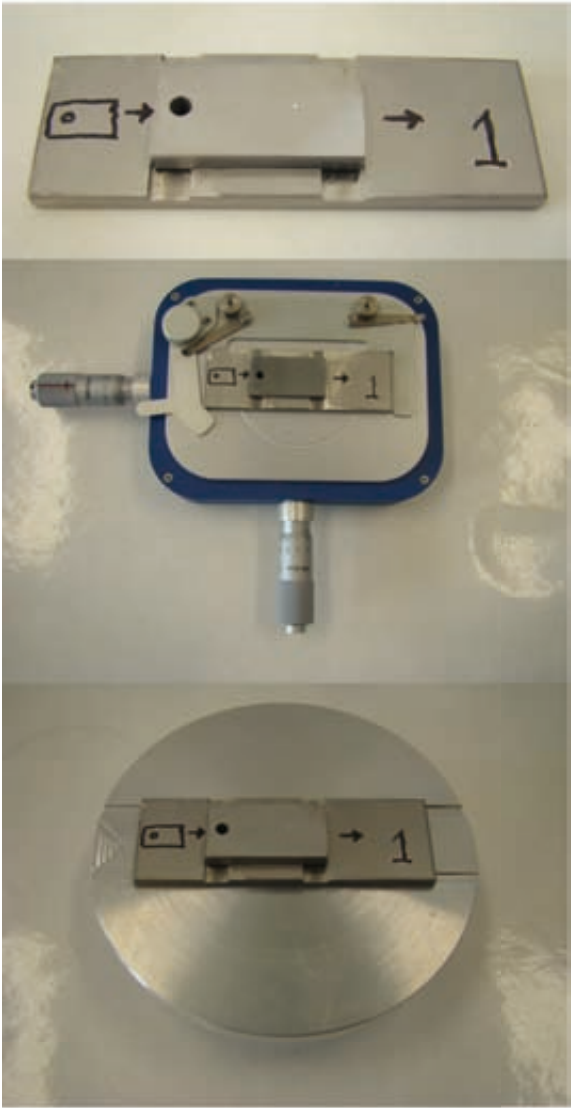


Fig. 1. Sample stages for combining three microscopes; (a) in-house made sample holder,(b) sample holder on AFM shuttle stage, (c) sample holder placed on home-made SEM shuttle stage.

## 2.3 Microscopes

### *Optical/Epifluorescence microscope (OM/EFM)*

An upright optical/epifluorescence microscope (Olympus BX 51, Japan) with a 40 x water-immersible objective (LUMPlanFLN 40x, Olympus) without using coverslips were combined using the shuttle stage as base stage on the microscope. By using a water-immersible objective, images of the natural state of the biofilm *in situ* could be taken.

### *Atomic force microscopy (AFM)*

A NanoWizard II atomic force microscope (JPK Instruments, Germany) was used for contact mode imaging in air of the metal substrate. For AFM imaging a silicon cantilever CSC37 A (Mikromasch, Estonia) with the following features was used: typical length, 250  $\mu\text{m}$ ; width, 35  $\mu\text{m}$ ; thickness, 2  $\mu\text{m}$ ; resonance frequency, 41 kHz; and nominal force/spring constant, 0.65 N/m. Each AFM image consists of 512 by 512 pixels. The AFM image acquisition details are given in the legends of the each figure.

### *Scanning electron microscope (SEM)*

SEM analysis was performed with a JSM-5800LV (Joel, Japan) scanning electron microscope. Images were taken with a working distance of 7-12 and 800 x magnification. For Energy Dispersive X-Ray (EDX) spectroscopic analysis the system was equipped with a Noran 5 elemental analyser (Thermo Scientific, Germany). An accelerated voltage of 12 kV was used for both secondary electron imaging and EDX. The analysis software NSS 2.2 x-ray microanalysis (Thermo Scientific, Germany) was used for elemental analysis.

## 2.4 Imaging steps

### *Step 1 – combination of optical microscope/EFM and AFM*

For a successful combination of both microscopes, meaning the visualization of the same sample spot, the variable position of the AFM cantilever had to be aligned to the static optical axis of the optical/epifluorescence microscope to match the AFM scan region with the microscope's field of view. The first step includes the alignment of optical microscope and AFM. This was carried out using a glass calibration-slide with a marked centered cross in detail explained by [34]. The AFM shuttle stage can be transferred between the AFM and the optical/epifluorescence microscope, giving a precise positioning of the stage on both microscopes. Furthermore, a sample clamp guaranteed a tight and accurate fixation of the sample to the shuttle stage, thereby allowing the retrieval of the same sample spot with AFM and EFM with an error of no more than 3 to 5  $\mu\text{m}$ . The alignment procedure of EFM and AFM is intensively described by [34]. The new approach in here was to visualize the same spot afterwards by SEM and SEM-EDX by using an in-house made sample holder as well as transfer stage.



To combine AFM imaging with SEM an additional surface indent has to be placed on the sample coupon, which corresponded to the center of the glass calibration slide, which was used to align EFM and AFM. Once the spot of interest was fixed by x and y coordinates (by adjusting front and side knobs of the AFM shuttle stage, Fig. 1b) the respective optical microscope image and the AFM scan were combined in  $\mu\text{m}$  scale. For sequential investigations of different spots of interest (i.e. different coordinates of the AFM shuttle stage can be used), shuttling between the instruments could be repeated as often as required, without losing position. Additionally, two AFM scans were combined to increase the sample area up to  $(180 \times 100 \mu\text{m})$  with a 20 % overlap. This up scaled AFM surface image corresponds to the central part of the EFM image. Fig. 2 shows the combined AFM contact scan of a stainless steel sample (20 % overlap represented by orange square) with grain boundaries that correspond to the center of EFM image (yellow square).

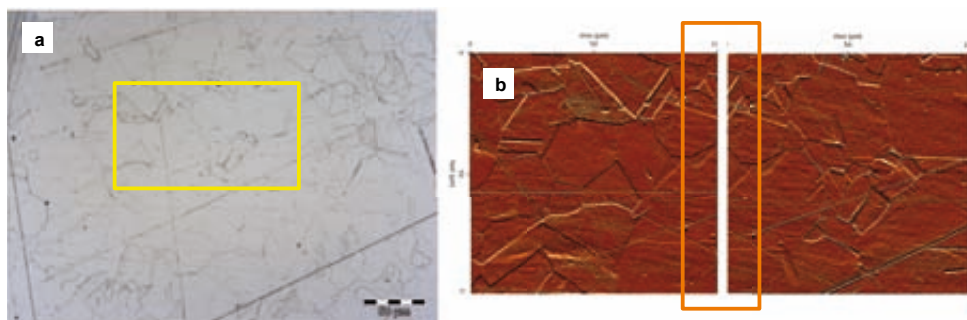


Fig. 2. (a) Optical microscope image (Yellow frame indicates the area of AFM scan); (b) AFM contact scans of the same spot of a stainless steel sample with grain boundaries; AFM scans acquired by contact mode in air (scan area  $100 \times 100 \mu\text{m}$ ; line rate 0.2 Hz, orange frame indicates overlapping area of 20 % of two scans).

### *Step 2 – combination of EFM (bacterial imaging) and AFM*

After the initial AFM scans the sample was immersed in natural seawater for a period of 48 hours. The bacteria attached to the stainless steel surface were first gently rinsed with deionized water and subsequently stained with DAPI. After re-alignment of the instruments, using the calibration slide as detailed in the first step, we could locate the sample spot back again. EFM and AFM imaging of the same spot were performed.

### *Step 3 – combination with SEM*

Finally the same sample holder containing the metal coupon was mounted on the SEM stage for imaging of the same spot area. At this step the indent, which corresponds to the centre of the SEM stage (point 0 of the SEM axis) is traced back. Interestingly, one complete rotation of x or y coordinate of the AFM shuttle stage is equivalent to 0.5 mm and corresponds to 0.5 coordinate of the SEM working stage (x or y-axis). This similarity in scaling of the sample stages made it much easier for locating any spot on the sample from the centered indent in the enclosed SEM chamber.

### 3. Results and Discussion

The combination of microscopes with the above alignment steps were carried out to illustrate the performance of the methodology and possible achievements, which can be expanded by using this new tool for surface science. Figure 3 demonstrate the optical microscope and AFM surface scan of the same spot of the stainless surface before immersion in natural seawater. The grain structure can be easily made visible by the light microscope Fig. 3a and the AFM scan Fig. 3b provides additional information on height structures of the sample including imperfections.

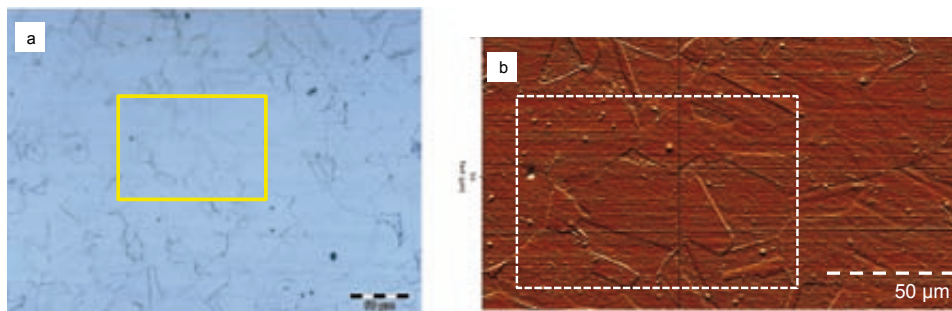


Fig. 3. (a) Optical microscope image of stainless steel surface with the grain boundaries. Square marked area indicates same imaging spot for all microscopes used; (b) combined vertical deflection images of two AFM contact scans with 20 % overlap. AFM scan acquired in contact mode in air (100 x 100  $\mu\text{m}$ , line rate 0.2 Hz, square marked area in this figure indicates area used for height profiles as detailed in Fig. 4 and Fig. 6).

Besides, it was also possible to characterize the roughness of the surface by AFM contact scan in air. This helps in determining the attachment of bacteria with respect to surface roughness. Figure 4a is the example of the height profile of the microstructure surface, which was taken before immersion. The blue line in Fig. 4a shows the scan line along which the profile was measured as shown in Fig. 4b.

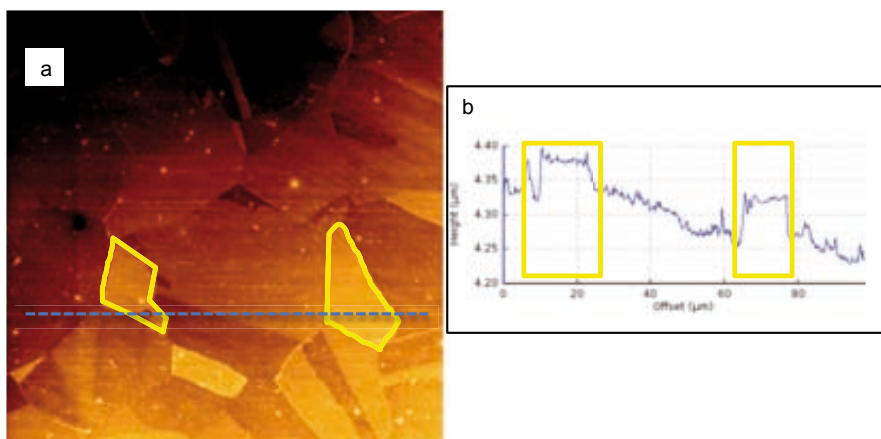


Fig. 4. Quantitative analysis of the height profile determined by AFM scan (a) height image of contact scanned area in Fig. 3b); (b) height profile data in  $\mu\text{m}$  across the dotted line in Fig. 4a.

After imaging of the specific area spot of the coupon using different microscopes, it was then immersed in natural seawater for the period of 48 h. Subsequently the coupon was retrieved, rinsed and scanned to the same area spot using different microscopes as detailed before. Fig. 5 illustrates the metal surface (with microstructure) after immersion to natural seawater over the period of two days. Optical microscopic imaging reveals the grain structure and same spot area as before immersion, Fig. 5a. Epifluorescence microscopy reveals blue stained single bacterial cells on the surface by DAPI staining Fig. 5b. The bacteria were randomly attached to surface. Bacterial numbers are relatively low, a result of the short immersion time of 48 h and the additional rinsing procedure, which will detach loosely attached cells from the surface. Additional AFM imaging provides detailed topography study of the surface Fig. 5c.

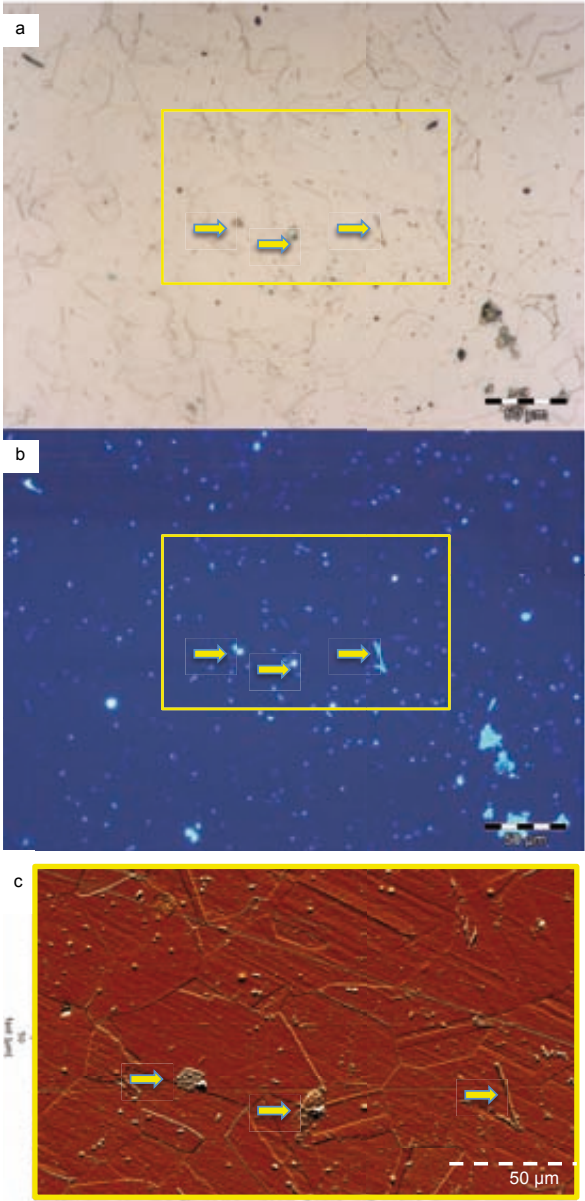


Fig. 5. Series of combined optical microscope, EFM and AFM images of a natural bacterial cells attached to stainless steel surface after exposure to seawater for 48 h: (a) optical microscope image of stainless steel surface; (b) EFM image of coupon surface stained with DAPI in liquid after exposure, frame indicates corresponding AFM scan area; (c) Two combined AFM scans vertical deflection image with 20 % overlap acquired in contact mode in air (100 x 100 μm, line rate 0.2 Hz).

Besides, it was possible to study bacterial cell cluster on a very local scale, and to determine height and width of a certain biological residues on the surface. Fig. 6 is the height profile AFM scan of the same surface spot of the sample after 48 h of immersion in natural seawater. Fig. 6b provide the height profile line of the same surface spot as given in Fig. 4b before immersion, and thus characterizing bacterial cells attachment by contact mode measurements.

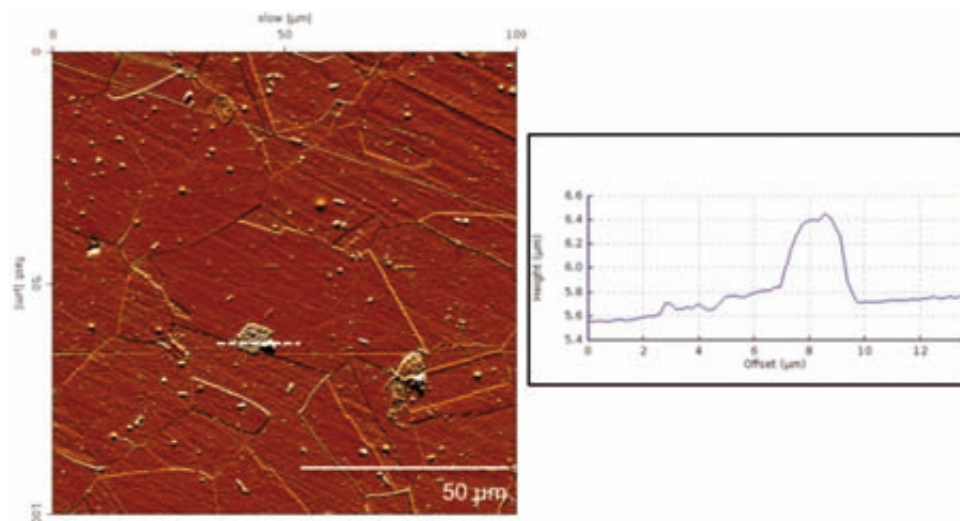


Fig. 6. AFM contact scan of stainless steel surface and corresponding height profiles of marked spots. (a) surface topography image of stainless steel after 48 h immersion, image corresponds to Fig. 4a; (b) height profile of cell cluster (dotted line), image corresponds to Fig. 4b.

A repeated height profile line was taken after immersion for one of the biological residue on the surface that was previously identified by DAPI staining technique, Fig. 5b. The height profile line in Fig. 6b resembles exactly to the structural pattern of the contact scanned surface in Fig. 5c. The rough surface spots that were identified before immersion as in Fig. 4b are now replaced by two peaks in Fig. 6b, suggesting biological accumulation at these spots. The profile shows at these specific spots biological accumulation on the surface is in the range of 0.2  $\mu\text{m}$  to 0.4  $\mu\text{m}$  maximum in height. This pattern can be identified as an initial single cell cluster attached to the surface (average bacteria width is about 0.2 to 0.5  $\mu\text{m}$ ). The drying of the sample before imaging will also decrease the cell volume. It appears that the initial attachment sites for bacterial attachment are preferable on rougher surface parts, as intensively discussed in literature [35–37]. Thus these observations could be supported by AFM height imaging scans, allowing determining the rough parts on the metal surface beforehand. The corresponding SEM scan of the same spot was carried out as shown in Fig. 7. Grain boundaries and surface features are clearly distinguishable. Small bacterial footprints in the form of EPS residues can be also identified as black residue on the surface (arrow indication), which corresponds to blue stained bacteria cells in the EFM/DAPI stained image (Figure 5).

The marked arrows are used as a reference to the surface spot with bacteria and it can be recognized in all different microscopic images, supporting our method that imaging of the same spot is possible by all three instruments before and after immersion of the sample.

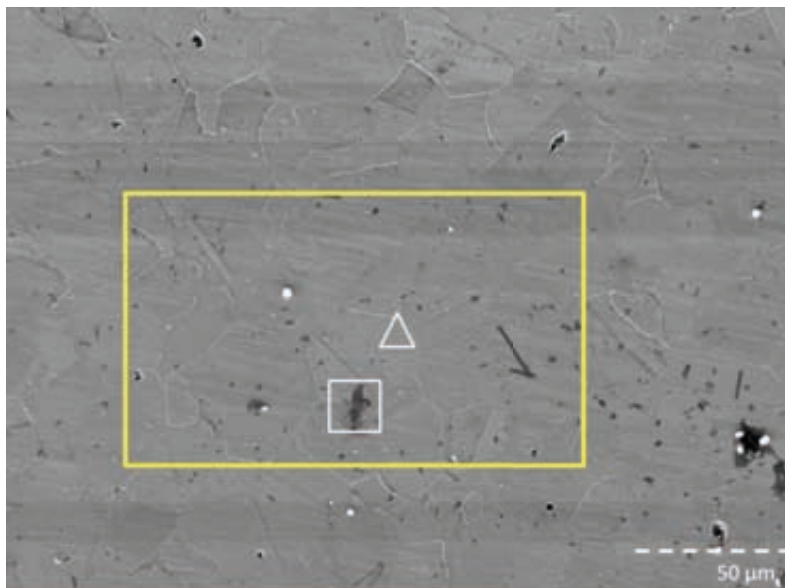


Fig. 7. SEM image of metal coupon after exposure, yellow frame indicates same sample spot as given in Fig. 5. Frames indicate EDX spectra scans, a) bacterial residues, b) plane surface, see spectra in Fig. 8.

Subsequently, SEM/EDX measurements were performed on the same spot, which provide useful information about the surface residue at the end of the experiment. Fig. 8 gives the EDX spectra of the presented sample surface after 48 h in natural seawater. Typical peaks for Fe, Cr and Mo can be found for the stainless steel in Fig. 8a. A preliminary colonized bacterial cell spot was additionally chosen and the corresponding EDX spectrum is given in Fig. 8b. The peaks of carbon in the spectra clearly identify that the footprints are from biological origin. The small sulphur peak is a result of the sulphate from the water phase. For the future we can state that it is possible to study the source of the origin of corrosion products, whether it is generating from general corrosion or of biological origin. For example, MIC will be identified by carbon and sulphur element peaks in the spectrum in the presence of corrosive sulphate reducing bacteria with the combination of other microscopes.

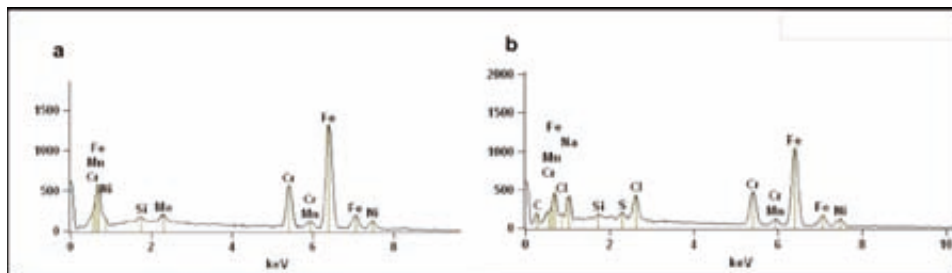


Fig. 8. Energy Dispersive X-Ray (EDX) spectroscopic analysis of the stainless steel coupon after 48 h of immersion in natural seawater; (a) a single point analysis of surface without bacteria (blue cross Fig. 7); (b) a single point analysis of bacterial cell cluster residues identified by SEM in Fig. 7 (white cross).

In summary, EFM imaging gives information of the spatial distribution of bacterial cells on the surface, which cannot be seen with an optical microscope alone. AFM imaging allows a clear identification of these structures by high-resolution topography imaging including height and profile imaging. The SEM image can give additional information on the grain boundaries and grains and can be complemented by Energy Dispersive X-Ray (EDX) spectroscopic analysis of the elemental composition of the surface residue formed either due to corrosion or deposition on the surface.

#### 4. Conclusions

A novel technique has been developed for the preparation and visualization of metal surfaces, suitable for combined imaging by EFM, AFM and SEM. By combining three different microscopes, we have investigated and proven the complementary use of these high-resolution techniques to study surface changes and accumulation of biological substances on stainless steel surfaces. Interestingly, if all these three instruments are used within their whole analysing potential, the scheme of Table 1 can be applied with combination of different techniques. This will integrate combination of seven independent microscopic techniques that can be used for characterizing the same sample spot before and after immersion in a solution.

**Table 1** Combination of microscopic techniques, which can be applied on one sample spot.

Microscopic technique	Analytical information	Detection level
Light microscopy (OM)	Surface characteristics (grain boundaries, impurities such as inclusions, coatings)	Micrometer
Fluorescent microscopy (EFM)	Biological samples (fluorescent stained bacterial cells attached to surface)  Auto fluorescent composite materials  Corrosion study under coating by fluorescent probes	Micrometer
Atomic Force Microscopy (AFM)	Surface characteristics (roughness, quantification of inclusions or accumulated substances)	Submicron Molecular level
AFM – Scanning Kelvin Probe Force Measurements (AFM-SKPFM)	Surface potential measurements (metal or polymer coated surface)	Submicron Molecular level
Scanning Electron microscope (SEM)	Metal surfaces (Grain structures, impurities in high resolution)  Polymer layers, oxide films	Micrometer
SEM- Energy dispersive X-ray (SEM-EDX)	Quantitative chemical analysis of particles, corrosion products or accumulated compounds	—

By combining all these techniques on one sample spot a big step is achieved in corrosion science research. Although, all these techniques are already in use for corrosion research but an elegant and easy to handle set-up for a combined use of these techniques on one sample spot has not been reported before.



## References

- [1] S.W. Borenstein, *Microbiologically Influenced Corrosion Handbook*, 5<sup>th</sup> ed., Woodhead Publishing, Cambridge, UK, 1994, p. 288.
- [2] H. C. Flemming, Biofouling and microbiologically influenced corrosion MIC – an economical and technical overview, in: E. Heitz, W. Sand, H.C. Flemming (Eds.), *Microbial Deterioration of Materials*, Springer, Heidelberg, Germany, 1996, pp. 5-14.
- [3] W.P. Iverson, *Adv. Appl. Microbiol.* 32 (1987) p. 1.
- [4] T. Ford, R. Mitchell, N.J. Dowling, M.W. Mittelman, J.C. Danko (Eds.), *Microbially Influenced Corrosion and Biodeterioration*, Knoxville, TN: University of Tennessee (1991) 3/94-3/98.
- [5] J.M. Odom, *The sulfate-reducing bacteria: Contemporary Perspectives*, R. Singleton ed. New York: Springer (1992) 1-248.
- [6] I.B. Beech, V. Zinkevich, L. Hanjansit, R. Gubner, R. Avci, *Biofouling* 15 (2000) 3–12.
- [7] K.R. Sreekumari, Y. Sato, Y. Kikuchi, *Mater. T. JIM* 46 (2005) 1636–1645.
- [6] J.T. Walker, C.W. Keevil, *Int. Biodeter. Biodegr.* 33 (1994) 223–236.
- [7] E. Defranchi, E. Bonaccorso, M. Tedesco, M. Canato, E. Pavan, R. Raiteri, C. Reggiani, *Microsc. Res. Technol.* 67 (2005) 27.
- [8] J.H. Priester, A.M. Horst, C.L. van de Werfhorst, J.L. Saleta, L. A.K. Mertes, P. A. Holden, *J. Microb. Methods* 68 (2007) 577-587.
- [9] J.T. Walker, J. Verran, R.D. Boyd, S. Percival, *Methods Enzymol.* (2001) 243-255.
- [10] M.P. Sibi, Z. Zong *Progress in Organic Coatings* 47 (2003) 8–15.
- [11] *Letter Corrosion Science* 42 (2000) 1661-1668.
- [12] S. Manne, P. Hansma, J. Massie, V. Eling and A. Gewirth, *Science* 251, 183 (1991).
- [13] R.M. Rynders, C.H. Paik, R. Ke and R. Alkire, *J. Electrochem. Soc.* 141, 1439 (1994).
- [14] Y.F. Dufrene, *Nat. Rev. Microbiol.* 2 (2004) 451–460.
- [15] L.-C. Xu, Chan, H.H.P. Fang, *Mater. Charact. Materials* 48 (2002) 195-203.
- [16] L.-C. Xu, H.H.P. Fang, K.Y. Chan, *J Electrochem Soc* 146 (1999) 4455-60.

- 
- [17] I.B. Beech, J.R. Smith, A.A. Steele, I. Penegar, S.A. Campbell. *Colloids Surf. B* 23 (2002) 231–247.
- [18] S.J. Yuan, S.O. Pehkonen, *Colloids Surf. B* 59 (2007) 87–99.
- [19] S.J. Yuan, S.O. Pehkonen, *Corros. Sci.* 51 (2009) 1372–1385.
- [20] F.A. Martin, C. Bataillon, J. Cousty, *Corros. Sci.* 50 (2008) 84–92.
- [21] J. Madl, S. Rhode, H. Stangl, H. Stockinger, P. Hinterdorfer, G.J. Schütz, G. Kada, *Ultramicroscopy* 106 (2006) 645–651.
- [22] C. Obuekwe, D.W.S. Westlake, F.D. Cook, J.W. Costerton, *Appl. Environ. Microbiol.* 41 (1981) 766–774.
- [23] S.N. Semerak, C.W. Frank, *Macromolecules* 14 (1981) 443.
- [24] J.S. Royal, J.M. Torkelson, *Macromolecules* 26 (1993) 5331.
- [25] D.E. Miller, R.H. Krueger, J.M. Torkelson, *J. Polym. Sci. B* 33 (1995) 2343.
- [26] C.S.P. Sung, J.C. Song, *Macromolecules* 26 (1993) 4818.
- [27] C.S.P. Sung, N.H. Sung, *Mater. Sci. Eng. A* 162 (1993) 241.
- [28] R.O. Loutfy, *J. Polym. Sci. B* 20 (1992) 825.
- [29] A. Worobiec, S. Potgieter-Vermaak, A. Brooker, L. Darchuk, E. Stefaniak, R. van Grieken, *Microchemical Journal* 94 (2010) 65–72.
- [30] D.A. López, W.H. Schreiner, S.R. de Sánchez, S.N. Simison *Applied Surface Science* 207 (2003) 69–85.
- [31] F. Fay, I. Linossier, V. Langlois, D. Haras, K. Vallee-Rehel, *Progress in Organic Coatings* 54 (2005) 216–223.
- [32] S. Mangold, K. Harneit, T. Rohwerder, G. Claus, W. Sand. 2008. *Appl. Env. Microbiol.* 74 (2) 410–415.
- [33] L.R. Hilbert, D. Bagge-Ravn, J. Kold, L. Gramb, *Int. Biodeter. Biodegr.* 52 (2003) 175–185.
- [34] K. Truong, R. Lapovok, Yuri S. Estrin, S. Rundell, J.Y. Wang, C. J. Fluke, R.J. Crawford, E.P. Ivanova, *Biomaterials* 31 (2010) 3674–3683.
- [35] C. Tide, S. R. Harkin, G. G. Geesey, P. J. Bremer, W. Scholz, *Journal of Food Engineering.* 42 (1999) 85–96.

## **4.2      *Early-stages of Pseudomonas biofilm formation on stainless steel by means of local electrochemical techniques***

### **Abstract**

Biofilm formation on metal surfaces leads to significant and complex changes at the metal/solution interface. A change of oxygen reduction kinetics is one of the possible effects of the respiratory activity of aerobic bacteria like *Pseudomonas* species. In this work in-situ changes related to electrochemical processes at the metal/solution interface after addition of *Pseudomonas* are monitored. Taking advantage of the high-spatial resolution of scanning electrochemical techniques such as the scanning vibrating electrode technique (SVET) and the scanning electrochemical microscope (SECM) the early-stages of the biofilm formation can be monitored. Changes of the ionic-current fluxes in solution by SVET experiments are observed with a significant increase of incoming ionic-currents towards the metal surface (stainless steel) when bacteria are present. SECM measurements showed that the dissolved oxygen concentration decreases as a function of the biofilm formation process. Both in-situ local techniques together with supplementary ex-situ fluorescent microscopy allowed to study the biofilm impact at the metal/solution interface. It was possible to establish the direct relation between oxygen reduction catalysis and the early stages of biofilm formation by *Pseudomonas*.

## 1. Introduction

Microorganisms, with their ability to influence the corrosion of many metals normally considered corrosion resistant in a wide range of environments, are a real threat to the stability of those metals (Beech et al. 1999). Biocorrosion or microbiology influenced corrosion (MIC) is recognized as a major destructive force in aqueous environments. The main types of bacteria associated to MIC are sulphate reducing bacteria (SRB), sulfur-oxidising bacteria, iron-oxidising/reducing bacteria, manganese-oxidising bacteria and bacteria secreting organic acids or slime. These organisms typically coexist in naturally occurring biofilms, forming complex consortia on corroding metal surfaces (Baker 2003, Kjellerup 2003; Zhang 2003). The key to altering the corrosion behavior of metals by microbial activity is the formation of a biofilm. The term biofilm involves a wide range of surface associations: exopolymeric substances (EPS), inorganic precipitates derived from the bulk aqueous phase and/or corrosion products of the metal substrate (Beech et al. 1999, Baker et al. 2003; Kjellerup et al. 2003; Zhang et al. 2003). Several models have been proposed to explain the mechanisms, by which bacteria enhance the corrosion process of mild steel (Ford et al. 1988). A number of factors are involved and a single predominant mechanism is not existing (Hamilton, 1998; Lee et al. 1995). The contrary effect is described as microbiologically influenced corrosion inhibition (MICI) in which the presence of biofilm decreases the corrosion rate of the metals. It is considered that corrosion inhibition by biofilms may take place following different mechanisms: (a) the biofilm forms a diffusion barrier to corrosion products, which stifles metal dissolution (Alber, 1989); (b) respiring aerobic microorganisms within the biofilm consume oxygen, decreasing the concentration of that reactant at the metal surface, for example *Pseudomonas* (Dubiel et al. 2002; Lee et al. 2003); (c) microorganisms produce metabolic products that act as corrosion inhibitors, for example enzymes (Thielen et al. 2005) or EPS (Beech et al. 2000; Gubner et al. 2000); (d) microorganisms produce specific antibiotics that prevent the proliferation of corrosion causing organisms, for example, *sulfate-reducing bacteria* (SRB) (Zuo, 2004). Most research studies indicate that aerobic bacteria like *Pseudomonas* have been shown to decrease metal corrosion by microbial respiration. This activity can decrease the cathodic rate by reducing the amount of reactants available for the cathodic reaction. The presence of a biofilm on the surface has to be considered as a highly non-uniform, dynamic, three-dimensional and microscopic system. This imposes a big experimental and interpretative challenge in studying its influence on MIC and MICI processes on metals.

Application of multidisciplinary techniques including microscopy and surface chemical analysis has lead to a better understanding of biochemical reactions taking place at the biofilm/metal interface (Beech et al. 2004; Wang et al. 2006). However, all this information was obtained after microbial adhesion (measurements ex-situ and on dead cells). They provide no insight in the changes taking place during microbial activity (Little et al. 2007). From an electrochemical point of view numerous studies using conventional electrochemical methods have evidenced the (un)desirable effects of the microorganism presence and its impact on the metal stability (Jayaraman et al. 1997; Beech et al. 2004; Dinh et al. 2004; Dubiel et al. 2002).

However in their interpretation it is assumed that there is a homogeneous electrochemical process with a uniform biofilm attached to a homogeneous metal surface, which is far from reality. Therefore there is a need to use electrochemical techniques with spatial resolution that will allow to distinguish the electrochemical heterogeneities of the system under microbiological influence. The scanning vibrating electrode technique (SVET) allows monitoring variations in current densities over a metal surface by measuring the potential gradients developed in solution due to ionic flow. The method has been widely applied by the study of corrosion phenomena (de Wit et al. 1996; Sekine et al. 2002; Krawiec et al. 2004) and MIC processes (Mansfeld and Little 1991; Little et al. 1991; Angell et al. 1995). SVET mapping may provide information of anode and cathodes distribution on the surface. Another technique frequently used in biological studies (Brehm-Stecher and Johnson 2004) and more recently in corrosion research (Bard et al. 1989, 1991; Casillas et al. 1993, 1994; Wipf et al. 1994; Serebrennikova and White 2001; Souto et al. 2004) is the scanning electrochemical technique (SECM). In SECM a microelectrode probe (smaller than 25  $\mu\text{m}$  diameter) is polarized to an adequate potential to monitor a specific electrochemical reaction with high spatial-resolution. The chemical selectivity of the SECM is one of the advantages of this technique for its application in biological and corrosion research.

In the work of Amemiya et al. (Amemiya et al. 2006) the main advantages of SECM for biological applications are summarized as follow: (a) living cells attached to opaque samples can be studied in an electrolyte solution directly (in situ) without tip-sample contact; (b) oxygen as a metabolic reaction indicator can be monitored selectively and with high sensitivity; (c) reactivity of chemical species and surface topography can be studied with high spatial resolution down to single cell level.

The objective of this paper is to study the early stages of *Pseudomonas* respiratory activity in contact with stainless steel by using in-situ local electrochemical techniques. Changes in ionic-currents and oxygen concentration in the metal/solution interface due to the formation of biofilm are monitored by complementary application of SVET and SECM measurements.

## 2 Experimental details

### 2.1 Sample preparation

Stainless steel 316 coupons (distributed by Salomon Metalen, Groningen, The Netherlands) were ground up to 2400 grid to obtain a mirror like finish and a test surface area of 1x0.5  $\text{cm}^2$  was mounted in epoxy resin. The mounted sample was washed thoroughly with Millipore deionized water and finally surrounded by an acrylic ring fixed with tape, thus creating a small container for the electrolyte solution with a volume of 2.5 ml. For location identification and reproducible current scans, 4 indents in a square arrangement (100x100  $\mu\text{m}$ ) were applied. Furthermore, for the SECM sample an additional scratch was applied as a reference point within the SECM maps (defect). Samples were mounted horizontally facing upwards to obtain optimum bacterial attachment and growth conditions. The test electrolyte was introduced to the cell with end-volume of 2ml.

Testing was carried out in aqueous 0.05M NaCl solution (sterile filtrated, conductivity  $17.68\text{mS cm}^{-1}$ ) and experiments were conducted at ambient temperature.

## 2.2 Biofilm

*Pseudomonas fluorescens* DSM 4358, a bacterium present in natural waters, was used as a biofilm producer (DSMZ, Braunschweig, Germany). The bacteria were maintained continuously in a recommended medium (*Pseudomonas* DSM 220) of DSMZ. For the experimental approach the culture was grown and cultured in artificial seawater to ensure efficient extracellular polymeric substances (EPS) production. The experiment described was performed in sterile NaCl supplemented with yeast (0.2%) (Noghabi et al. 2007). Experimental bacterial cultures were taken from ASW liquid medium in the exponential growth phase after 4 days ( $10^8$  cells/ml) to have a metabolic active culture. A volume of 100  $\mu\text{l}$  of the liquid culture was added under sterile conditions to the electrochemical cell filled with supplemented sterile NaCl.

## 2.3 SVET experiment

Local current measurements were performed using a SVET (Applicable Electronics, USA). Further details on software and instrumentation can be found in literature (Bastos et al. 2004; Bastos et al. 2005). The microelectrode had a platinum tip with a diameter of approximately  $20\mu\text{m}$ . All the experiments were performed at a distance of  $100\mu\text{m}$  above the surface. The microprobe was moved using a computer-controlled micromanipulator. A calibration routine converted the measured potentials into current density at the corroding surface (Isaacs and Ishikawa 1986). The current density was measured and plotted as a function of the location over the measured surface (scan area  $0.0124\text{cm}^2$ ). In this format, positive and negative current densities represent anodic and cathodic sites respectively. Incoming negative currents can be used as an indication for the respiratory activity of bacteria. Whereas the positive outcoming currents can be used to study the corrosion reaction. This allows us to correlate both reactions: the corrosion reactions and respiratory activity of the biofilm by SVET at the metal/solution interface. To avoid negative effects by biofilm formation on the probe (Chen et al. 1997), the tip was removed from the electrolyte after each measurement and gently rinsed with sterile Millipore water to remove contaminations.

## 2.4 SECM experiment

The SECM experiments were carried out with the Scanning Electrochemical Workstation Model370 (Princeton Applied Research, AMETEK Inc.). A  $5\mu\text{m}$ -radius platinum-disk microelectrode was used as SECM tip. All potential values are referred to the Ag/AgCl/KCl saturated reference electrode and a stainless steel counter electrode completed the micro-electrochemical cell. Further details of the technique and its limitations can be found in (Bard et al. 1991). No polarization was applied to the metal specimen. The experiments were performed at an approximate tip height of  $30\mu\text{m}$  above the surface (relative to approach curve of 70% in current change). The positioning motors were set to move the tip over the surface covering parts of the micro-scratch and the area marked by indents.

The second experiment covered the surface investigation by SECM (scan area 0.0025 cm<sup>2</sup>) followed by fluorescent staining of the biofilm. The microelectrode was removed after each scan from the electrolyte to avoid clogging of the probe by attachment of bacterial cells. Electrolyte was replaced prior to scanning to eliminate contamination by planktonic free floating bacterial cells; the set up was left for 30min for stabilization and SECM scans were performed afterwards. The test specimen and all components were sterilized with 70% EtOH, prior to assembly and mounting up.

## 2.5 Microscopic imaging

Microscopic imaging of the biofilm attached to the stainless steel samples was performed after electrochemical measurements. In a first step the metal surface was gently rinsed with sterile deionized water. Afterwards the biofilm was fixed in 2.5% (v/v) glutaraldehyde in cacodylate buffer (0.01M) for 2 hours. In a third step staining was performed with the nucleic acid dye SYTO 9 (5μM) for 10 min in the dark at room temperature. Visualization of the colonized surface was performed with a Zeiss Confocal microscope Axiovert 100 M BP (Zeiss, Germany) equipped with an argon laser (488nm excitation wavelength and a LP 505 detection filter). Pictures were taken at 10x and 40x magnification (Plan-Neofluar 10x and 40x) and the corresponding images were analyzed with the software packages 3D for LSM and ImageVisArt (Zeiss).

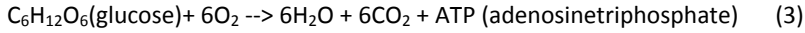
## 3. Results and Discussion

The 316L stainless steel is known for its high corrosion resistance due to the high concentration of Cr and Mo. This performance is primarily attributed to the passive film composed of mainly chromium (hydr)oxide. Under the action of aggressive ions, especially chlorides, local breakdown of passivity may occur, mainly at sites of local heterogeneities, causing pitting corrosion. The chlorides penetrate the passive film. The main reactions involved in the initiation of the local corrosion process are further the oxidation of iron and chromium (1a-1d) and the reduction of dissolved oxygen (2) in the case of a neutral pH solution. The oxygen is thus responsible for preservation of the passivity as long as metastable pitting does not end up in stable pitting. In a stable growing pit acidification takes place resulting in a local increase of the H<sup>+</sup> concentration and an increased pitting rate.



In the presence of aerobic microbial activity, the complex biofilm formation takes place on the metal surface. At the initial stages, a conditioning film (CF) is built up which is mainly constituted by exopolymeric compounds (EPS).

In the case of *Pseudomonas* the glucose metabolism (equation 3) is one of the main reactions for the biofilm formation (Fuhrer 2005). This was for the first time identified in the field of microbial corrosion by Scotto (Scotto et al. 1985) and it is known as microbial electro-catalysis of oxygen reduction.



### 3.1 In-situ SVET measurements of the ionic current distribution during biofilm formation

SVET measurements at different immersion times allow monitoring of the ionic currents in solution above a stainless steel surface at open circuit potential. Firstly SVET scans were performed on the control sample not influenced by bacterial attachment. The total exposed surface area was limited with tape to assure a well-defined area. In Figure 1 (a-c) SVET current-density maps corresponding to control specimen indicated a low activity over the course of the experiment with current values in the range of  $\pm 20 \mu\text{A cm}^{-2}$ .



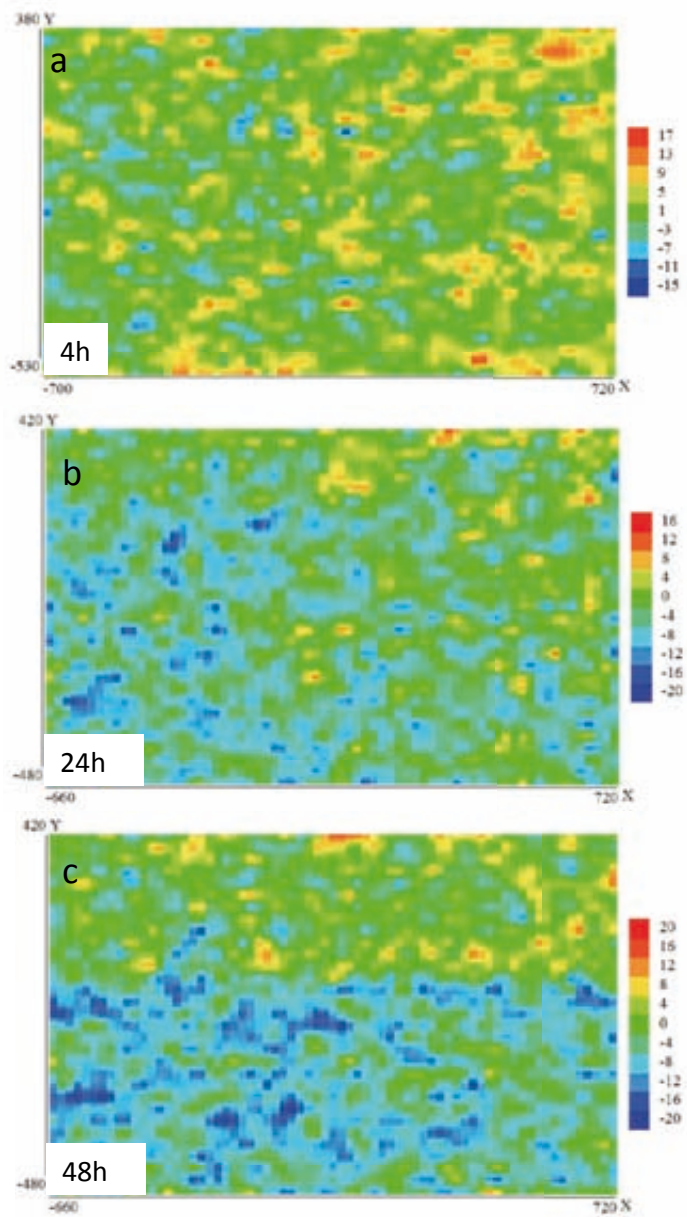


Fig. 1: Local ionic-current maps of stainless steel sample in 0.05M NaCl solution (blank control sample) obtained by SVET measurements at open circuit potential. The 2D-maps correspond to the surface after (a) 4, (b) 24 and (c) 48 hours of immersion. Color scale:  $\mu\text{A cm}^{-2}$ .

The image sequence of Fig. 1(a-c) illustrates very localized minor events on the stainless steel surface. Anodic and cathodic activities were spread over the surface with very low current values. The dynamic location of these current fluctuations along the image sequence may be an indication of metastable pitting on the surface.

These events are a well-documented feature of pitting corrosion of stainless steel in chloride solution (Frankel et al. 1987; Stockert and Böhni 1989; Carroll and Howley 1990) and consisted of reinitiation and repassivation of pits. In general SVET maps showed a balance of anodic and cathodic currents that leads to a total current over the measured and exposed surface close to zero. A different behaviour is observed in the sequence of SVET images of the stainless steel in presence of aerobic bacteria as is presented in Figure 2. After 4 hours (Fig. 2(a)) of exposure to microbial activity, the SVET map of the surface showed current values up to  $\pm 30 \mu\text{A cm}^{-2}$ . After 24h of immersion both positive (outcoming) and negative (incoming) currents are more clearly identified on the map, and remained high in magnitude with values in the range of  $\pm 90 \mu\text{A cm}^{-2}$ . Positive currents are very localized on the map while negative currents appear preferentially in the center of the area. This separation between incoming and outcoming currents is even more evident after 48h of immersion (see Fig. 2(c)). Now negative currents are homogenously distributed on half of the area (blue arrow) while lower positive currents remain still relatively localized in some areas of the sample (yellow arrows).

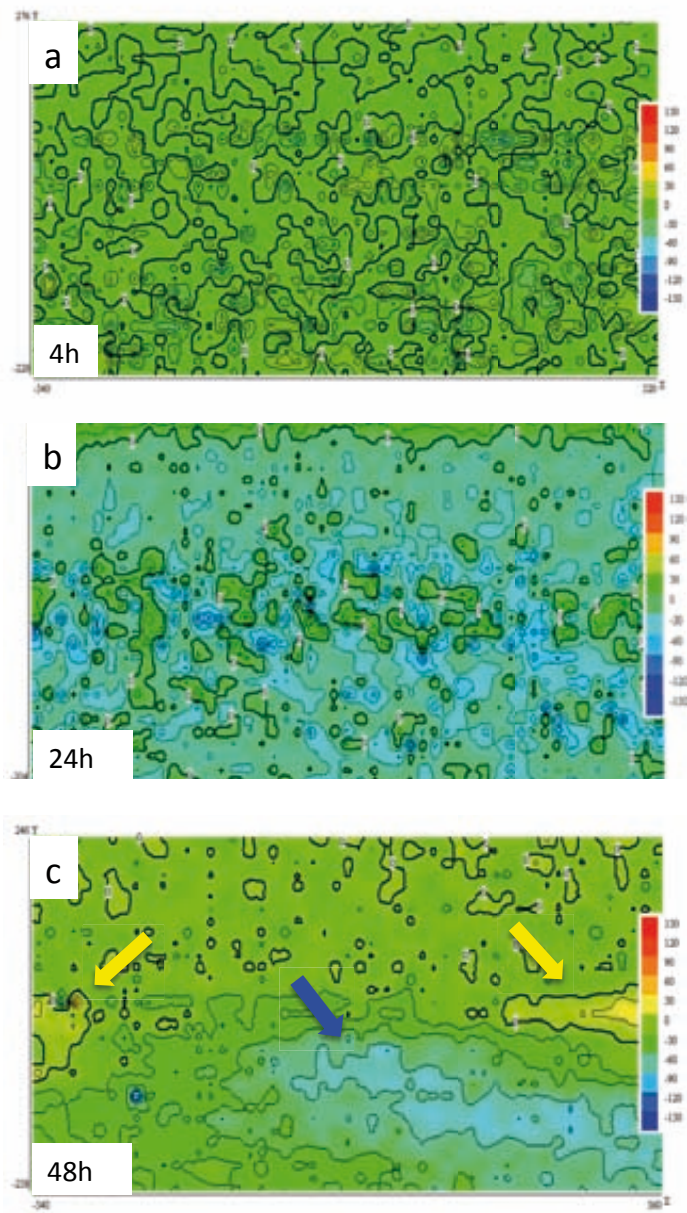


Fig. 2: SVET ionic-current maps of stainless steel sample at open circuit potential during immersion in 0.05M NaCl solution containing *Pseudomonas* bacteria obtained. Before addition of bacteria sample was exposure to chloride solution during 12hours. The 2D-maps correspond to the surface after (a) 4hours, (b) 24 hours and (c) 48 hours of exposure to microbial solution. Color scale:  $\mu\text{Acm}^{-2}$ .

Bacterial activity in the initial 24 hours is high and planktonic cells from the water phase (electrolyte) will attach to the metal surface and start the formation of the biofilm. The initial step is dominated by forming a conditioning film (CF) mainly composed of exopolymeric compounds (Jayaraman et al. 1997; Gunasekaran et al. 2004). These complex processes that involve local electrochemical and biochemical changes in the metal/solution interface may be evidenced by the high current values measured compared to the blank sample. SVET maps in Figure 2 show an unbalanced distribution of incoming (negative) and outgoing (positive) currents in the presence of bacteria in solution. This fact is more clearly presented in Figure 3 the absolute current values (positive and negative integrated currents) are plotted as calculated from each map in Figure 2 as a function of time. Ionic currents measured in the absence of bacteria remained balanced during immersion in chloride solution. This observation is expected when the ionic current changes are solely related to electrochemical reactions (corrosion) at the metal surface since during corrosion a balance between anodic and cathodic currents is required. After the addition of the biotic solution outgoing and incoming currents presented a different evolution with immersion time. A significant increase of the incoming current is observed while outgoing currents tend to decrease. The increase of incoming currents values and its homogenous distribution over the map scan is related to the first cell attachment and later growth of the conditioning film. It must be noted that now monitored incoming currents are a consequence of both bioactivity (glucose metabolism) and corrosion activity. The later decrease of the positive currents can be related to the presence of a well-formed film that shields the ionic flux from the metal substrate.

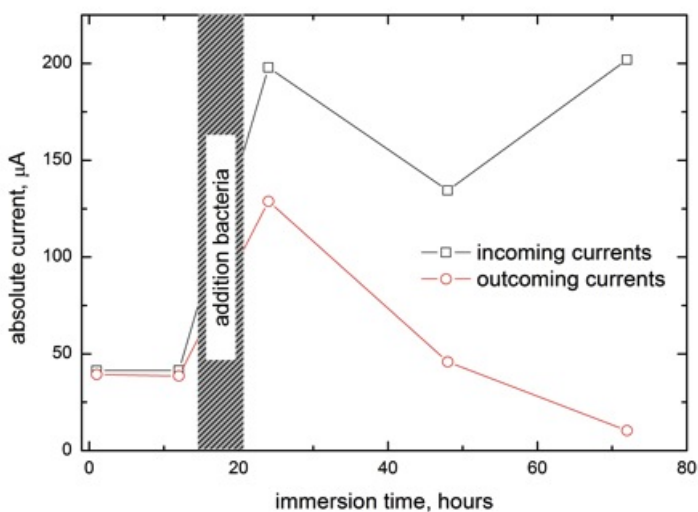


Fig. 3: Absolute current values (incoming and outgoing) as a function of immersion time. Currents are integrated from the SVET maps presented in Figure 2.

In summary SVET results showed the influence of microbial activity on the ionic fluxes at the metal/solution interface. The increase of negative currents observed in SVET maps may be related to the increasing demand of oxygen necessary for the biofilm formation (electrocatalysis of the oxygen reduction). However, the SVET technique has the disadvantage of lacking chemical specificity that does not allow to prove the direct relation between incoming currents and oxygen reduction.

### 3.2 In-situ SECM measurements of oxygen concentration changes during biofilm formation

SECM experiments were performed to study the biofilm development and its effect on the oxygen concentration at the metal-solution interface with higher spatial resolution than SVET measurements. Oxygen reaction in aqueous solution involves heterogeneous charge transfer processes coupled with homogeneous chemical reactions (Casillas et al. 1993). The voltammetric curve (CV) in the range of 0 to -1V vs. Ag/AgCl/KCl electrode shows a single wave at potential range of -0.5 to -0.7V corresponding to the oxygen reduction. This value is obtained by checking the CV of oxygen obtained with a microelectrode of platinum, a current plateau was observed at -0.6V which corresponds to limiting current conditions in the operational working range of the SECM. Concentration of oxygen in the proximity of a corroding surface will vary with time due to its consumption at the cathodic sites (Bastos et al. 2004; Bastos et al. 2005) and especially in this case influenced by actively respiring bacteria (consumption of oxygen). Consequently changes in oxygen concentration due to corrosion reactions valid for Eq. 1 and 2 and in this approach to monitor bacterial respiratory activity in the solution can be monitored at the tip of the SECM. Fig. 4(a-c) presents the SECM current maps of  $O_2$  reduction measured at different times of immersion of the sample-control (stainless steel) in 0.05M NaCl solution. As can be seen in the sequence, the current distribution is fairly homogeneous and gives values in the range of -2.5 to -3.0nA. Averaged current values are in agreements with oxygen concentration expected for chloride solution in saturated dissolved oxygen condition (Hitchman, 1978). It is possible to observe the location of the scratch on the surface (indicated by the arrow in the right-bottom of the image) due to the irregular morphology of the defect. Same area monitored by using ferrocenemethanol as a mediator (SECM operating in negative feedback mode) showed same features (data not shown). This confirmed that variations in current around that zone are uniquely resulting from the topographic effect.

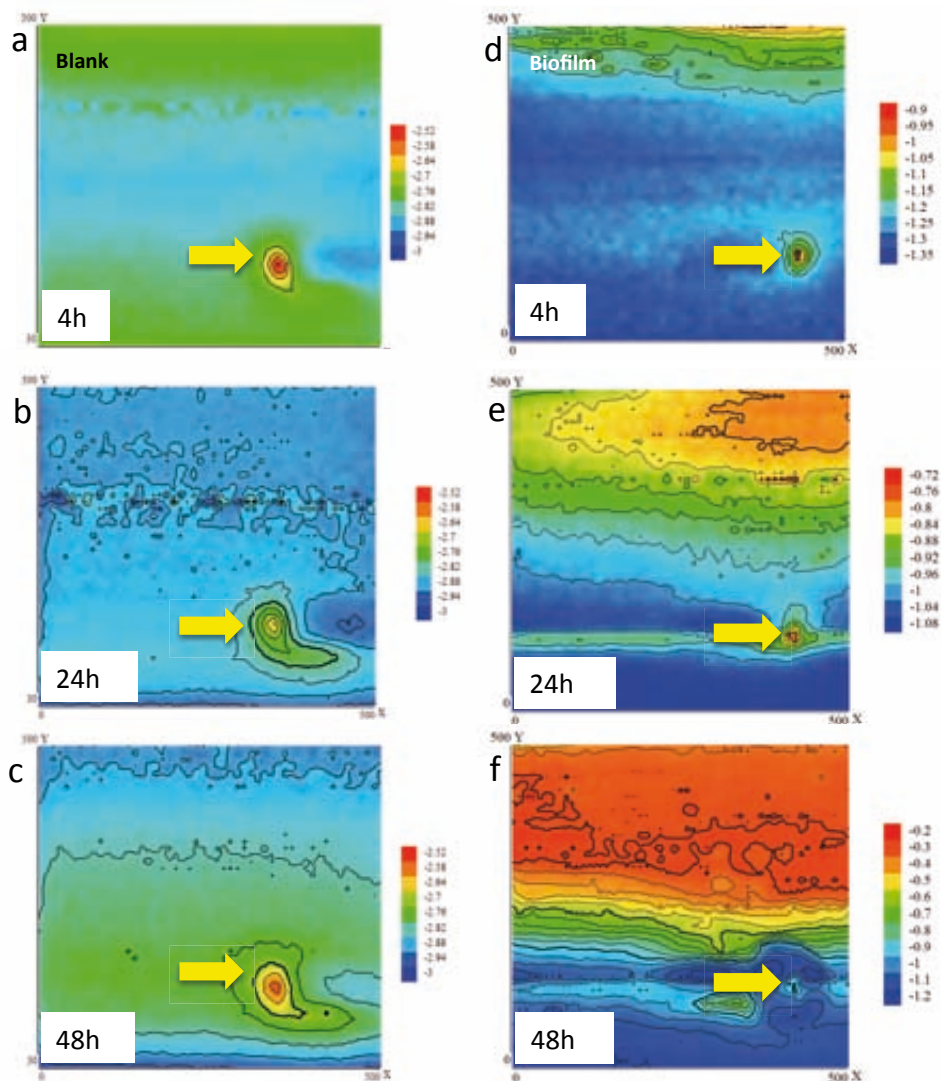


Fig. 4: SECM 2D images of stainless steel surface immersed in 0.05M NaCl. Blank surface (a) 4 hours, (b) 24 hours and (c) 48hours of exposure; Bacterial set-up (d) 4 hours, (e) 24 hours and (f) 48hours of exposure. All images indicate the surface defect in the right base corner as a reference point. Color scale: current at the tip, nA.

In-situ SECM measurements in the presence of bacteria are represented in Fig. 4(d-f). A very different behavior could be found for the bacterial set-up over the course of the experiment. After the initial first hours of experiment Fig. 4(d), SECM maps show two distinctive regions with different current values (Fig. 4e-f). The image corresponding to 24h of immersion (Fig. 4(e)) presented a homogeneous drop of current located at the top of the map, while the current near the defect did not change significantly. The lowest oxygen concentration at the top of this area reached a value about  $-0.8\text{nA}$  and up to  $-0.95\text{nA}$  close to the defect.

This gradient of oxygen concentration can be attributed to sessile cells floating free in the NaCl solution and by initial attachment of cells on parts of the surface. After 48 hours the decrease in oxygen concentration becomes highly significant and spreads over time covering two-third of the initial surface area. The initial Fig. 4(d) indicates a first bacterial attachment in the upper region of the current map that showed a lower oxygen concentration at the interface due to respiratory activity. This is rather different for Fig. 4(e), where the biofilm is grown for already 24h on top of the stainless steel surface. The growth can be monitored in the SECM map indicating a zone increasing in shape and size in combination with a significant decrease in oxygen concentration down to a current value of  $-0.8\text{ nA}$ . This is a clear indication that a biofilm is already established several micrometers in height (Rittmann and McCarty, 1980) consuming oxygen by respiratory activity. Consequently, a lower current corresponding to a lower oxygen concentration is measured. A direct use of  $\text{O}_2$  is discussed for aerobic microorganisms by Peterson et al. (1991) reporting that *Pseudomonas* could protect unalloyed steel in chloride containing medium in the form of pure cultures. The experiment indicated that living biofilms cause higher protection effects compared to planktonic cells. This result is supported by our findings showing higher activity rates for attached cells compared to sessile in the beginning. The highest impact on the oxygen concentration at the interface could be found after 48h. This period of time is enough to establish a thick biofilm and the decrease in oxygen concentration becomes obvious in the current map showing current values of  $-0.2\text{ nA}$  compared to the bare surface showing a value of  $-1.2\text{ nA}$ . The presence of bacteria leads to a massive consumption of oxygen in solution due to respiratory activity according to Eq. (3) which is evidenced by the development of a homogenous drop of current with time.

In Fig. 5 the general growth curve of *Pseudomonas* species in minimal medium (as used for this experimental set-up) at  $25^\circ\text{C}$  (Maier, 2000) is compared to the mean values of the current measured for each SECM map. A good agreement between biological growth kinetics (biofilm development) and the depletion of oxygen concentration in solution is evident. This confirms that changes in oxygen concentration measured with the SECM-probe can be related to the growth of a biofilm on the surface during the bacteria respiratory process.



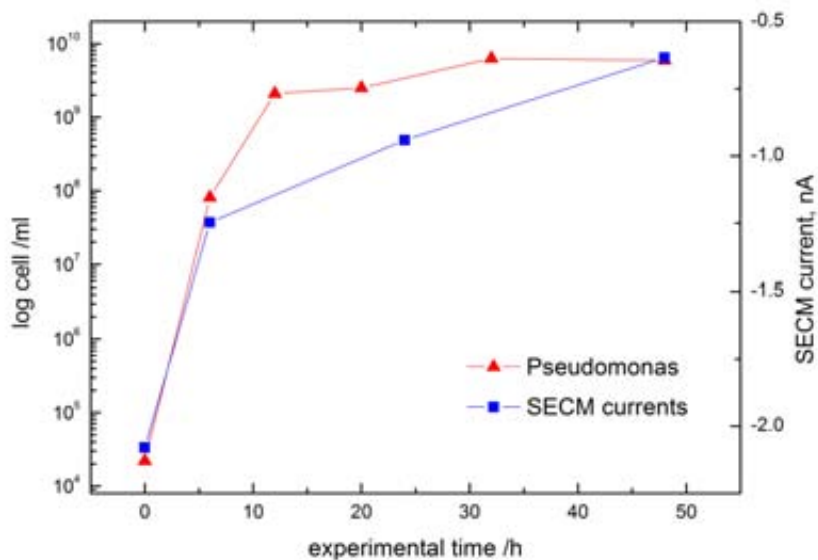


Fig. 5: Comparison of growth curve of *Pseudomonas* (red line) and averaged currents of  $O_2$  reduction (blue line) measured during SECM experiments in Figure 4.

### 3.3 Ex-situ fluorescent microscopy analysis

Fluorescent microscopy was used to assess the stainless steel surface (working electrode) and its coverage by bacteria. This method allowed a verification of possible bacterial attachment sites. Fig. 6(b-c) present the fluorescent microscopy images after terminating the experiment corresponding to the SECM map in Fig. 4(f). The yellow frame indicates the detailed fluorescent images given in Fig. 6(b-c) and the additional arrow indicates the edge of the scratch/defect which can be recognized in all images. The green fluorescent dots dispersed within the black background correspond to bacterial clusters and cells on the metal surface. The yellow-framed area on the bottom of the image indicates the location of the artificial scratch. As can be derived from the fluorescent image no bacterial cells can be found in the scratched area. The corresponding topography image in Fig. 6(c) is given to underline the presence of bacteria on the plane metal surface indicated in green with several microns in height, whereas the surface defect is colored in blue (yellow frame) representing the defect (hole) on the surface. These images confirm the existence of bacteria on the surface corresponding to the current drop observed in the SECM map. One of the phenomena that could be found in the SECM current map was the separation of two zones: one biofilm zone with low oxygen concentrations and a second zone with higher oxygen concentrations.



The front of lower currents corresponds to the formation and growth of the biofilm which is accompanied for a massive consumption of oxygen due to respiratory activity according to Eq. (3).

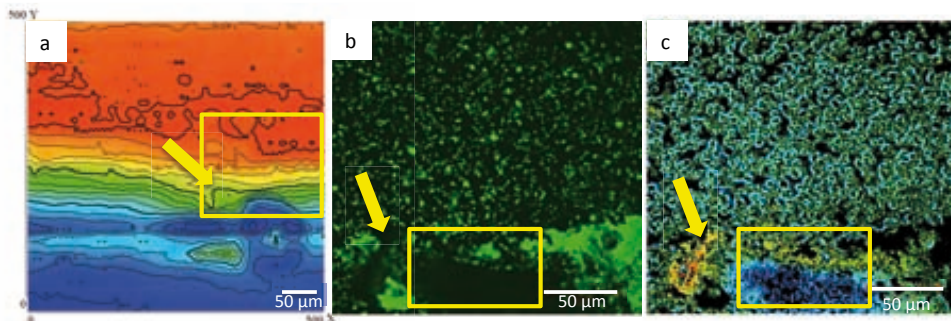


Fig. 6: (a) SECM surface map as reference image (frame indicates the fluorescent images (b-c); arrow indicates the boarder of the defect in all images); (b) SYTO 9 stained biofilm formed on stainless steel after 48h; (c) Topography image gained from confocal scan. Scale bar 50  $\mu\text{m}$ .

## Conclusions

In this work the early-stages of respiratory activity of *Pseudomonas* bacteria on stainless steel is studied by using in-situ local electrochemical techniques. SVET measurements showed that the presence of bacteria leads to significant increase of incoming ionic currents toward the metal during a 2-days experiment. This is related to the electrochemical changes at the metal/solution interface during formation of a conditioning film on the surface. SECM measurements of oxygen in solution confirmed that the incoming ionic current observed in SVET mapping is related to the catalysis of oxygen reduction reaction necessary for the respiratory metabolism of bacteria. A gradual decrease of oxygen concentration in solution was observed in the SECM maps in agreement with the kinetics of the biofilm growth. Complementary ex-situ fluorescent microscopy analysis supported the SECM results, showing higher agglomeration of cells (patches) in the areas corresponding to lower concentration of oxygen. It is demonstrated that the application of local scanning electrochemical techniques with high-spatial resolution is a powerful tool for a better understanding of microbial activity on metals providing in-situ information of the processes taking place at the metal/biofilm/solution interface.

## References

- Alber, X., 1989. Studie über temporären mikrobiologischen Korrosionsschutz, Diplomarbeit, Regensburg.
- Amemiya, S., Guo, J., Xiong, H., Gross, D.A., 2006. Biological applications of scanning electrochemical microscopy: chemical imaging of single living cells and beyond analytical and Bioanalytical Chemistry 386, 458-471.
- Angell, P., Sonnerson, A., Wagner, P.A., White, D.C., Little, B.J., 1995. Role of Oceanospirillum exopolymer in marine copper corrosion, NACE Symposium of Microbiologically Influenced Corrosion. NACE, Houston, Texas, p. paper 347.
- Baker, P.W., Ito, K., K, Watanabe., 2003. Marine prosthecate bacteria involved in the ennoblement of stainless steel. Environmental Microbiology 5, 925-932.
- Bard, A.J., Denuault, G., Friesner, R.A., 1991. Scanning Electrochemical Microscopy: Theory and Application of the Transient (Chronoamperometric) SECM Response. Analytical Chemistry 63, 1282-1288.
- Bard, A.J., Fan, F.R.F., Kwak, J., Lev, O., 1989. Scanning Electrochemical Microscopy. Introduction and Principles. Principles in Analytical Chemistry 61, 138-144.
- Bastos, A.C., Simoes, A.M., Gonzalez, S., Gonzalez-Garcia, Y., Souto, R.M., 2004. Imaging concentration profiles of redox-active species in open-circuit processes with the scanning electrochemical microscope. Electrochemistry Communications 6, 1212-1215.
- Bastos, A.C., Simoes, A.M., Gonzalez, S., Gonzalez-Garcia, Y., Souto, R.M., 2005. Application of the scanning electrochemical microscope to the examination of organic coatings on metallic substrates. Progress in Organic Coatings 53, 177-182.
- Beech, I.B., 2004. International Biodeterioration and Biodegradation 53, 177-183.
- Beech, I.B., Gaylarde, C.C., 1999. Revista de Microbiologia 30, 177-190.
- Beech, I.B., Gubner, R., Znkevich, V., Hanjansit, L., Avci, R., 2000. Characterization of conditioning layers formed by exopolymeric substances of Pseudomonas NCIMB 2121 on surfaces of AISI 316 stainless steel. Biofouling 16 (2-4), 93-104.
- Brehm-Stecher, B.F., Johnson, E.A., 2004. Single-Cell Microbiology: Tools, Technologies, and Applications. Microbiol. Mol. Biol. Rev. 68, 538-559.
- Carroll, W.M., Howley, M.B., 1990. The influence of temperature, applied potential, buffer and inhibitor addition on the passivation behaviour of a commercial grade 316L steel in aqueous halide solutions. Corros. Sci. 30 (6-7), 643-655.

Casillas, N., Charlebois, S.J., Smyrl, W.H., White, H.S., 1993. Scanning electrochemical microscopy of precursor sites for pitting corrosion on titanium. *Journal of Electrochemical Society*, 142.

Casillas, N., Charlebois, S.J., Smyrl, W.H., White, H.S., 1994. Pitting corrosion of titanium. *Journal of Electrochemical Society* 141, 636.

Chen, G., Palmer, R.J., White, D.C., 1997. Instrumental analysis of microbiologically influenced corrosion. *Biodegradation* 8:189-200.

Dinh, H.T., Kuever, J., Musmann, M., Hassel, A.W., Stratmann, M., Widdel, F., 2004. Iron corrosion by novel anaerobic microorganisms. *Nature* 427, 829-832.

Dubiel, M., Hsu, C.H., Chien, C.C., Mansfeld, F., Newman, D.K., 2002. Microbial iron respiration protects steel. *Appl Environ Microbiol* 68, 1440-1445.

Ford T.E., Maki J.S., Mitchell R. (1988) Involvement of bacterial expolymers in biodeterioration of metals. In: Houghton D.R., Smith R.N., Eggin H.O.W. (eds) *Biodeterioration 7, Proceedings of the Seventh International Biodeterioration Symposium*, Cambridge, June 1987. Elsevier Applied Science, Barking, UK, pp 378-384.

Frankel, G.S., Stockert, L., Hunkeler, F., Böhni, H., 1987. Metastable pitting of stainless steel. *Corrosion* 43, 429.

Gubner, R., Beech, I.B., Zinkevich, V., Hanjansit, L., Avci, R., 2000. The effect of EPS on the attachment of *Pseudomonas NCIMB 2121* to AISI 304 and 316 stainless steel *Biofouling* 15 (1-3), 25-36.

Hamilton, W.A., 1998. Sulphate reducing bacteria – physiology determines their environmental impact. *Geomicrobiological Journal* 15, 19-28.

Hitchman, M.L., 1978. *Measurement of Dissolved Oxygen*. Wiley, New York, p. 2.

Isaacs, H.S., Ishikawa, Y., 1986. *Electrochemical Techniques for Corrosion Engineering*, in: Baboian, R. (Ed.). NACE, Houston, p. 17.

Jayaraman, A., Cheng, E.T., Earthman, J.C., Wood, T.K., 1997. Corrosion inhibition of SAE 1018 steel by aerobic biofilms. *Applied Microbiology and Biotechnology* 47, 62-68.

Kjellerup, B.V., Olesen, B.H., Nielsen, J.L., Frolund, B., Odum, S., Nielsen, P.H., 2003. Monitoring and characterisation of bacteria in corroding district heating systems using fluorescence in situ hybridisation and microautoradiography. *Water Science Technology* 47 (5), 117-22.

Krawiec, H., Vignal, V., Oltra, R., 2004. Use of the electrochemical microcell technique and the SVET for monitoring pitting corrosion at MnS. *Communication* 6, 655-660.

Lee, A.K., Newman, D.K., 2003. Microbial iron respiration: impacts on corrosion processes. *Applied Microbiology and Biotechnology* 62, 101-106.

Lee, W., Lewadowski, Z., Nielsen, P.H., Hamilton, W.A., 1995. Role of Sulfate-reducing Bacteria in Corrosion of Mild Steel : a Review. *Biofouling* 8, 165-194.

Little, B., Lee, J.S., 2007. Microbiologically Influenced Corrosion, in: Winston, R. (Ed.), *Microbiologically Influenced Corrosion*. Wiley-Interscience Wiley & Sons, Hoboken.

Little, B.J., Wagner, P., Mansfeld, F., 1991. An overview of microbiologically influenced corrosion. *Electrochem. Acta* 37 (12), 2185-2194.

Maier, R.M., Pepper, I.L., Gerba, C.P., 2000. *Bacterial Growth, Environmental microbiology*. Academic Press, London, UK, p. 47.

Mansfeld, F.B., Little, B.J., 1991. A technical review of electrochemical techniques applied to microbiologically influenced corrosion. *Corros. Sci.* 32 (3), 247-272.

Noghabi, K.A., Zhahiri, H.S., Yoon, S.C., 2007. The production of a cold-induced extracellular biopolymer by *Pseudomonas fluorescens* BM07 under various growth conditions and its role in heavy metals absorption. *Process Biochemistry* 42 (5), 847-855.

Pederson, A., Hermansson, M., 1991. Bacterial corrosion of iron in seawater in situ, and in aerobic and anaerobic model systems. *FEMS Microbiol. Lett.* 86 (2), 193ff.

Rittmann, B.E., McCarty, P.L., 1980. Model of steady-state-biofilm kinetics *Biotechnology and Bioengineering* 22 (11), 2343-2357.

Scotto, V., Cintio, R.D., Marcenaro, G., 1985. The influence of marine aerobic microbial film on stainless steel corrosion behavior. *Corros. Sci.* 25 (3), 185-194.

Sekine, I., Yuasa, M., Hirose, N., Tanaki, T., 2002. Degradation evaluation of corrosion protective coatings by electrochemical, physicochemical and physical measurements. *Progress in Organic Coatings* 45, 1.

Serebrennikova I., White H., Wall D., Missert N., Sullivan J.P., Barbour C., *Scanning Electrochemical Microscopy Investigations of Aluminum Oxide Films* in *Oxide Films*, K.R. Hebert, R.S. Lillard, B.R. MacDougall, eds., *Proceedings Volume 2000-4*, Electrochemical Society: Princeton, NJ, p. 139, 2000.

Souto, R.M., Gonzalez-Garcia, Y., Gonzalez, S., Burstein, G.T., 2004. Damage to paint coatings caused by electrolyte immersion as observed in situ by scanning electrochemical microscopy. *Corros. Sci.* 46, 2621.

Stockert, L., Böhni, H., 1991. Susceptibility to Crevice Corrosion and Metastable Pitting of Stainless Steels *Materials Science Forum* 44-45, pp. 313-328.

Thielen, P., 2005. Einfluss extrazellulärer Enzyme auf die Struktur und die Eigenschaften von Biofilmen von *Pseudomonas aeruginosa*. University Duisburg.

Wang, W., Wang, J., Xu, H., Li, X., 2006. Electrochemical techniques used in MIC studies. *Materials and Corrosion* 57.

Wipf, D.O., 1994. Initiation and study of localized corrosion by scanning electrochemical microscopy. *Colloid and Surface Science A93*, 251.

de Wit, J.H.W., Lenderink, H.J.W., 1996. Electrochemical impedance spectroscopy as a tool to obtain mechanistic information on the passive behaviour of aluminium. *Electrochem. Acta* 41, 1111-1119.

Zhang, T., Fang, H.H.P., Ko, B.C.B., 2003. Methanogen population in a marine biofilm corrosive to mild steel. *Applied Microbiology and Biotechnology* 63, 101-106.

Zuo, R., Wood, T.K., 2004. Inhibiting mild steel corrosion from sulfate-reducing bacteria and iron oxidizing bacteria using gramicidine-S-producing biofilms. *Appl Microbiol Biotechnol* 65, 747-753.



## Conclusions

In this thesis three different ways were followed to study the impact and presence of MIC in ship ballast tanks.

In Chapter 1 a review is given to explain the problem of MIC in ship ballast tanks. MIC is a very serious problem for the ship industry as it reduces structural lifetime and increases maintenance costs. This review aims to focus on the importance and mechanisms of MIC in ship ballast tanks (SBTs). It considers the practical aspects of MIC detection, identification and possible counterstrategies for engineers and inspection personal. An integral approach for SBTs is introduced, linking environmental parameters such as oxygen concentration, corrosion rate, nutrient availability and the microbial species of this environment. The model specifies the SBT zones, oxygen concentration, corrosion rate, microbial species and metabolic process related to MIC. For each zone, oxygen concentration, corrosion rate, abundant microorganisms and the possible MIC process can be derived. The gas phase and the sediment zone are separated, creating extreme zones within the ballast tank. The splash zone and the immersion zone in the middle of the tank are taken together because similar environmental parameters and microorganisms apply. The scheme indicates that with decreasing oxygen concentrations increasing corrosion rates result in combination with bacterial activity in the system. This is an important observation because a decrease in oxygen concentration within ballast tanks is being discussed in industry as a practical corrosion mitigation measure, which however ultimately not seems to reduce but enhance MIC. Based upon this review, following conclusions were drawn:

- The tank can be divided into three different risk regions for MIC; zone 1 low; zone 2 and 3 medium; zone 4 high;
- SBTs are prone to MIC because of their enclosed structure and their constant nutrient supply due to water exchange processes. Within the four different zones, gradients in oxygen, nutrients and flow conditions are established; these environmental conditions generate a diverse bacterial community;
- The corrosion process is characterized by rapid material loss forming deep pits. This corrosion condition is quite different from typical seawater corrosion, where low oxygen concentrations slow down the overall corrosion process;
- Structural changes which simplify cleaning strategies by reducing sediment accumulation – the source of MIC – should be considered;

- Perfect coating application should be aspired (no voids) to decrease the number of possible attachment sites for microorganisms. Biodegradation of ballast tank coatings should be considered in the future in order to develop new strategies to overcome microbial deterioration processes of the applied coatings. This will reduce the risk of MIC and will additionally fulfill the international coating guidelines provided by IMO;
- Ultimately, bacterial activity and diversity have a significant impact on the corrosion process. Biofilm formation and metabolic interactions are key mechanisms of MIC in problematic accessible SBTs. Bacterial accumulation can be circumvented by pre-treatment of the ballast water, e.g., filtration and ozonation, to minimize the risk of MIC.

From this general overview on MIC in SBT a new road was followed in chapter 2, including molecular techniques (DGGE) to assess bacterial communities involved in biofilm formation in ship ballast tanks. A thorough understanding of the microbial ecology and electrochemical environments where microbial corrosion occurs is necessary to implement preventive measures or appropriate controls to improve structural integrity. The use of traditional culture methods (involving liquid culturing) is inadequate to comprehensively assess the composition of microbial communities and their interactions, since the great majority of microorganisms in nature occur as biofilms and are yet uncultivated. In the last decades, molecular tools have been developed to overcome the limitations imposed by traditional cultivation techniques to study bacterial diversity in corrosive biofilms that form in diverse environments. However, detailed information regarding the microbial corrosion of SBTs exposed to seawater is practically non-existent. The current work is a large-scale approach of a direct investigation of microbial community in the ship ballast tank and also their corrosiveness simultaneously. The approach to determine the corrosiveness in the ship ballast tanks includes monitoring the electrochemical activity of carbon steel exposed to seawater by measuring the corrosion potential by OCP and the corrosion rate by LPR. Measurements results have been analyzed and related to literature sources to obtain insight in the corrosion process of bare metal under natural conditions. The outcome of this experiment indicated that bacterial accumulation and growth is continuously ongoing in ship ballast tanks. It was possible to confirm that bacterial growth and activity had a contribution to localized corrosion. This long term experiment proved the findings of the literature survey supporting the assumption that on the one hand MIC biofilms contain diverse bacterial communities and on the other hand shifts in the environment composition driven by nutrient supply are well established in SBTs. Overall it can be said that the bottom zone was more dominated by MIC bacteria such as (*Gallionella*, *Thiomicrospira* and *Desulfobacteraceae*) than the immersion zone (irrespective planktonic or sessile).



Higher pitting rates could be due to synergetic effects of various bacterial groups such as acid producing bacteria, slime producing bacteria, sulphur-oxidizing, sulphate reducing and metal oxidizing bacteria enabling the proliferation of local corrosion damage. All these results highlight the strong genetic diversity among these bacterial populations and their fast adaptability to different conditions, underlining once more the difficulty in finding a correlation between electrochemical activity and composition of microbial populations. Reliable corrosion monitoring of MIC is essential to obtain an efficient corrosion control and furthermore necessary for mechanistic corrosion studies. The presented techniques in chapter 2 revealed that the choice of monitoring technique can have a large impact on the results obtained in mechanistic studies. One of the recommended electrochemical techniques is EIS, as a reliable monitoring technique for MIC, although data interpretation is difficult.

Chapter 3 summarized 3 different experimental approaches of MIC monitoring and recognition based on electrochemical impedance spectroscopy and microscopy work.

Equivalent circuit modeling representing structures of passive films and coatings in simple aqueous solutions has been used to interpret EIS measurements of MIC. Despite the fact that the time-dependence of the impedance parameters showed quite some scatter, still valuable mechanistic information has been derived from the measurement results. Especially in later stages of bacterial growth, when a biofilm is formed on the metal surface, EIS clearly has indicated various processes related to biofilm formation (e.g. diffusion, formation of conductive pathways) can be identified with this technique.

The first experimental approach included the use of isolated anaerobic bacteria from a corrosion spot of a ship ballast tank. The results show that the corrosion rate increased in the presence of bacteria, in comparison with that observed in the sterile medium for the same exposure time. Localized corrosion attack in the form of pitting was observed on the steel surface in the presence of bacteria. The combination of two anaerobic species decreased pit size and local defects of carbon steel. This indicates that bacterial communities can have beneficial properties increasing or decreasing the corrosion rate depending on the environmental conditions.

These outcomes lead to the second experimental approach to study the corrosion impact of a natural MIC community isolated from a ship ballast tank. Standard laboratory techniques for MIC include in most cases a standard electrochemical cell containing reference electrode and counter electrode plus a working electrode of the material of interest, typically measurements are performed under static undisturbed conditions. To gain more realistic corrosion data a set-up representing natural conditions was introduced. For this a ship tank model system was implemented to study specifically the different zones of ship ballast tanks including sediment and wave movement.

Corrosion models are available predicting corrosion rates for diverse areas of ships, but no model includes the occurrence of MIC bacteria so far that will lead to an increase in corrosion rates preferably on the bottom of the tank.

The study confirmed that the metabolic activity of bacterial species as well as environmental conditions have a strong influence on local corrosion attack.

Electrochemical LPR measurements performed in the presence of the natural community, comprising SRB, SOB, IRB and APB isolated from a SBT biofilm and grown under semi anaerobic shaking conditions, confirmed higher corrosion rates of steel samples exposed to ASW containing these microorganisms. Values of 0.59 and 0.47 mm/y were found for the carbon steel, respectively, in the presence of the isolated community, compared to that of 0.02 mm/y for the control, corresponding to a 20-fold increase in corrosion.

The conclusions have shown that the presence of bacteria in SBTs can have a significant impact on the local corrosion of the bottom plating over time. These findings are addressing ship engineers and corrosion specialists similarly and will help to establish new maintenance programs for SBTs considering MIC as one of the causes for localized rapid corrosion failure. Coatings are applied for corrosion protection and act as a barrier layer between environment and metal surface. Prevention of corrosion is therefore one of the most important aspects of maintaining vessel safety plus preserving asset value. The success of any program for protecting water ballast tank depends on:

- The correct selection of the coating scheme during building
- Correct surface preparation and application of the coating scheme at new building
- Planned coating inspection in service
- Planned and effective coating maintenance throughout the vessel's life

Neglect or poor practice at any of these four stages can lead to coatings defects and the rapid onset of de-adhesion and corrosion with possible, serious consequences. Beside these practical application problems coating degradation can be influenced by the presence of microorganisms termed „biodeterioration effect“. Ballast water tanks are extreme environments as could be derived from chapter 1; in case of this severe conditions, it is tremendously important to have a coating that is most suitable for these site-specific conditions. As a third experimental approach the biodegradation process for ballast tank coatings in marine environments was investigated. For this methodology a natural bacterial community was chosen to explore progression of the interaction of natural biofilms with the coating, an aspect, which is not covered in standard procedures of coating test procedures.

The overall effect of this degradation was examined using the EIS technique. EIS is currently the most commonly used electrochemical method for evaluation of the protective properties of coatings. Samples not exposed to biological activity (blanks) exhibited a reasonable corrosion resistance. However, the bacterial affected coatings (both those exposed to acid producing bacteria and those exposed to a natural ballast tank community) showed a decrease in corrosion resistance. For the acidic environment with a low pH, EIS measurements indicate a decline in corrosion resistance over the course of the experimental time regardless of whether there were bacteria present.

This demonstrates that low pH solution has a significant impact on the coating barrier property, resulting in crack and hole formation. It is also revealed that the coating corrosion resistance declines after 40 days of exposure for the natural community, leading to the formation of blisters. Bacterial settling could be linked to some specific biofilm patterns affecting different types of coating attack. Overall, the natural bacterial community shows a less aggressive type of deterioration than the pure culture alone.

Literature studies showed that EIS is being applied for MIC studies. However the findings in chapter 3 have now proven that the response for long-term exposure of a steel electrode covered by biofilm / ferrous sulphide deposits is complex and cannot be modeled by a simple Randles circuit. It is necessary to model the capacitive, adsorptive and diffusional effects in order to understand the response.

However, EIS cannot be used as a stand-alone technique for MIC studies. However with the support of other techniques (OCP, microscopy) and additional information on the environment (nutrients, pH) specific conclusions can be drawn.

Beside these electrochemical monitoring techniques that provide corrosion rates and information on biofilm formation it is necessary to understand and follow up MIC initiation on a fundamental level by using high spatial resolution microscopic techniques. Currently, the most common way of using microscopic methods e.g. fluorescent microscopy, atomic force microscopy or SEM use the individual techniques as a standalone technique for evaluation of MIC. In most cases the sample is exposed to different instruments after each other, without following up the same sample. To overcome this problem a new technique was developed combining EFM, AFM and SEM for one sample specimen.

By combining three different types of microscopes it is possible to study bacterial attachment on opaque sample surfaces and all three instruments can image the same sample spot. By combining all these techniques on one sample spot a new methodology has been achieved, which is very straightforward and can also be employed in other corrosion science research. Application of these techniques in a systematic way will enable to analyze and visualize the different microstructural features to corrosion initiation. While all these techniques are already in use for corrosion research an elegant and easy to handle set-up for a combined use of these techniques on one sample spot has not been reported before.

The application of SECM was introduced in biology to monitor metabolic activity of biological cells and was afterwards transferred to corrosion science to study pit initiation and coating performance on a very local scale. Therefore the idea arose to use this local electrochemical scanning technique in combination with SVET to study local oxygen concentrations and depletion influenced by biofilm formation. MIC in natural environments is occurring in the biofilm mode of life. That comprises all microorganisms in aquatic environments. Biofilm formation causes changes in the metal/biofilm/interphase by creating localized anodic sites with larger surrounding cathodic areas.

In chapter 4 the findings of the SVET and SECM experiment have been presented and discussed. Based on these results, conclusions have been drawn upon the ability of SVET and SECM for evaluation of biofilm formation on metal surfaces.

The two local electrochemical techniques used in this study, offer complementary information: ionic fluxes corresponding to anodic and cathodic areas could be related to biofilm consumption of oxygen by SVET measurements and oxygen concentrations established in the interphase could be determined by SECM. Therefore the results showed that SECM is powerful in studying biofilm formation due to its high spatial resolution and in situ information of oxygen concentrations in aquatic biological systems, whereas the SVET proved the existence of an oxygen consuming biofilm. On the basis of the correlation that has been found between SVET and SECM, it is possible to use SECM to monitor changes of oxygen concentration in situ over time with high spatial resolution. This quantitative data can be used as a database for modeling and understanding MIC initiation and propagation mechanisms. Consequently localized electrochemical techniques should be used to gain a proper understanding of these complex phenomena and an extensive exchange of ideas between corrosion engineers and biologists is necessary for further improvements in the field of MIC and MICI.

## Future Outlook

The study of microbiologically influenced corrosion (MIC) has progressed from phenomenological case histories to mature interdisciplinary science including electrochemical, metallurgical, surface analytics and microbiology. The ways in which new techniques can be used to understand fundamental mechanism and to discriminate MIC was part of this thesis.

Detection of MIC in natural environment is still a difficult research field with numerous parameters to study.

As the different chapter of this thesis indicate, MIC is a complex topic that needs information to be obtained from many techniques. However, it has to be highlighted that no method is universally applicable and that the methods should be selected by taking into account the different aspects of the problem of concern.

Based on the findings, the following conclusions were drawn:

The test methods should be divided into two main groups; (i) laboratory tests, (ii) field tests.

- (i) Laboratory studies have the advantage that controlled environmental conditions can be explored such as temperature and nutrient availability. Over the last decades MIC was modelled and studied under precise environments gaining reproducible results.
- (ii) Field tests on the other hand are limited by 3 main factors:
  - a. longer time
  - b. masking of localized corrosion behaviour by natural fluctuations in the environment
  - c. single parameters are difficult to distinguish

The main advantage of field tests is their direct application to the system of interest. Therefore we recommend the combination of laboratory tests and field experiments to determine the mechanisms of corrosion. For control and mitigation of MIC we recommend the following diagram.

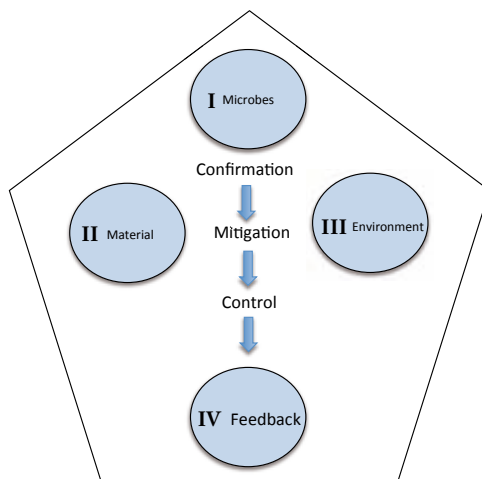


Diagram 5.1: MIC failure analysis scheme including the main categories (microbes, material, environment) making a system vulnerable for MIC in combination with a practical step by step guideline for corrosion engineers.

- (i) Confirmation that the case has been caused by MIC.
- (ii) Mitigation includes the physical or chemical mitigation and design modifications of environment and material.
- (iii) Control will include continuous monitoring of the system after application of mitigation procedures.
- (iv) Feedback covers a complete documentation of all performed steps to have a detailed advice/reference procedure in the future.

A simple one-method approach as a counterstrategy does not exist it will be rather the use of a multidimensional model including MIC mitigation and practical treatment steps that will lead to advanced control strategies in the future. MIC confirmation should be regarded as an essential part of the mitigation and control of corrosion in natural and industrial waters. Diagram 5.2. provides the different phases of MIC mitigation in practise.

Phase 1 Recognition of MIC			
	Material	Environment	Microbes
Analysis Confirmation On site	Pit morphology Corrosion products	Electrochemical techniques: OCP, LPR, EIS	Culture techniques Rapid tests
Phase 2 Advanced techniques to study extent of MIC			
Techniques Confirmation In the lab	SEM-EDX	Local electrochemical techniques: Microelectrodes, SVET	Identification of Organisms: Culture techniques Cell Activity Genetic Techniques Microscopic Techniques
Phase 3 Treatment of MIC			
Techniques Mitigation & Control	Physical mechanical: Pigging, UV radiation, Ultrasonic treatment	Electrochemical methods: Cathodic protection, Coating	Biological methods: Bio-competitive exclusion Chemical treatments: Chlorine, Bromine, Ozone, Aldehydes
Phase 4 Feedback - documentation			

Diagram 5.2: Confirmation, mitigation and control of MIC failure based on a multidimensional approach.

The multidimensional approach can be divided into 4 phases covering the material, environment and microorganisms involved. The first phase is based on analysing techniques used on site to prove the existence of MIC such as corrosion products, electrochemical techniques if applicable and rapid test to identify bacterial groups. If the failure identified can be related to MIC the second phase of the diagram should be followed.

This step involves laboratory work including advanced surface analysis techniques such as SEM-EDX or molecular analysing tools to determine abundance and activity of microorganisms in the system. The third phase incorporate the treatment of MIC by physical, chemical and biological methods. Following these three phases the system under MIC attack can be treated in the most efficient way to prevent further failure. The concluding documentation and feedback in phase four is obligatory to develop counterstrategies based on previous cases.

## Summary

Microbiologically influenced corrosion (MIC) is known to be a dangerous process in ship tanks due to its rapid and yet unpredictable occurrence, leading to extremely fast local corrosion, possibly jeopardizing the structural integrity, in a relatively short time. This project focuses on a fundamental understanding of MIC processes in ship ballast tanks (SBTs) as a basis for the development of effective counterstrategies that offer an appropriate protection against MIC attack. Local conditions typically consist of oxic-anoxic environments where both aerobic and anaerobic biofilms develop resulting in aggressive corrosion. Fundamental understanding of the dominant parameters considering material, environment and microbes were addressed. In chapter 1 a review of the conditions in ship ballast tanks, possible MIC mechanisms and practical counterstrategies is presented.

Two central points were addressed in this thesis:

(i) fundamental understanding of interactions between biological and electrochemical processes on metal surfaces and (ii) identification of counterstrategies that offer the potential to improve MIC control.

Chapter two deals with the impact of MIC in a real scale SBT to understand community characteristics within SBTs. The study highlights the impact of attached biofilms on local corrosion in a ship ballast tank environment. The application of molecular techniques in combination with electrochemical techniques provides a better and synergistic monitoring tool in the enclosed seawater environment. The use of denaturing gradient gel electrophoresis (DGGE) as a screening tool can be one of the potential techniques to monitor corrosion behaviour in enclosed seawater environments in combination with open circuit potential (OCP) and linear polarization resistance (LPR) measurements. The work in this chapter provides a systematic future research and analysis approach to build up a database of bacterial species, which are involved in corrosion or coating degradation on-board of ships. A more effective treatment system for treating biofilms on sidewalls of ship ballast tanks will help to reduce costly material replacements.

Hence, any measure in the future for controlling aquatic invasive species in ballast tanks should also consider the impact on corrosion from sessile communities, which has been underestimated so far.

In chapter three the usability of electrochemical techniques for monitoring MIC is discussed in detail. Three individual approaches were studied in the lab comprising: (i) corrosion impact of a dual species biofilm, (ii) implementation of a simulated ship tank model system and (iii) the study of the biodeterioration of a ship ballast tank coating.



(i) The influence of localized corrosion on carbon steel by two anaerobic bacterial strains isolated from a ship ballast tank were investigated by using linear polarization resistance (LPR), electrochemical impedance spectroscopy (EIS), scanning electron microscopy (SEM) and energy dispersive analysis (EDX). The LPR results show that the corrosion potential  $E_{\text{corr}}$  decreased in the presence of bacteria, in comparison with those observed in the sterile medium for the same exposure time interval. To confirm the electrochemical data weight loss measurements were performed. Additional surface analysis by SEM demonstrated enhanced local corrosion on the carbon steel in presence of the bacterial community as compared to abiotic controls.

(ii) For the first time a model system was used to study the impact of sediment and wave movement in different levels of a simulated SBT. The study confirmed that the metabolic activity of bacterial species as well as environmental conditions have a strong influence on local corrosion attack. A contrary effect for the corrosion rates could be found in the sediment zone for bacterial set up and control. The presence of sediment in the test cell supported anaerobic conditions favourable for the growth of anaerobic and acid producing bacteria increasing the potential risk of pitting corrosion. Additionally the severity of pitting attack increased due to metabolic interactions. The results confirmed that interactions of mixed communities need time on the one hand but on the other hand once established local corrosion attacks become rapid and severe. The model system could be successfully implemented to gain reproducible and comparable corrosion data simulating natural conditions.

(iii) The behaviour of a ballast tank coating against microbial degradation was studied. It was shown that biological activity significantly affected the coating properties. As a result of such microbial attack, numerous cracks and holes were produced as identified by atomic force microscopy (AFM). The overall effect of such degradation was studied by EIS. It was observed that the non-bacterial exposed samples (blank) exhibited a reasonably proper corrosion resistance. However, the bacterially affected coatings (exposed to acid producing bacteria and natural ballast tank community) showed a decrease in corrosion protection performance. For the acidic environment with a low pH regardless of bacteria presence or not EIS measurements indicated a decline in corrosion protection performance over the course of the experimental time. Finally, it can be concluded that the bacterial deterioration effect is as severe as other types of degradation, causing the coating system to be very vulnerable to deterioration under realistic environmental conditions. Therefore it is necessary to include natural communities in coating degradation studies to identify possible degradation mechanisms and the severity of attack over time.

The fourth chapter comprises different highly sensitive and spatially resolved techniques to study MIC on a very local scale. The first step included the development of a novel analysis approach for the preparation and visualization of metal surfaces, suitable for combined imaging by epifluorescent microscopy (EFM), AFM and SEM. By combining three different microscopes, the complementary use of these high-resolution techniques to study surface changes and accumulation of biological substances on stainless steel surfaces was proven. Although all these techniques are already in use for corrosion research, an elegant and easy to handle set-up for a combined use of these techniques on one sample spot has not been reported before.

The last experimental part of the thesis covers the use of local electrochemical techniques. The scanning vibrating electrode technique (SVET) and scanning electrochemical microscope (SECM) were used for their high spatial resolution close to the metal/solution interface. By combining these techniques in-situ changes at metal/solution interfaces in the presence and absence of aerobic bacteria could be followed up. Aerobic bacteria like *Pseudomonas* have been shown to decrease metal corrosion by microbial respiration. This activity can decrease the cathodic rate by reducing the amount of reactants available for the cathodic reaction. SECM measurements showed that the dissolved oxygen concentration decreases as a function of formation stages of the biofilm. It was possible to establish a direct relation between oxygen reduction catalysis and early stages of biofilm formation by *Pseudomonas*. Therefore it was possible to demonstrate that the application of local scanning electrochemical techniques with high-spatial resolution is a powerful tool for a better understanding of microbial activity on metal systems providing in-situ information of the processes taking place at the metal/biofilm/solution interface.

Chapter five summarises the conclusions drawn in the preceding chapters. In addition, the general discussion in this chapter links together some of the preceding results and suggestions. The last part of the thesis gives a future outlook on MIC monitoring and prediction and reviews options to mitigate MIC failures based on a multidimensional approach.

---

## Samenvatting

Corrosie veroorzaakt door micro-organismen (microbiële geïnitieerde corrosie, MIC) is onvoorspelbaar en leidt in korte tijd tot ernstige plaatselijke aantasting. Met name water ballast tanks (WBT) van schepen zijn gevoelig voor deze corrosievorm. MIC in WBT kan in korte tijd ernstige verzwakking van de structurele integriteit van het schip en zelfs perforaties veroorzaken. Dit project onderzoekt de fundamentele aspecten van MIC in WBT om hieruit oplossingen te vinden om MIC of de gevolgen ervan te voorkomen.

In hoofdstuk 1 wordt een overzicht gegeven van de voorwaarden en van de praktische milieu eigenschappen in de WBT, waarbij MIC kan optreden. Deze kunnen zuurstofhoudende of zuurstofarme omstandigheden zijn; hierin kunnen zowel aërobe als anaërobe biofilms zich ontwikkelen en aanleiding geven tot de agressieve corrosie. Fundamentele kennis van de belangrijkste parameters zoals materiaal, omgeving en type micro-organismen is essentieel. Twee centrale lijnen zijn hierbij gevolgd: (i) fundamenteel begrip van interacties tussen biologische en elektrochemische processen op metalen en (ii) identificatie van maatregelen die kunnen leiden tot MIC-beheersing.

In hoofdstuk 2 wordt MIC onderzocht in een reële situatie, namelijk in een echte WBT. Deze studie laat voor het eerst de rol zien van de aanwezige biofilms op de lokale corrosie. De toepassing van moleculaire technieken in combinatie met elektrochemische technieken levert een beter en synergetische controlemiddel in de omringende zeewateromgeving. Het gaat hier met name om het gebruik van “Denaturerende gradiënt gelelektroforese” (DGGE) als een screening methode in combinatie met de open-circuit potentiaal (OCP) en de lineaire polarisatieweerstand metingen. Met deze laatste technieken wordt het corrosiegedrag onderzocht. Het werk in dit hoofdstuk biedt een systematische onderzoeks- en analyseaanpak om een database van bacteriële soorten op te bouwen, die betrokken zijn in het MIC proces aan boord van schepen.

Door een effectiever behandelingssysteem voor het bestrijden van biofilms op de wanden van WBT van schepen kan dure materiaalvervanging worden voorkomen. Een consequentie hiervan is ook dat bij toekomstige metingen voor het controleren van aquatisch invasieve soorten ook rekening dient te worden gehouden met de impact op de corrosie door de reeds aanwezige groepen, wat tot nu toe onderschat is.

In hoofdstuk drie wordt de bruikbaarheid van elektrochemische technieken bij het MIC onderzoek nader uitgewerkt. Drie benaderingen zijn in een laboratorium gevolgd: (i) de invloed op corrosie van een biofilm die uit twee soorten micro organismen bestaat, (ii) implementatie van een gesimuleerde tank van een schip op schaal en (iii) het bestuderen van aantasting van de beschermende coating door micro organismen.

(i) De invloed van corrosie op koolstof staal door twee anaërobe bacteriestammen die geïsoleerd werden in een WBT is onderzocht door gebruik te maken van diverse elektrochemische en oppervlakte analyse technieken (respectievelijk potentiaal, lineaire polarisatieweerstand, elektrochemische impedantie spectroscopie en scannen met behulp van elektronenmicroscopie en energie-dispersieve analyse).

Hieruit blijkt dat de corrosiepotentiaal daalt door de aanwezigheid van bacteriën, dit vergeleken met koolstof staal in een steriel medium. Oppervlakte analyse toonde geïntensiverde lokale corrosie van het koolstof staal aan in aanwezigheid van een bacteriegemeenschap, dit in tegenstelling met abiotische controlegroepen. Om de elektrochemische en oppervlakte analyse resultaten te bevestigen zijn ook gewichtsverlies metingen uitgevoerd

(ii) Voor het eerst is een modelsysteem gebruikt om de invloed van sediment en de beweging van de golven op een gesimuleerde WBT te onderzoeken. Deze studie bevestigt de metabolische activiteit van bacteriën evenals de grote invloed van de omgevingsparameters op de lokale corrosie. Voor de hoeveelheid corrosie is in de sedimentzone voor de bacteriële set-up en de controle een tegengesteld effect geconstateerd.

De aanwezigheid van sediment in de testcel toont aan dat anaërobe omstandigheden gunstig zijn voor de groei van anaërobe en zuurproducerende bacteriën waardoor het potentiële risico van putcorrosie verhoogd werd. Bovendien wordt de mate van putcorrosie verhoogd door de metabolische interacties. De resultaten bevestigden dat interactie van gemengde groepen enerzijds tijd nodig hebben, maar anderzijds, zodra lokale corrosie begonnen is, de aantasting sneller verloopt. Door het simuleren van de natuurlijke omstandigheden kan het modelsysteem met succes geïmplementeerd worden om reproduceerbare corrosiegegevens te verzamelen.

(iii) Bestudeerd is ook het gedrag van de (epoxy)coating van WBT op microbiologische degradatie. Het blijkt namelijk dat biologische activiteit een significant invloed heeft op de coatingeigenschappen. Een dergelijke microbiële aanval heeft tot gevolg, dat tal van scheuren en gaten ontstaan die met behulp van de atoomforcemicroscoop (AFM) zijn vastgesteld. Het effect van een dergelijke degradatie op de corrosiebescherming van de coating is met behulp van elektrochemische impedantie spectroscopie verder onderzocht. Hieruit volgt dat de non-bacterieel blootgestelde coatings (blanco) de gewenste corrosieweerstand vertonen. De door bacteriën aangetaste coatings (blootgesteld zowel aan zuurproducerende bacteriën als aan de van nature in een WBT aanwezige bacteriën) toonden een afname in corrosiebescherming. Voor een zure omgeving (lage pH), ongeacht of er bacteriën aanwezig zijn of niet, is een afname van van corrosiebescherming aangetoond. Dit is het resultaat van de interactie tussen de soorten, bijv. soorten die van zuur leven, verminderen het aantal direct zuurproducerende bacteriën die schadelijk zijn voor de coating. Tenslotte kan men concluderen dat het bacteriële aantasting van de coating net zo erg is als MIC zelf. Daarom is het noodzakelijk de natuurlijke gemeenschappen bij de studies van de degradatie van de coating te betrekken, dit om de aard en de ernst van het degradatiemechanisme vast te stellen.

In het vierde hoofdstuk worden twee gevoelige technieken besproken om MIC op zeer lokale schaal te onderzoeken. De eerste betreft een nieuwe analyse-aanpak voor de visualisatie van metaaloppervlakken met biofilms: het gaat hierbij om de combinatie van epifluorescentiemicroscopie (EFM), AFM en SEM. Alhoewel deze technieken afzonderlijk bij het onderzoek naar corrosie al worden gebruikt, zijn hierbij voor het eerst in een gecombineerde opstelling de voordelen van alle drie technieken samen optimaal benut.

De tweede techniek betreft het gebruik van lokale elektrochemische technieken: de scanning vibrerende elektrodeteknik (SVET) en scanning elektrochemische microscopie (SECM). Deze zijn gebruikt vanwege hun hoge ruimtelijke resolutie dicht bij het metaal/oplossing overgang. Door deze technieken in situ te combineren kunnen de veranderingen tijdens de aan- en afwezigheid van aërobe bacteriën worden onderzocht. Bij aërobe bacteriën, zoals de *Pseudomonas*, is een afname van metaalcorrosie door microbiologische respiratie aangetoond. Deze activiteit zorgt voor de afname van het kathodische reactie. SECM-metingen hebben aangetoond dat de zuurstofconcentratie afneemt gedurende de formatiestadia van de biofilm. Hiermee is aangetoond dat de toepassing van lokale scanning elektrochemische technieken met hoge ruimtelijke resolutie een zeer geschikt gereedschap is voor een beter begrip van microbiologische activiteiten op metalen oppervlakken.

In hoofdstuk vijf worden de conclusies van de voorafgaande hoofdstukken samengevat. Ook worden in een algemene discussie enkele van de voorafgaande resultaten en suggesties aan elkaar gekoppeld. Tenslotte geeft het laatste gedeelte van dit proefschrift een toekomstige verwachting op MIC-voorspelling en MIC-controle en analyseert mogelijkheden om schade door MIC te beperken uitgaande van de multidimensionale aanpak.

## Zusammenfassung

Mikrobiologisch beeinflusste Korrosion (Microbiologically Influenced Corrosion, MIC) ist aufgrund ihres schnellen und unvorhersehbaren Auftretens, das zu extrem schneller, lokaler Korrosion führt, ein nicht zu unterschätzendes Problem in Schiffballasttanks. Die in dieser Arbeit vorgestellten Ergebnisse konzentrieren sich auf die Entwicklung von effektiven Gegenstrategien, die einen geeigneten Schutz vor MIC bieten sollen. Desweiteren wurden Versuche dahingehend konzipiert um das fundamentale Verständnis von MIC-Prozessen in Ballasttanks von Schiffen (Ship Ballast Tanks, SBTs) zu vertiefen. Die Umgebungsparameter in Ballasttanks sind typischerweise oxisch-anoxisch, in denen sich aerobe und anaerobe Biofilme entwickeln können, welches eine aggressive Korrosion begünstigt. Kapitel eins fasst die grundlegenden Ballasttank Parameter in Bezug auf Material, Umweltbedingungen und Mikroorganismen zusammen und stellt zusätzlich praktische Gegenstrategien gegen MIC vor.

In dieser Arbeit werden zwei zentrale Punkte angesprochen:

(i) Das grundlegende Verständnis von Interaktionen zwischen biologischen und elektrochemischen Prozessen auf Metalloberflächen und (ii) die Entwicklung von Gegenstrategien, die zu einer Verbesserung der MIC-Kontrolle führen sollen.

Kapitel zwei befasst sich mit den Auswirkungen von MIC in einem SBT von realer Größe, dessen mikrobiologischen Organismen charakterisiert wurden. Die Studie dokumentiert die Auswirkungen von sessilen Biofilmen auf die lokale Korrosion in Schiffballasttanks. Der Einsatz von molekularen Techniken wie der denaturierender Gradientengelelektrophorese (DGGE) kombiniert mit elektrochemischen Messmethoden wie dem Ruhepotential (Open Circuit Potential, OCP) und des linearen Polarisierungswiderstandes (Linear Polarization Resistance, LPR) bietet ein besseres und komplementierendes Überwachungshilfsmittel in diesen geschlossenen schwer zugänglichen Schiffssektionen.

Die Arbeit in diesem Kapitel stellt einen systematischen Forschungs- und Analysenansatz vor, auf dessen Basis eine Datenbank aufgebaut werden kann, die korrosive Bakterien detailliert beschreibt und klassifiziert. Die somit gewonnenen Daten können dafür genutzt werden ein effektiveres Kontroll- und Überwachungssystem für Ballasttanks zu entwickeln.

In Kapitel drei wird die praktische Anwendung von elektrochemischen Messmethoden für die Kontrolle und den Nachweis von MIC detailliert besprochen. Im Labor wurden drei individuelle experimentelle Ansätze verfolgt: (i) die Auswirkungen eines mikrobiellen Biofilms auf die Korrosion, (ii) die Implementierung eines simulierten Schiffstank-Modellsystems und (iii) das Studium der biologischen Interaktion mit einem Ballasttankanstrich (Beschichtung).

(i) Zwei anaerobe Bakterienstämmen (isoliert aus einem Ballasttank) und deren Einfluss auf die lokale Korrosion wurde unter Verwendung verschiedener elektrochemischer Methoden wie des linearen Polarisationswiderstands (Linear Polarization Resistance, LPR) und der Impedanzspektroskopie (Electrochemical Impedance Spectroscopy, EIS) im Labor untersucht. Die LPR-Ergebnisse zeigten, dass das Korrosionspotential  $E_{\text{corr}}$  im Vergleich zu jenem, das im sterilen Medium über das gleiche Zeitintervall aufgezeichnet wurde, in der Anwesenheit von Bakterien abnahm. Um die elektrochemisch gemessenen Korrosionsraten zu bestätigen wurden Gewichtsverlustmessungen mittels Korrosionscoupons vorgenommen. Zusätzliche Oberflächenanalysen der verwendeten Korrosionscoupons mittels Rasterelektronenmikroskopie (SEM) zeigten im Vergleich zu den abiotischen Kontrollen, fortgeschrittene lokale Korrosion in Gegenwart der bakteriellen Gemeinschaft.

(ii) Zum ersten Mal wurde ein Modellsystem implementiert, um die Auswirkungen von Sediment- und Wellenbewegung in einem SBTs zu untersuchen. Die Studie bestätigte, dass die metabolische Aktivität von Bakterien sowie die Umweltfaktoren einen starken Einfluss auf lokale Korrosion haben. Die Zugabe von Sedimenten im Testtank unterstützte anaerobe Bedingungen, die günstig für das Wachstum von anaeroben und säureproduzierenden Bakterien sind. Die Präsenz der Mikroorganismen erhöhte das potentielle Risiko von Lochfraß der exponierten Korrosioncoupons. Darüber hinaus erhöhte sich der Schweregrad der Korrosion aufgrund von metabolischen Interaktionen der Bakterien. Die Ergebnisse bestätigten, dass durch Interaktionen von gemischten mikrobiellen Gemeinschaften lokale Korrosionsattacken schneller und schwerwiegender werden. Das Modellsystem konnte erfolgreich implementiert werden, um vergleichbare und natürliche Wachstums- und Korrosionsbedingungen zu simulieren.

(iii) Im dritten Versuchsansatz wurde eine Ballasttankfarbe (Beschichtung) verschiedenartigen Bakterien ausgesetzt um den biologischen Einfluss auf die Farbe zu studieren. Dabei zeigte sich, dass biologische Aktivitäten die Eigenschaften der Farbe erheblich beeinflussen können. Als Ergebnis dieser mikrobiellen Interaktion entstanden zahlreiche Risse und Löcher die mittels Atomkraftmikroskopie (Atomic Force Microscopy, AFM) nachgewiesen wurden. Die Gesamtauswirkungen der mikrobiellen Zerstörung wurde mit EIS über einen längeren Zeitraum von 60 Tagen untersucht. Die den Bakterien ausgesetzten Beschichtungen zeigten eine Abnahme der Korrosionsschutzleistung. In saurer Umgebung mit einem niedrigen pH-Wert, ungeachtet dessen, ob Bakterien vorhanden waren oder nicht, zeigten die EIS-Messungen im Laufe des Experimentes eine Abnahme der Korrosionsschutzleistung. Daraus kann man schlussfolgern, dass der bakterielle Zersetzungseffekt genauso schwerwiegend ist, wie andere Arten der Zerstörung wie z.B. durch Säure, wodurch das Beschichtungssystem unter realistischen Umgebungsbedingungen wie mikrobiologische Gemeinschaften, sehr anfällig für biologische induzierte Zerstörung ist.

Daher ist es notwendig, in Studien über biologische Zersetzung von Farben und Beschichtungen natürliche Bakteriengemeinschaften zu integrieren, um mögliche Zersetzungsmechanismen und den Schweregrad der Zerstörung/Interaktion so zeitnah und realistisch wie möglich festzustellen.

Das vierte Kapitel umfasst unterschiedliche, hochempfindliche und räumlich auflösende Techniken um MIC zu studieren. Der erste experimentelle Arbeitsschritt beinhaltete die Entwicklung einer neuartigen Methodik zur Visualisierung von Metalloberflächen. Dazu wurden Fluoreszenzmikroskopie, Atomkraftmikroskopie und der Rasterelektronenmikroskopie über einen gemeinsam zu nutzenden Probenträger verbunden. Diese Technik erlaubt es eine Probe unter verschiedenen Mikroskopen zu betrachten und zu analysieren. Obwohl alle diese Techniken einzeln bereits in der Korrosionsforschung zum Einsatz kommen, wurde zuvor noch nie von einem einfach zu handhabenden System für die Kombination der einzelnen Mikroskope berichtet.

Der zweite und letzte Teil der experimentelle Arbeit in Kapitel vier deckt die Anwendung von lokalen elektrochemischen Techniken ab. Die Vibrationssondenraftermessung (Scanning Vibrating Electrode Technique, SVET) und elektrochemische Rastermikroskopie (Scanning Electrochemical Microscope, SECM) wurden wegen ihrer hohen räumlichen Auflösung nahe an der Metall-/Elektrolytgrenzfläche eingesetzt. Durch das Kombinieren dieser Techniken in situ konnten Veränderungen an den Metall-/Elektrolytgrenzfläche in Präsenz und Abwesenheit von aeroben Bakterien nachverfolgt werden. Es konnte eine direkte Beziehung zwischen Sauerstoffabnahme und der Biofilmbildung durch aerobe Bakterien (*Pseudomonaden*) aufgezeichnet werden. Die Ergebnisse zeigten dass die Anwendung von lokalen elektrochemischen Scantechniken mit hoher räumlicher Auflösung dazu geeignet sind, in-situ-Informationen über die an der Metall-/Biofilm-/Elektrolytgrenzfläche stattfindenden Prozesse zu liefern.

Kapitel fünf fasst die in den vorherigen Kapiteln gezogenen Schlussfolgerungen zusammen. Darüber hinaus verknüpft die allgemeine Diskussion in diesem Kapitel einige der vorangehenden Ergebnisse und Vorschläge. Der letzte Teil der These gibt einen Zukunftsausblick über eine mögliche MIC-Überwachung und Vorhersage, die auf Basis von wissenschaftlichen Erkenntnissen umgesetzt werden kann.



## **Publications**

### **Talks**

#### **COST D33 2009 Final Workshop 2009**

A. Heyer, F. D'Souza, G. Ferrari, J.M.C. Mol and J.H.W. de Wit, May 2009, Cluj, Romania  
"Microbiologically Influenced Corrosion in ship tank environments part II" Working group:  
Nanoscale Electrochemical and Bioprocesses at Solid-aqueous interphases of Industrial  
Materials.

#### **Studiekern Corrosie 2009**

A. Heyer, F. D'Souza, G. Ferrari, J.M.C. Mol and J.H.W. de Wit, May 2009, Den Helder,  
The Netherlands. "MIC in ballast tanks". De Sectie Corrosie van de Bond voor Materialkennis

#### **MIC workshop TNO/MIP/Senter Novem/M2i 2009**

A. Heyer, F. D'Souza, G. Ferrari, J.M.C. Mol and J.H.W. de Wit, Den Helder May 2009,  
The Netherlands "A fundamental approach in studying - Microbial corrosion in ship ballast  
tanks" De mega impact van micro bio-corrosie.

#### **Eurocorr 2009,**

A. Heyer, F. D'Souza, G. Ferrari, J.M.C. Mol and J.H.W. de Wit, September, Nice, France  
"Combining microscopy and electrochemical studies on microbial influenced corrosion (MIC) in  
seawater environments" Paper number: 7581

#### **M2i Annual Conference, 2009**

A. Heyer, F. D'Souza, G. Ferrari, J.M.C. Mol and J.H.W. de Wit, December 2009, Nordwijkerhout,  
The Netherlands "Using state of the art techniques to study Microbiologically Influenced  
Corrosion (MIC) in a model system"

#### **15<sup>th</sup> Nordic corrosion congress (NKM) 2010**

A. Heyer, F. D'Souza, G. Ferrari, J.M.C. Mol and J.H.W. de Wit, May 2010 Stockholm Sweden  
"A new approach in understanding microbiologically influenced corrosion (MIC) based on  
electrochemistry and microscopy in a ship tank model system. "  
Theme: Fouling and microbially influenced corrosion oral presentation

#### **15<sup>th</sup> International congress on marine corrosion and fouling (ICMCF 2010)**

A. Heyer, F. D'Souza, A. Bruin, G. Ferrari, J.M.C. Mol and J.H.W. de Wit, July 2010, Newcastle  
England. "Using Electrochemical Impedance Spectroscopy and microscopy for evaluation of  
ballast tank coating degradation by microorganisms." Paper number: 28-B-1-8

**Eurocorr 2010**

A. Heyer, F. D'Souza, G. Ferrari, J.M.C. Mol and J.H.W. de Wit, September 2010 Moscow, Russia. "A study of electron transfer processes through biofilms in marine environments."  
Paper number: 9458

A. Heyer, G. Ferrari, F. D'Souza, X.Zhang, H. Bakuwel, J.M.C. Mol and J.H.W. de Wit September 2010 Moscow, Russia. "Susceptibility of epoxy coatings to microbial influenced degradation."  
Paper number: 9489

**NACE 2011**

A. Heyer, F. D'Souza, G. Ferrari, J.M.C. Mol and J.H.W. de Wit , March 2011, Houston, Texas USA. "EIS study of MIC in three different zones derived from ship ballast tank model system"  
Paper number: 19148

**Eurocorr 2011**

A. Heyer, G. Ferrari, F. D'Souza, J.M.C. Mol and J.H.W. de Wit September 2011, Stockholm Sweden. "A combined EFM, AFM and SEM study for visualization of bacteria on metal to study local corrosion processes (MIC)" Paper number: 9461

**Dancorr Workshop**

A. Heyer, G. Ferrari, F. D'Souza, J.M.C. Mol and J.H.W. de Wit, September 2011, Aarhus, Denmark. "Microbiologically Influenced Corrosion in ship ballast tanks"  
Invited speaker.

**NACE 2012**

A. Heyer, F. D'Souza, G. Ferrari, F.S.L. Marty, G. Muyzer, J.M.C. Mol and J.H.W. de Wit, March 2012 Salt Lake City, Utah USA. "Study of MIC impact in a full-scale ship ballast tank" Paper number: 1246

**Poster****M2i Conference 2008,**

A. Heyer, F. D'Souza, G. Ferrari, J.M.C. Mol and J.H.W. de Wit, Nordwijkerhout, The Netherlands "Microbiologically influenced corrosion in MIC in ship tanks" Poster number: 6.6

**Eurocorr 2009,**

A. Heyer, F. D'Souza, G. Ferrari, J.M.C. Mol and J.H.W. de Wit, Nice, France "Microbiologically Influenced Corrosion in a simulated ship tank model system" Poster number: 7582

**5<sup>th</sup> ASM conference on biofilms,**

A. Heyer, F. D'Souza, G. Ferrari, J.M.C. Mol and J.H.W. de Wit, November 2009, Cancun, Mexico  
"Microscopic characterization of MIC biofilms on stainless steel" Poster number: C276

**M2i Conference 2009,**

A. Heyer, F. D'Souza, G. Ferrari, J.M.C. Mol and J.H.W. de Wit, Nordwijkerhout, The Netherlands  
"MIC – detection of pit initiation: A microscopic approach" Poster number: 6.1

**Dechema, Jahrestagung der Biotechnologen,**

A. Heyer, F. D'Souza, G. Ferrari, J.M.C. Mol and J.H.W. de Wit, September 2009, Mannheim, Germany  
"Mikrobielle Korrosion in maritimen Ballasttanks" Poster number: 7887

**Eurocorr 2010**

A. Heyer, F. D'Souza, G. Ferrari, J.M.C. Mol and J.H.W. de Wit, September 2010 Moscow Russia  
"Characterization of microbial attachment on metal surfaces by Scanning Kelvin Probe and Epifluorescence Microscopy." Paper number: 9461

**JPK 9<sup>th</sup> International Symposium on Scanning Probe Microscopy & Optical Tweezers  
in Life Science 2010**

A. Heyer, A. Bruin, M. Bakker, G. Ferrari, F. D'Souza, G. Strijk, P. Willemsen, "A multidisciplinary microscopy approach to study MIC on steel surfaces." Poster number: P25

**Reservoir microbiology forum (RMF) 2010**

A. Heyer, A. Bruin, M. Bakker, G. Ferrari, F. D'Souza, G. Strijk, P. Willemsen, December 2010, London England. "A combination of diverse local techniques for the characterization of biofilm/metal interactions."

**M2i Conference 2010**

A. Heyer, F. D'Souza, G. Ferrari, J.M.C. Mol and J.H.W. de Wit, Nordwijkerhout, The Netherlands  
"A new approach to study local corrosion processes on steel surfaces by combining diverse microscopic techniques" Poster number 6.4

**M2i Conference 2011**

A. Heyer, F. D'Souza, G. Ferrari, J.M.C. Mol and J.H.W. de Wit, Nordwijkerhout, The Netherlands  
"The Use of Scanning Vibrating Electrode Technique in Microbial Influenced Corrosion Research" Poster number 6.4

## Scientific paper

A. Heyer, F. D'Souza, A. Bruin, G. Ferrari, J.M.C. Mol and J.H.W. de Wit, "A new approach to study local corrosion processes on steel surfaces by combining different microscopic techniques", *Applied Surface Science* 2012, Vol 258, 22, 8431-9104.

A. Heyer, F. D'Souza, G. Ferrari, C. F. Leon Morales, J.M.C. Mol and J.H.W. de Wit, "Molecular Microbiology Methods applied on ship ballast tank samples", Skovhus, T.L., Caffrey, S., and Hubert, C. (2014). *Molecular Methods and Applications in Microbiology* (Norfolk, UK: Caister Academic Press). In press.

A. Heyer, X. Zhang, G. Ferrari, J.M.C. Mol and J.H.W. de Wit, "Biodegradation of ballast tank coating investigated by impedance spectroscopy and microscopy", accepted for publication in *Biodegradation*

A. Heyer, F. D'Souza, C. F. Leon Morales, G. Ferrari, J.M.C. Mol and J.H.W. de Wit, "Ship ballast tanks a review from microbial and electrochemical point of view", under review in *Ocean Engineering*

A. Heyer, F.S.L. Marty, G. Muyzer, F. D'Souza C.F. Leon Morales J.M.C. Mol and J.H.W. de Wit, "A molecular and electrochemical approach to study corrosiveness and population dynamics of MIC biofilms inside ship ballast tanks", under review in *Biofouling*

A. Heyer, F. D'Souza, C. F. Leon Morales, G. Ferrari, J.M.C. Mol and J.H.W. de Wit, "Corrosion of carbon steel in a simulated ship ballast tank in the presence of a natural microbial community", to be published

A. Heyer, Y. Gonzalez-Garcia, J.M.C. Mol and J.H.W. de Wit, "Early-stages of *Pseudomonas* biofilm formation on stainless steel by means of local electrochemical techniques", to be published

## Dankwoord

Zum Schluss möchte ich mich bei den Menschen bedanken, die es mir möglich gemacht haben diese Arbeit zu verfassen.

First of all, I would like to express my gratitude to Prof. Hans de Wit and Dr. Arjan Mol for giving me the chance to participate in this interesting project. I thank both of you for educating me the aspects in doing research work. Many inspiring discussions between us contribute a lot too the development of the present work.

I greatly thank Fraddry D'Souza all my work is based on your confidence and interest in research. I am very lucky to know you and a really like your way of approaching new ideas and for your kindness, patience and persistence guidance and competent assistance all these years.

Grazie Gabriele per avermi dato la possibilità di approfondire la conoscenza, e risvegliare in me l'interesse, nel campo dell'elettrochimica. Certamente non ci si può augurare un mentore migliore. Grazie per aver posto la fiducia per 4 anni nel mio lavoro, accompagnato da discussioni critiche e costruttive, che mi hanno aiutato ad intraprendere la strada giusta in un campo così difficile. Durante la mia permanenza a TNO ho imparato molto di più del solo lavoro scientifico. Il vasto orizzonte nordico ha ampliato anche i miei orizzonti personali, mi mancheranno le nostre trasferte.

Mijn collega's bij TNO in Den Helder ben ik veel dank verschuldigd. Zij hebben mij altijdbijgestaan bij het uitvoeren van de experimenten. Vooral met Fraddry D'Souza en Xiaolong Zhang heb ik veel gediscussieerd over de resultaten. De gehele Helderse groep wil ik bedanken voor de steun en de bijdrage aan mijn onderzoek en ook voor de prettige werksfeer die ik heb ervaren gedurende bijna 4 jaar.

I would further thank Prof. Gerard Muyzer for scientific knowledge transfer and Florence Marty for her assistance in experimental work to finalize chapter 2 of this thesis.

Thanks to the people of my group in Delft especially Önnaz and Olga for their option to stay in Delft when it was necessary and to make me feel home. Without you two it would not have been such an inspiring time. Thanks Yaiza for your support in experimental work and being a nice accompany during conferences.

Finally I would like to say thanks to my friends and fellow students for their support over years and years.

Special thanks are due to my family, my father, Rita and Horst, for their never ending support throughout my education. Ohne Euch, wäre diese Arbeit nicht zustande gekommen.

Anne Heyer  
Oberhausen, 2013

## Curriculum Vitae

Anne Heyer was born on March 7, 1980 in Duisburg, Germany. She obtained her bachelor's degree in water science in 2005 and participated in a research internship under the supervision of Prof. Dr. Hans Curt Flemming and Dr. Kirsten Habicht entitled "Temperature effect on isotopic fractionation during sulphate reduction of *Archaeoglobus fulgidus* strain z" at the University of Southern Denmark in Odense.

For her master's degree in water science, she wrote a thesis entitled "Effect of EPS films on attachment and biofilm formation by sulphate-reducing bacteria on metal surfaces" under the supervision of Prof. Dr. Wolfgang Sand and Prof. Dr. Hans Curt Flemming at the University Duisburg-Essen. After receiving her master's degree in 2007, she participated in a six-month intership entitled „Neuartiger Korrosionsschutz durch verwendung mikrobieller extrazellulärer polymerer Substanzen (Biofilm-induzierte Korrosionsinhibition)" in a joint program between the University of Duisburg-Essen in Germany and the Karl Winacker Institute in Frankfurt, Germany.

From 2008 to 2012, she worked as a PhD student in the Materials Innovation Institute (M2i) and the Materials Surface and Interface group at the Delft University of Technology in the Netherlands. For her research, she was directly situated at TNO at the Maritime Materials Performance Center (MMPC) in Den Helder, the Netherlands. Under the supervision of Prof. Dr. Hans de Wit, Dr. ir. Arjan Mol, MSc. Gabriele Ferrari and Dr. Fraddy D'Souza, she performed the research that is presented in this thesis. Currently she works as department manager of Microbiology at RWW (Rheinisch-Westfälische Wasserwerksgesellschaft) in Mülheim an der Ruhr, Germany.